The analysis of event-related potentials following the presentation of near-simultaneous stimuli under dual-task conditions

Thesis

THE ANALYSIS OF EVENT-RELATED POTENTIALS FOLLOWING THE PRESENTATION OF NEAR-SIMULTANEOUS STIMULI UNDER DUAL-TASK CONDITIONS.

Jane Ross Denton, BSc (Newcastle), MSc (CNAA)

Date of Submission: 1.10.85
Date of Award 10.6.86

Submitted in part fulfilment of the requirements
for the degree of Doctor of Philosophy at
the Open University

Discipline: Psychology

Date of submission: 31 October 1985

To my parents: Donald Ross Carstairs and

Freda Maud Carstairs

ABSTRACT

Event-related potential (ERP) research frequently utilises research designs from cognitive psychology to investigate ERPs as indices of cognitive processes. There are, however, restrictions on the use of certain experimental paradigms arising from the nature of the physiological activity being recorded. One such restriction relates to the duration of the event-related response, which can extend beyond 500mS. The presentation of stimuli at constant intervals of less than 500mS results in complex waveforms which are composed of partially overlapping activity associated with the successively presented stimuli. This thesis concerns the methodology of separating overlapping ERP components recorded following the presentation of temporally close, or 'near-simultaneous', stimuli.

Three analytical procedures are considered. The first utilises an elementary subtraction process whereby the waveform recorded to one stimulus in isolation is subtracted from the complex waveform recorded to the same stimulus when presented in close temporal proximity to a second stimulus. The result of this subtraction is assumed to be the waveform associated with the second stimulus. An important restriction on the use of this technique, however, is that it fails to allow the assessment of any interaction (of either a sensory or a psychological nature) which results from the close presentation of two stimuli.

The second procedure involves the application of two digital filters, the first in the time domain and the second in the frequency domain. The third procedure employs a generalised least-squares (GLS) regression analysis. The advantage of these techniques over that of elementary subtraction is that they are applied directly to the complex overlapping waveform, and allow a direct assessment of any interactions

between task stimuli. Both procedures, however, require the presentation of stimuli such that the activity recorded to one stimulus is partially time-unlocked from that recorded to the other stimulus.

Three main approaches are utilised in the consideration of the three analytical procedures:

- the problem of ERP component overlap, and the method of stimulus presentation necessary for the application of the filtering and GLS solutions, are demonstrated using data recorded during a dual-task experiment which investigates the 'distribution' of attention through the simultaneous performance of two experimental tasks;
- the theoretical foundations of the analytical procedures are considered and the assumptions and restrictions associated with each are discussed;
- simulations are used which enable an assessment of the analytical procedures under ideal conditions.

Evidence is presented which indicates that the estimation of ERP activity through the elementary subtraction process is appropriate for the present dual-task data, and the behavioural and electrophysiological data are evaluated.

It is concluded that elementary subtraction procedures provide a powerful solution to the problem of separating overlapping ERP components, but only if the assumptions associated with the technique can be shown to hold.

The adequacy of the filtering and GLS solutions is assessed by comparing ERP estimates obtained through these procedures with those obtained through elementary subtraction. These comparisons provide an

adjunct to assessments made through the use of simulations.

Whilst in theory the filtering process provides an optimum solution, the technique is limited in its usefulness due to the severe distortions of ERP estimates resulting from spectral leakage in the frequency domain representation of the waveforms. Methods of reducing the effects of spectral leakage are considered but are found to result in residual distortions of the very low frequency, late components of the ERP.

A potentially more useful procedure than either elementary subtraction or digital filtering was found to be that of GLS estimation. The solution allows the detection and assessment of interactions between stimuli and is carried out in the time domain, thus obviating the problems of spectral leakage associated with analysis in the frequency domain. Methods by which the solution can be optimised are discussed.

DECLARATION

None of the material contained in this thesis has been submitted previously for a degree or other qualification to this or any other university or institution.

The experimental work and its interpretation in this thesis are entirely my own.

ACKNOWLEDGEMENTS

I should like to express my gratitude to my supervisor, Dr. Martin LeVoi (Psychology Discipline, O.U.), for his impeccable guidance and advice, his unfailing interest, and his inimitable good humour during all stages of this work. I am also indebted to Dr. LeVoi for developing much of the computer software used throughout this thesis.

I should like also to express my gratitude to Professor John Monk (Faculty of Technology, O.U.), for his invaluable help in developing the analytical procedures presented in Chapters 4 and 5.

My thanks go to Mr. Danny Waite (Psychology Discipline, O.U.), for his technical help during the setting-up of a psychophysiology laboratory at the Open University, and for designing and constructing ancilliary equipment used during the experimental stage of this project.

I am indebted to Dr. Michael Cook (Psychology Department, Australian National University), for statistical advice and for the use of computing facilities, and to Mr. Martin Schaefer and Mr. Greg Preston (both at the Australian National University) for their help in the arduous task of transferring data onto the Univac 1100.

I am indebted further to the Australian Public Service for granting me study leave in which to complete the written component of this work, and to my colleagues and friends at the Office of the Australian Public Service Board for their continued support and encouragement.

Special thanks are due to Dr. Chris Denton for the numerous hours spent preparing many of the figures and tables, and to Ms Barbara Piper for her excellent typing and sanguine disposition when confronted with the various drafts of this thesis.

Finally, there are many friends who should be thanked for the support and encouragement they have provided. In particular, I should like to thank Chris Denton, Julia Irwin, Sue Poultney and Martin Schaefer. Without their optimism and encouragement this thesis would probably never have been completed.

CONTENTS

LIST OF FIGURES

LIST OF TABLES

LIST OF OVERLAYS

CHAPTER 1: INTRODUCTION

1.1 The event-related potential

The human sensory event-related potential (ERP), also known as the evoked potential (EP), can be recorded from the scalp following the presentation of a discrete stimulus, such as an auditory click or a flash of light. The potential consists of a characteristic series of positive and negative voltage oscillations which starts as early as 1mS after stimulus onset, and persists for up to 500mS. Such specific brain responses were first noted in 1875 by Caton, recording from the cortex of the rabbit. In 1929 Berger recorded similar voltage fluctuations from the intact human scalp. The small amplitude of these responses relative to the spontaneous activity of the brain, the electroencephalogram (EEG), precluded any systematic investigation, however, until a means of improving the signal (ERP) to noise (EEG) ratio became available. This technical advance was achieved by Dawson (1947; 1951) who first introduced Galton's (1878) procedure of photographic superimposition to ERP research, and then, four years later, described an analogue signal averager. A further development came when Clynes and Kohn (1960) developed the first digital averager. The principle underlying these techniques is that the ERP is an invariant response which is closely synchronised with the onset of the stimulus, whereas the EEG is a random process, and its contributions to successive ERPs are statistically independent of one another. Consequently, the point by point summation (or averaging) of successive digitised epochs of activity, recorded time-locked to the onset of the stimulus, cancels out the unwanted EEG and leaves the wanted response intact.

The effect of signal averaging is to attenuate the background noise in proportion to the square root of the number of epochs being summed (Glaser and Ruchkin, 1976), and its use in any experimental investigation can require the presentation of many trials under a

particular experimental condition. Generally, about 64 trials are needed to distinguish large amplitude potentials from the background EEG, and as many as 1600 trials are necessary to distinguish small amplitude components (Picton and Hink, 1974). Although there are methods for improving the signal to noise ratio on a single trial basis (see for example John, Ruchkin and Vidal, 1978; Otto, 1978, section IX), this approach is unsuitable for detecting small amplitude components. Therefore, the majority of research presents ERPs as averaged waveforms, and as Donchin (1979) aptly stated: "the key to the study of the human ERP has been the signal averager".

The non-invasive methods employed for recording human ERPs necessarily means that these waveforms reflect the gross electrical activity of synchronously-activated neuronal populations, rather than the discrete functioning of individual nerve cells. Generally it is agreed that the ERP represents the algebraic summation of excitatory post-synaptic potentials (EPSPs) and inhibitory post-synaptic potentials (IPSPs), but the complex cytoarchitecture of the brain makes it impossible to assess the relative contributions of these two types of graded potentials to a particular ERP component (Goff, Allison and Vaughan, 1978). However, intracellular recordings from animal 'models', and studies of the scalp topography of ERPs in humans, are providing information about the specific generators of various ERP components (see Goff *et al.*, 1978; Vaughan, 1974, 1982; Wood, 1982 for reviews of ERP sources and discussion of the volume conduction model). ERP components have been identified as originating in afferent pathways, in or near the primary sensory cortex, and in motor and association cortex. In general, the origin of a component, in terms of the position of its generator in the sensory pathway or cortex, is reflected by its latency.

Figure 1.1 shows the human average ERP recorded to a brief auditory stimulus (after Picton, Hillyard, Krausz and Galambos, 1974; Hillyard and Kutas, 1983). Figure 1.1A shows the idealised response plotted against a logarithmic timebase in order to illustrate the high frequency, early components, as well as the lower frequency, late components. Figure 1.1B shows the early, middle and late components of the response plotted separately on different timebases[1]. The early components of the auditory ERP comprise seven wavelets (waves I-VII) which represent activity in the auditory sensory pathway from the cochlea to the inferior colliculus of the thalamus (Jewett and Williston, 1971; Picton *et al.*, 1974). The source of the middle latency components, occurring between 10 and 80mS, is less clear, but it has been suggested that these are generated by the medial geniculate and the polysensory nuclei of the thalamus (Picton *et al.*, 1974), and possibly the primary auditory cortex (Goff *et al.*, 1978). The P_1, N_1 and P_2 late components (also called the 'vertex potentials', because they are recorded maximally at or near the vertex of the scalp) have been suggested to arise from modality-nonspecific cortical areas (Roth, Shaw and Green, 1956), including frontal association cortex (Picton *et al.*, 1974), or conversely, from primary and secondary auditory

[1] It should be noted that various labelling conventions have been applied to ERP components, and Figure 1.1 illustrates three of these conventions. The early latency components are labelled with Roman numerals, in the order of their temporal sequence, whereas middle latency and late components are labelled P or N according to their polarity. The polarity convention used in Figure 1.1 is negative up. The subscripts attached to the middle latency components (N_o, N_a, N_b) simply reflect the temporal order of components having the same polarity, whereas subscripts attached to the late components (e.g. P_{300}) refer to their modal latency in milliseconds. If the peak latency of a late component approaches a unit-multiple of 100mS, then a single digit subscript often is used, e.g. N_1 is equivalent to N_{100}.

cortex (Vaughan and Ritter, 1970). The precise origins of these late components are, therefore, equivocal and await clarification.

The components of the auditory ERP described so far invariably occur following the presentation of an auditory stimulus, and their amplitudes and latencies are sensitive to stimulus parameters such as intensity and rate of presentation. Such components have been termed 'obligatory', 'stimulus-bound' or 'exogenous', as they always appear in response to external stimulation (Donchin, Ritter and McCallum, 1978). The absence or distortion of these exogenous components can provide useful indicators of neurological or sensory impairment (see, for example, Starr, Sohmer and Celesia, 1978, for a review of these clinical applications). In contrast, the N_2, P_3 and N_d waves shown in Figure 1.1A, superimposed on the vertex potentials, are termed 'non-obligatory' or 'endogenous', as their occurrence and amplitude depends largely on the psychological context in which the stimuli are presented, rather than the stimulus parameters *per se*. Indeed, the N_2 and P_3 components can be recorded following the omission of an expected stimulus (e.g. Klinke, Fruhstorfer and Finkenzeller, 1968; Picton and Hillyard, 1974).

Whilst all components of the ERP are influenced to some extent both by stimulus parameters and the internal state of the organism, Donchin, Ritter and McCallum (1978) have emphasised the heuristic value of the exogenous-endogenous distinction:

> "The useful distinction, which can serve as a guide for experimentation, is that whenever variance in the ERP cannot be attributed to variance in the physical stimulus, the ERP component will be considered endogenous. Whenever the variance is attributable to the physical nature of the stimulus we consider the components exogenous", (p.356).

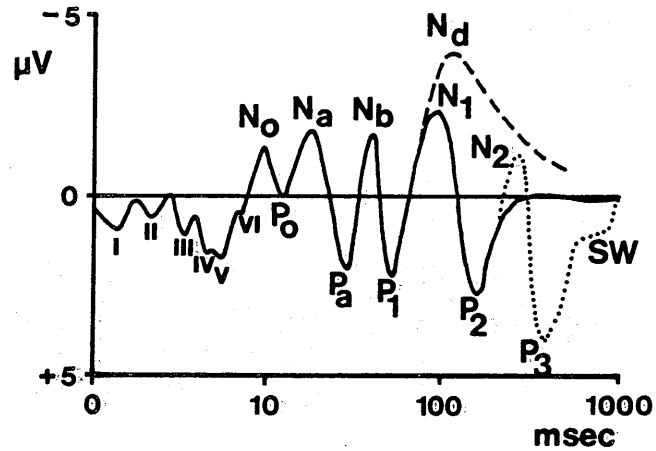

A. Idealised waveform of average auditory ERP to a brief sound plotted against a logarithmic timebase. (After Hillyard and Kutas, 1983).

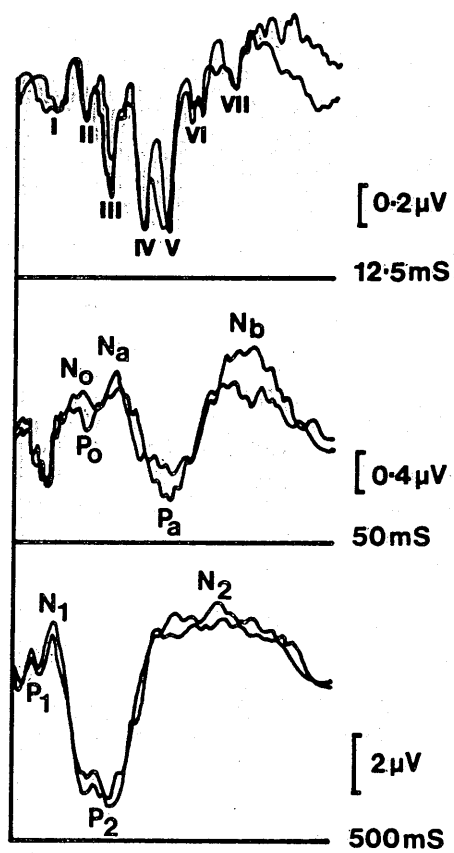

B. Auditory ERPs to 60dBSL clicks. Each trace represents the average of 1024 responses from vertex-mastoid electrodes. (After Picton, Hillyard, Krausz and Galambos, 1974).

Figure 1.1. Auditory event-related potential.

It is, therefore, the endogenous components of the ERP which can provide insight into the psychological basis of human cognitive functioning.

1.2 ERP research and cognitive psychology

The technological advances which allowed the non-invasive recording of the human ERP, and the development of signal extraction techniques, occurred within the same time frame as the emergence of the information processing approach as a major influence in cognitive psychology (Haber, 1974). The result of this influence was a 'paradigm shift' (Kuhn, 1962; Segal and Lachman, 1972), whereby psychological theory moved away from the view that all behaviour could be explained in terms of simple S-R connections, and began to conceptualise humans as active processors of information who adopted strategies, generated and tested hypotheses, established expectancies and made decisions. Furthermore, the information processing model proposes 'stages' of processing such as encoding, selection, storage and retrieval, all of which may be manifested as endogenous components of the ERP. Contemporary cognitive psychology, therefore, provides a theoretical framework and a wealth of research designs within which 'cognitive psychophysiologists' (Donchin, 1982) can explore the relationship between endogenous ERP components, behavioural measures and specific stages of information processing. Through combined studies of humans and animals the identification of the physiological generators of endogenous ERPs ultimately may lead to the localisation of those brain systems that subserve specific cognitive activities (Galambos and Hillyard, 1981).

The present understanding of the relationships between endogenous ERPs and cognitive processes is catalogued in the proceedings of a number of recent symposia (Callaway, Tueting and Koslow, 1978;

Otto, 1978; Begleiter, 1979; Desmedt, 1979; Lehmann and Callaway, 1979; Kornhuber and Deecke, 1980; Galambos and Hillyard, 1981; Donchin, 1982; Karrer, Cohen and Tueting, 1984).

1.3 Practical limitations of ERP research

Whilst research in cognitive psychophysiology can draw fruitfully on the research designs of cognitive psychology, there are some restrictions on the use of particular experimental tasks and task requirements. These restrictions result directly from the nature of the physiological activity being recorded. An obvious example is that the recording and averaging of ERP activity requires the presentation of discrete stimuli which have a reasonably abrupt onset, and which are exactly reproducible (Picton and Hink, 1974). Slowly changing stimuli, such as those used in visual tracking tasks or monitoring situations, are unsuitable for eliciting time-locked responses. The average ERP also is subject to contamination by other cerebral and non-cerebral activity, if this happens to be time-locked to the evoking stimuli. Sources of possible contamination are due to motor potentials associated with overt (and possibly covert) responding (Tueting, 1978), muscle potentials associated with sustained muscle tension or gross body movements (Picton and Hink, 1974), and ocular artefacts resulting from eyeblinks and vertical eyemovements (Hillyard and Galambos, 1970; Corby and Kopell, 1972; Weerts and Lang, 1973). The need to control for these sources of contamination requires the careful adaptation of some experimental designs, whilst other designs prove to be unsuitable for ERP research.

A further difficulty with the application of experimental paradigms from cognitive psychology to cognitive psychophysiology concerns the temporal relationship between task stimuli, and this thesis considers methods of assessing ERP waveforms recorded to stimuli presented in close temporal proximity.

Late components of the ERP can be recorded for up to 500mS after stimulus onset, and a problem arises if stimuli are presented at a constant rate with an inter-stimulus interval (ISI) of less than, say, 400mS. In this situation, the late components of the ERP to one stimulus will not be fully resolved, and will overlap the early components of the ERP to the next stimulus. As the late components of one ERP are effectively time-locked to the occurrence of the next stimulus, averaging over a timebase equal to the ISI will result in a waveform with spurious short-latency components. The obvious solution to this problem is to use ISIs of at least 500mS. There are, however, many situations in which ISIs of this duration are undesirable. For example, in selective attention paradigms, stimuli generally are presented at high rates in order to ensure that subjects attend to the task-relevant 'channel' and cannot switch their attention to a task-irrelevant channel (Näätänen, 1975).

An alternative solution to the problem of overlapping components is to present stimuli in an aperiodic manner, that is, with variable ISIs (Ruchkin, 1965). The effect of such a procedure is to time-unlock the late components of each ERP from the subsequent stimulus. Overlapping activity will be treated as random 'noise', and will cancel out during averaging. There are many instances of the application of this technique in the literature. For example, Hillyard, Hink, Schwent and Picton (1973) presented tonal stimuli dichotically with an ISI range of 100-800mS (mean ISI 450mS), and averaged over a 200mS or a 500mS timebase. The unpredictable time of arrival of stimuli, and the occasional very short ISIs, prevented subjects from switching between channels (Hillyard *et al.*, 1973), and there is no evidence of spurious early components in their data. A rule of thumb for the use of this technique is that

ISIs should range over a time-span which is greater than the period of overlapping activity to be attenuated (John *et al.*, 1978). The 700mS ISI range used by Hillyard and his colleagues resulted in the attenuation of components down to approximately 2Hz, which is appropriate for attenuation of most long-latency components.

In the example provided above, the precise timing of successive stimuli was not important, and it was possible to use a wide range of ISIs; but what of those paradigms in which the actual temporal relationship between stimuli is important? Backward masking experiments provide an example of such a paradigm. In these experiments, the interval between two stimuli (a test stimulus and a subsequent masking stimulus) is systematically manipulated to assess the effects of the masking stimulus on the perception of the test stimulus (Kahneman, 1968; Turvey, 1973) and such manipulations often involve the presentation of stimuli at constant ISIs of 50mS or less.

Several researchers have recorded ERPs under conditions of backward visual masking (e.g. Donchin and Lindsley, 1965; Andreassi, Stern and Okamura, 1974; Andreassi, De Simone and Mellers, 1976; Schwartz and Pritchard, 1981) with the result that ERP traces consist of composite waveforms representing overlapping activity to both test and masking stimuli. The relative contribution of the two stimuli to the recorded potentials has been assessed through the use of elementary subtraction procedures. That is, the ERP recorded to the masking stimulus in isolation is subtracted from the composite waveform and the residual of this subtraction is assumed to be the ERP evoked by the test stimulus. The use of this technique, however, is problematic as it rests on the assumption that the ERP recorded to the masking stimulus in isolation is identical to that recorded to the masking stimulus when presented in conjunction with the test stimulus. Consequently, the technique fails to

allow for any psychological or physiological interaction which may take place between the two stimuli in the masking situation. Under such circumstances the use of elementary subtraction procedures will lead to an inaccurate estimation of activity associated with the test stimulus. Alternative methods of analysis are necessary to allow for a more precise estimation of component waveforms.

The topic of this thesis is the methodology of separating overlapping ERP components recorded to temporally close, or 'near-simultaneous' stimuli. To this end, three analytical techniques are investigated. The first technique utilises traditional elementary subtraction procedures. The other techniques allow the estimation of component waveforms directly from the composite waveform, and are designed to enable the assessment of interactions between task stimuli. This thesis utilises three approaches:

- the problem of component overlap is demonstrated using ERP data recorded during a dual-task experiment which investigates the 'distribution' of attention through the simultaneous performance of two experimental tasks. While the results of this experiment may be of interest, the primary reason for its inclusion is to allow a comparison of the different analytical procedures following their application to 'real' data which might be expected to reflect interactions between task stimuli;
- the theoretical foundations of the three analytical techniques are explored, and the assumptions and restrictions associated with each procedure are discussed;
- simulations are utilised which enable an assessment of the analytical procedures under ideal conditions.

The following section provides an overview of the theoretical basis of dual-task paradigms, and introduces the experimental task used to demonstrate the analytical procedures. The use of dual-task paradigms in the study of ERP correlates of attentional processes provides a natural extension to those paradigms used to assess the ERP under conditions of focussed or selective attention (for reviews of this area see Näätänen, 1975, 1982; Näätänen and Michie, 1979; Hansen and Hillyard, 1980; Hillyard, 1981).

1.4 Dual-task paradigms

The resurgence of interest in dual-task performance over the last fifteen years resulted from the formulation of capacity theories of attention (Moray, 1967; Kahneman, 1973; Norman and Bobrow, 1975; Navon and Gopher, 1979). Kahneman's model, for example, views attention as an undifferentiated resource of limited supply which can be allocated to different information processing activities. The interference between concurrently performed tasks can be explained in terms of a competition for this limited processing resource, and the extent of this interference will depend upon the overall resource requirements of the competing activities. Navon and Gopher, on the other hand, propose that processing resources are differentiated into a number of structure-specific capacities, each of which is limited. For example, perceptual, memory, motor and verbal activities might draw on such separate limited capacities. This multi-processor model predicts that interference between concurrently performed tasks will occur only if both tasks draw on the same limited capacity 'pool'. These different capacity models have been formulated from observations of dual-task performance, and in turn, dual-task paradigms can be utilised to test their various predictions.

In the dual-task situation the processing demands of one task, the primary task, can be inferred from performance on the other task, the secondary task. For example, an increase in difficulty (processing requirements) of the primary task will result in a decline in secondary task performance, as long as primary task performance is maintained at some predefined criterion of speed or accuracy (Norman and Bobrow, 1975), and as long as the joint demands of the task exceed the total available resources. Secondary task methodology (Kerr, 1973) can, therefore, be used to describe a task, or the individual processing stages involved in that task, in terms of the demands made on the limited capacity system. It is not the intention here to review the large body of literature on dual-task performance, but rather to give a flavour of the broad theoretical framework underlying the use of these paradigms. Reviews of this area and recent formulations regarding the structure of attentional resources are provided by Duncan (1980), Navon and Gopher (1980), Wickens (1980) and Posner and McLeod (1982).

An example of the application of dual-task paradigms to ERP research is provided by the work of Isreal and his colleagues, who investigated the endogenous P_3 component of the ERP (see Figure 1.1A) as an index of task difficulty or 'workload'. The amplitude of the P_3 component, elicited by a secondary tone discrimination task, was found to decrease when a primary visual tracking task was introduced. No further effect on the amplitude of this component was evident, however, when tracking difficulty was increased by manipulating tracking dimensionality or band-width (Wickens, Isreal and Donchin, 1977; Isreal, Chesney, Wickens and Donchin, 1980). Conversely, when a similar auditory task was paired with a visual display monitoring task,

which required the detection of changes in target trajectories, the auditory P_3 was found to be sensitive to changes in primary task difficulty. P_3 amplitude decreased significantly when the number of visual task elements to be monitored was increased from four to eight (Isreal, Wickens, Chesney and Donchin, 1980). Thus, the P_3 component elicited by secondary task stimuli was sensitive to increases in primary task difficulty when the primary task involved an increase in perceptual demands (i.e., the monitoring task), but not when the primary task involved an increase in response-related demands (i.e., the tracking task). These results have been interpreted in terms of those capacity theories which posit multiple sources of limited processing capacity, each of which deals with a specific processing activity (see Navon and Gopher, 1979; Wickens, 1980). The tone discrimination task used by Isreal and his co-workers emphasised perceptual processing rather than responding, and could be presumed to be drawing upon the same processing resources as the display monitoring task. The authors therefore concluded that P_3 provided an indirect index of the primary task's demand for perceptual processing resources. Consistent with this interpretation is the evidence which indicates that the P_3 indexes aspects of stimulus evaluation and classification, rather than response-related processes (Squires, Donchin, Squires and Grossberg, 1977; Donchin, 1978; Duncan-Johnson and Donchin, 1982).

It should be emphasised that the aim of the experiments described above was to investigate the ERP as an index of overall task difficulty or 'workload', rather than as an index of the processing demands of specific mental operations. Hence the precise temporal relationship between primary

and secondary task stimuli was of little importance, and the continuous nature of the primary tasks precluded the possibility of recording complex waveforms resulting from overlapping visual and auditory ERPs.

There are, however, dual-task paradigms which do allow the investigation of processing demands associated with specific stages of the primary task, as well as an assessment of overall processing demands during different levels of primary task operation. Such paradigms present the cognitive psychophysiologist with problems of ERP component overlap. The dual-task used in this thesis is adapted from a behavioural study by Posner and Boies (1971) who applied such a paradigm. Their experiments required subjects to perform a primary visual letter-matching task and at the same time respond to secondary task auditory 'probe' stimuli which were presented during various phases of the primary task. Each trial of the letter-matching task consisted of a warning signal, followed by a first letter and then a second letter to which a 'same' or 'different' manual reaction-time response was to be made according to physical match or name match rules. The visual task falls into three natural segments, each of which can be associated with specific processing operations: the warning signal is associated with preparation for the following task stimuli, presentation of the first letter is associated with the operations of encoding and rehearsal, and presentation of the second letter involves response selection and initiation.

Posner and Boies assessed the processing demands of these different operations by reference to the speed with which subjects made a manual response to the auditory probe stimuli: long reaction-times to the probe were assumed to indicate large processing demands of the primary task. The close temporal relationship between visual and

auditory stimuli was essential for exploring the time course of the processing demands of different primary task operations, and some probe stimuli were presented after an interval of only 50mS following the onset of a visual stimulus.

The Posner and Boies experiment has previously been adapted to ERP research to investigate the effect of preparatory set and task difficulty on the auditory event-related potential (Nash and Williams, 1982). While probe stimuli were presented in both the warning interval and in the interval between the first and second letter onset, the minimum time between any two stimuli was set at 480mS to obviate problems of ERP component overlap. The authors state that:

> "The specific positions within these intervals were selected to minimize temporal overlap between the auditory potentials elicited by the probes and any visual evoked potentials elicited by the letters themselves", (p.19) .

1.5 Overview of analytical techniques and chapter organisation

The three analytical techniques to be reported are illustrated using average ERP data recorded during a modified version of the Posner and Boies dual-task experiment. The first method involves the use of elementary subtraction techniques, whereby the ERP recorded to a visual stimulus in isolation is subtracted from the complex waveform recorded following the near-simultaneous presentation of the same visual stimulus and an auditory stimulus. The residual of this subtraction is assumed to be the auditory response. The second method employs a time-series analysis, and individual ERPs are derived from complex waveforms through the application of two digital filters, the first in the time domain and the second in the frequency domain. The third method to be reported utilises an alternative approach to the analysis of time-series

data, and estimation of component waveforms is achieved in the time domain through a least squares regression analysis.

The advantage of the latter two techniques over the elementary subtraction method is that the solutions are derived directly from the complex waveforms. The application of these techniques, however, requires that ERP activity evoked by one stimulus is partially time-unlocked from ERP activity evoked by the other stimulus. This is achieved by varying the interval between the presentation of stimuli in the two modalities over successive experimental trials. In the example presented here, ISIs are varied over a window of 100mS, although this time period is quite arbitrary, and can be reduced if near constant ISIs are required. The implementation of both of these techniques depends on an accurate knowledge of the range of ISIs used in the presentation of stimuli. The method by which ERP data are collected and averaged is also central to the application of these procedures. Chapter 2 describes the dual-task experiment, placing particular emphasis on the method of stimulus presentation and data collection. Preliminary results are presented also in this Chapter. Chapters 3, 4 and 5 each present one of the three signal recovery techniques and the assumptions and restrictions associated with each are discussed. Chapter 6 presents the analysis of behavioural and electrophysiological data recorded during the dual-task experiment and Chapter 7 provides a comparison of the three analytical procedures used to separate overlapping ERP components.

CHAPTER 2: EXPERIMENTAL METHODS

2.1 Introduction

The three methods of separating out overlapping ERPs are illustrated using data recorded during a modified version of the Posner and Boies (1971) dual-task paradigm. The primary task consisted of a visual letter-matching task which required subjects to categorise letter-pairs according to three levels of letter-match. The concurrently performed secondary task required subjects to detect near-threshold auditory signals against a background of white noise.

Auditory signals were presented within eight temporal windows with respect to visual task stimuli, each temporal window corresponding to a different signal condition. Consequently, the extent to which auditory ERPs overlapped visual ERPs varied over the eight signal conditions.

The dual-task was designed to avoid response interference between the two component tasks (see for example, McLeod, 1978), and subjects were required to confine their responses to the inter-trial intervals (ITIs) rather than make speeded movements. Thus, performance on both visual and auditory tasks was measured in terms of accuracy rather than speed. This response requirement provided the added advantage of avoiding the possible contamination of ERPs with response-related motor potentials (Gilden *et al.*, 1966; Ritter *et al.*, 1972; Tueting, 1978).

The following sections provide a description of the dual-task and the method by which primary and secondary task stimuli were presented to effect the partial time-unlocking of visual and auditory ERPs. Subsequent sections describe the collection and averaging of ERP data and present group averages recorded under the different conditions of the dual-task experiment.

2.2 Overview of stimulus control and experimental arrangement

The dual-task experiment was run on-line from a Digital PDP-11/34 computer running under the multi-user operating system RSX-11-M. The computer was equipped with sixteen digital input and output points, and a sixteen channel, 12-bit analogue to digital converter (AD11-K) having an input voltage range of $\pm$ 5V and a resolution of 0.0024 volts (1 part in 4096).

Throughout the experiment, the electroencephalogram (EEG) was recorded from the midline Central (Cz) and midline Parietal (Pz) scalp locations. Details of the techniques used for physiological recording are given in Section 2.5. The vertical electro-oculogram (EOG) also was monitored, in order to identify eyeblinks and eye-movements which could contaminate the EEG. Excessive eyemovements, of the order of 200μV, were identified by means of a moving window algorithm described in Section 2.5.1.

The presentation and timing of task stimuli, monitoring of subjects' behavioural responses, and sampling and averaging of physiological data were all under computer control. Figure 2.1 shows a block diagram of the hardware arrangement for stimulus presentation and data collection.

Experimental testing was carried out in a dimly lit, electrically screened and sound-attenuated room measuring 2 x 3 metres. Subjects were seated at a small table on which was placed a Sony video monitor (model CVM 110UK) driven by a Cifer video terminal (model 026). The Cifer keypad was positioned in front of the video monitor, and subjects pressed particular keys to register their responses during the experiment. The input terminals to the physiological recording

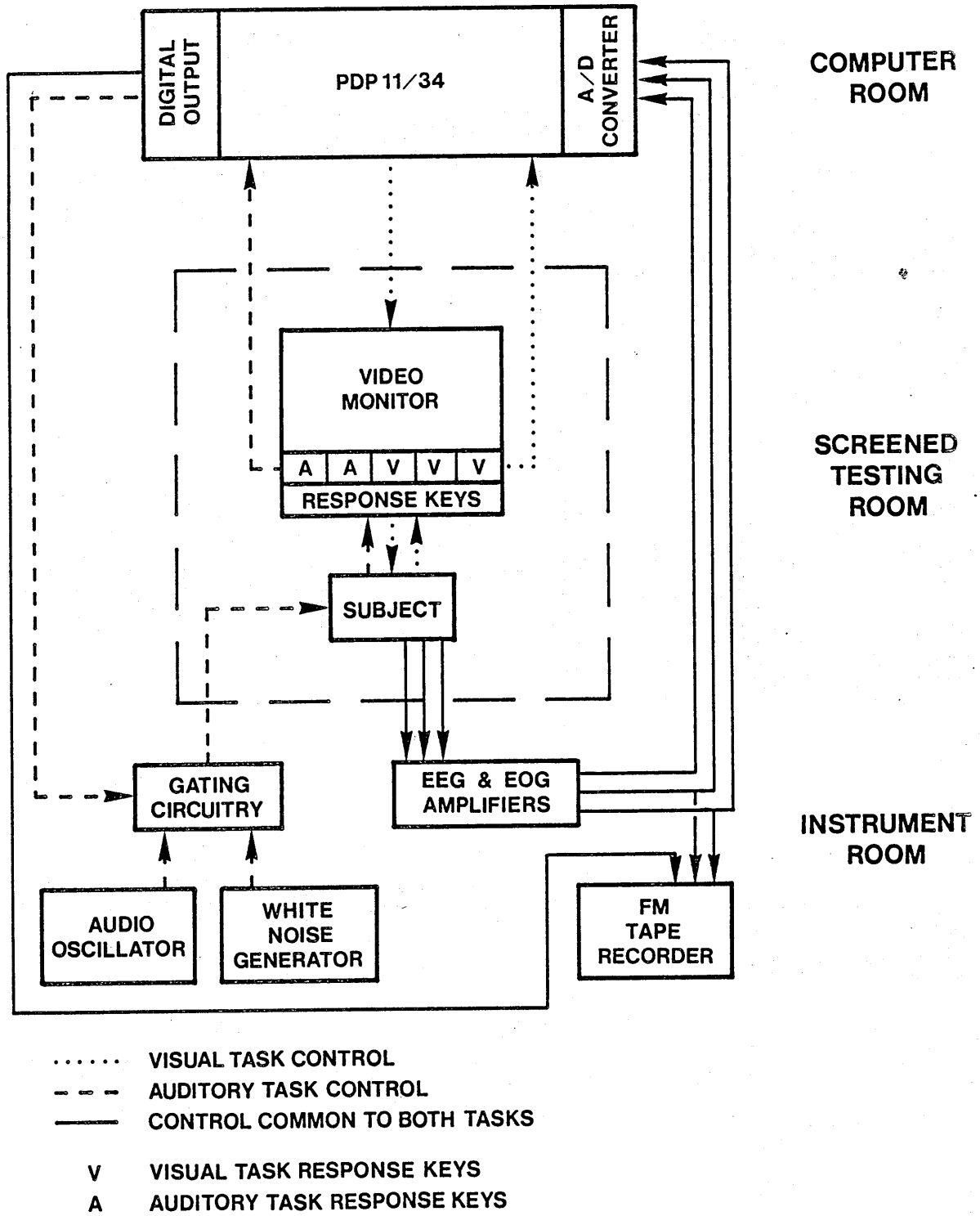

Figure 2.1. Block diagram of stimulus presentation and data collection arrangements.

equipment were positioned on a wall immediately behind the subject. Additional stimulus control apparatus and the physiological recording equipment were located in an adjoining instrument room. Communication between the computer and the experimental apparatus was achieved through coaxial cables which ran overhead from the computer room and terminated in the instrument room.

2.3 Subjects

Subjects were eight female and four male volunteers, whose ages ranged from 23-40 years. All subjects were familiar with the experimental arrangement, having attended three previous sessions during which they practised the component tasks of the dual-task experiment. Ten subjects were right handed and all had normal or corrected vision. No subject was taking any drug during the course of the experiment or had any history of neurological disorder. Subjects were paid £1.00 per hour for their participation.

2.4 Dual-task

The dual-task combined a visual letter-matching task and an auditory signal detection task, and required subjects to make judgements about letter-pairs whilst also monitoring for auditory signals in a background of white noise. The task was presented in blocks of 96 trials, every trial lasting for 2 seconds with a mean inter-trial-interval of 4.5 seconds. A description of the component tasks and the experimental design follows.

2.4.1 Visual letter-matching task.

The letter-matching component of the dual-task required subjects to categorise pairs of upper case letters according to three levels of letter-match. Letter-pairs corresponded to one of the following categories:

(1) Physical match (PM): letter-pairs were designated PM if they were physically identical, e.g. EE, PP.

(2) Rule match (RM): letter-pairs were designated RM if they were not physically identical but did conform to the rule of being either both vowels or both consonants, e.g. AE, BQ.

(3) Mismatch (MM): letter-pairs were designated MM if they belonged to neither of the above categories; that is, mismatch letter pairs consisted of one vowel and one consonant, e.g. AT, MU.

The task was presented on the Sony video monitor, which had a screen measuring 17 x 23cm. Subjects sat at a viewing distance of 50cm. Every two-second trial was composed of three visual events: a centrally placed fixation cross which remained in view for 1 second, followed by a first letter positioned to the left of centre and presented for 500mS, and then a second letter positioned to the right of centre, also presented for 500mS. The size of each character was 6mm high and 5mm wide, and the three characters presented on each trial occupied adjacent positions. Thus, the total display was 15mm wide, and at a viewing distance of 50cm, was foveal, the visual angle subtended by both letters and the fixation cross being less than 1 degree vertically and less than 2 degrees horizontally (Cogan, 1966, p.17).

At the end of every trial, subjects indicated their decision concerning the preceding letter-pair by pressing one of three adjacent keys on the Cifer keypad using the index, middle or ring finger of their right hand. Designation of response keys to the three stimulus conditions was counterbalanced across subjects.

2.4.2 Auditory signal detection task.

The stimulus parameters of the signal detection component of the dual-task were similar to those used by Hillyard, Squires, Bauer and Lindsay (1971). Continuous white noise (5kHz bandwidth) generated by a DAWE type 419 white noise generator was presented binaurally over headphones (AKG type K140S). The loudness of the white noise was adjusted to 60dB SPL as measured at a distance of one inch from the headphone cushion by a 1 inch Bruel and Kjaer microphone and measuring amplifier (Bruel and Kjaer, type 2608). On signal trials, a computer-generated pulse activated gating circuitry which enabled a 1kHz tone (generated by a Gould Advance oscillator) to mix with the white noise for 50mS. Only one signal occurred on any given signal trial at a constant signal intensity of 41dB SPL. Pilot studies had found this intensity to result in approximately 80% correct signal detection, which was consistent with detection rates reported by Hillyard *et al.* (1971) at similar intensities. Subjects were told that signals would occur on only half of the trials, and that the signal would be presented at any time within the 2 second trial period.

At the end of every trial, subjects were required to indicate whether or not a signal had been presented during that trial by pressing one key on the Cifer keypad with the index finger of their left hand for 'No Signal', or a second, adjacent key with the middle finger of their left hand for 'Signal'.

2.4.3 Experimental design

For each block of 96 trials, letter-pairs were generated from a population of fifteen letters, five vowels (A E I O U) and ten consonants (B C D G K N P Q T V). Letter-pairs were generated

randomly with the constraints that 32 trials conformed to each letter-match condition, and that within each condition, vowels and consonants occupied first and second letter positions an equal number of times. Half of the trials in each letter-match condition were signal trials and half were non-signal trials.

Although subjects were told that a signal could occur at any time during a trial, signals were presented equally often in one of eight discrete 100mS signal windows, corresponding to eight signal conditions. These windows were 100-200mS, 548-648mS, 1048-1148mS, 1200-1300mS, 1348-1448mS, 1548-1648mS, 1700-1800mS and 1848-1948mS, timed from the start of each trial. Within each window, the onset of the signal occurred at one of 25 time-points, spaced 4mS apart. The precise timing of signals within a particular window was randomly determined according to a rectangular distribution, so that over 25 trials, a signal was presented at each of the 25 time-points. Thus, signal detection performance during any signal condition represented mean performance over a 100mS time interval.

The onset of auditory signals was staggered with respect to visual task stimuli in order to partially time-unlock auditory event-related activity from visual event-related activity when trials were averaged across each signal condition. This staggering procedure is crucial to two of the methods of analyses to be presented and will be discussed further in Chapters 4 and 5.

Figure 2.2 illustrates the eight temporal windows during which the onset of the 50mS signal could occur, and the temporal relationship between visual and auditory events. The near-simultaneous onset of visual and auditory stimuli is evident from this diagram, with the interval between the onset of a visual and an auditory stimulus being as short as 48mS on some trials.

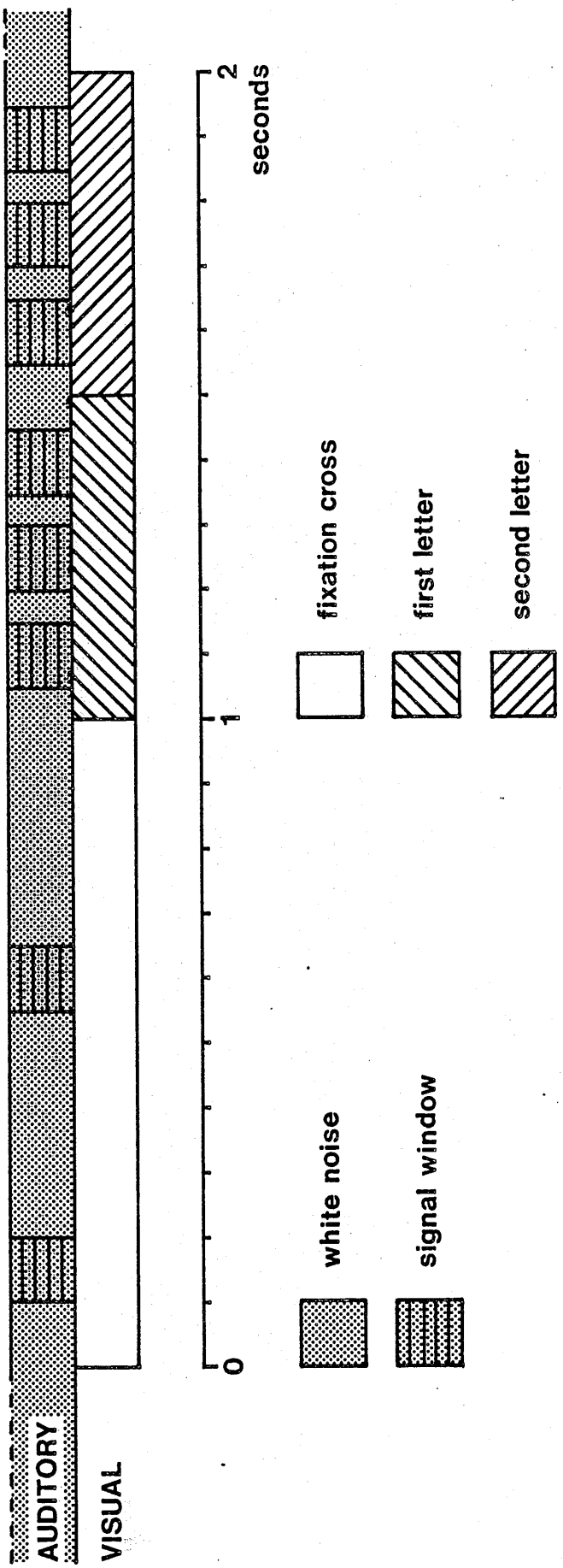

Figure 2.2. Temporal relationship between visual and auditory stimuli.

Within each block of trials an equal number of signals was presented within each signal window, at each level of visual letter-match. Table 2.1 shows the design of one block of dual-task trials. The ordering of letter-match trials, the ordering of signal detection trials and the ordering of signal conditions were randomised over each block, and the randomisation sequences were unique for every block of trials and for every subject.

All subjects worked through a total of 25 blocks of dual-task trials over three, 3hr sessions which were held on consecutive days. Eight blocks of trials were presented during both sessions one and two, and nine blocks of trials were presented during session three. Subjects initiated the start of each block of trials by pressing the return key on the Cifer keypad, and were encouraged to rest for a few minutes between each trial block.

Overall, subjects received 1200 signal trials (50 signals within each signal window, at each level of visual letter-match; 50 x 8 x 3 = 1200 trials) and 1200 non-signal trials (400 trials at each level of visual letter-match). Of the 50 signals presented within each signal window, 2 signals were presented at each of the 25 time points within the 100mS staggering interval.

The experimental design was thus a within-subject, two-way factorial design, the factors being: 'letter-match category' (physical match (PM), rule match (RM) and mismatch (MM)); and 'signal condition' (signal conditions 1-8, and no signal). There was a total of 24 experimental or 'dual-task' conditions (8 signal conditions at each of 3 levels of letter-match), and 3 control or 'single-task' conditions (1 at each level of letter-match when no signal was presented).

Table 2.1. Design of one block of Dual-Task trials.

Dual-Task						
Visual				Auditory		
Letter-match condition	Number of trials	Letter pairs		Signal condition	Number of trials	Number of trials at each signal condition
		Type	Number of trials			
PM	32	V-V	16	NS	8	-
				S	8	1
		C-C	16	NS	8	-
				S	8	1
RM	32	V-V	16	NS	8	-
				S	8	1
		C-C	16	NS	8	-
				S	8	1
MM	32	V-C	16	NS	8	-
				S	8	1
		C-V	16	NS	8	-
				S	8	1

PM = Physical match
RM = Rule match
MM = Mismatch

V = Vowel
C = Consonant

NS = No signal
S = Signal

2.4.4 Instructions to subjects

Subjects were instructed to fixate the warning cross at its onset and to attempt to retain their fixation point throughout the trial. If excessive eyemovements occurred during a trial, the message 'PLEASE TRY NOT TO MOVE YOUR EYES' was presented on the monitor for two seconds during the following inter-trial-interval.

The importance of the visual task was stressed (see Section 1.4 of Chapter 1), and subjects were instructed to keep visual task errors to a minimum and were told that two or three errors per block was an acceptable rate. At the end of each trial, subjects first made their response to the visual task by pressing one of three keys with their right hand, and then made their response to the auditory task by pressing the appropriate key with their left hand. Subjects were instructed to withhold making their first response until 500mS after the offset of the second letter in an attempt to avoid contaminating the EEG with response-related motor activity. Response latencies of less than 500mS were followed by the warning 'YOU ARE RESPONDING TOO SOON' displayed on the monitor for two seconds in the following inter-trial-interval. Subjects reported little difficulty in refraining from responding until the required interval had elapsed.

At the end of every block of trials, the total number of incorrect responses made to the visual task, and the number of 'Signal' and 'No Signal' responses given during the block were displayed on the monitor, in order to encourage subjects to keep visual task errors to a minimum and to make roughly equal numbers of signal/no signal responses.

2.5 Electrophysiological recording

The EEG was recorded concurrently from two scalp locations throughout the experiment. Recording was monopolar, electrical activity being recorded between an active scalp electrode and an inactive reference electrode which was common to both channels. An additional electrode was used to ground the subject. Vertical eyemovements also were monitored throughout the experiment. Details of the recording techniques are given in the following sections.

2.5.1 Application of electrodes

2.5.1.1 Active electrodes. Midline Central (Cz) and Parietal (Pz) sites were located according to the '10-20' electrode system (Jasper, 1958; see Figure 2.3), and marked with a chinagraph pencil. The electrode sites were cleaned by rubbing the scalp with cotton wool soaked in acetone, and electrodes were attached by the following method, described by Picton, Woods and Proulx (1978). A small hole was cut in the centre of a 3cm x 3cm pad of gauze which was placed over the electrode site and glued in position with collodion (Specialized Laboratory Equipment). The small area of scalp exposed through the gauze was gently scratched with a sterile hypodermic needle in order to eliminate interference from skin potential artifacts and to minimize inter-electrode impedance (Picton and Hink, 1974). Camjel electrode jelly (Cambridge Medical Instruments) was rubbed into the exposed scalp, and Beckman Standard Biopotential Ag/AgCl pellet electrodes were filled with electrode jelly and attached to the gauze by means of Beckman double-sided adhesive collars. A thin strip of adhesive plaster was placed over each electrode and stuck to the gauze on either side.

2.5.1.2 EEG reference electrode. The area of skin over the right mastoid process was cleaned with acetone, abraded with a sterile needle

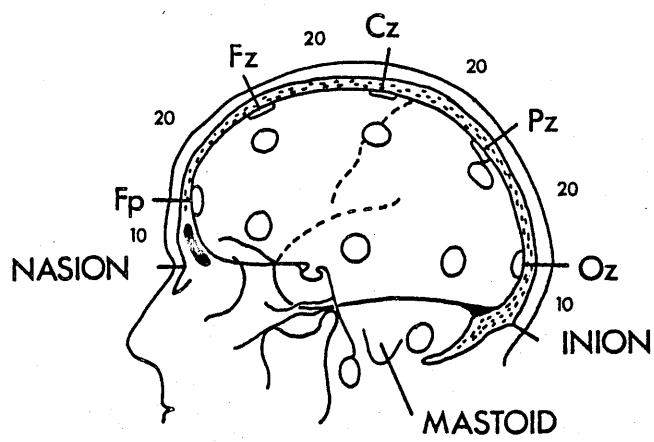

Figure 2.3. Lateral view of the left hemisphere, showing standard placements of the '10-20' electrode system. (After Jasper, 1958).

and rubbed with electrode jelly. The electrode was attached directly to the skin by means of a double-sided adhesive collar, and was further secured with a strip of adhesive plaster. The electrode, electrolyte and adhesive collar were of the same type as those used at active electrode sites.

2.5.1.3 Ground electrode. A 9mm gold disc electrode (Grass Instruments) was covered with electrode jelly and attached to the left ear lobe of the subject by means of a plastic ear clip. This electrode was used to ground the subject through the recording equipment and mains electricity supply.

2.5.1.4 EOG electrodes. Eyemovements and eyeblinks were monitored by continuous recording of the vertical EOG. Nine millimetre Ag/AgCl cup electrodes (Specialised Laboratory Equipment) were positioned on the upper and lower orbital ridges of the right eye, equidistant between inner and outer canthi (Picton *et al.*, 1978). The electrode sites were prepared by rubbing the area with a cotton-bud dampened with acetone. Electrodes were filled with isotonic electrolyte (Johnson and Johnson KY Jelly) and covered with small pieces of cotton wool soaked in 5% KCl to reduce drying of the electrolyte. The electrodes were held in position with thin strips of adhesive plaster.

2.5.2 Impedance testing of EEG electrodes

After a stabilisation period of fifteen minutes, the impedance between each active EEG electrode and the reference electrode was measured at 20Hz using an impedance meter (Specialised Laboratory Equipment). Electrodes were reapplied if inter-electrode impedances exceeded 5KΩ (Goff, 1974). The method of electrode application described above normally resulted in impedances of less than 2KΩ.

2.5.3 EEG and EOG recording

Electroencephalograms and the electro-oculogram were recorded on a Grass Model 7 polygraph, fitted with Model 7DAF driver amplifiers (IRIG standard: maximum full scale signal output level 1 volt RMS). EEG and EOG signals were fed into 3 channels of the analogue to digital converter for on-line sampling and signal averaging. The two channels of EEG activity and appropriate stimulus markers were recorded also on an FM instrumentation recorder (Racal, Store 4), which provided an off-line back-up facility.

EEG activity was amplified by Grass 7P1 chopper-type preamplifiers, each having an input impedance of 1 Megohm. Input was capacity-coupled with a half amplitude (50% cut-off) low frequency response of 0.4Hz (corresponding to a decay time constant of ~ 0.25 seconds), and a half amplitude high frequency response of 0.5kHz. The sensitivity of all EEG channels was set at 50μV/cm. 50Hz notch filters were used during all recording sessions. The EOG was amplified by a Grass 7P5 capacity-coupled preamplifier having an input impedance of 44 Megohms. The half amplitude low frequency response of the amplifier was set at 1Hz (decay time constant of 0.1 seconds) and the half amplitude high frequency response was set at 35Hz. The EOG was recorded at a sensitivity of 0.5mV/cm.

2.5.4 Calibration

Prior to the commencement of every testing session, all driver amplifiers and individual EEG and EOG preamplifiers were calibrated using the internal calibration signals of the equipment. The gain of the entire amplifier-averaging system was then determined separately for each channel by sending the internal calibration signal

through the system and running a computer program which sampled the output of the channel at 250Hz (Goff, 1974). The resulting digitised values of the calibration signals were used later to determine the amplitudes of average ERPs and eyemovements recorded during that session (see Section 2.7).

2.5.5 Removal and storage of electrodes

At the end of every recording session electrodes were removed from the subject and immediately washed in distilled water. A soft artist's brush was used to remove electrode jelly from electrode cavities. Beckman Ag/AgCl electrodes were stored in 1% saline solution; other electrodes were stored dry.

The collodion-impregnated gauze was detached from the subject's hair using cotton wool soaked in acetone. Excess electrolyte from EOG and ground electrode sites was wiped off with cotton wool and warm water.

2.6 On-line sampling, signal averaging and saving of EEG and EOG data

Fortran-callable Real Time Sampling routines were used to control the analogue to digital conversion of physiological data. Each channel of EEG activity was sampled at a rate of 250Hz, which was sufficient to provide adequate resolution of event-related activity and to avoid significant aliasing (Vaughan, 1974). The lower frequency EOG activity was sampled at a rate of 50Hz.

EEG and EOG sampling always commenced 500mS prior to the start of every trial, and continued for 3.5 seconds. Relevant sections of these 3.5 second epochs were then averaged into data files during the following inter-trial-interval, and saved for further analysis. A description of the manner in which EEG and EOG data were saved is provided in Section 2.6.2 below.

2.6.1 Criteria for saving EEG and EOG data

Two criteria had to be satisfied for physiological data to be saved at the end of a trial. The first required that the subject had responded correctly to both the visual letter-matching task and the auditory signal detection task. Following every trial, a computer check was made to determine if the subject had responded correctly to both elements of the dual-task. If an incorrect response had been given, physiological data were not saved for that trial. This criterion was imposed in order to minimize the variance of averaged ERPs, as the morphology of the ERP has been shown to reflect the correctness and/or certainty of decisions made about the evoking task stimulus (e.g. Hillyard *et al.* 1971; Squires, Hillyard and Lindsay, 1973). The importance of this criterion for the accurate estimation of overlapping ERP components is discussed in Chapter 4.

The mean percentage of incorrect letter-match responses and the mean percentage of incorrect signal detection responses were found to be 1.3% and 22% respectively, averaged across all experimental conditions and all subjects.

The second criterion for physiological data-saving was the absence of excessive eyemovements during the trial. The computer test for eyemovements was carried out during the inter-trial-interval, and consisted of a comparison between digitised EOG values recorded 80mS apart (4 sample intervals). An eyemovement was deemed to have occurred if the difference between these values exceeded 100 computer units (corresponding to approximately 200μV). This criterion was found to be effective in identifying gross eyemovements without placing undue stress on the subject. Successive comparisons of EOG values were made every 40mS over a window of 2.6 seconds. The test was started 400mS after the onset of the fixation cross, to allow for initial eye fixation by the subject, and ended 1 second

after the offset of the last visual event, thereby covering the response phase of the trial. Following the detection of one or more eyemovements, a warning message was presented to the subject, and physiological data were discarded for that trial. Excessive eyemovements were detected on 4.0 $\pm$ 4.6% of trials, averaged across all subjects. The large standard deviation associated with this mean reflects differences in individual subjects' abilities to control their eyemovements and eyeblinks.

Pilot tests showed the reliability of the eyemovement test to be high, but as an additional precaution the EOGs recorded on non-rejected trials were averaged together by task condition and saved for off-line inspection. No evidence of excessive eyemovements was apparent from these traces (see Section 2.9).

2.6.2 EEG and EOG data saving

If both of the above criteria were satisfied, relevant sections of the digitised EEG and EOG data were averaged into appropriate data files according to condition of task and electrode placement. These sections of data always contained 500mS of pre-stimulus activity which was subsequently used to determine the isoelectric 'zero' or baseline of averaged responses (see Section 2.7). A description of the timing and length of EEG and EOG epochs saved is provided below and is summarised in Table 2.2.

On all signal trials, four stimulus events occurred. These were the three visual events, consisting of the fixation cross, first letter and second letter, and the single auditory signal presented within one of the eight signal windows. Digitised EEG data recorded over these trials were saved in two ways. Firstly, the data were averaged and saved so that traces were time-locked to the visual events of the task. Data

Table 2.2: Summary of EEG and EOG data saving

Signal Condition	Time-locked Modality*	Input Channel	Sampling Rate	Data Saving Begins	Data Saving Ends	Epoch Duration	Data Storage
Signal	Visual	Cz, Pz	250Hz	500mS prior to fixation cross onset	500mS after end of trial	3 sec	Data averaged according to: 1) electrode placement 2) letter-match condition 3) signal condition 2 x 3 x 8 = 48 records
	Auditory	Cz, Pz	250Hz	500mS prior to signal onset	1 sec after signal onset	1.5 sec	Data averaged according to: 1) electrode placement 2) letter-match condition 3) signal condition 2 x 3 x 8 = 48 records
	Visual	EOG	50Hz	500mS prior to fixation cross onset	500mS after end of trial	3 sec	Data averaged according to: 1) letter-match condition 2) signal condition 3 x 8 = 24 records
No Signal	Visual	Cz, Pz	250Hz	500mS prior to fixation cross onset	500mS after end of trial	3 sec	Data averaged according to: 1) electrode placement 2) letter-match condition 2 x 3 = 6 records
	Staggered pure visual	Cz, Pz	250Hz	500-400mS prior to fixation cross onset	400-500mS after end of trial	3 sec	Data averaged according to: 1) electrode placement 2) letter-match condition 2 x 3 = 6 records
	Visual	EOG	50Hz	500mS prior to fixation cross onset	500mS after end of trial	3 sec	Data averaged according to: 1) letter-match condition = 3 records

*Indicates stimulus modality to which averages time-locked.

saving commenced 500mS prior to the onset of the fixation cross and continued for 3 seconds. These epochs were then averaged into data files according to electrode placement, visual letter-match condition and signal condition. In this way a total of forty-eight separate 'visual' averages was saved for each subject. Each average was based on a total of up to 50 trials and represents activity time-locked to the visual events of the task plus any time-unlocked or 'staggered' activity associated with the presentation of auditory stimuli over the 100mS signal window.

Secondly, data were averaged and saved so that traces were time-locked to the auditory events of a particular condition. Data saving commenced 500mS prior to the onset of the auditory stimulus and lasted for 1.5 seconds. These data similarly were averaged into data files according to electrode placement, letter-match condition and signal condition. A total of forty-eight 'auditory' averages was saved for each subject, each average based on a total of up to 50 trials. It should be stressed that these latter averages were time-locked to the onset of the auditory stimuli. That is, for a particular signal condition, data saving commenced at precisely 500mS prior to the onset of every auditory stimulus presented within the 100mS window, and these data were averaged so that the time of onset of the auditory stimuli was coincident across all records. The resulting averages, therefore, represent activity evoked by the auditory stimuli plus any time-unlocked or 'staggered' activity associated with the onset or offset of one or more visual events that occurred during the 1.5 second epoch. The essential point to note is that corresponding averages in both sets of 'visual' and 'auditory' records are generated from identical data. They differ only in the onset of data saving and the duration of the epoch saved.

On non-signal trials, EEG data again were collected in two ways. Firstly, data saving was time-locked to the visual events of each trial. These epochs commenced 500mS prior to the onset of the fixation cross and continued for 3 seconds. The data were then averaged according to electrode placement and letter-match condition. A total of six averages was saved, each of which was derived from a maximum of 400 trials. These averages will be referred to as 'pure visual' averages as they represent time-locked visual activity recorded in the absence of auditory task stimuli.

Secondly, the same data were used to derive a series of 'staggered pure visual' averages. For these averages, data saving commenced at one of 25 sample intervals between 500 and 400mS prior to the onset of the fixation cross, and continued for 3 seconds. The onset of data saving was randomly determined over the 100mS interval, with the constraint that saving commenced at each time point an equal number of times. These data were averaged according to electrode placement and letter-match condition and a total of six averages was saved, each based on a maximum of 400 trials. These staggered pure visual averages, therefore, simulate the visual component of those averages recorded time-locked to auditory stimuli over signal trials.

EOG data saving always commenced 500mS prior to the onset of the fixation cross and continued for 3 seconds. EOG data were averaged and saved separately for each task condition, and a total of twenty-seven EOG averages was computed for each subject. Twenty-four of these averages represent EOG activity during dual-task signal trials, recorded separately for each letter-match condition and each signal condition. These averages are based on a total of up to 50 trials. Three averages were recorded over non-signal trials, one corresponding to each letter-match condition. Each of these latter averages is derived from a maximum of 400 trials.

2.7 Electrophysiological data conditioning

The analogue to digital conversion of EEG and EOG activity yielded digitised values within the range of 1 to 4096 computer units, with zero voltage represented by the value of 2048. To allow meaningful quantification and comparison of EEG and EOG averages, two transformations were applied to all records.

The first transformation involved subtracting the mean prestimulus activity, recorded over the initial 500mS period, from every value in the record. For EEG averages, the mean prestimulus level was calculated from the first 125 samples of each record; for EOG averages this value was derived from the first 25 samples. The transformation removed any offset from a digital value of zero due to small biases in the EEG and EOG amplification systems, provided an isoelectric baseline against which ERP amplitudes and eyemovements could be measured, and adjusted averages to an overall mean approaching zero (Buchsbaum and Coppola, 1974, p.233).

The second transformation scaled EEG and EOG averages according to the gain of the amplification system, and converted the digitised values to microvolt equivalents. This was achieved by multiplying each value in a record by an appropriate scaling factor determined during the calibration procedure conducted at the start of every recording session (see Section 2.5.4). For every subject, averages recorded over each of the three experimental sessions were saved separately, and the above transformations were applied using the respective calibration factors obtained at the start of the session. The three sets of records were then averaged together to provide 'overall' averages for each subject.

Following the data conditioning described above, all electrophysiological data were transferred to a Univac 1100/82 at the Australian National University, Canberra, for hard copy data plotting and further analysis.

2.8 Electrophysiological data plotting

Plot files were generated using a locally-written library of Fortran-callable plotting subroutines (the PLOTLIB package). These files were then copied onto magnetic tape and plotted on a Calcomp 960 electromechanical plotter interfaced with a Calcomp 925 controller. The polarity convention used in all plots is negative up. Upward deflection of EEG traces signifies negativity at the active electrodes with respect to the reference electrode, and upward deflection of EOG traces signifies negativity at the lower orbital lead with respect to the upper orbital lead (i.e. an upward eyemovement). Table 2.3 provides a key to all figures presented throughout this thesis which depict plots of average waveforms.

2.9 Preliminary results

The electrophysiological data to be presented represent group data, averaged across all subjects. The total number of trials contributing to these averages is given in Table 2.4. All averages recorded under a particular dual-task condition are based on an identical number of trials. For example, a total of five group averages was derived from data recorded under the non-signal, physical match condition of the dual-task. These are: the pure visual averages recorded from both the Cz and the Pz placements, the staggered pure visual averages recorded from both the Cz and Pz placements and the EOG average recorded time-locked to the visual events of the task. As indicated in Table 2.4, all of these averages are based on a total of 3619 trials.

Table 2.3. Key to Figures depicting average waveforms.

Cz : Central electrode placement	0 : No auditory signal
Pz : Parietal electrode placement	1-8 : Auditory signal conditions
EOG : Electro-oculogram	⊢⊣ : Auditory signal window
PM : Physical match condition	$\vdash\!\!\vdash_{+}$: Fixation cross onset window
RM : Rule match condition	$\vdash\!\!\vdash_{1}$: First letter onset window
MM : Mismatch condition	$\vdash\!\!\vdash_{2}$: Second letter onset window
	$\vdash\!\!\vdash_{2off}$: Second letter offset window

Table 2.4. Number of trials contributing to average waveforms.

		Letter match condition		
		Physical match	Rule match	Mis match
Signal condition	8	397	398	408
	7	416	425	444
	6	431	447	432
	5	406	413	412
	4	437	440	420
	3	458	432	445
	2	401	387	381
	1	399	403	409
	No signal	3619	3540	3487

Figure 2.4 depicts group averages recorded from Cz, Pz and EOG leads at each level of letter-match over non-signal trials. All averages are time-locked to the visual task stimuli. Each EEG average shows three distinct ERPs: the first associated with the onset of the fixation cross at zero seconds, the second associated with the onset of the first letter at 1 second, and the third associated with the onset of the second letter at 1.5 seconds. ERPs recorded from Cz and Pz placements show morphological differences; however, within each placement, the amplitudes and latencies of ERPs to the fixation cross and first letter are almost identical. Differences associated with the three conditions of the visual letter-matching task become apparent only following the onset of the second letter, when a large amplitude late positive wave (P_3) distinguishes the physical match condition from the rule match and mismatch conditions.

Averaged EOG activity, presented in the lower portion of Figure 2.4, indicates the occurrence of small vertical eyemovements, but no systematic effects which could differentially contaminate EEGs recorded over the three letter-match conditions are apparent.

Figure 2.5 shows the six staggered pure visual averages recorded over non-signal trials. The *mean* time of onset of the fixation cross is indicated at time zero seconds. It is clear from these traces that staggering over a 100mS interval fails to eliminate visual event-related activity. This finding is not surprising as the interval used is effective only in removing frequencies down to about 10Hz (Ruchkin, 1965; see also Section 1.3 of Chapter 1). The staggering procedure, therefore, produces the effect of a low pass filter which

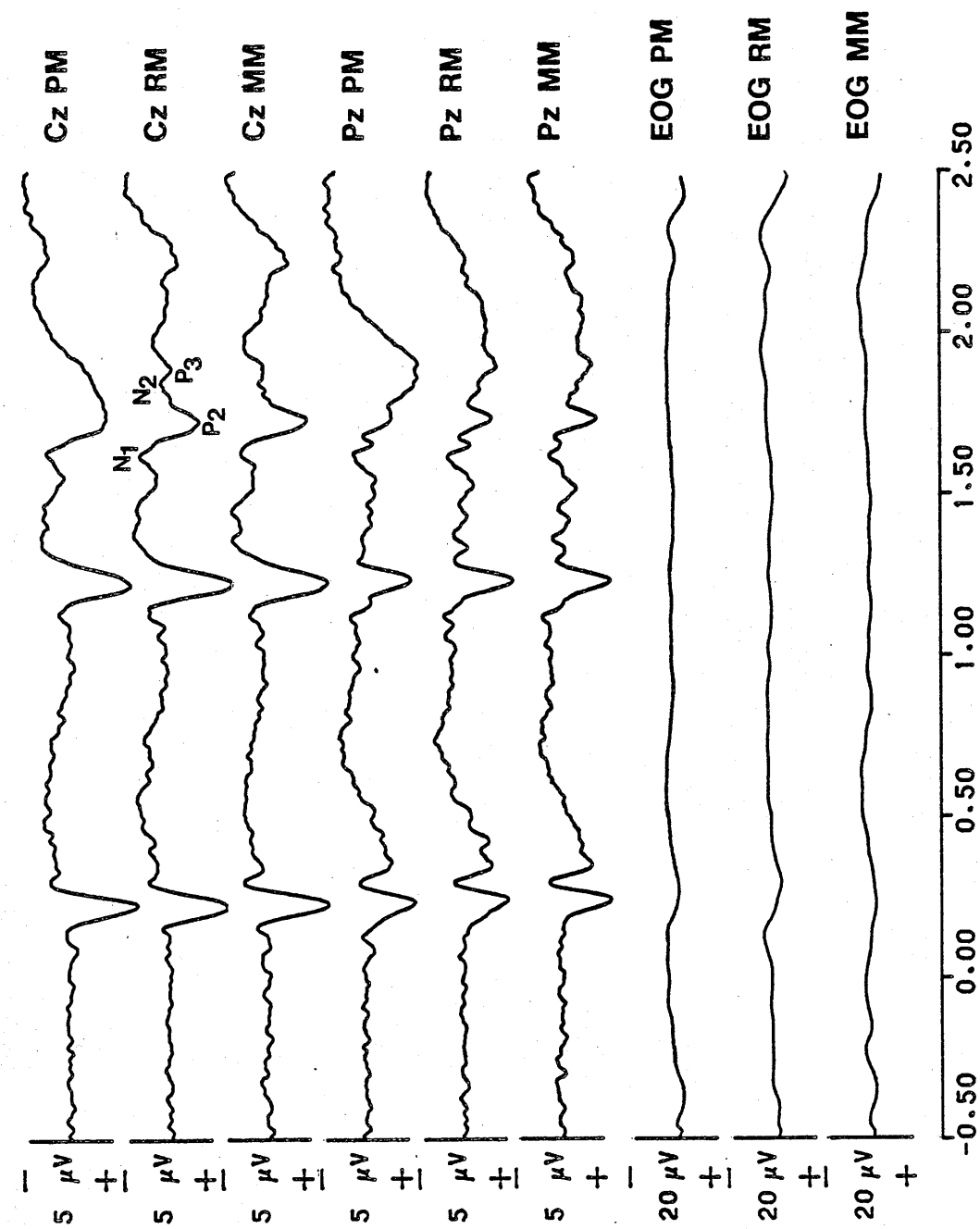

Figure 2.4. EEG and EOG averages recorded over non-signal trials.

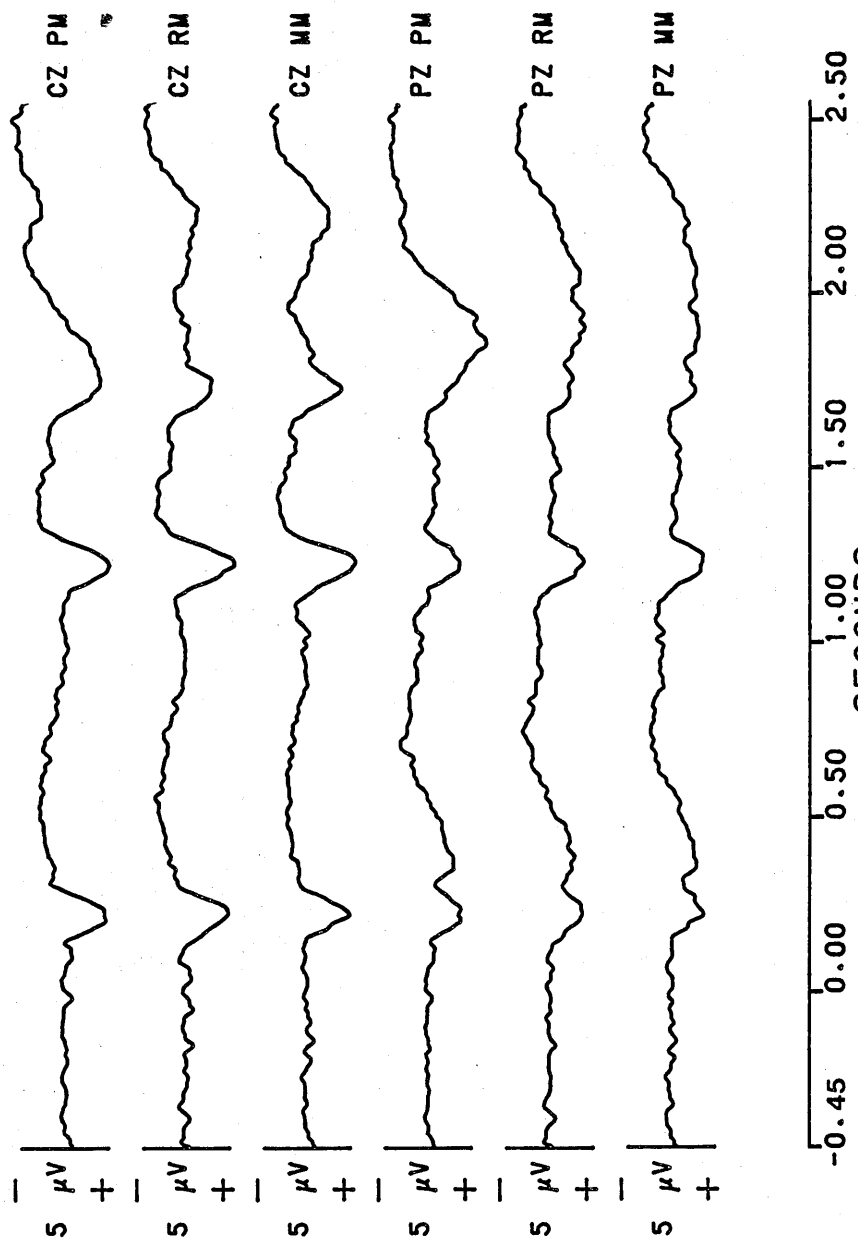

Figure 2.5. Staggered pure visual traces recorded over non-signal trials.

removes high frequency components, but fails to filter out low frequency activity which characterises the late components of the ERP. These staggered pure visual averages, however, can be used to assess the extent of the 'visual contamination' in those averages recorded time-locked to the auditory stimuli over signal trials (see Chapter 3).

Figures 2.6 to 2.20 show group averages recorded over dual-task signal trials. These figures are presented in three sets, each set corresponding to data collected over one of the three levels of visual letter-match. The following description refers to those data recorded during physical match trials, presented in Figures 2.6 to 2.10. This description is equally applicable to those data recorded during the rule match condition of the visual task (Figures 2.11 to 2.15) and the mismatch condition of the visual task (Figures 2.16 to 2.20).

Figure 2.6 shows group averages recorded from the Cz lead during physical match trials, and time-locked to visual task stimuli. The eight averages correspond to those data recorded under each of the eight signal conditions, with the bar under each trace indicating the signal window for that condition. ERPs associated with the three events of the visual task can be identified in these traces. However, a biphasic waveform, displaying varying degrees of overlap with visual ERPs also is evident in each trace. Each average, therefore, consists of time-locked visual event-related activity plus the partially time-unlocked auditory event-related activity, starting some time after the onset of the first visual event. Figure 2.7 shows the same data recorded time-locked to the onset of auditory stimuli, which occur at

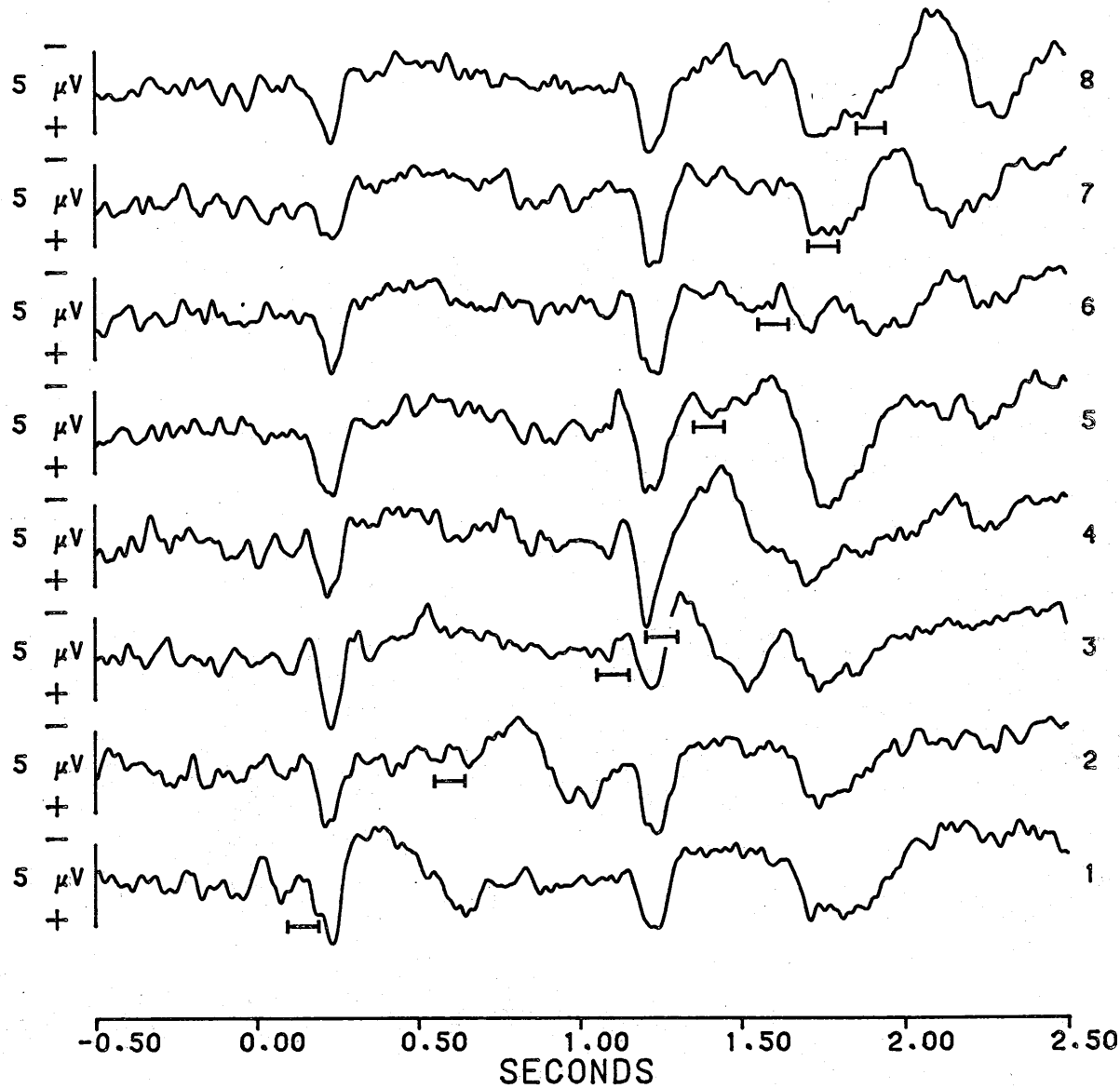

Figure 2.6. Time-locked visual averages recorded from the Cz lead under the physical match condition of dual-task signal trials.

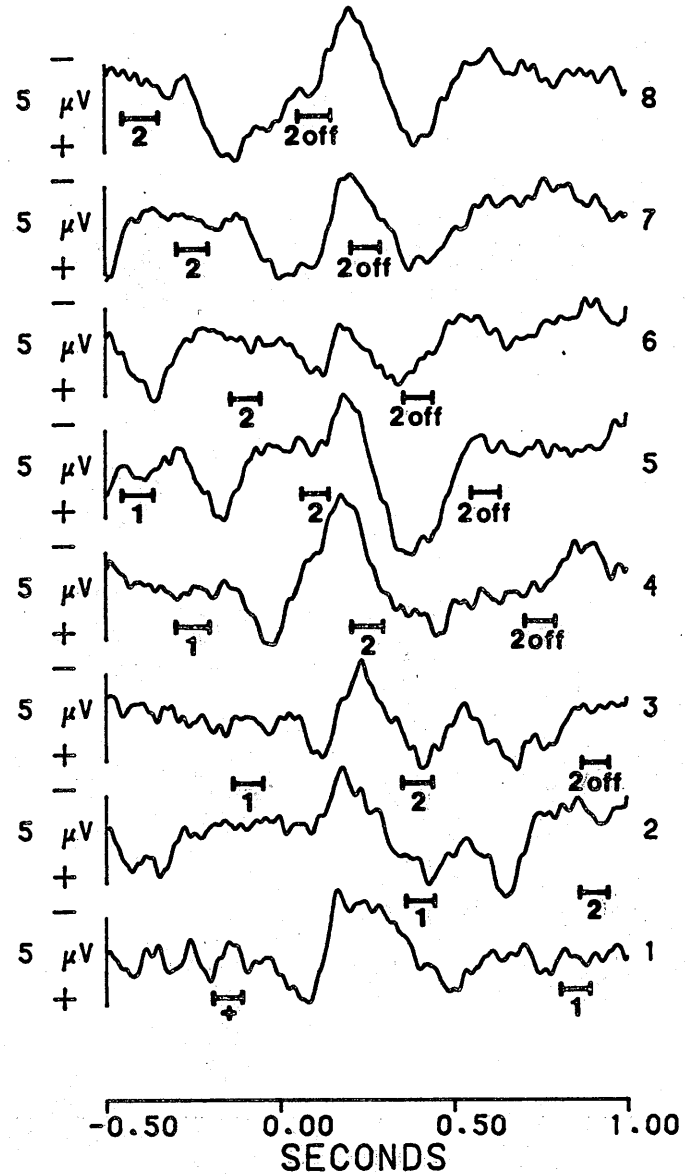

Figure 2.7. Time-locked auditory averages recorded from the Cz lead under the physical match condition of dual-task signal trials.

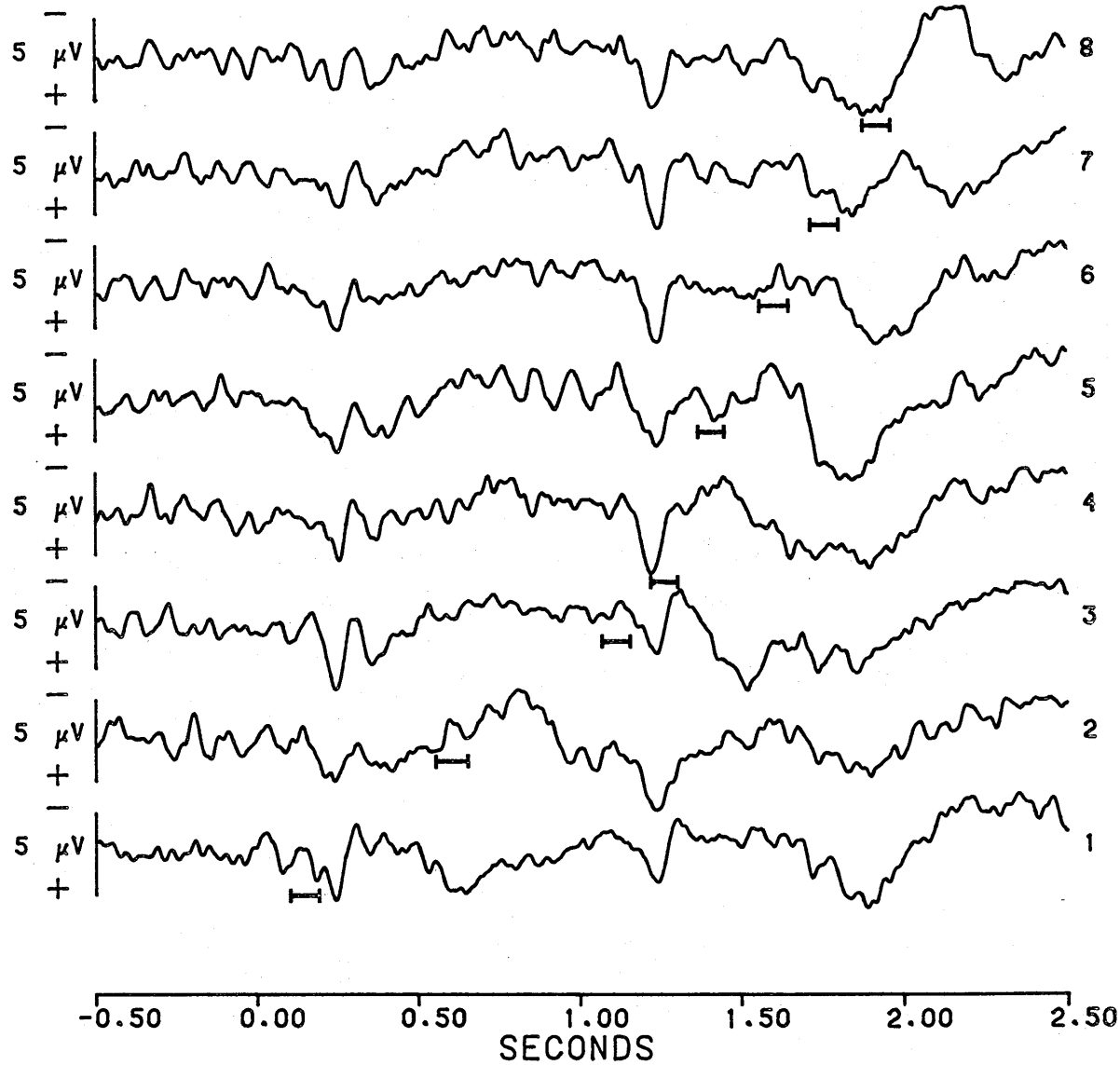

Figure 2.8. Time-locked visual averages recorded from the Pz lead under the physical match condition of dual-task signal trials.

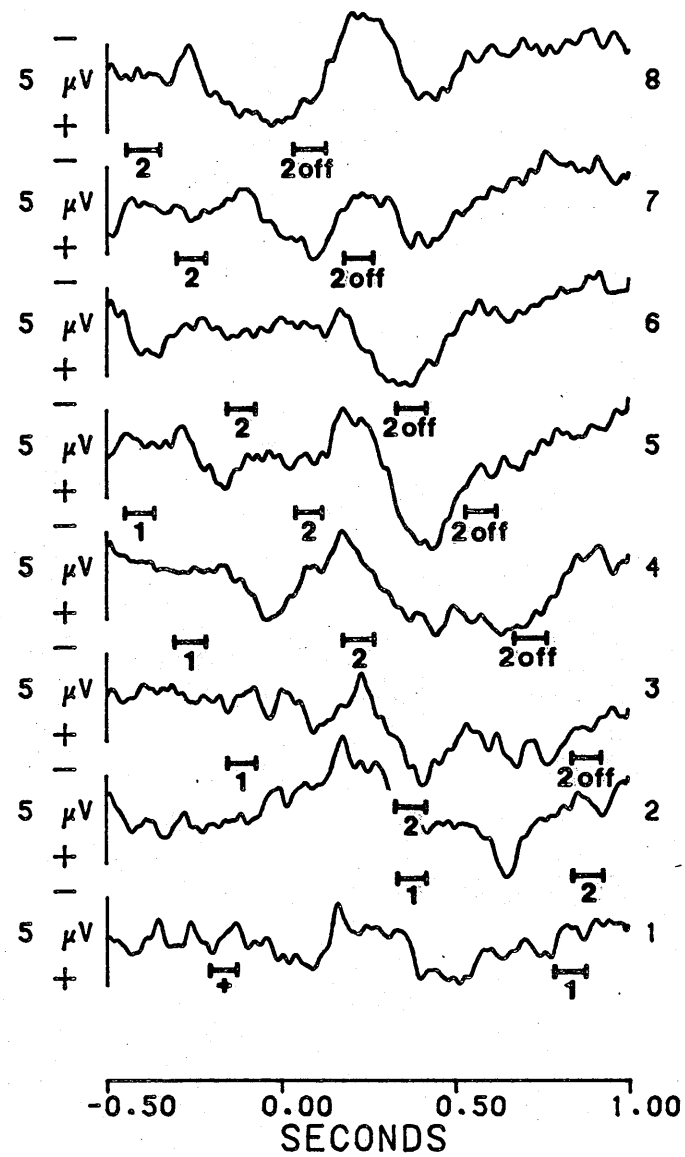

Figure 2.9. Time-locked auditory averages recorded from the Pz lead under The physical match condition of dual-task signal trials.

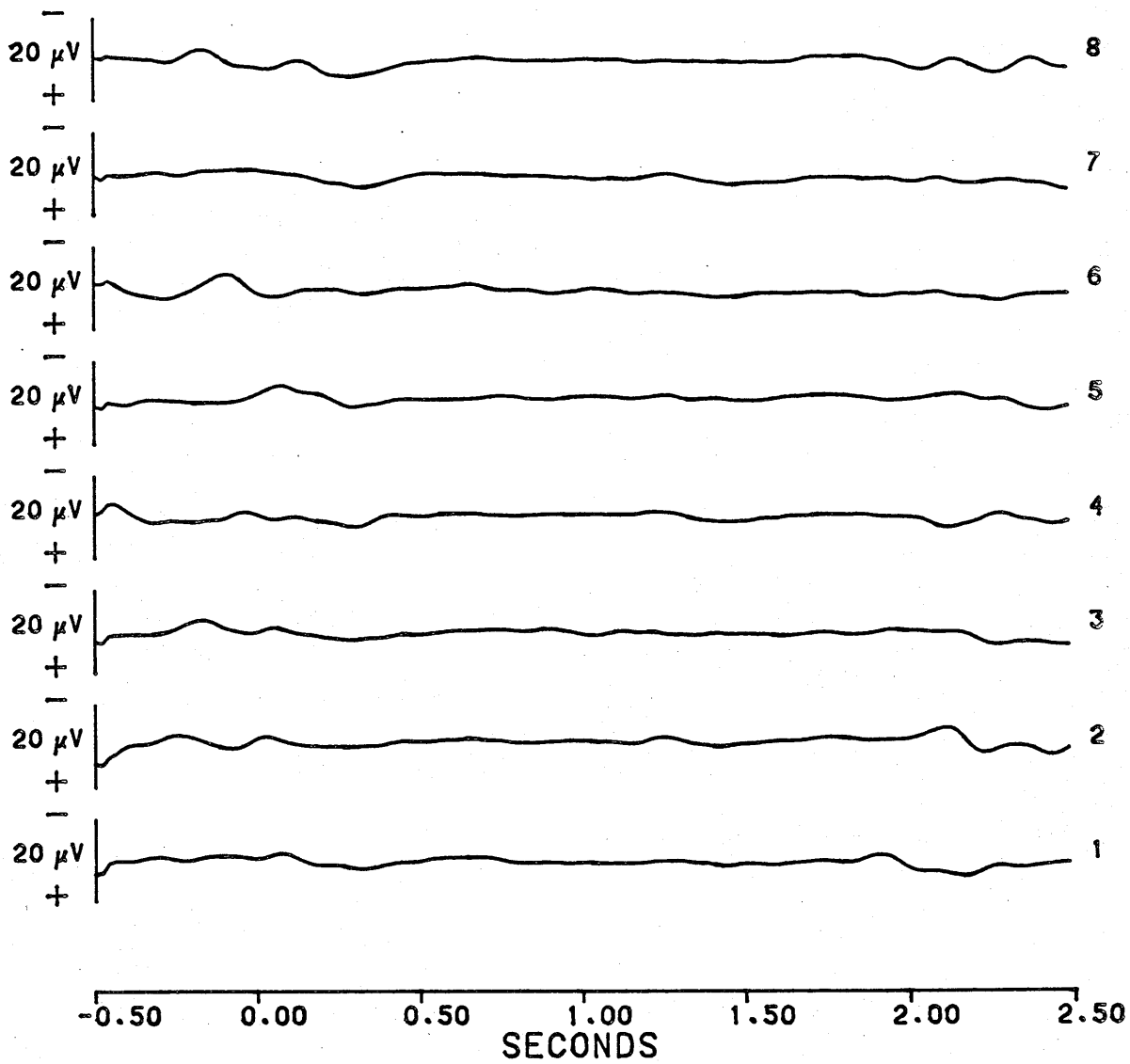

Figure 2.10. EOG averages recorded under the physical match condition of dual-task signal trials.

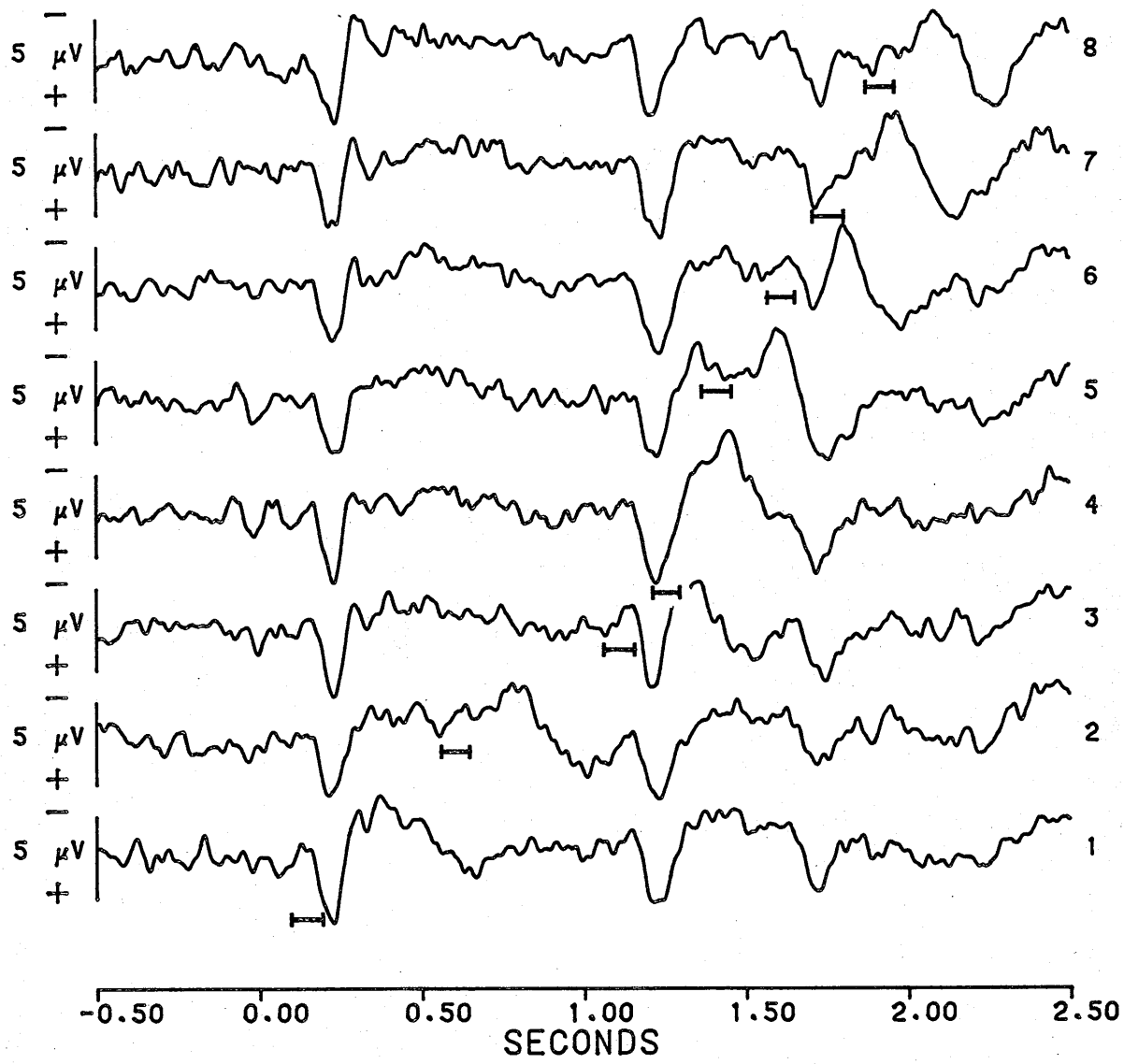

Figure 2.11. Time-locked visual averages recorded from the Cz lead under the rule match condition of dual-task signal trials.

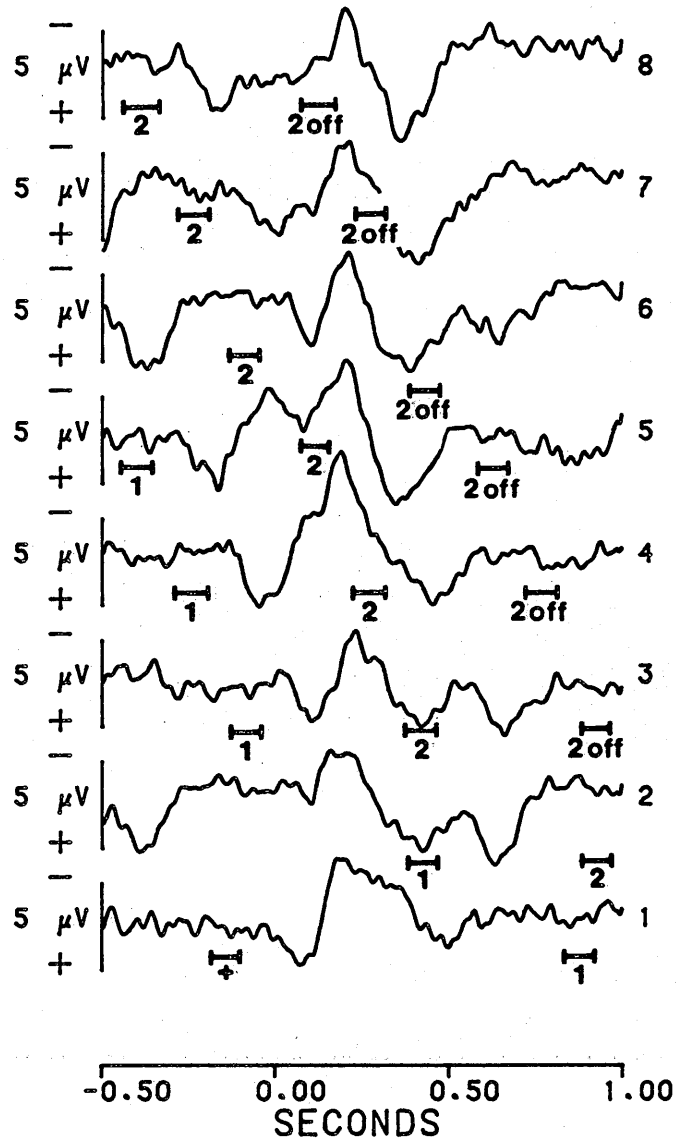

Figure 2.12. Time-locked auditory averages recorded from the Cz lead under the rule match condition of dual-task signal trials.

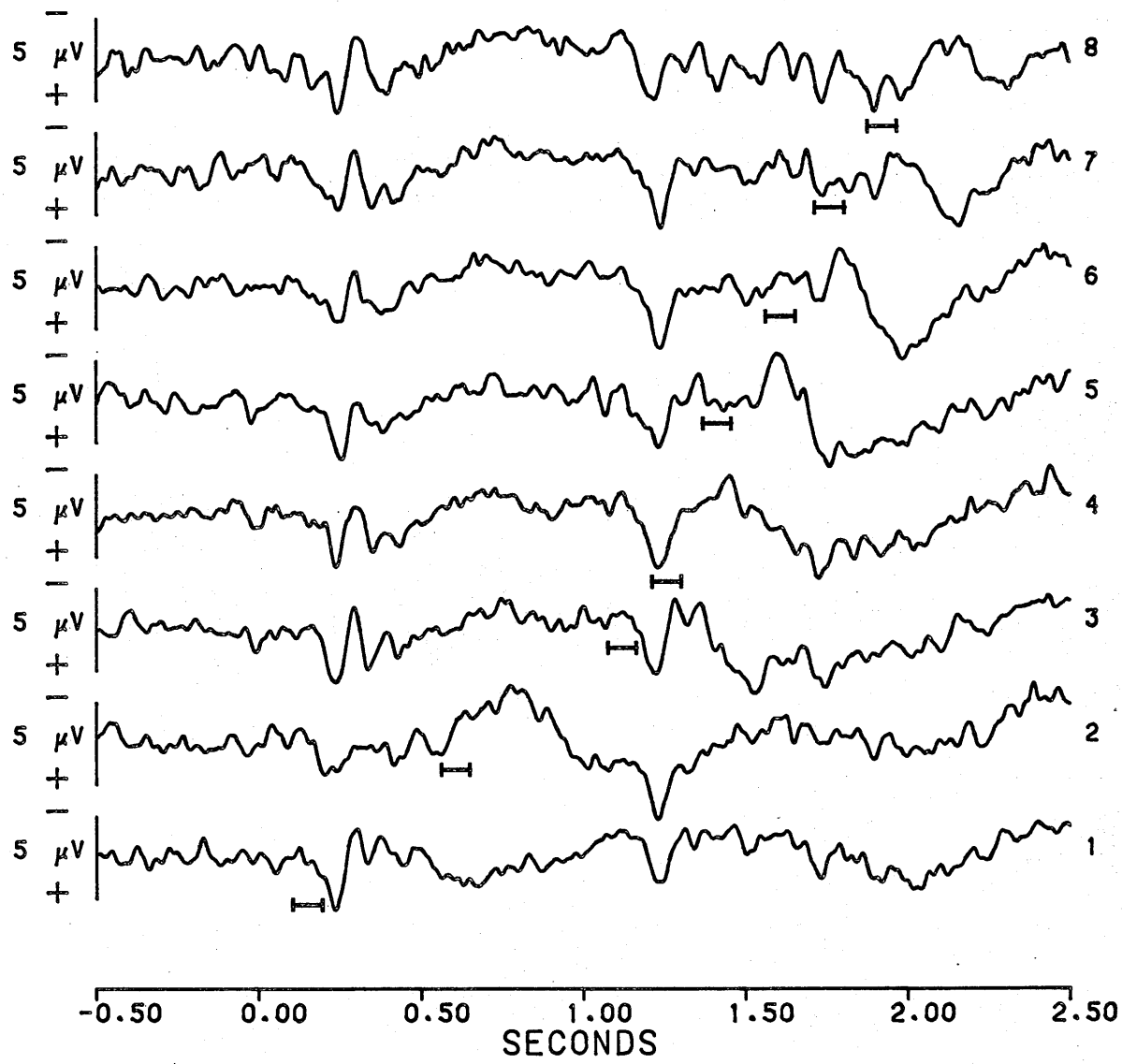

Figure 2.13. Time-locked visual averages recorded from the Pz lead under the rule match condition of dual-task signal trials.

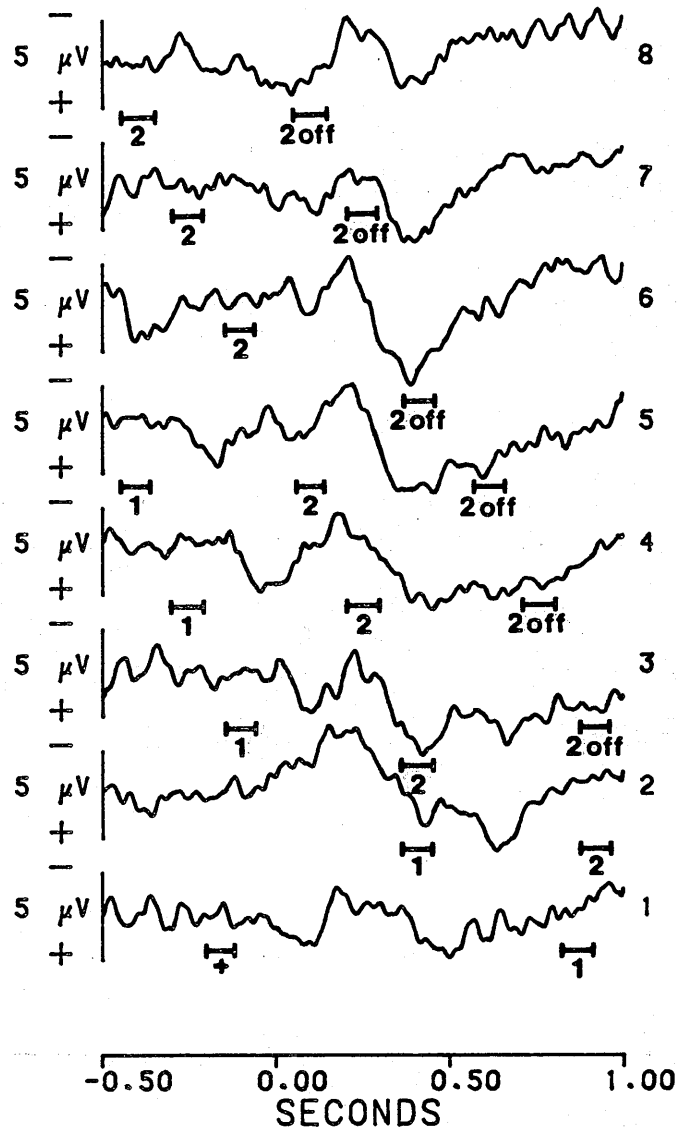

Figure 2.14. Time-locked auditory averages recorded from the Pz lead under the rule match condition of dual-task signal trials.

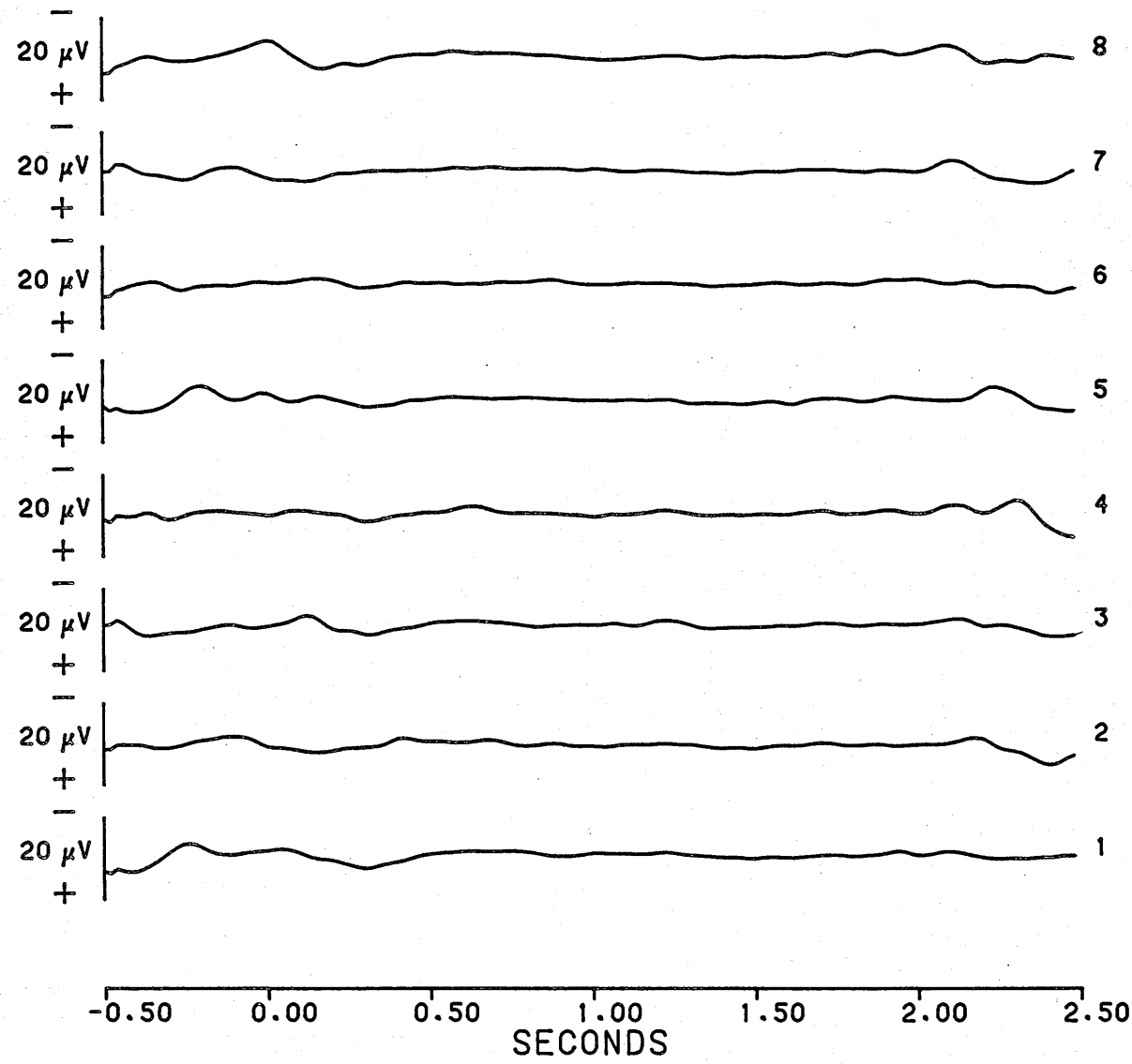

Figure 2.15. EOG averages recorded under the rule match condition of dual-task signal trials.

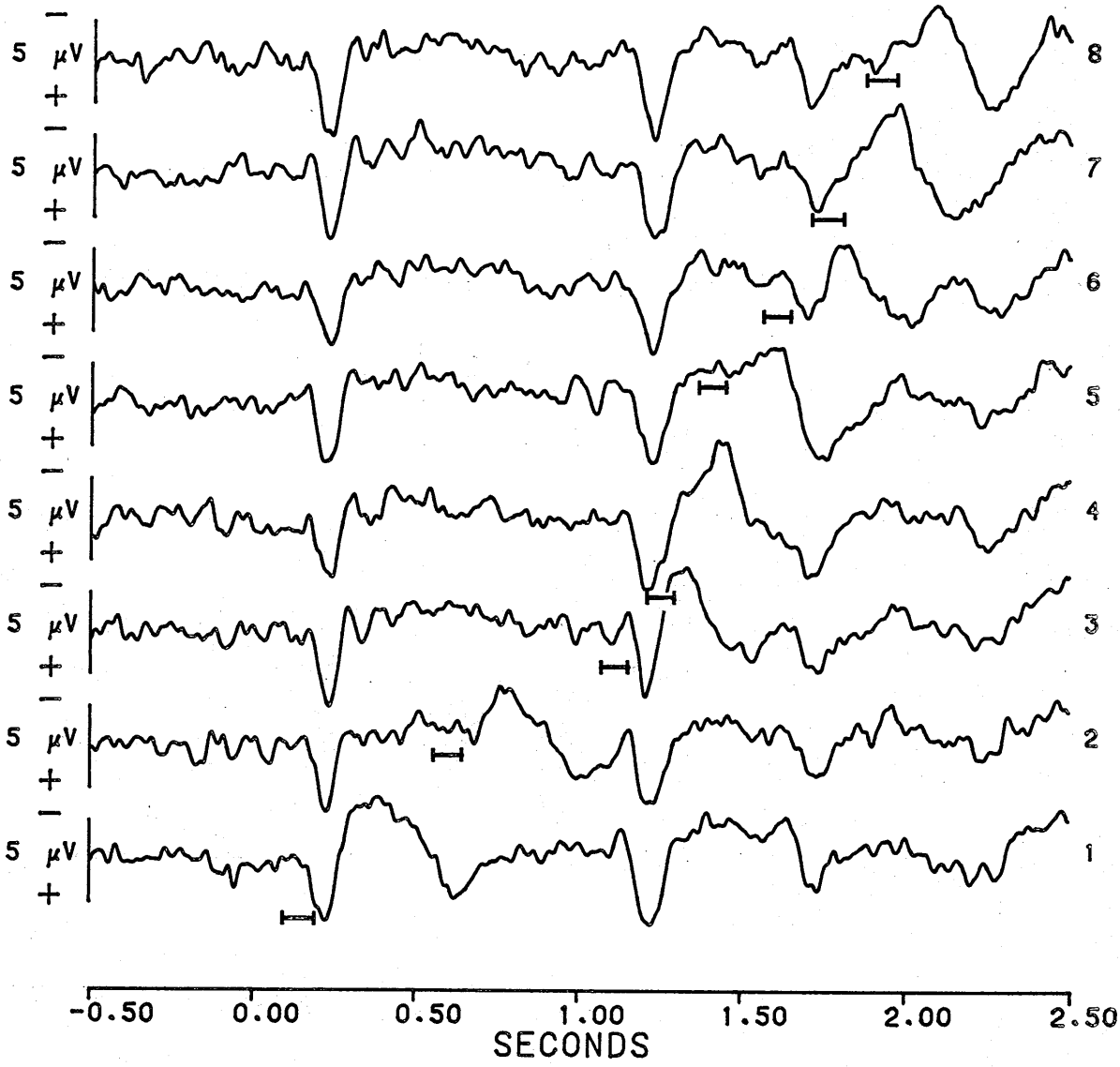

Figure 2.16. Time-locked visual averages recorded from the Cz lead under the mismatch condition of dual-task signal trials.

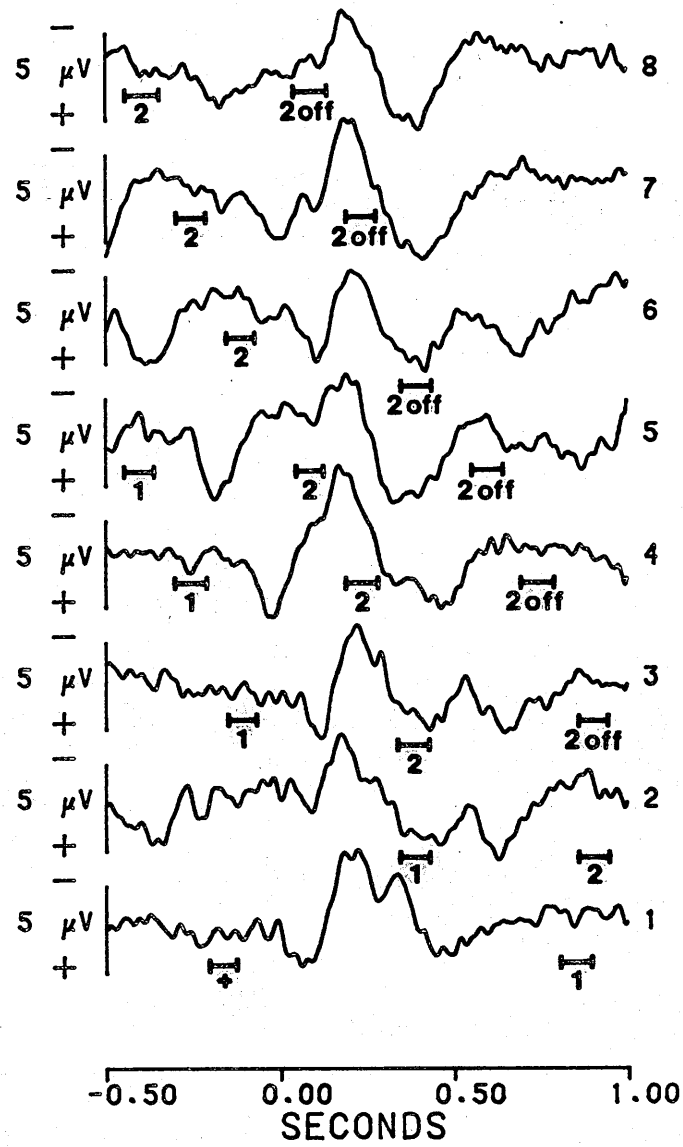

Figure 2.17. Time-locked auditory averages recorded from the Cz lead under the mismatch condition of dual-task signal trials.

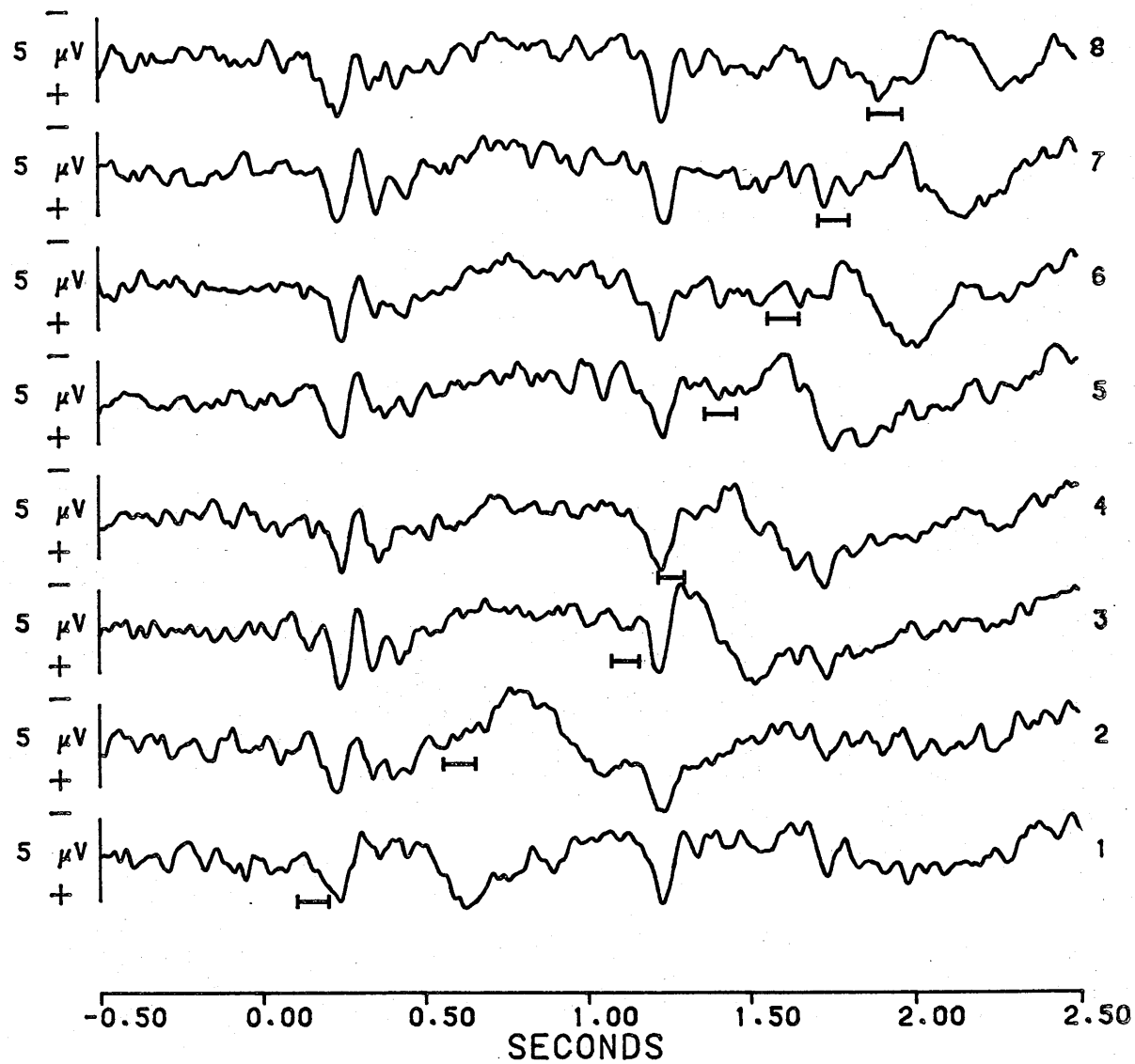

Figure 2.18. Time-locked visual averages recorded from the Pz lead under the mismatch condition of dual-task signal trials.

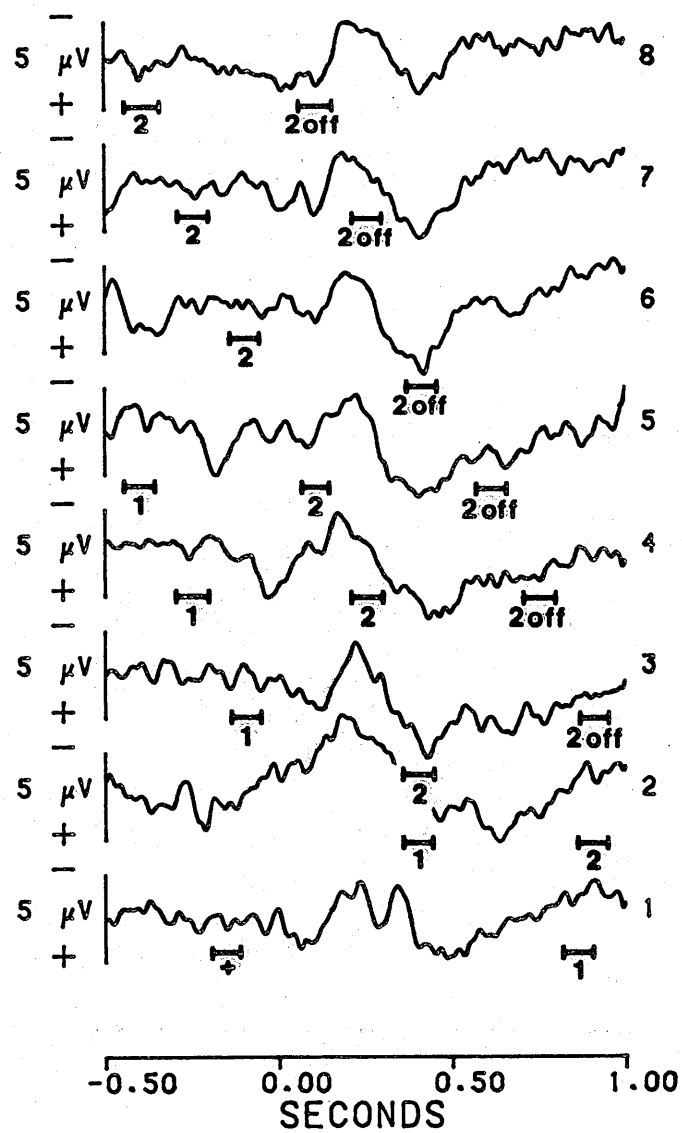

Figure 2.19. Time-locked auditory averages recorded from the Pz lead under the mismatch condition of dual-task signal trials.

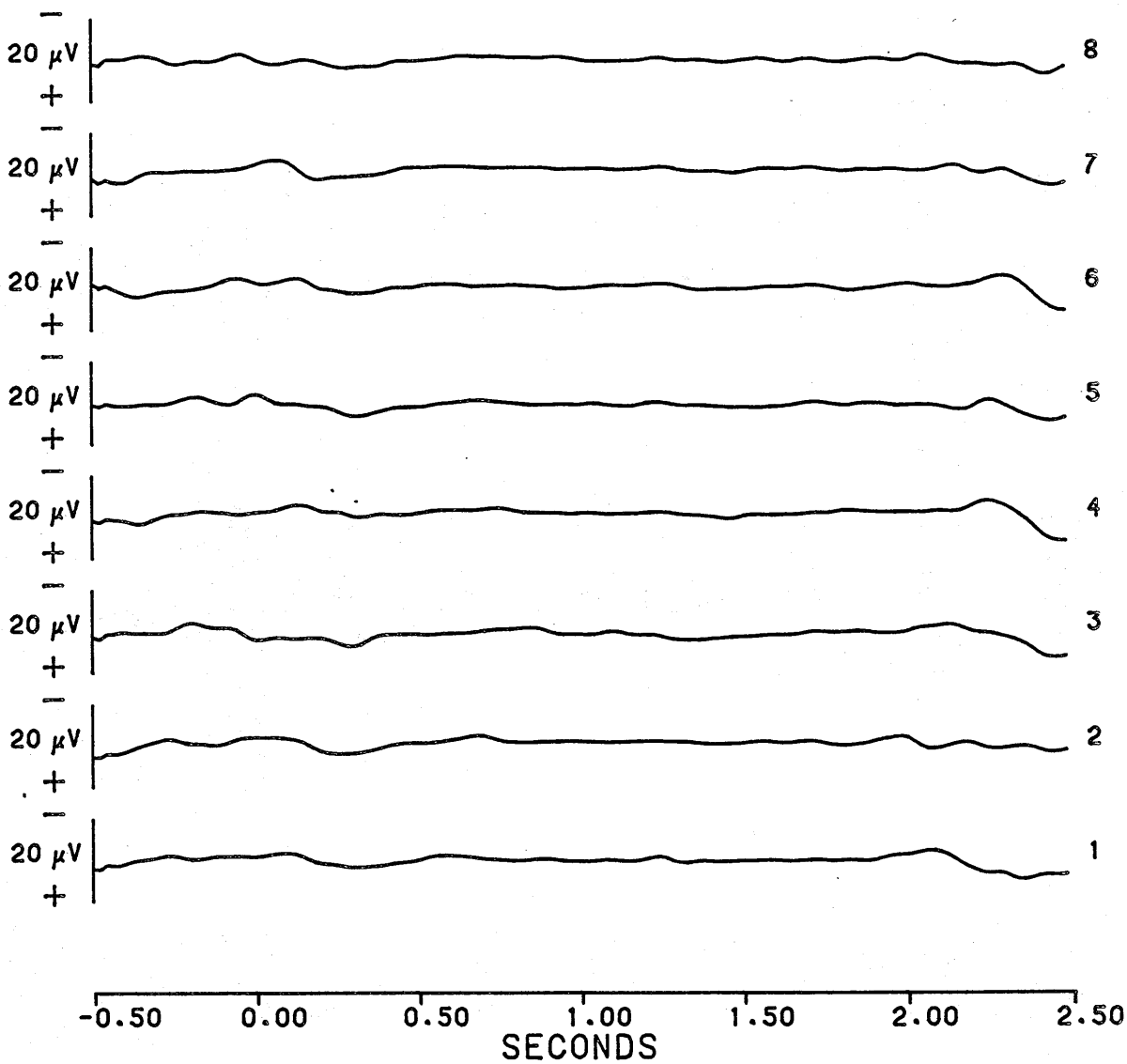

Figure 2.20. EOG averages recorded under the mismatch condition of dual-task signal trials.

zero seconds. The bars under each trace indicate the 100mS windows during which the onset or offset of visual task stimuli occur within the 1.5 second epochs. Unwanted activity similarly is evident in these traces, this time associated with the visual events of the task.

Equivalent data, recorded from the Pz lead are shown in Figures 2.8 and 2.9. The amplitude of auditory ERPs is somewhat reduced in these traces, which is consistent with studies of scalp distribution which show the auditory ERP to be maximal at the Cz placement (e.g. Picton, Hillyard, Krausz and Galambos, 1974; Snyder, Hillyard and Galambos, 1980).

Figure 2.10 shows EOG activity recorded during the eight signal conditions over physical match trials and time-locked to the visual events of the task. All traces are similar in form and show no evidence of eyemovements which might differentially contaminate EEG averages recorded under different experimental conditions.

2.10 Discussion

The dual-task experiment provides an example of a paradigm which involves the close temporal presentation of visual and auditory stimuli with the consequence that, under most experimental conditions, ERPs elicited by stimuli in one modality overlap components of ERPs elicited by stimuli in the other modality.

The first step towards separating out these overlapping waveforms was to stagger the presentation of auditory stimuli with respect to visual stimuli over a window of 100mS, at intervals of 4mS. This staggering procedure allowed two averages to be generated from the same data, each average consisting of a wanted, time-locked response plus an unwanted, partially time-unlocked response.

The two averages may be represented thus:-

$$R_v = V + f(A) \qquad \{2.1\}$$

$$R_a = A + f(V) \qquad \{2.2\}$$

where: R_v is the average recorded time-locked to the visual stimuli,

R_a is the average recorded time-locked to the auditory stimuli,

V is the idealised visual response,

A is the idealised auditory response and

f is the function applied through the staggering procedure.

The method of stimulus presentation and data collection allows the unwanted responses, represented by $f(A)$ and $f(V)$ in the above equations, to be defined precisely. Each takes the form of the idealised response, A or V, after it has been passed through a 'running' or 'moving' average digital filter.

If we assume that the idealised visual response and the idealised auditory response remain invariant over successive trials of a particular dual-task condition, then in general each element of the output vector containing $f(A)$ and $f(V)$ can be defined numerically as follows:

$$f(A) = y_{(i)} = \frac{1}{N} \sum_{n=0}^{N-1=24} A_{(i+n)} \qquad \{2.3\}$$

$$f(V) = y_{(i)} = \frac{1}{N} \sum_{n=0}^{N-1=24} V_{(i+n)} \qquad \{2.4\}$$

where y is the output vector containing the function of A or V and

N is the number of samples over which staggering takes place, in this case $N = 25$.

Each element of the output vector, y, therefore contains the average of twenty-five elements of the 'idealised' auditory or visual input vector. The first element of the input vector contributing to successive average values advances through the time series at intervals of one sample, and so the average progressively 'moves' through the idealised response.

More formally the action of such a filter can be specified as follows (Otnes and Enochson, 1972, p.68):

$$y_{(i)} = \frac{1}{N} \sum_{n=0}^{N-1} g_{(n)} \cdot x_{(i+n)} \qquad \{2.5\}$$

where: x is the input time series,

g is the impulse response of the filter,

N is the length of the filter series and

y is the output vector.

The filter consists of a set of fixed weights, $g_{(n)}$, and the process of filtering consists of determining the sum of products from the set of filter weights and the input vector. Such a process, termed 'convolution', consists essentially of correlating one time series with another. In the present case the filter weights are set to unity and hence $g_{(n)}$ has been omitted from the numerical representations given in equations {2.3} and {2.4}.

The problem in the further analysis of these data is to remove the running average of activity associated with stimuli in one modality from averages recorded time-locked to stimuli in the other modality.

The following chapter explores the ways in which elementary subtraction techniques can be applied to this problem.

CHAPTER 3: ELEMENTARY SUBTRACTION PROCEDURES

3.1 Introduction

Elementary subtraction procedures provide one solution to the problem of separating out time-locked and partially time-unlocked ERPs recorded over signal trials of the dual-task experiment. The use of these procedures rests on two major assumptions.

The first assumption is that of electrical additivity of the time-locked and time-unlocked waveforms recorded over signal trials. That is, the output of the visual and auditory ERP generators is assumed to sum linearly at the site of the recording electrode (cf. equations {2.1} and {2.2}). If this assumption is valid, and estimates of $f(A)$ and $f(V)$ are available, then these unwanted responses can be removed from time-locked visual and auditory traces by means of simple subtraction:

$$V = R_v - f(A) \qquad \{3.1\}$$

$$A = R_a - f(V) \qquad \{3.2\}$$

Such an estimate of $f(V)$ is available if we consider that the distortion due to $f(V)$ is simulated by the staggered pure visual traces generated from data collected over non-signal trials (Section 2.6.2; Figure 2.5). The second assumption, therefore, is that for each level of visual letter-match the visual ERPs recorded under dual-task conditions (signal trials) are identical to visual ERPs recorded under single task conditions (non-signal trials). This assumption is tenable to the extent that secondary task methodology, as described in Section 1.4 of Chapter 1, is designed to assess the allocation of processing capacity across tasks by monitoring the pattern of secondary task interference when primary task performance is maintained at some predetermined level of speed or accuracy. As the visual letter-matching task was presented to subjects as

the primary task (Section 2.4.4 of Chapter 2), it can be argued that any 'costs' associated with the introduction of the secondary task will be borne by that task, and that manipulations of cognitive load will be reflected by ERPs evoked by secondary task auditory stimuli rather than primary task visual stimuli. If we accept this proposition then $f(V)$ can be removed from time-locked auditory traces by subtracting appropriate sections of the staggered pure visual traces. The residuals of these subtractions will be the idealised auditory responses.

The assumption of visual response invariance over signal and non-signal conditions renders the estimation of idealised visual responses from time-locked visual traces somewhat redundant. However, these estimations will provide a check on visual response invariance. Although $f(A)$ was not independently measured during the dual-task experiment, the resultant auditory traces from equation {3.2} may be used to calculate a running average of the auditory response. This average can then be subtracted from appropriate sections of those traces recorded time-locked to the visual events of the task over signal trials.

The following section illustrates the application of these elementary subtraction procedures. The assumptions and problems associated with the use of this technique are explored further in this section and in Section 3.3.

3.2 Application of elementary subtraction procedures to dual-task data

The elementary subtraction technique is illustrated using those averages recorded from the Cz placement over physical match trials.

The first stage in the procedure was to estimate the idealised auditory responses. This required that sections of the appropriate staggered pure visual trace were subtracted from traces recorded time-locked to the onset of auditory stimuli. For purposes of illustration, Figure 2.7 is duplicated as Figure 3.1, and shows traces time-locked to the onset of auditory stimuli under the eight signal conditions. The running average of visual activity can be identified in these traces as occurring before, during and/or following activity associated with the auditory stimuli. Sections of the appropriate staggered pure visual average (CzPM) shown in Figure 2.5 are presented in Figure 3.2, with each section corresponding to a particular signal condition. These sections were taken from the staggered pure visual trace following an interval equal to the minimum time period between the onset of the fixation cross and the presentation of auditory stimuli in that particular signal condition. These minimum times were: 100, 548, 1048, 1200, 1348, 1548, 1700 and 1848mS respectively (see Chapter 2, Section 2.4.3). Those sections of trace corresponding to signal conditions 1 to 5 are all of 1.5 seconds duration (375 samples). Those sections corresponding to signal conditions 6, 7 and 8 are of 1.45, 1.3 and 1.15 seconds respectively, being limited by the time period over which staggered pure visual averages were saved.

The running average of visual activity was removed from time-locked auditory traces by subtracting corresponding time points of the staggered pure visual trace. The results of these subtractions are presented in Figure 3.3.

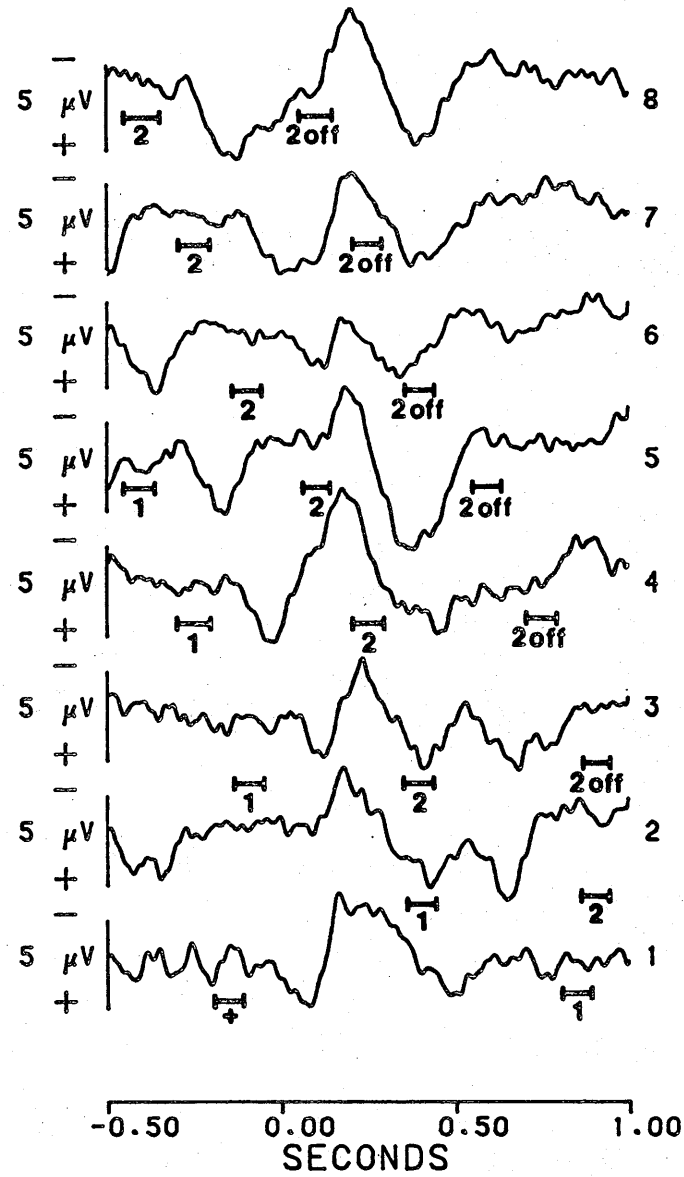

Figure 3.1. Time-locked auditory averages recorded from the Cz lead under the physical match condition of dual-task signal trials.

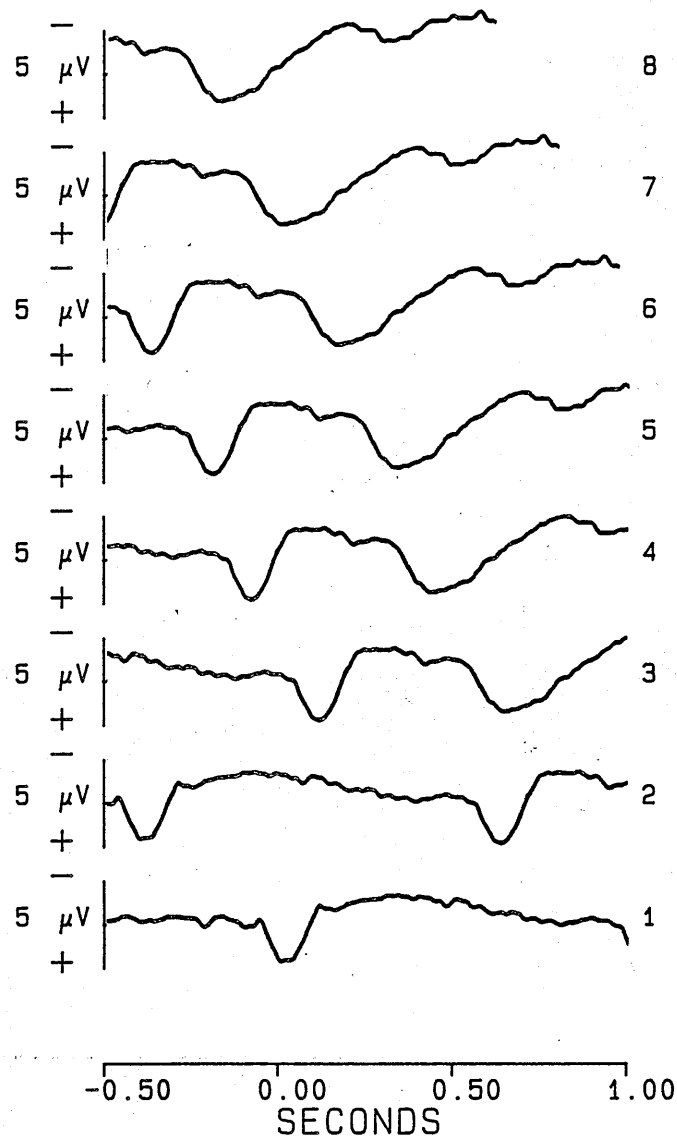

Figure 3.2. Sections of staggered pure visual trace (CzPM) simulating 'visual distortion' in time-locked auditory averages.

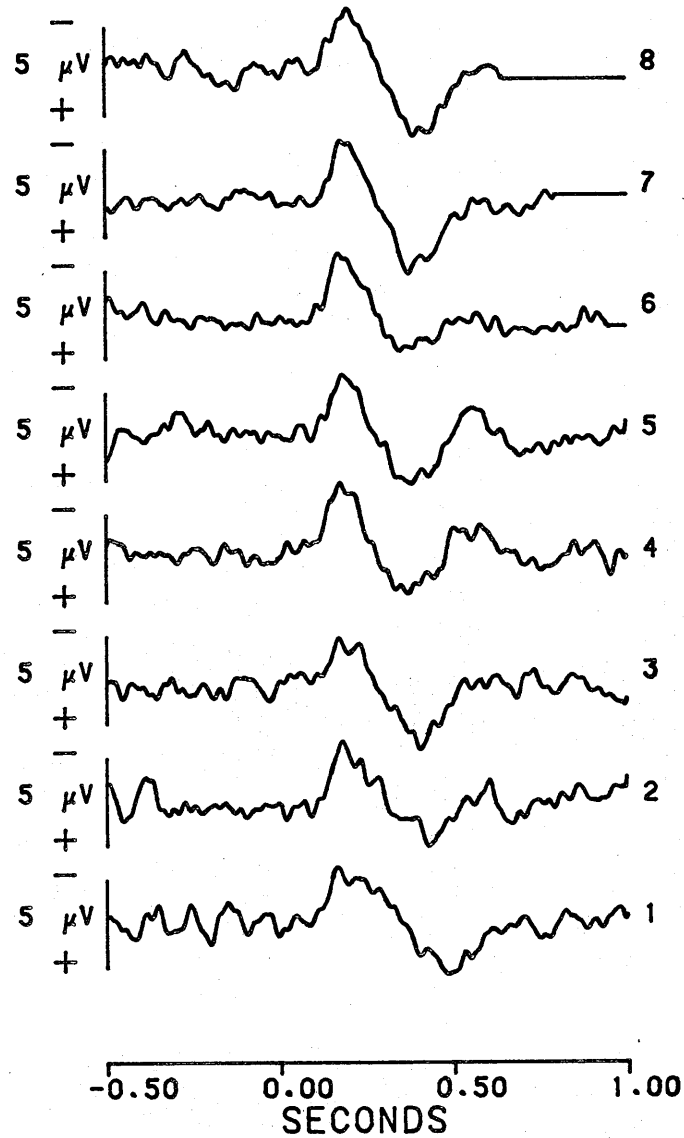

Figure 3.3. Time-locked auditory averages (CzPM) following subtraction of visual distortion.

A comparison of Figure 3.3 with Figure 3.1 indicates that the subtraction procedure has successfully removed the visual distortion from time-locked auditory traces. The effect is particularly striking for signal condition 6 where the second letter onset preceded the auditory stimuli by 48 - 148mS. Removal of the visual distortion has resulted in a significant increase in the amplitude of the auditory ERP.

The second stage in the procedure was to estimate the idealised visual response by subtracting the acoustic running average from time-locked visual traces recorded over signal trials. Figure 3.4 replicates Figure 2.6 and shows those time-locked visual traces recorded from the Cz placement during physical match trials. The running sum of each 'idealised' auditory response shown in Figure 3.3 was calculated by summing the value at each time point with the values at the following 24 time points, according to the algorithm given below (see also equation {2.3}):

$$f(A) = y_{(i)} = \sum_{n=0}^{N-1=24} A_{(i+n)} \qquad i = 1,399 \qquad \{3.3\}$$

Note that the output vector y is larger than the input vector A, and to allow an estimation of the first and last 24 values of the running sum, the vector A was padded out with nulls. Special treatment of these values was required to produce correct averages. Equations {3.4} to {3.6} specify the algorithms used to ensure appropriate normalisation.

$$f(A) = y_{(i)} = \frac{1}{i} \sum_{n=0}^{24} A_{(i+n)} \qquad i = 1,24 \qquad \{3.4\}$$

$$f(A) = y_{(i)} = \frac{1}{25} \sum_{n=0}^{24} A_{(i+n)} \qquad i = 25,375 \qquad \{3.5\}$$

$$f(A) = y_{(i)} = \frac{1}{400-i} \sum_{n=0}^{24} A_{(i+n)} \quad \text{for } i = 376,399 \qquad \{3.6\}$$

Note, however, that accuracy at the tails of the output vector is not essential to the technique and vectors may be truncated to ensure the validity of the data.

The first 125 samples of the calculated running averages were discarded, as they represented activity over the 500mS period prior to the onset of the auditory stimuli. The remaining samples were padded out with nulls within a 3 second epoch to provide temporal correspondence with auditory activity contributing to time-locked visual traces (see Figure 3.5). The point by point subtraction of the running average of auditory activity from time-locked visual traces resulted in the 'idealised' visual waveforms shown in Figure 3.6, numbered 1-8. The lower trace in this figure represents activity recorded time-locked to visual stimuli over non-signal physical match trials and has been included for purposes of comparison. Visual inspection of these traces indicates that the subtraction procedure has successfully removed the auditory distortion from time-locked visual traces. Furthermore, the resultant traces all closely resemble the pure visual trace recorded over non-signal trials.

The above procedures were applied also to those data recorded from the Pz lead during physical match trials, and the resultant 'idealised' averages are shown in Figures 3.7 and 3.8. Figures 3.9 to 3.12 show the 'idealised' auditory and visual averages similarly derived from traces recorded from Cz and Pz placements over rule match trials, and Figures 3.13 to 3.16 show equivalent data for mismatch trials. Overlay 1 shows the 100mS windows over which the onset and offset of visual task stimuli occurred within each 1.5 second epoch of the auditory traces,

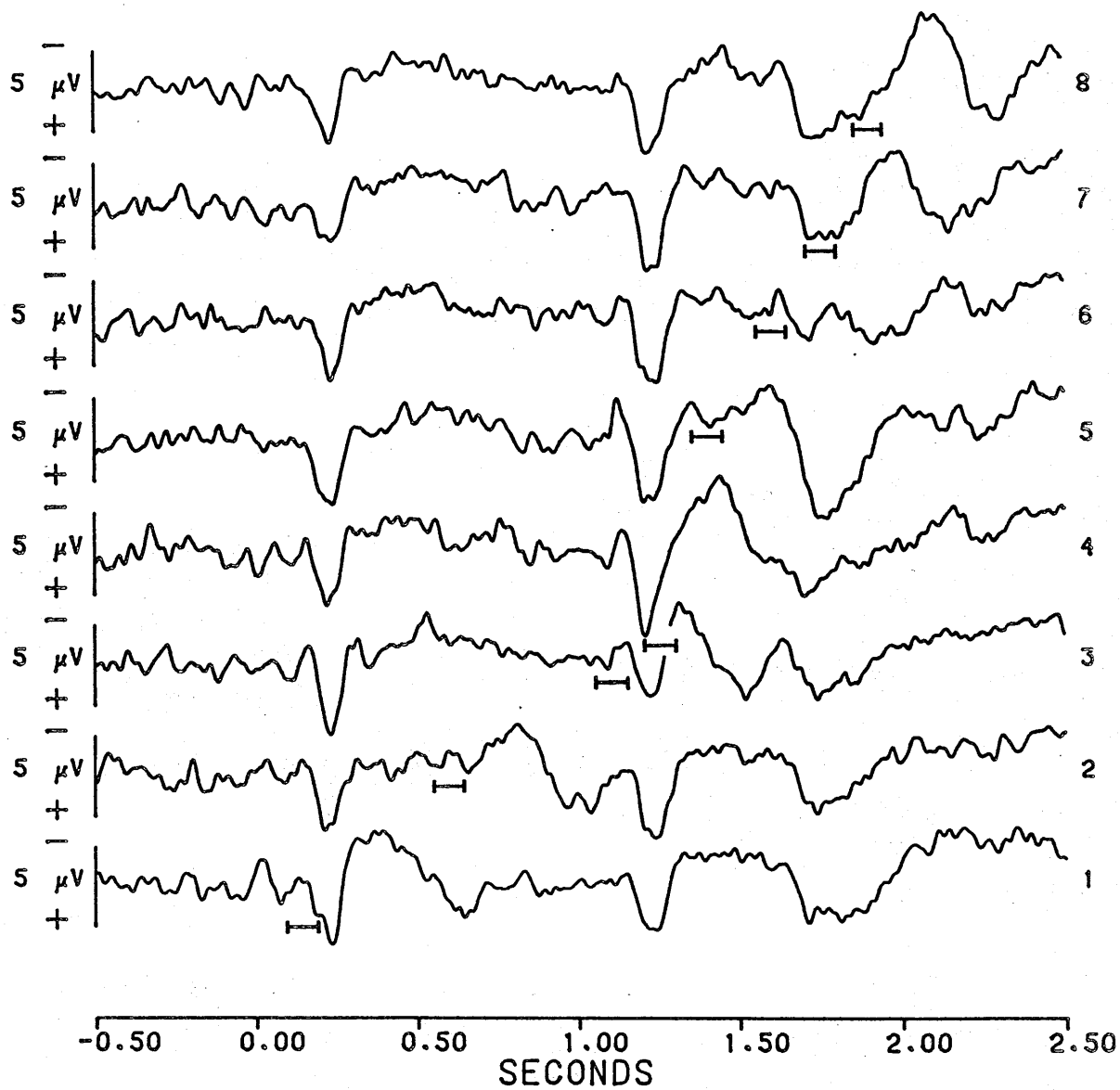

Figure 3.4. Time-locked visual averages recorded from the Cz lead under the physical match condition of dual-task signal trials.

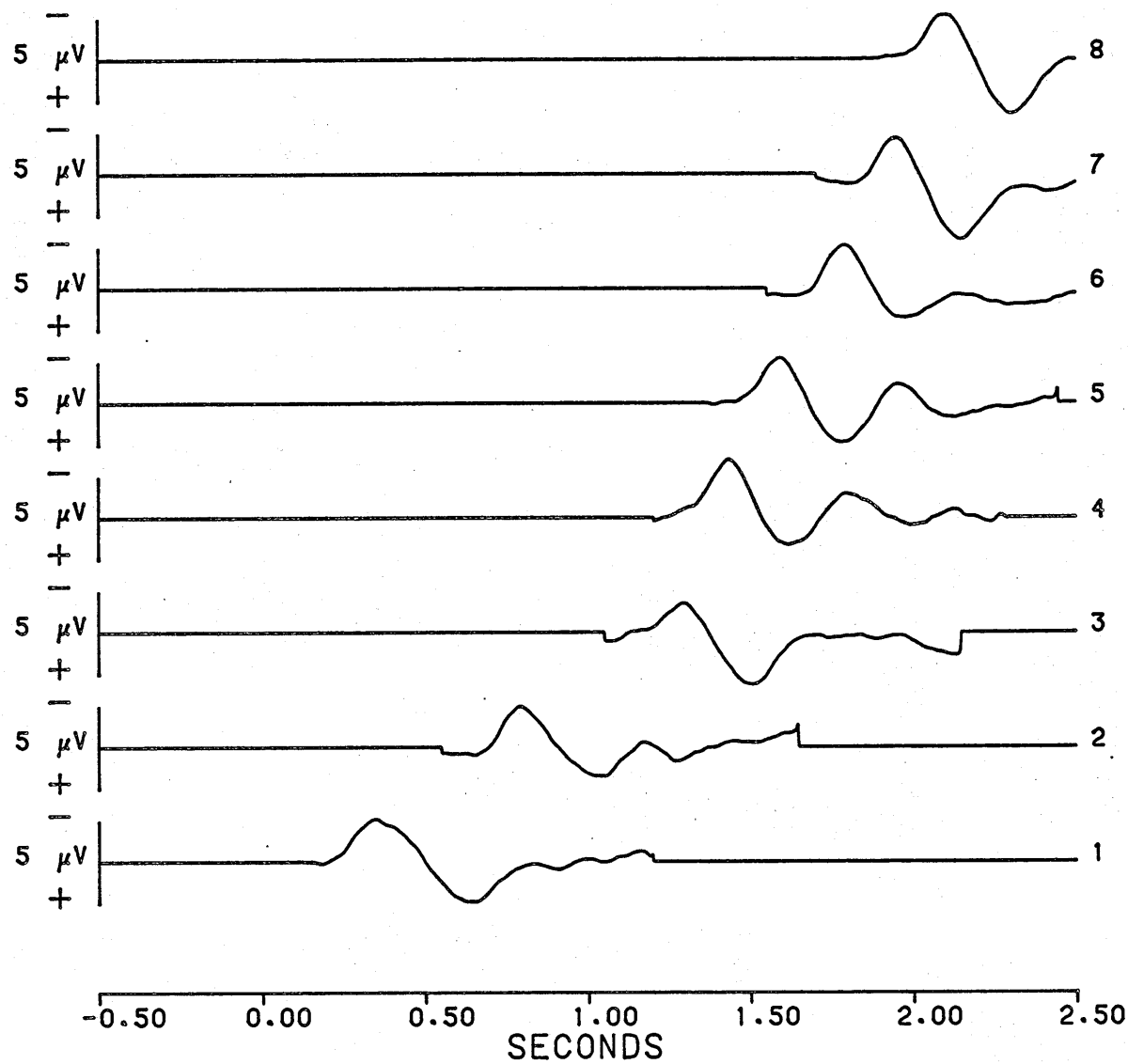

Figure 3.5. Running averages of 'idealised' auditory ERPs (CzPM) simulating distortion in time-locked visual averages.

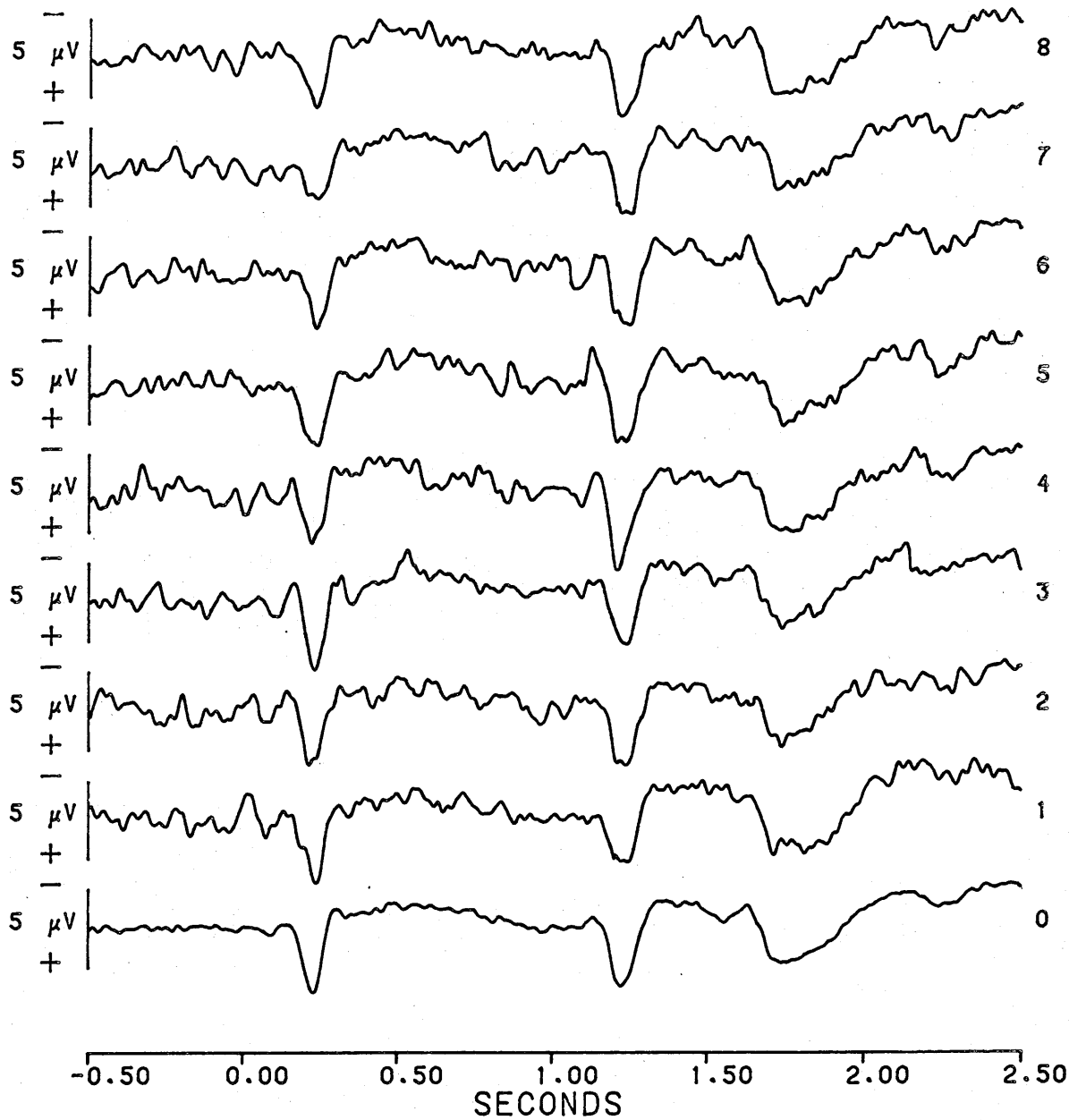

Figure 3.6. Time-locked visual averages (CzPM) following subtraction of auditory distortion.

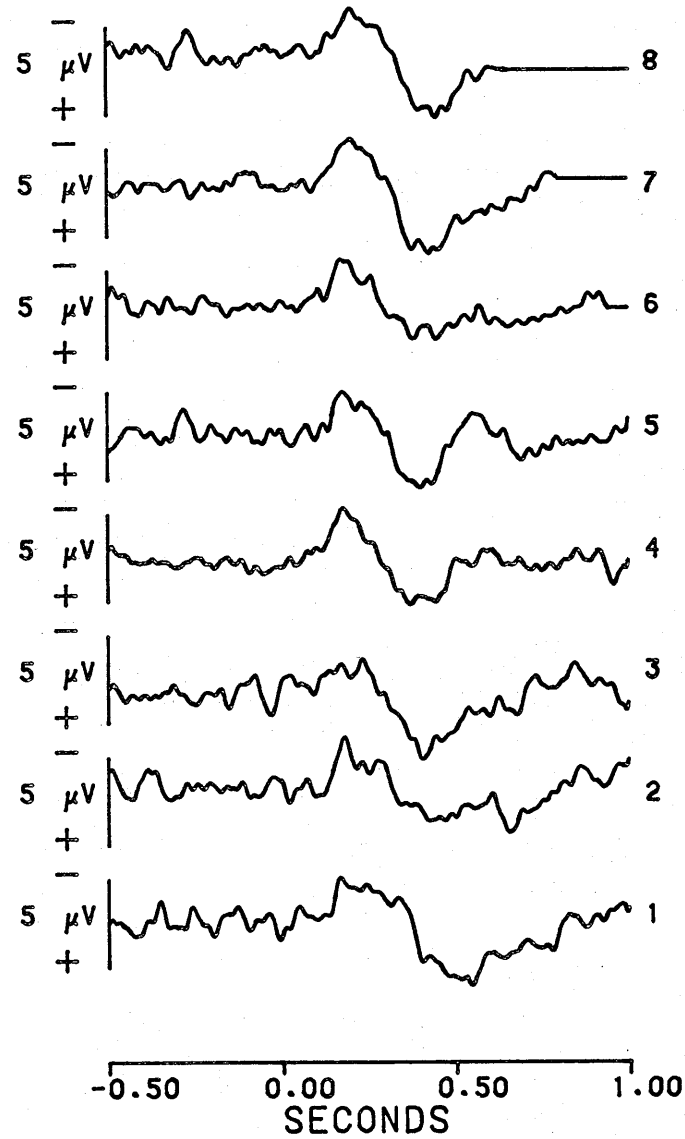

Figure 3.7. Time-locked auditory averages (PzPM) following subtraction of visual distortion.

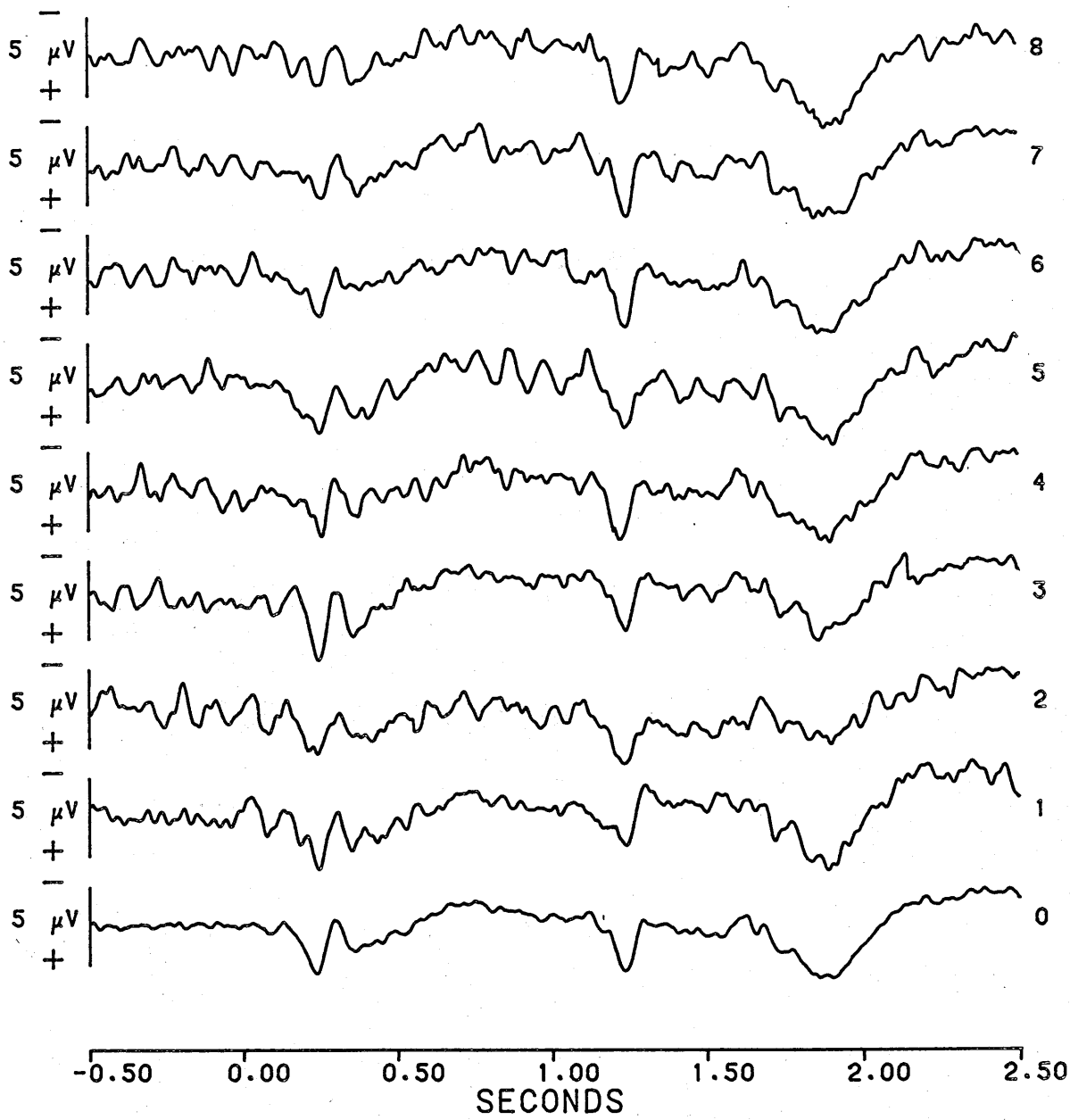

Figure 3.8. Time-locked visual averages (PzPM) following subtraction of auditory distortion.

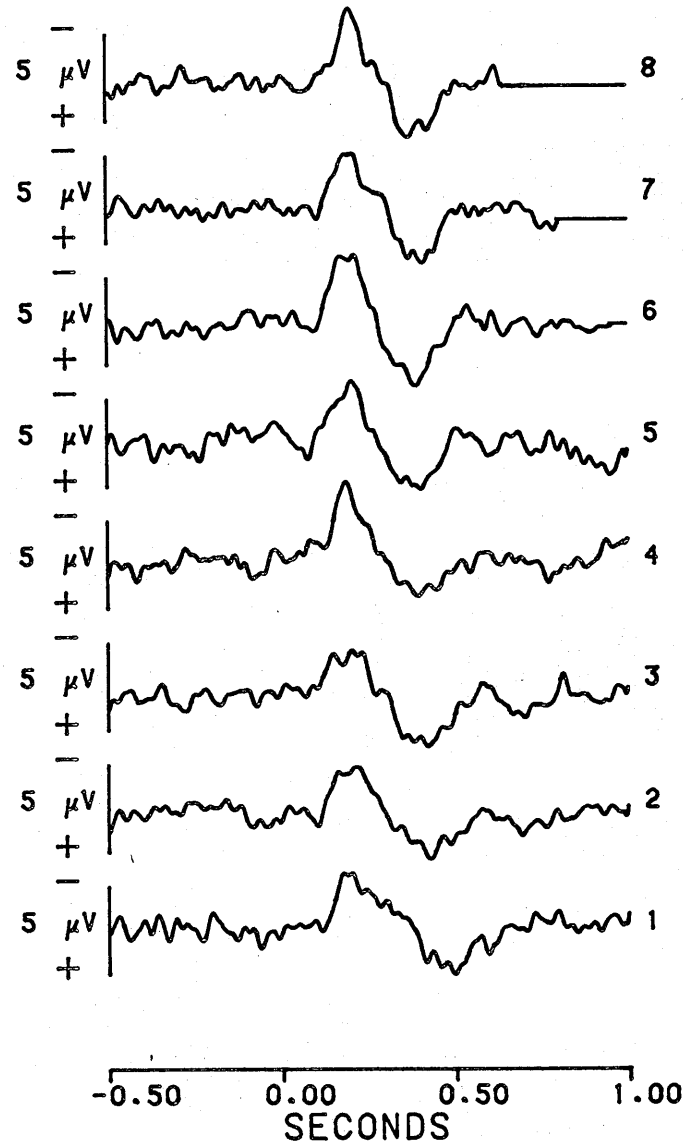

Figure 3.9. Time-locked auditory averages (CzRM) following subtraction of visual distortion.

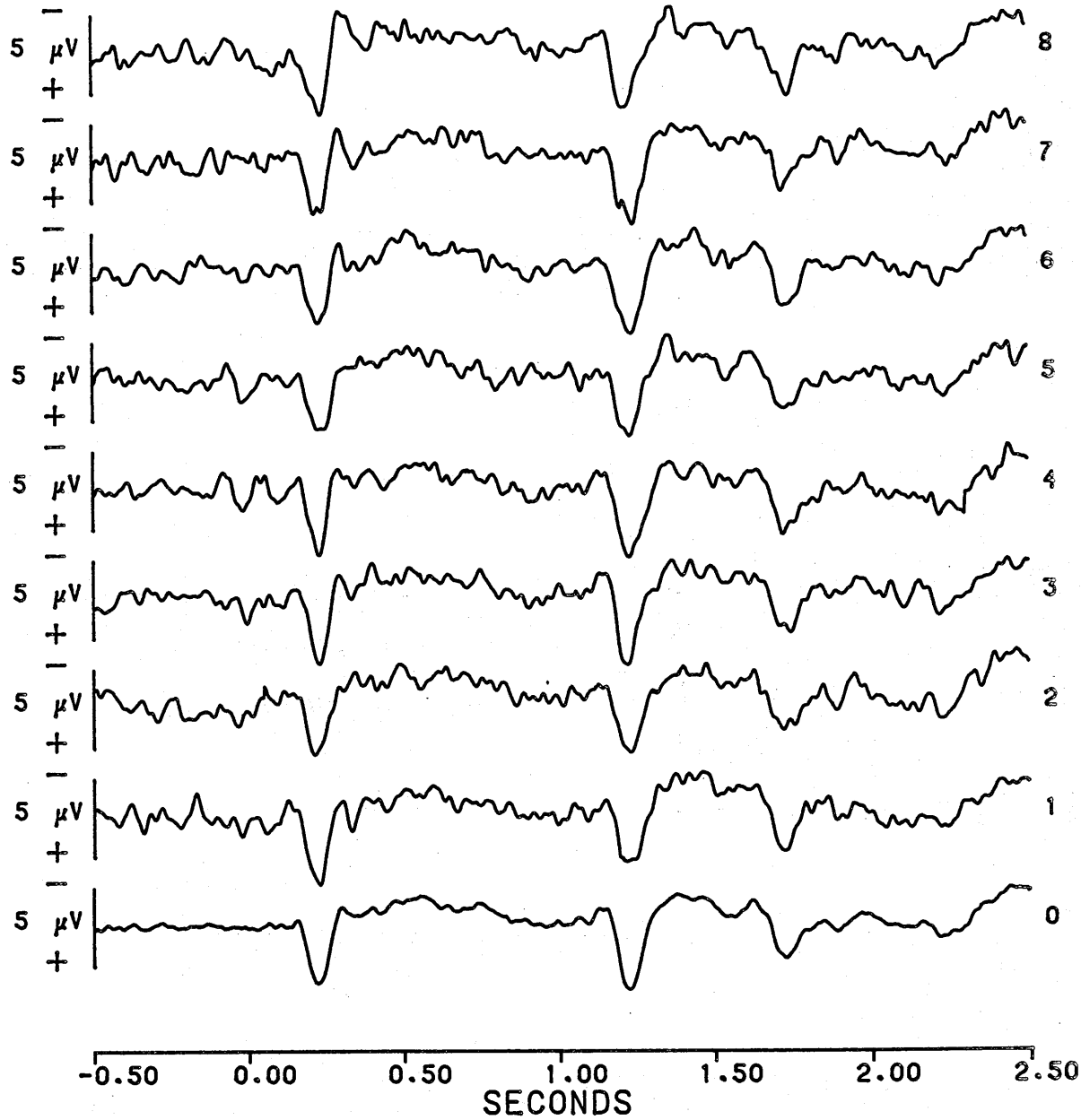

Figure 3.10. Time-locked visual averages (CzRM) following subtraction of auditory distortion.

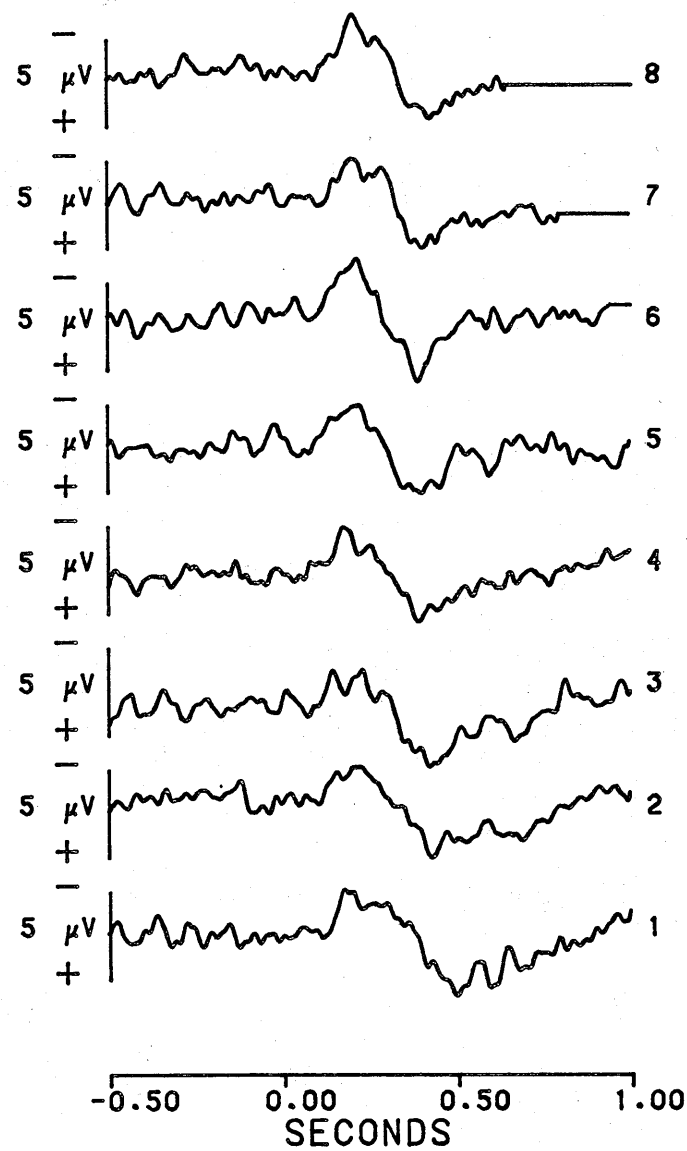

Figure 3.11. Time-locked auditory averages (PzRM) following subtraction of visual distortion.

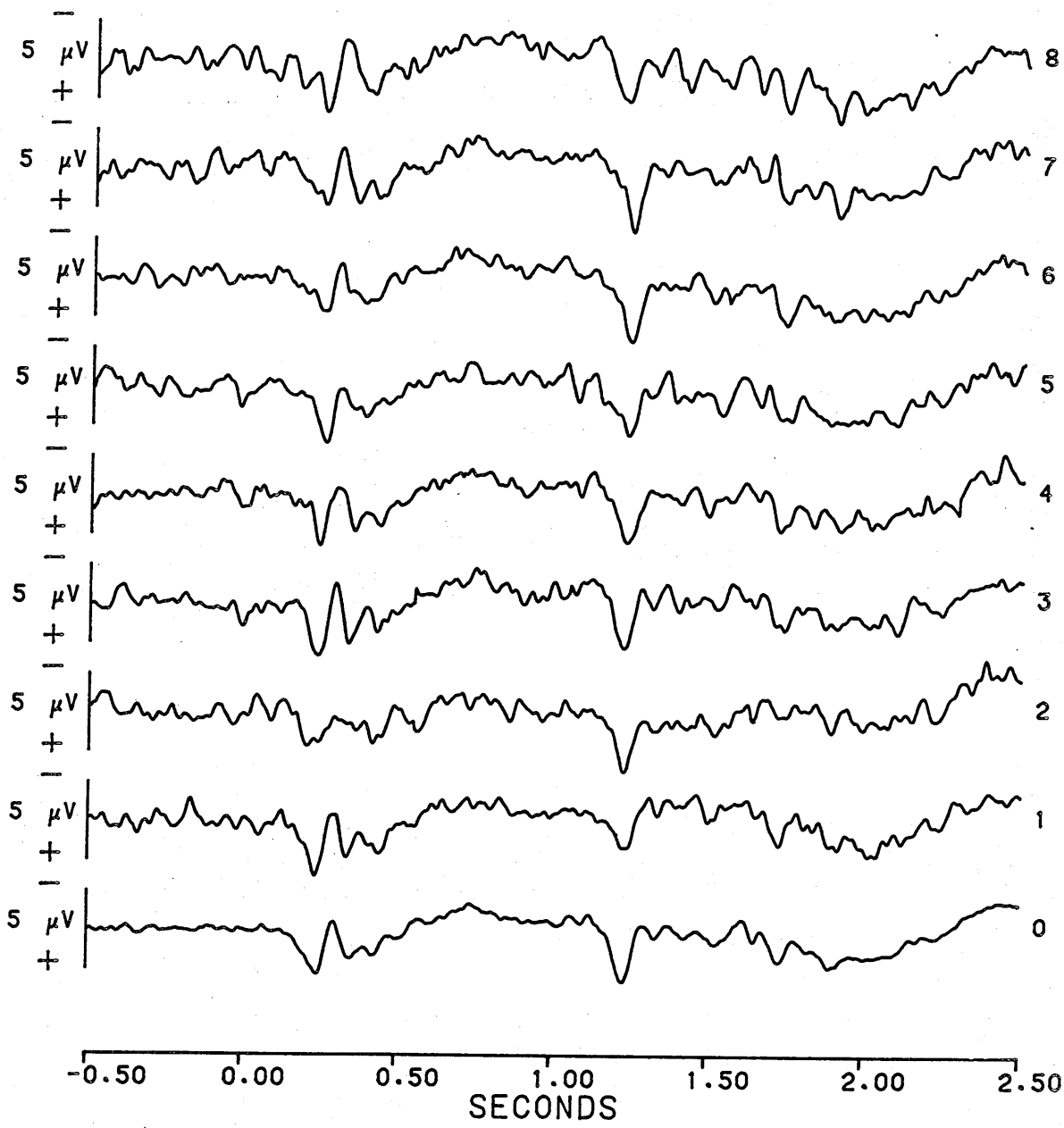

Figure 3.12. Time-locked visual averages (PzRM) following subtraction of auditory distortion.

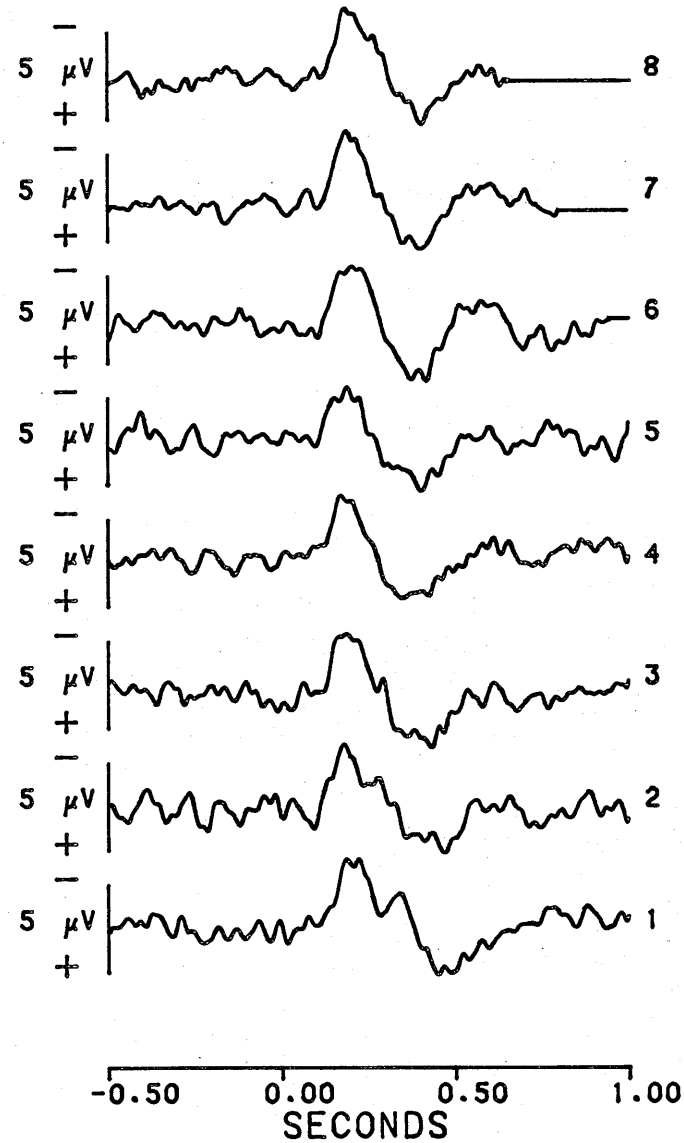

Figure 3.13. Time-locked auditory averages (CzMM) following subtraction of visual distortion.

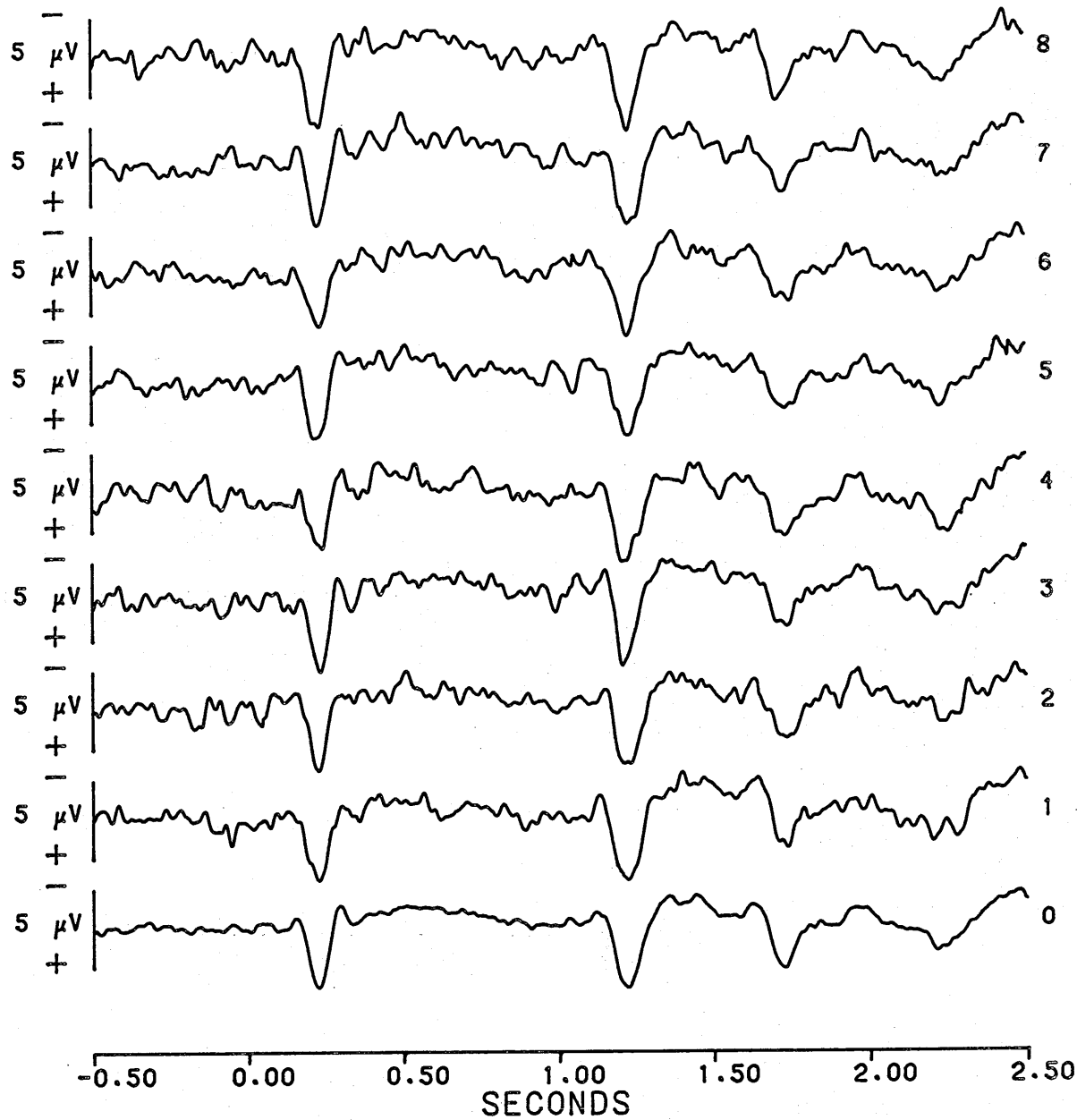

Figure 3.14. Time-locked visual averages (CzMM) following subtraction of auditory distortion.

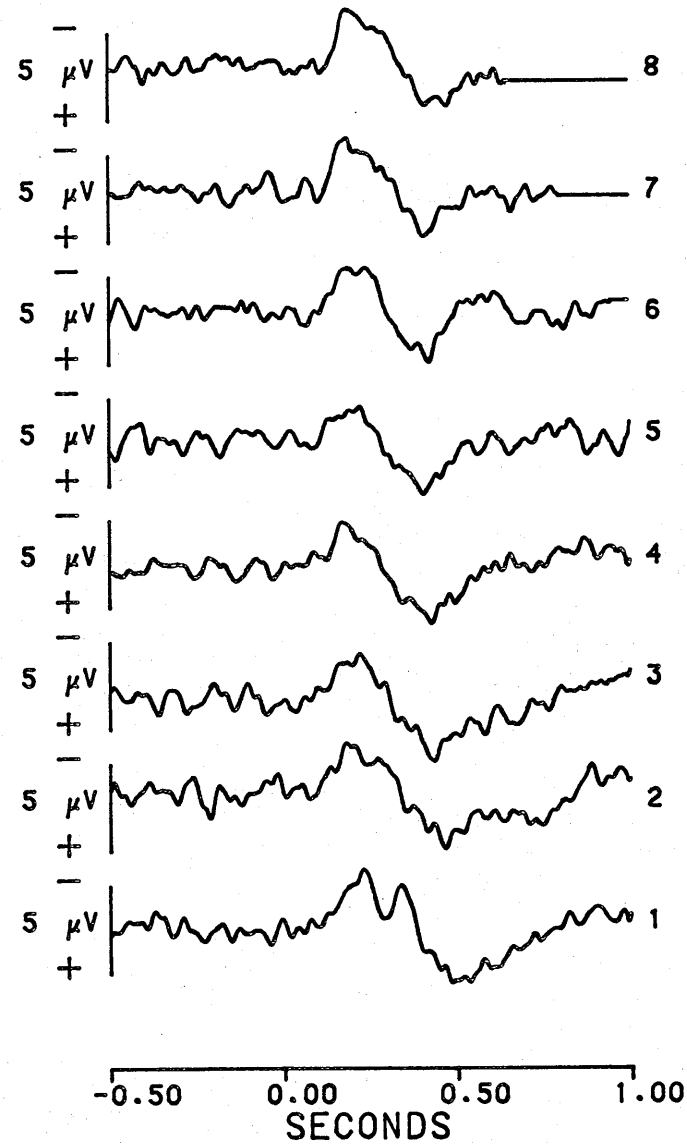

Figure 3.15. Time-locked auditory averages (PzMM) following subtraction of visual distortion.

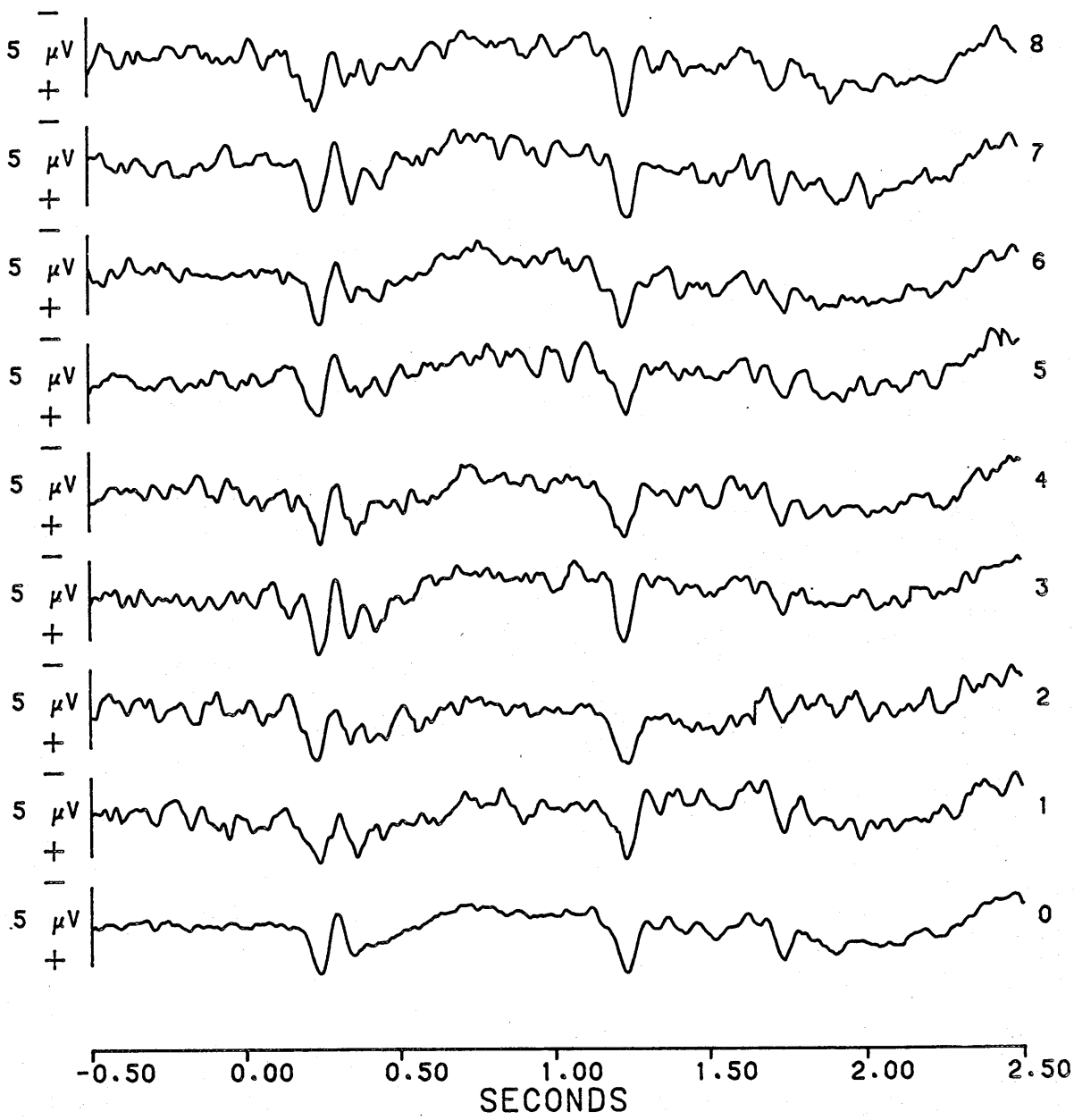

Figure 3.16. Time-locked visual averages (PzMM) following subtraction of auditory distortion.

and Overlay 2 indicates the 100mS windows over which the onset of auditory stimuli occurred with respect to those averages recorded time-locked to the visual task stimuli. These overlays can be used on all figures showing the 'idealised' auditory and visual responses, to check the adequacy with which elementary subtraction procedures have removed the distortion associated with the presentation of stimuli in the other modality.

In order to assess the similarity between visual traces recorded over signal trials and pure visual averages recorded over non-signal trials, every 'idealised' visual average was subtracted from the pure visual average recorded under the same conditions of letter match and electrode placement. The resulting 'difference' traces are shown in Figures 3.17 to 3.22. All traces show residual 'noise', and there is no evidence of any systematic effect to indicate that visual averages recorded over signal trials differ from visual averages recorded over non-signal trials. The use of Overlay 2 confirms that these difference traces show no systematic effects associated with the onset of auditory stimuli in any signal condition.

3.3 Discussion

Elementary subtraction procedures provide one means of separating out time-locked and partially time-unlocked activity recorded during the dual-task experiment. It will be apparent, however, that staggering the presentation of auditory stimuli with respect to visual stimuli is not a necessary requirement if elementary subtraction techniques are to be used to separate out overlapping waveforms. The subtraction procedure can be assumed to work equally well on overlapping, time-locked responses. Under these conditions, time-locked visual traces recorded over non-signal trials can be subtracted directly from the complex waveforms to yield the 'idealised' auditory responses.

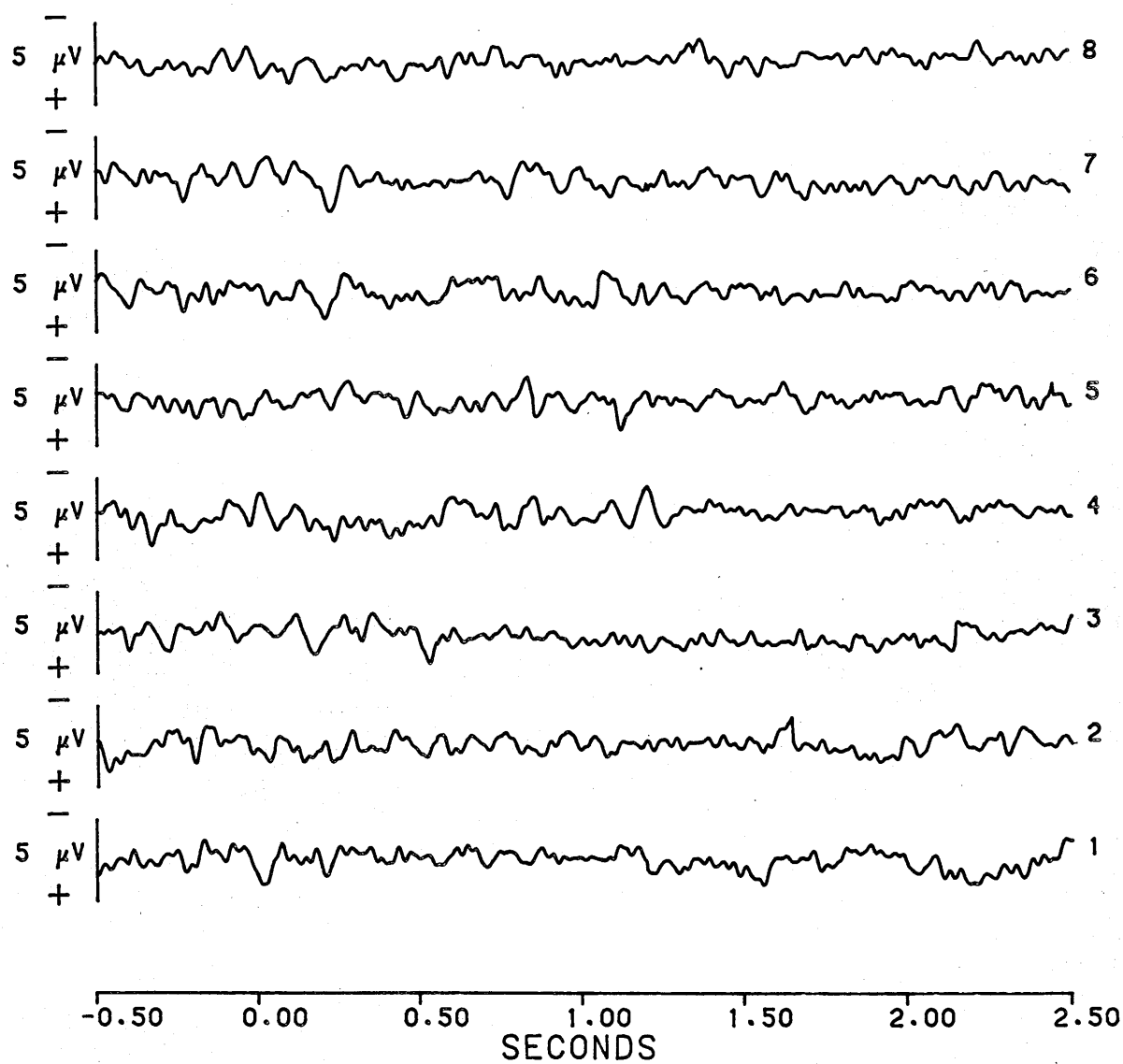

Figure 3.17. Difference traces (CzPM): subtraction of idealised visual averages (signal trials) from pure visual average.

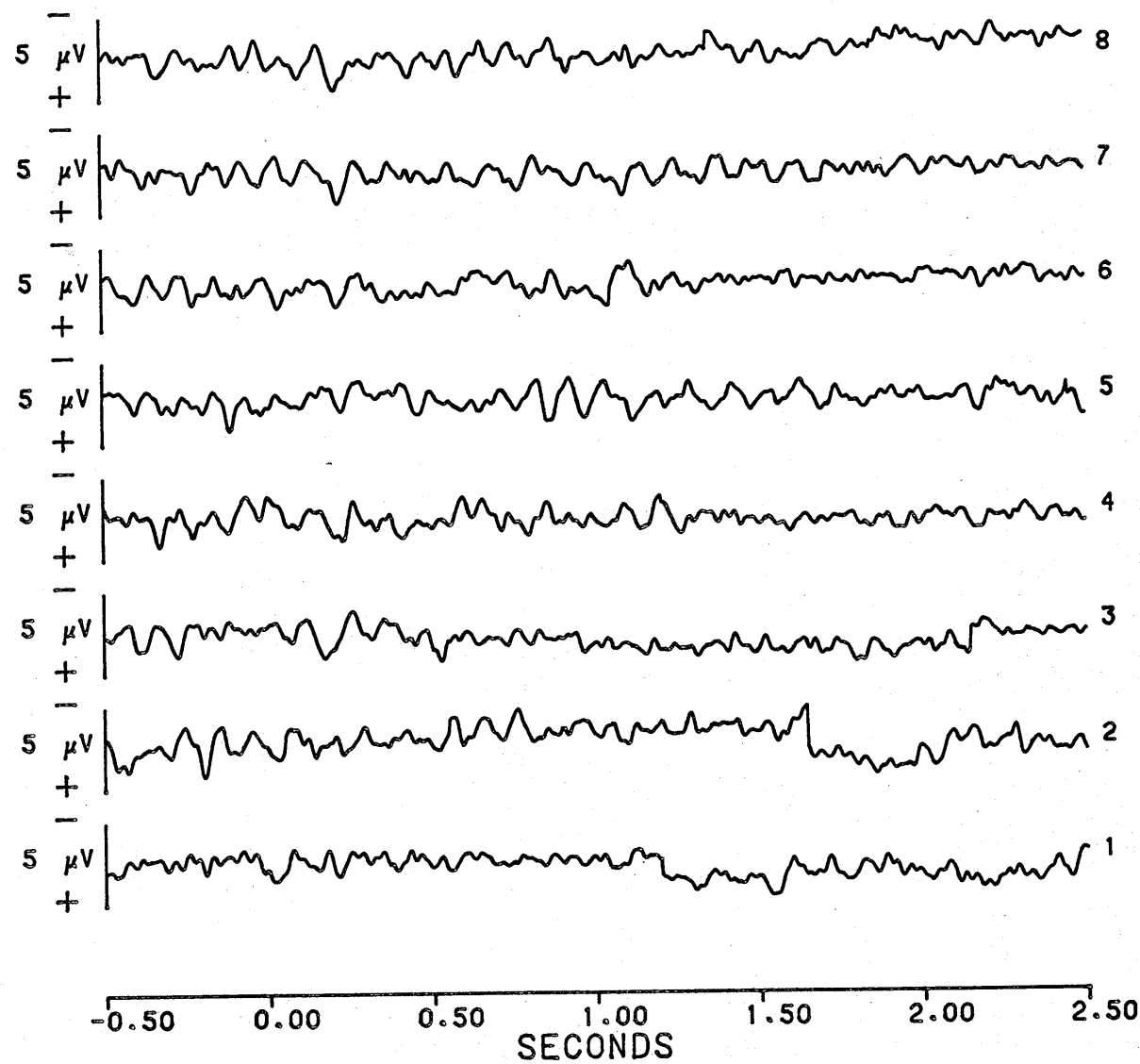

Figure 3.18. Difference traces (PzPM): subtraction of idealised visual averages (signal trials) from pure visual average.

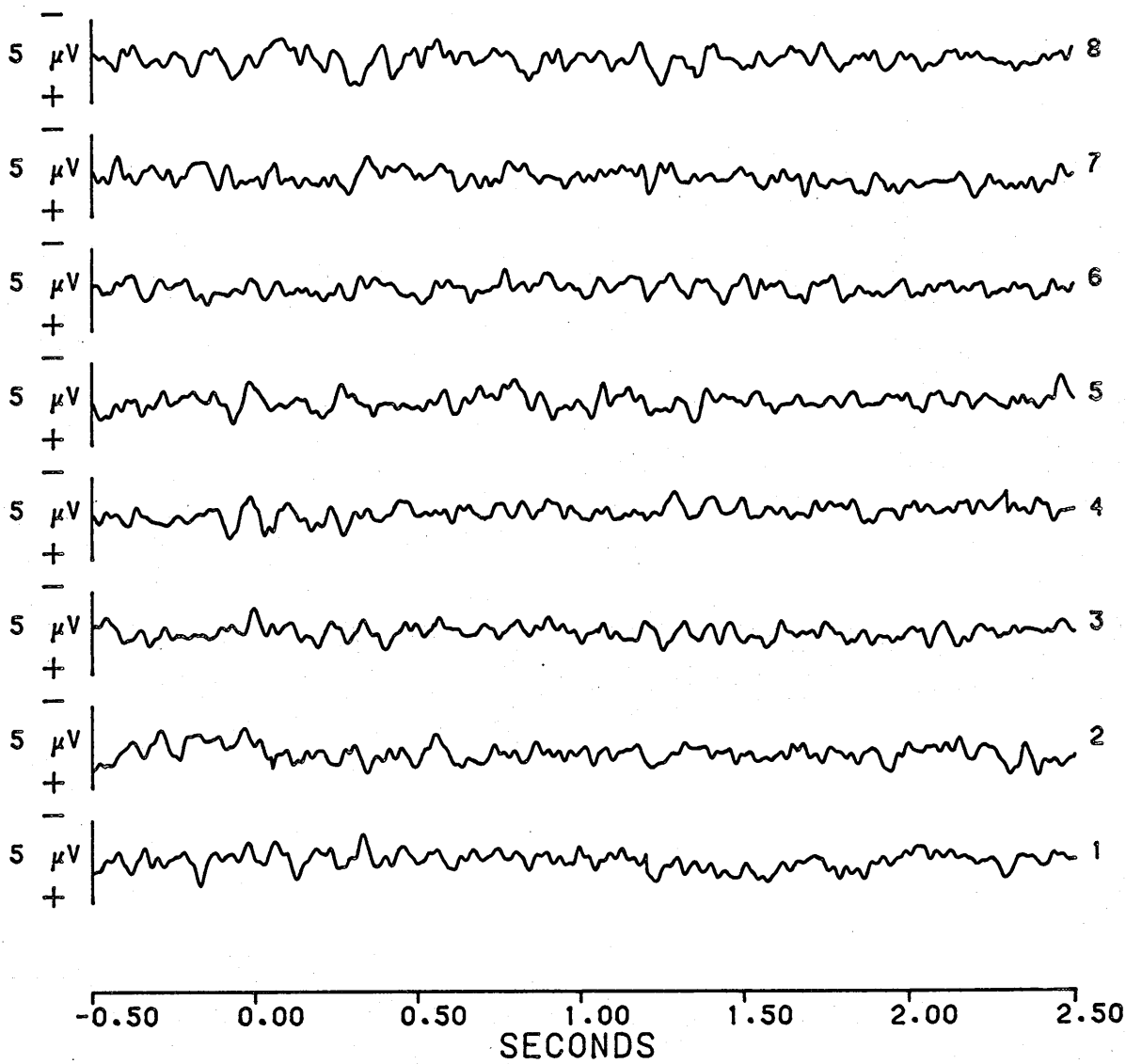

Figure 3.19. Difference traces (CzRM): subtraction of idealised visual averages (signal trials) from pure visual average.

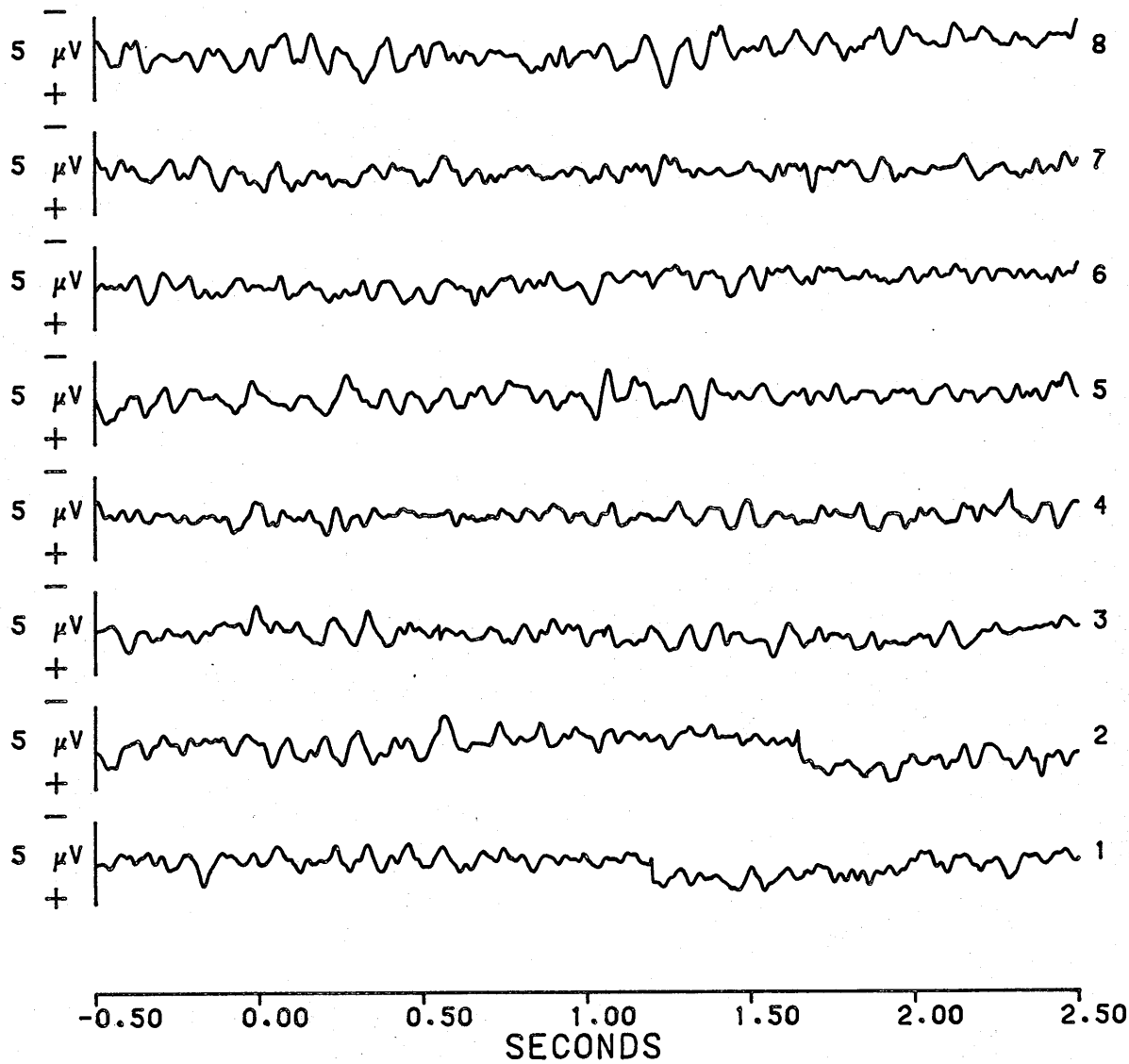

Figure 3.20. Difference traces (PzRM): subtraction of idealised visual averages (signal trials) from pure visual average.

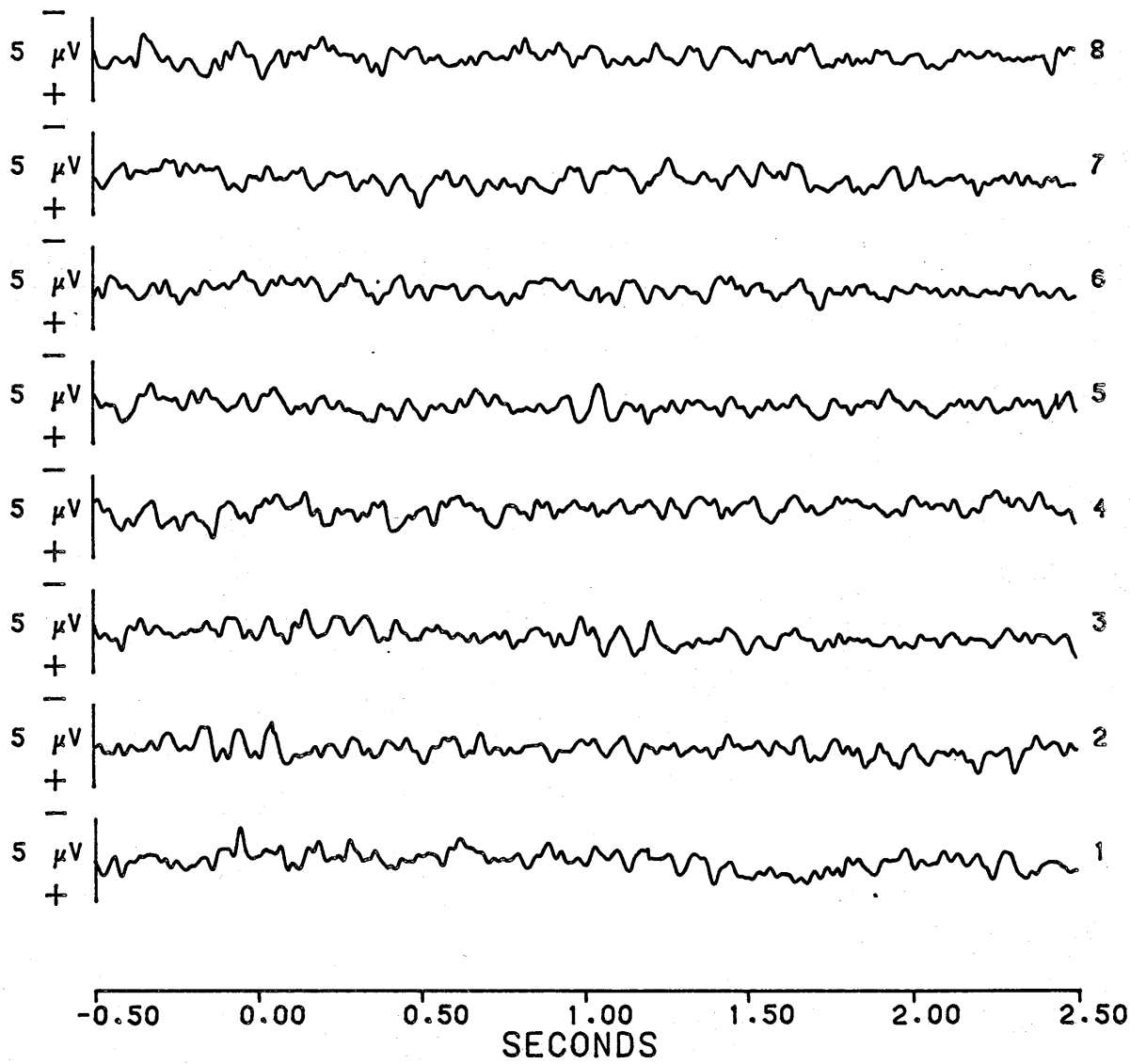

Figure 3.21. Difference traces (CzMM): subtraction of idealised visual averages (signal trials) from pure visual average.

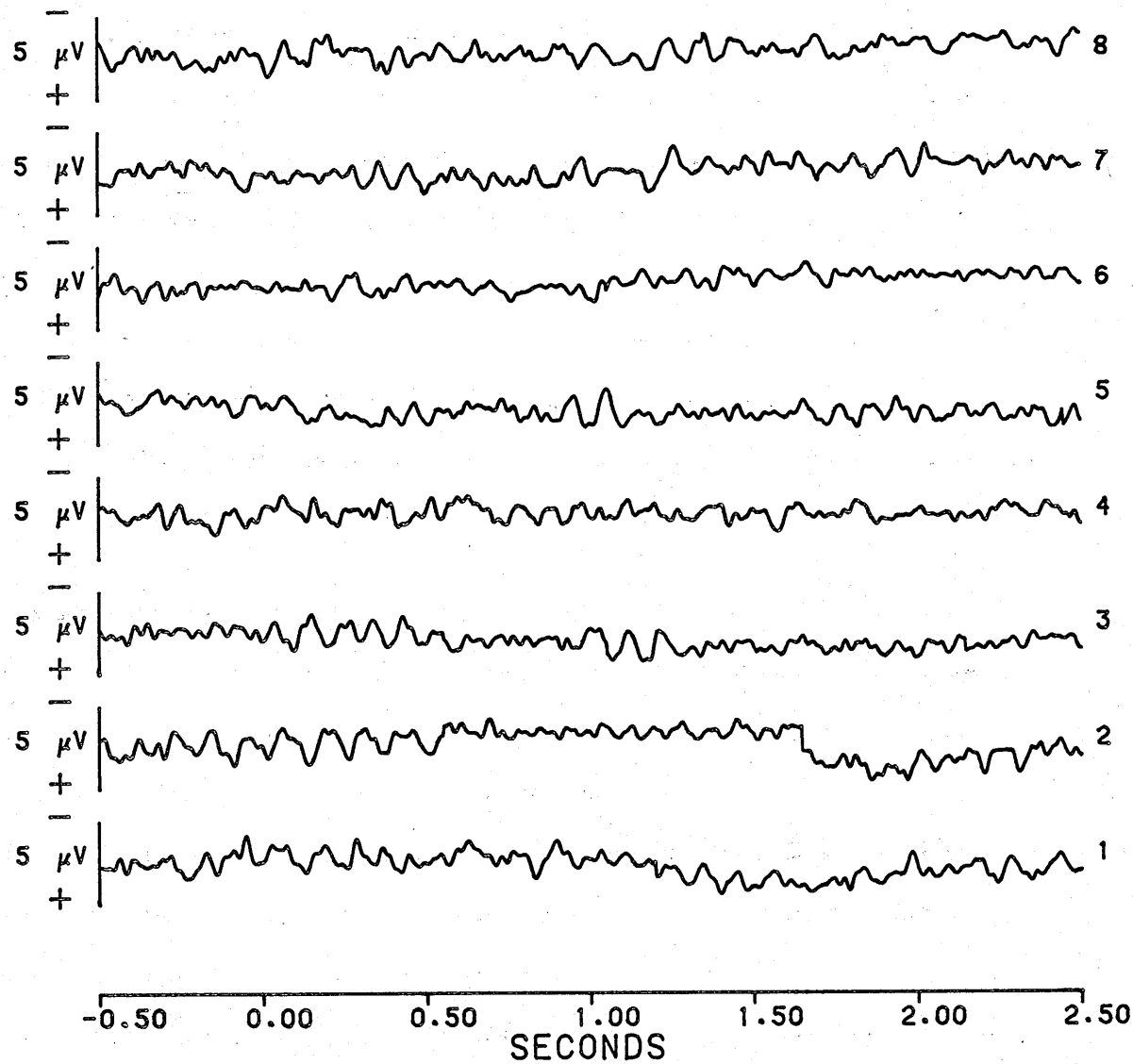

Figure 3.22. Difference traces (PzMM): subtraction of idealised visual averages (signal trials) from pure visual average.

The use of elementary subtraction procedures hinges on two major assumptions. The first assumption, that of electrical additivity of the overlapping waveforms, is no different from the assumption which underlies many aspects of ERP research. For example, it is inherent in all summation and averaging procedures used to improve the signal to noise ratio of recorded ERPs, as it is assumed that the wanted signal is accompanied by noise which has simply been added to it (see, for example, Vaughan, 1974, p.165). If the signal and noise combine non-additively, then the signal resolved by the averaging technique would be, to some degree, a product of the noise which occurred during recording, and not a true representation of the underlying waveform.

The second assumption necessary for the application of elementary subtraction procedures to dual task data is that of visual response invariance over signal and non-signal trials of the task. Implicit in this assumption is the further assumption that the visual component of the complex waveforms remains invariant to the location of the auditory stimulus within the 100mS staggering interval. As noted above, staggering the presentation of auditory stimuli with respect to visual stimuli is an unnecessary requirement for the application of elementary subtraction procedures. The need for this latter assumption can easily be eliminated by maintaining a constant ISI between auditory and visual stimuli in any particular experimental condition. Consequently, it will not be considered further in relation to these elementary subtraction techniques. The assumption of ERP invariance over signal and non-signal trials, however, is more problematic.

If the visual and auditory components of the complex waveforms recorded over signal trials reflect any physiological or psychological interaction between the evoking stimuli, such that the ERPs to visual stimuli presented on signal trials differ from ERPs to visual stimuli presented on non-signal trials, then clearly this assumption is not met. Similar criticisms have been raised by Hillyard *et al.* (1978) with respect to the application of subtraction methods to perceptual masking paradigms (e.g. Donchin and Lindsley, 1965; Schwartz and Pritchard, 1981), because of possible interactions between the masked and masking stimuli.

It was argued (Section 3.1) that any increase in cognitive load due to the introduction of the auditory signal detection task would be reflected in ERPs associated with auditory task stimuli rather than ERPs associated with visual task stimuli. The difference traces presented in Figures 3.17 to 3.22 give support to this argument as they provide no evidence of systematic differences between visual ERPs recorded over signal trials and non-signal trials. Further support is provided through behavioural measures of visual task performance. Table 3.1 shows the mean proportion of correct visual trials for each combination of visual task and auditory task conditions, averaged across all 12 subjects. In addition, the row marginals show mean visual task performance under the three letter-match conditions, averaged across all signal conditions, while the column marginals represent mean visual-task performance under each signal condition, averaged across all letter-match conditions. A 2-way repeated measures analysis of variance (Kirk, 1968, p.238) on the arcsin transformation[1] of these data indicated a

[1] An arcsin transformation was used to remove the dependency between sample means and variances for every experimental condition (Kirk, 1968, p.66).

Table 3.1: Mean proportion of correct visual task trials under all conditions of the dual-task experiment.

Visual Task Conditions	Signal Conditions: No Signal	1	2	3	4	5	6	7	8	
PM	.992	.988	.987	.995	.993	.995	.995	.995	.995	.993
RM	.982	.980	.983	.985	.983	.985	.983	.978	.981	.982
MM	.985	.992	.985	.987	.986	.978	.988	.992	.983	.986
	.986	.987	.985	.989	.988	.986	.989	.988	.987	

significant effect due to visual task condition ($F_{2,22} = 7.136$; $p < .005$), no significant effect due to signal condition ($F_{8,88} = 0.551$; $p > .815$), and no significant interaction ($F_{16,176} = 0.801$; $p > .684$). A Newman-Keuls test of multiple comparisons indicated that performance on physical match trials was significantly better than performance on rule match trials ($p < .01$), and mismatch trials ($p < .05$), while there was no significant difference between performance on rule match and mismatch trials. Therefore, while visual task performance is influenced by the type of letter-match to be made, the introduction of the auditory signal detection task does not affect visual task performance. The above data support the assumption of visual response invariance over signal and non-signal trials. There is, however, much evidence to suggest the need for caution concerning this assumption.

In the dual-task experiment, non-signal trials differ from signal trials in two ways. Firstly, the stimulus environment is substantially different - on non-signal trials subjects receive stimuli in a single modality, at least 500mS apart; on signal trials subjects receive stimuli in two modalities and on some occasions these are separated by as little as 50mS. Evidence is provided through behavioural measures (Loveless, Brebner and Hamilton, 1970; Freides, 1974) that the processing of a stimulus can be altered by the close temporal presentation of a second stimulus in the same or different modality, even when the second stimulus is of no psychological significance. ERP measures are affected similarly by the temporal relationship between eliciting stimuli. For example, Davis, Osterhammel, Weir and Gjerdinger (1972) demonstrated intramodal and crossmodal depression of vertex potentials to stimuli 0.5 seconds apart when compared with vertex potentials to the same stimuli at ISIs of approximately 5 seconds. It could be that such differences do exist between visual ERPs

recorded over signal trials and non-signal trials of the present experiment, but that these differences are not large enough or systematic enough to be evident in Figures 3.17 to 3.22.

Secondly, the cognitive demands of the task alter between non-signal trials and signal trials, and this change could result in a trade-off between primary and secondary task performance which is reflected in the concomitantly recorded ERPs. While the behavioural data presented above show that in the present experiment subjects managed to maintain their visual task performance, attempts to keep primary task performance invariant are often unsuccessful (Rolfe, 1971; Kerr, 1973; Ogden, Levine and Eisner, 1979). Even if subjects strive to maintain their primary task performance, Kerr (1973, p.405) cites those critics who suggest that the introduction of a second task in itself affects the processing capacity available for primary task demands. Although Kerr suggests that the present paradigm is relatively immune to such an effect, as single and dual-task trials are presented randomly, any technique used for separating out overlapping waveforms should ideally generalise to those paradigms which are less robust in this respect.

There are, moreover, those experimental paradigms which are designed specifically to assess the degree of interaction between concurrently performed tasks. By manipulating the relative priorities of the component tasks Performance Operating Characteristic (POC) curves of dual-task performance can be obtained to provide a comprehensive assessment of how two tasks are time-shared (Norman and Bobrow, 1975; Navon and Gopher, 1979, 1980). ERPs recorded under such conditions would be *expected* to differ from ERPs recorded under single task conditions. Alternative methods of separating out

overlapping ERPs, therefore, are necessary to provide an accurate estimation of component waveforms.

An alternative approach to the analysis of ERPs recorded to near-simultaneous stimuli is considered in the following chapter. This method requires the application of a digital filter in both the time domain and the frequency domain and utilises only those data recorded over dual-task signal trials.

CHAPTER 4: DIGITAL FILTERING PROCEDURES

4.1 Introduction

As discussed in the previous chapter, the use of elementary subtraction procedures to separate out overlapping waveforms hinges on two major assumptions. It was argued that the first assumption, that of electrical additivity of the component waveforms, is no more remarkable than the assumption which underlies the majority of ERP research. However, the second assumption, that of ERP invariance over signal and non-signal trials, is of dubious validity if ERPs recorded to near-simultaneous stimuli reflect any interaction between the evoking stimuli. Furthermore, any technique for separating out overlapping waveforms ideally should generalise to those experimental paradigms which are designed specifically to detect and assess possible interactions between stimuli.

Equations {4.1} and {4.2} restate equations {2.1} and {2.2} and represent averages recorded time-locked to visual and auditory stimuli, respectively:

$$R_v = V + f(A) \qquad \{4.1\}$$

$$R_a = A + f(V) \qquad \{4.2\}$$

where: R_v is the trace recorded time-locked to the visual stimuli,
R_a is the trace recorded time-locked to the auditory stimuli,
V is the idealised visual response,
A is the idealised auditory response and
f is the function applied, a running average.

Idealised visual and auditory responses can be estimated accurately only if the unwanted activity, $f(A)$ and $f(V)$, can be defined precisely and removed completely from the composite waveforms. The present approach to the problem of removing the unwanted activity

rests on the fact that it is of a well-defined type. It should be noted however, that the following exposition assumes the absence of any noise component in the composite waveforms. The implications of this assumption are addressed in Section 4.3.4.

The means of removing the unwanted activity are implied by the above equations. As a result of the staggering used, the unwanted component of each trace consists of the wanted component of the other trace after it has been passed through a running average filter (see Section 2.10 of Chapter 2). If the running average of the R_a trace is calculated, the result is:

$$f(R_a) = f(A) + f[f(V)] \qquad \{4.3\}$$

Subtracting {4.3} from {4.1} completely removes the auditory distortion from the visual trace and gives:

$$R_v - f(R_a) = V - f[f(V)] \qquad \{4.4\}$$

Similar arguments apply to the removal of the visual distortion from the auditory trace, where the result of calculating the running average of the R_v trace is:

$$f(R_v) = f(V) + f[f(A)] \qquad \{4.5\}$$

and subtracting {4.5} from {4.2} gives:

$$R_a - f(R_v) = A - f[f(A)] \qquad \{4.6\}$$

Thus the distortion which appears as a result of the other trace may be removed by subtracting the running average of one recorded waveform from the other waveform. However, what is left is not the idealised waveform as can be seen from equations {4.4} and {4.6}. In fact each waveform comprises the idealised trace after it has been passed through a running average filter twice, and subtracted from

the original. The problem now becomes one of removing the 'second order' distortion resulting from the application of such a filter.

Fortunately, the action of the filter can be expressed precisely in the frequency domain, and its effect is easily reversed by passing the waveform through a filter which has exactly the opposite frequency response. The derivation of the filter can be shown by expressing equations {4.1} to {4.6} in the frequency domain.

In the case where an average has been time-locked to the visual events of the task, the visual input may be represented as an impulse to the visual processor (V) which has a response $H_{(v)}$ in the frequency domain. The input to the auditory processor (A), which has a response $H_{(a)}$ in the frequency domain, occurs at some minimum delay, t seconds, and also is represented by a rectangular function over the time period T seconds. This is a result of the staggering procedure. The two electrical activities add and are recorded as a composite waveform, whose representation (Y_1) in the frequency domain is:

$$Y_1 = H_{(v)} + H_{(a)} \exp^{-st} \left(\frac{1-\exp^{-sT}}{sT}\right) \qquad \{4.7\}$$

where: s is the complex Laplace variable, $s = j\omega$, with $j = \sqrt{-1}$ and ω is $2\pi f$, frequency in radians.

The second term on the right hand side of equation {4.7} is simply the representation of a running average filter in the frequency domain (see for example, Thomson, 1957, p.222).

In the case where an average has been time-locked to the auditory events of the task (cf. equation {4.2}), the visual events precede the auditory events by a maximum time period of $(T+t-\Delta)$ seconds, where Δ is the sampling interval (in this case 4mS), and the visual response also

is represented by a rectangular function over the time period T seconds. The frequency domain representation of the composite waveform (Y_2) is thus:

$$Y_2 = H_{(a)} + H_{(v)} \exp^{s(T+t-\Delta)} \left(\frac{1-\exp^{-sT}}{sT}\right) \qquad \{4.8\}$$

where {4·8} is in the same form as {4.7} with the appropriate synchronisation term.

Removing the auditory distortion from the time-locked visual trace, Y_1, requires the running average of the time-locked auditory trace, Y_2 to be calculated. As convolution in the time domain is equivalent to multiplication in the frequency domain (see Beauchamp and Yuen, 1979, p.229), this is achieved by multiplying {4.8} through by $\exp^{-st} \left(\frac{1-\exp^{-sT}}{sT}\right)$, to give:

$$Y_2 \exp^{-st} \left(\frac{1-\exp^{-sT}}{sT}\right) = H_{(a)} \exp^{-st} \left(\frac{1-\exp^{-sT}}{sT}\right) + H_{(v)} \exp^{s(T-\Delta)} \left(\frac{1-\exp^{-sT}}{sT}\right)^2 \qquad \{4.9\}$$

which may then be subtracted from {4.7} to give:

$$Y_1 - Y_2 \exp^{-st} \left(\frac{1-\exp^{-sT}}{sT}\right) = H_{(v)} \left[1-\exp^{s(T-\Delta)} \left(\frac{1-\exp^{-sT}}{sT}\right)^2\right] \qquad \{4.10\}$$

Symmetrical arguments can be applied to the auditory trace, firstly by multiplying {4.7} through by $\exp^{s(T+t-\Delta)} \left(\frac{1-\exp^{-sT}}{sT}\right)$ to give:

$$Y_1 \exp^{s(T+t-\Delta)} \left(\frac{1-\exp^{-sT}}{sT}\right) = H_{(v)} \exp^{s(T+t-\Delta)} \left(\frac{1-\exp^{-sT}}{sT}\right) + H_{(a)} \exp^{s(T-\Delta)} \left(\frac{1-\exp^{-sT}}{sT}\right)^2 \qquad \{4.11\}$$

and then subtracting {4.11} from {4.8}:

$$Y_2 - Y_1 \exp^{s(T+t-\Delta)}\left(\frac{1-\exp^{-sT}}{sT}\right) = H_{(a)}\left[1-\exp^{s(T-\Delta)}\left(\frac{1-\exp^{-sT}}{sT}\right)^2\right] \quad \{4.12\}$$

The left hand side of equations {4.10} and {4.12} amount to the subtraction of the running average of Y_2 from Y_1, and the subtraction of the running average of Y_1 from Y_2, respectively. The resultant waveforms are represented by the right hand side of these equations. Each takes the form of the wanted response in the frequency domain, which has been modified by the filter given by the values in parentheses. The first term of the filter is a synchronisation term. The second term corresponds to a triangular function which is the frequency domain representation of the double running average filter (see Thomson, 1957, p.222).

The filter is identical for both visual and auditory traces and is a finite impulse response (FIR) filter having zero phase shift. Its frequency response is plotted in Figure 4.1A, for T = 0.1 seconds and Δ = 0.004 seconds. It can be seen that the filter acts as a high pass filter which significantly attenuates frequency components of the wanted waveform below approximately 9Hz. This effect, however, can be reversed by passing the waveforms represented by equations {4.10} and {4.12} through a filter having the opposite frequency response. The frequency response of this inverse filter is plotted in Figure 4.1B.

The inverse filter coefficients can be calculated exactly for any frequency from the reciprocal of the filter function represented on the right hand side of equations {4.10} and {4.12}, as long as the time period of the staggering window, T, and the sampling interval, Δ, are known.

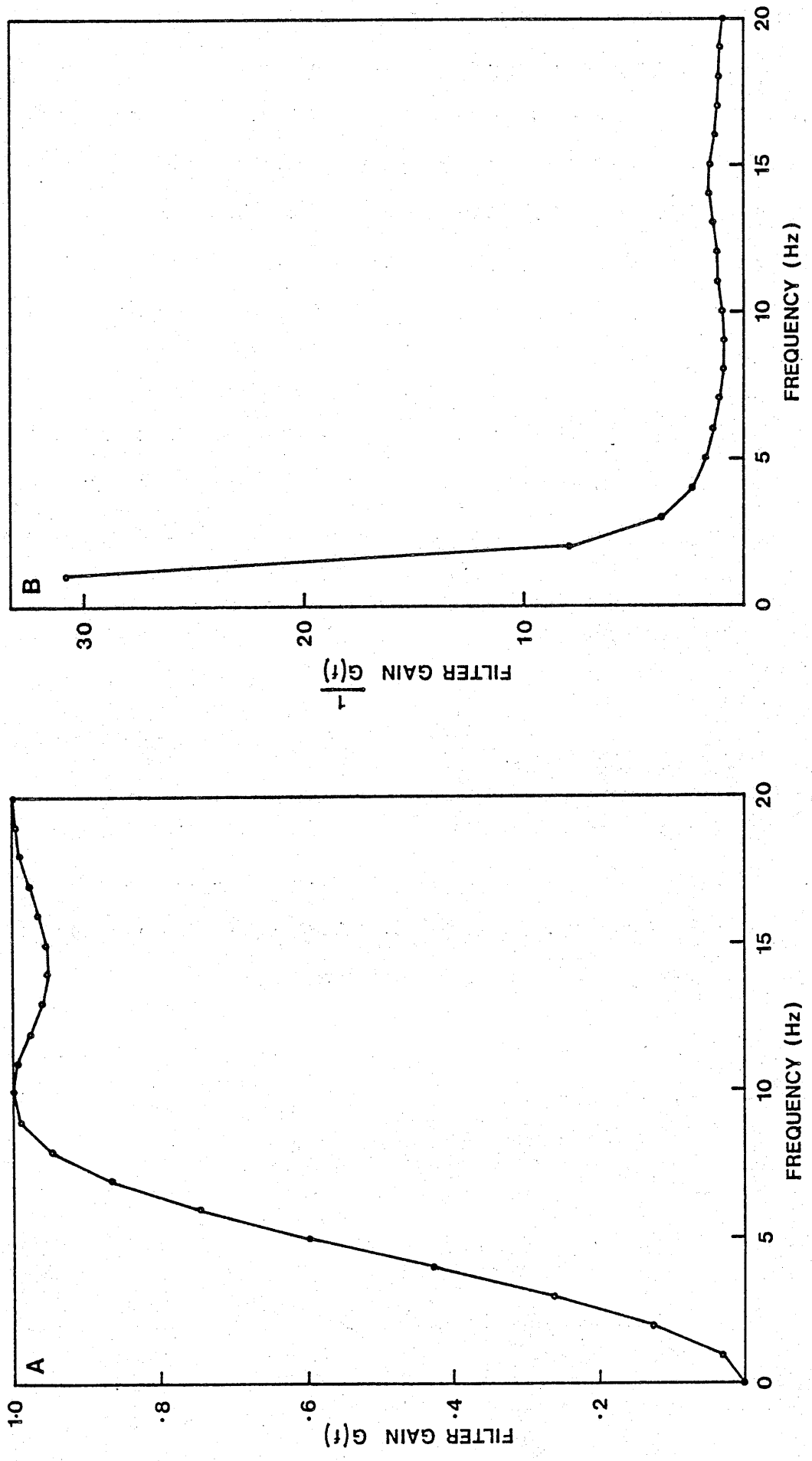

Figure 4.1. Frequency response functions of A: the double running average filter, and B: its inverse.

A two-stage procedure is necessary, therefore, to remove the distortion specified by equations {4.1} and {4.2}. Firstly, the running average of each trace is calculated and subtracted from the other trace. Secondly, the inverse filter is applied by performing a Fourier transform on the waveform resulting from the subtraction, multiplying the various frequency coefficients by the appropriate filter constants, and then performing an inverse Fourier transform to regenerate the data in the time domain.

Prior to applying this solution to experimental data the technique was tested on simulated data spanning different frequency ranges, and using staggering windows of different durations. Examples of these tests are provided in Section 4.3. By way of background information, the following section outlines the principles of Fourier analysis, the application of which is central to the use of this technique.

4.2 The Fourier transform

The Fourier transform converts a function in the time domain into an expression in the frequency domain. Each non-zero value of the resultant frequency function indicates that a sinusoid at that frequency is a component of the original time function.

For a continuous waveform, the continuous Fourier transform (CFT) can be written:

$$H(f) = \int_{-\infty}^{\infty} h(t)\ \exp^{-j2\pi ft} dt \qquad \{4.13\}$$

and the inverse CFT can be written:

$$h(t) = \int_{-\infty}^{\infty} H(f)\ \exp^{j2\pi ft} df \qquad \{4.14\}$$

where: $j = \sqrt{-1}$,

$h(t)$ is the time function to be transformed,

$H(f)$ is the Fourier transform of $h(t)$,

t is time, and

f is frequency in cycles per second.

However, when a waveform is sampled and of finite duration, the discrete Fourier transform (DFT) algorithm is used to approximate the CFT. The forward DFT can be written in the form:

$$H\left(\frac{n}{N\Delta}\right) = \sum_{k=0}^{N-1} h(k\Delta)\, \exp^{-j2\pi kn/N} \quad \text{for } n = 0,1,2,\ldots,N-1 \quad \{4.15\}$$

and the inverse DFT can be written as:

$$h(k\Delta) = \frac{1}{N} \sum_{n=0}^{N-1} H\left(\frac{n}{N\Delta}\right) \exp^{j2\pi nk/N} \quad \text{for } n = 0,1,2,\ldots,N-1 \quad \{4.16\}$$

where, in addition to the above definitions:

N is the number of samples taken from $h(t)$ or $H(f)$

Δ is the sampling interval.

Therefore, the DFT provides a reversible mapping of N terms of $H\left(\frac{n}{N\Delta}\right)$ into N terms of $h(k\Delta)$, and equation {4.15} shows that the result of the forward DFT conversion is a series of coefficients of harmonically related frequencies with the lowest, or fundamental, frequency of the series being given by $\frac{1}{N\Delta}$.

While the first $\frac{N}{2}$ terms of the DFT provide a good approximation to the CFT, the latter half of the frequency function is not a good approximation, but rather can be considered to be the 'negative' frequency harmonics between $\frac{-N}{2}$ and -1. This lack of correspondence arises because the input to the DFT is a finite set of discrete samples rather than a continuous waveform (Bergland, 1969). Consequently, the output of the

forward DFT can be considered to be associated with the frequency range:

$$-\left[\frac{N}{2}\cdot\frac{1}{N\Delta}\right] \text{ to } \left[\frac{(N-1)}{2}\cdot\frac{1}{N\Delta}\right]$$

In general, the output vector of the forward DFT is a complex series whereby the real part of each Fourier coefficient contains the value of sinusoids that are even functions (cosines) and the imaginary part contains the value of sinusoids that are odd functions (sines). The amplitude of the series is usually expressed in terms of the sum of the amplitudes of odd and even sinusoids, by taking the absolute value or modulus of each Fourier coefficient:

$$\left|H\left(\frac{n}{N\Delta}\right)\right| = \sqrt{ReH\left(\frac{n}{N\Delta}\right)^2 + ImH\left(\frac{n}{N\Delta}\right)^2}$$

where: $ReH\left(\frac{n}{N\Delta}\right)$ is the real part of the Fourier coefficient and

$ImH\left(\frac{n}{N\Delta}\right)$ is the imaginary part of the Fourier coefficient.

The amplitude spectrum of the transformed time series is constructed by plotting these absolute values as a function of frequency $\left(\frac{n}{N\Delta}\right)$, or as a function of the Fourier number (n), which is a simple linear transformation of the actual frequency. The amplitude spectrum, therefore, describes the importance of each frequency component within the original time series.

The transformed series also can be described in terms of its phase, which is the ratio of the contributions in the sine spectrum to the contributions in the cosine spectrum at a particular frequency. The phase spectrum is defined by:

$$\phi\left(\frac{n}{N\Delta}\right) = \arctan\left[ImH\left(\frac{n}{N\Delta}\right)/ReH\left(\frac{n}{N\Delta}\right)\right]$$

where, in addition to the above definitions, ϕ is the phase angle in radians.

The use of a finite set of discrete samples of data as input into the DFT poses special problems in the estimation of the frequency characteristics of a time series. For the DFT to yield a good approximation to the CFT, within the frequency range specified above, the input data must satisfy two conditions:

1. The function to be transformed must be band-limited and sampled at a rate which is at least twice that of the highest frequency component;
2. The function to be transformed must be periodic and should be truncated at exactly one non-zero integer multiple of the function's period.

The first condition applies to the representation of all continuous signals by discrete digital samples and the failure to meet this requirement results in a violation of the sampling theorem (Shannon, 1949) and gives rise to the phenomenon of aliasing. This means that higher-order frequencies, which cannot be represented by the sampled data, 'impersonate' lower frequency components. The frequency beyond which aliasing occurs, the Nyquist or folding frequency, is determined completely by the sampling interval of the time function, where the folding frequency $f_f = \frac{1}{2\Delta}$. Problems of aliasing can be avoided by ensuring that the data are sampled at a sufficiently high rate to provide an exact representation of the highest frequency of interest, and by removing all frequency components above the folding frequency with low pass filtering procedures prior to A to D conversion.

The second condition relates to the finite nature of the data input to the DFT. The input waveform is effectively 'viewed' through a rectangular data window which has its own Fourier transform representation in the frequency domain (the sin x /x function)

consisting of a main lobe and a series of highly oscillatory sidelobes. The Fourier estimation of the input waveform, therefore, results from the convolution of the input waveform with the rectangular window in the frequency domain (see, for example, Otnes and Enochson, 1972; p.200). The effect of the truncation factor is negligible if the frequency composition of the function to be transformed corresponds exactly to non-zero integer multiples (i.e. harmonics) of the fundamental frequency of the Fourier series (Bergland, 1969, p.45). However in practice this requirement rarely is satisfied. As a result, spectral 'leakage' occurs whereby the function is not localised to a given frequency but has a series of spurious peaks or sidelobes corresponding to those of the transformed data window. The power of the signal is smeared or spread out over a much broader range of frequencies.

The implication of spectral leakage for the successful application of the present technique is discussed in Section 4.3.3 and methods for reducing the degree of leakage are considered.

The following sections describe the application of the filtering procedures to simulated data and data recorded during the dual-task experiment. In all cases, Fourier transformation was achieved using a Fortran-callable fast Fourier transform (FFT) subroutine (FFT2C) from the International Mathematical and Statistical Libraries package (IMSL, 9th edition). The FFT is based on the DFT algorithm, but provides a computationally more economical method of moving between the time domain and the frequency domain (see Bergland, 1969).

4.3 Test data

The digital filtering technique was tested using simulated data consisting of sine waves of various frequencies. Examples of these tests are given below.

A similar procedure was followed for all tests and the results of each test are presented as a set of eight graphs. A description of the general procedure follows, while specific test manipulations are described prior to the presentation of test results.

4.3.1 General procedure

The first stage in testing involved the generation of two waveforms to simulate the 'idealised' visual and auditory responses. These waveforms are graphed separately and are labelled VIS1 and AC1, respectively.

Next, the running average of each waveform was calculated using a staggering window of 25 samples. Each staggered trace was appropriately normalised and added to the 'idealised' version of the other trace to simulate the time-locked visual and auditory traces represented by equations {4.1} and {4.2}. Each waveform, therefore, consisted of the idealised waveform plus the 'first order' distortion represented by $f(A)$ or $f(V)$. These data are plotted separately and labelled VIS2 and AC2.

The first order distortion was removed by calculating the running average of VIS2 and AC2 and subtracting each staggered waveform from the unstaggered version of the other waveform. The resultant traces, represented by equations {4.4} and {4.6} are plotted as graphs VIS3 and AC3.

Finally, the 'second order' distortion was removed by taking the FFT of VIS3 and AC3, multiplying each Fourier coefficient by the appropriate filter constant and then applying the inverse FFT to regenerate the data in the time domain. The filtered waveforms are presented as VIS4 and AC4, respectively. The success of the technique can be assessed by comparing VIS4 with VIS1 and AC4 with AC1.

All simulated traces consisted of 304 data points. The first and last 24 data points, however, were truncated prior to graph plotting and prior to the application of the inverse filter, in order to remove spurious data values resulting from the staggering process (see Section 3.2 of Chapter 3). Following truncation, all time series consisted of 256 data points and with an assumed sampling interval of 0.004 seconds each corresponds to a duration of 1.024 seconds. The fundamental frequency of the Fourier series was thus 0.977Hz and the folding frequency was 125Hz.

The inverse filter constants appropriate to these test data (for T = 0.1 seconds and Δ = 0.004 seconds) are plotted in Figure 4.2 as a function of Fourier number (n), where n=1 corresponds to 0.977Hz. As the double running average filter has a negligible effect on frequencies above 10Hz (see Figure 4.1A), the inverse filter was applied only to the first eleven Fourier coefficients returned by the forward FFT. These coefficients correspond to frequencies between 0Hz and 9.77Hz. It should be noted that a filter value corresponding to the first Fourier coefficient (n=0) cannot be calculated. Consequently, this value was set to unity.

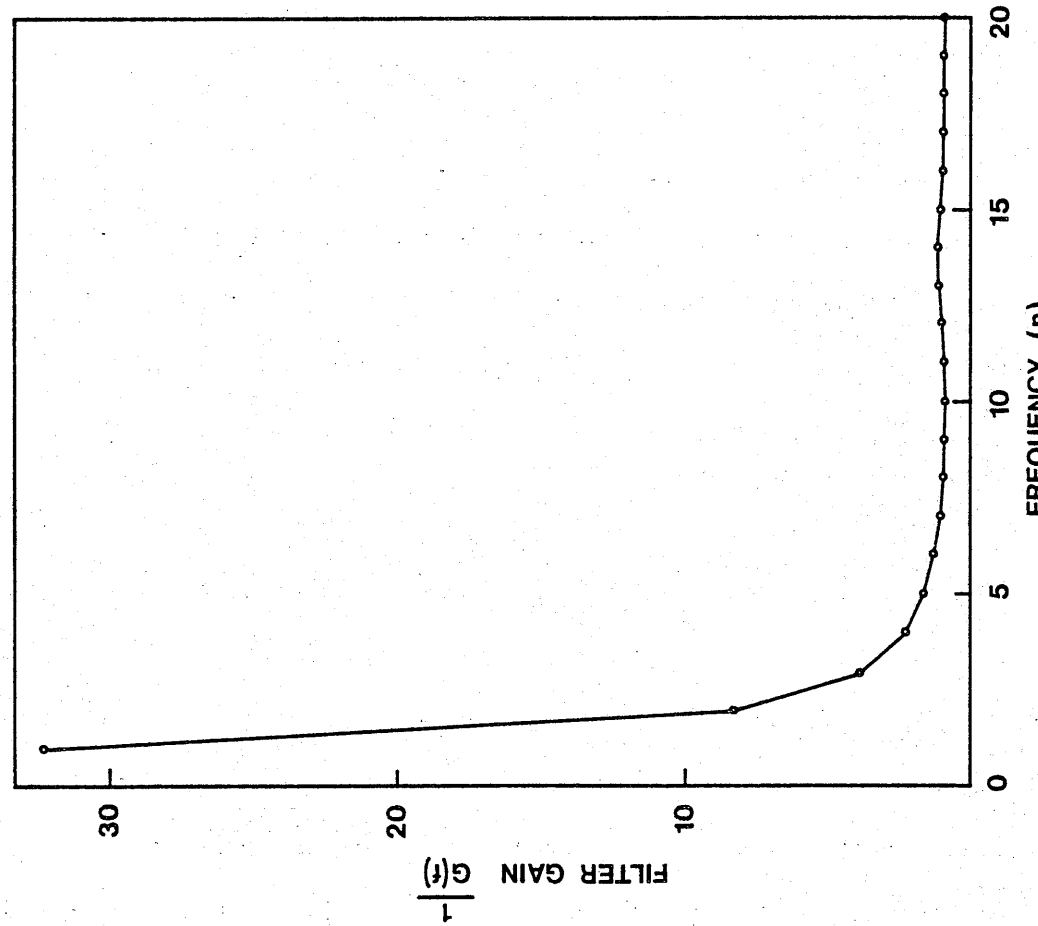

Figure 4.2. Gain of the inverse double running average filter as a function of Fourier number.

At every stage of the test procedure the amplitude spectrum of each waveform was calculated, and this is plotted below the time domain representation of the trace. These spectra are plotted as a function of the Fourier number, up to n = 50 only, as the amplitude of the Fourier coefficients beyond this frequency generally is negligible for these data. Note that in all graphs, the amplitude of the waveform as a function of time has been termed 'voltage', to distinguish these plots from those which present amplitude as a function of frequency.

4.3.2 Test 1: Simulated periodic waveforms

Figures 4.3 to 4.10 show the results of testing the filtering procedures using simulated periodic waveforms. The phase spectra of these waveforms also are plotted to demonstrate that neither the double running average filter, applied through the subtraction process, nor its inverse results in any phase shift occurring at any frequency.

The idealised 'visual' and 'auditory' traces, plotted in Figures 4.3 and 4.4, consist of one cycle of a 2.5Hz and 5Hz sine wave, respectively. Each sinusoid was padded with nulls to provide a trace of 304 samples. Figures 4.5 and 4.6 show the effect of adding the original waveform and the staggered version of the other trace. The effect of removing the first order distortion is shown in Figures 4.7 and 4.8 and the resultant second order distortion is evidenced by a marked reduction in frequencies below approximately 10Hz when compared with the original waveforms.

The second order distortion was removed by multiplying the Fourier coefficients of the transformed traces by the corresponding filter constants. The filtered waveforms are presented in Figures 4.9 and 4.10, and the idealised waves are regenerated so exactly that they can be superimposed over the original traces.

4.3.3 Tests 2 and 3: Limitations of the technique

While the preceding test indicates that the filtering technique provides a powerful method for separating out the components of overlapping waveforms, further tests using simulated data identified three conditions under which the solution was less than optimal. These are that:

1. Any DC offset is completely removed by the double running average filter and so cannot be restored by the application of the inverse filter;
2. If the waveform includes a frequency too high for the sampling rate used, distortion occurs as a result of aliasing in the FFT; and
3. Problems of spectral leakage in the FFT can lead to severe distortions in the recovered waveforms.

The first limitation can generally be considered a minor one as any DC offsets of interest can be evaluated easily prior to the restoration procedure and then added to the recovered waveforms. There are, however, conditions under which this limitation can be more problematic, as demonstrated by Test 2 below.

The second limitation results simply from a violation of the sampling theorem as discussed in Section 4.2, and can be avoided if all waveforms are bandlimited at a frequency equal to, or below the folding frequency of the FFT.

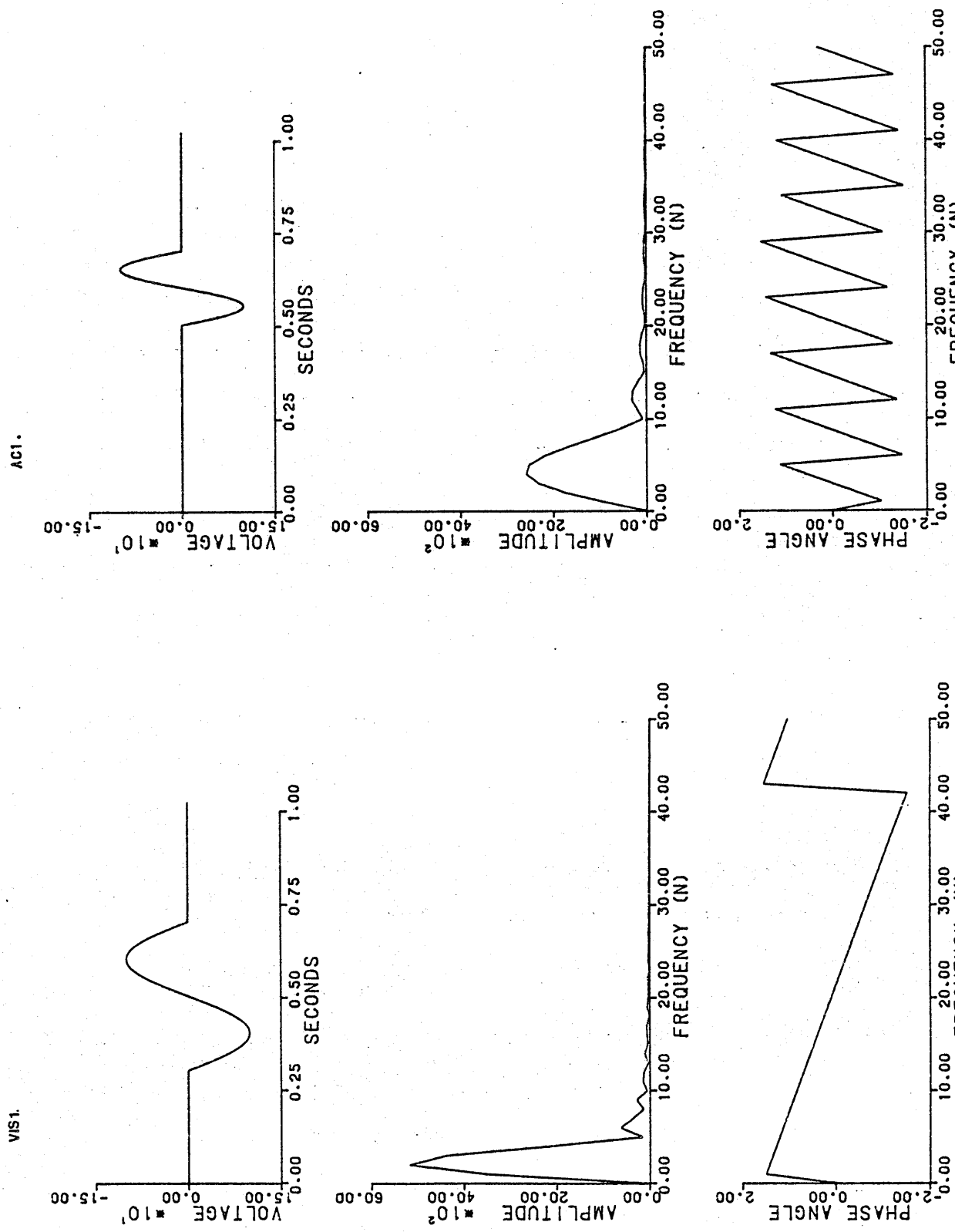

Figure 4.3. Test 1 : Idealised visual response - 2.5Hz.

Figure 4.4. Test 1 : Idealised auditory response - 5Hz.

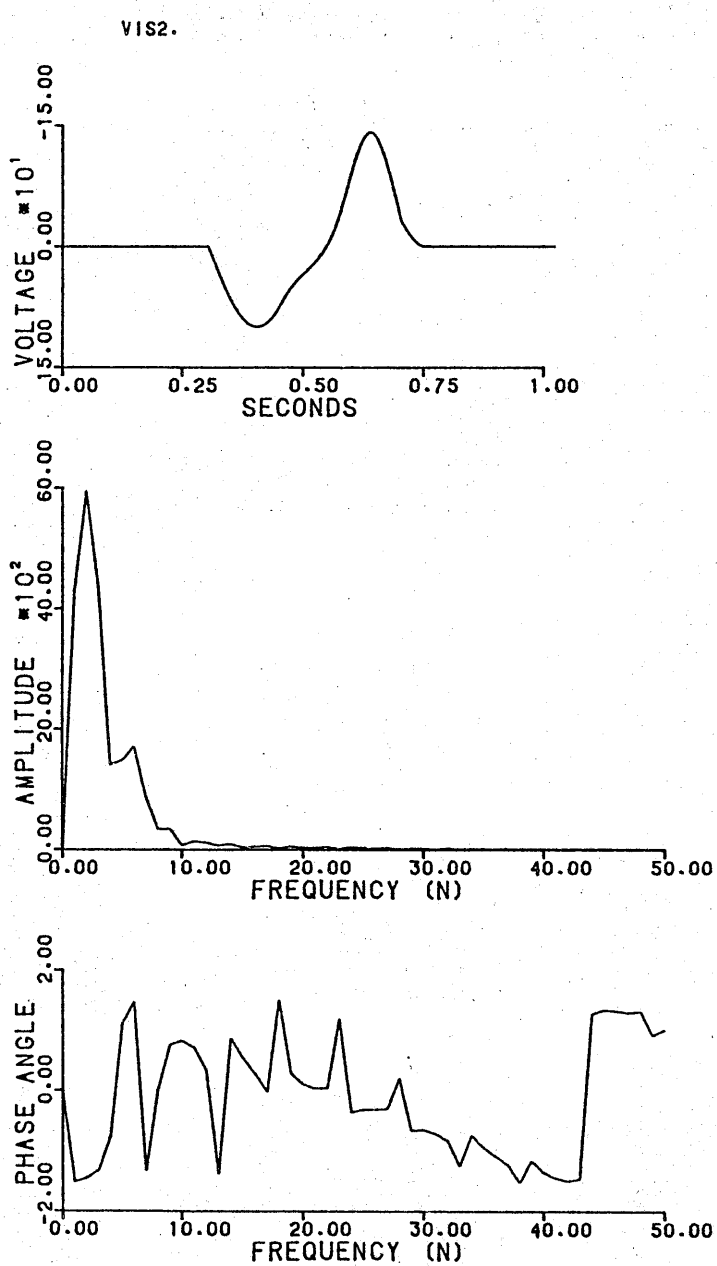

Figure 4.5. Test 1 : Visual response contaminated by the running average of the auditory response.

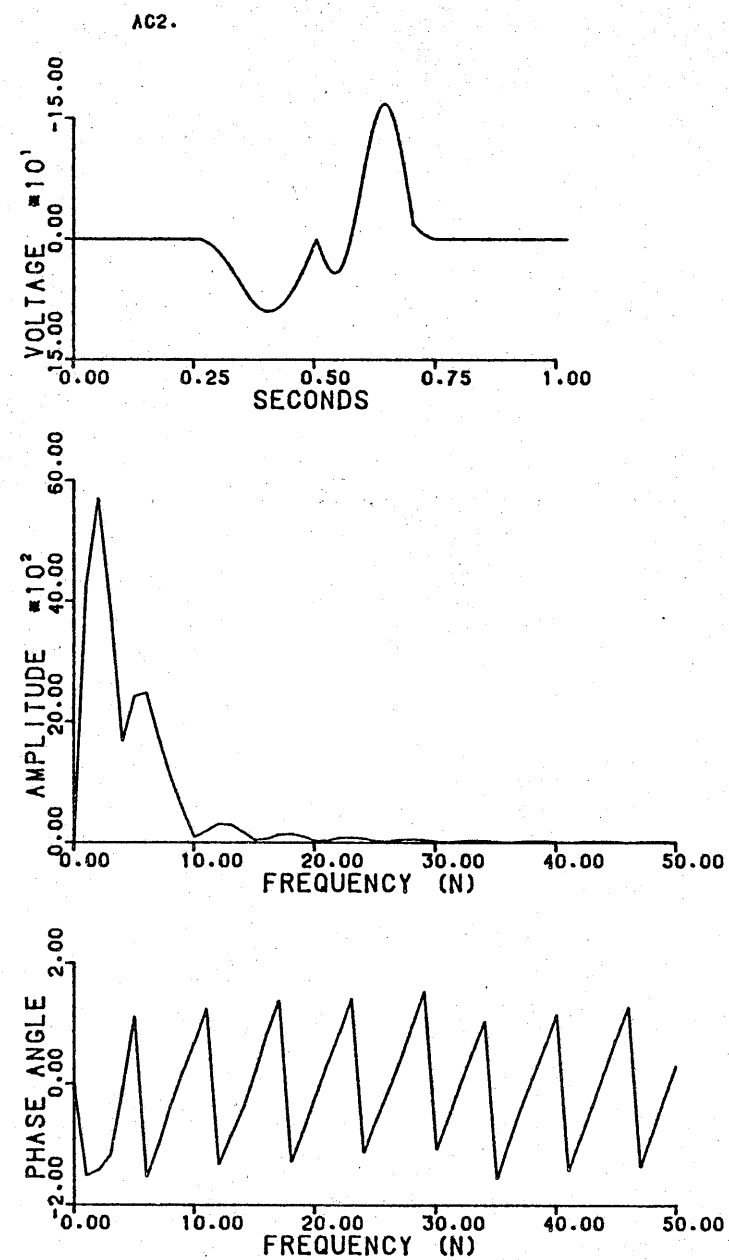

Figure 4.6. Test 1 : Auditory response contaminated by the running average of the visual response.

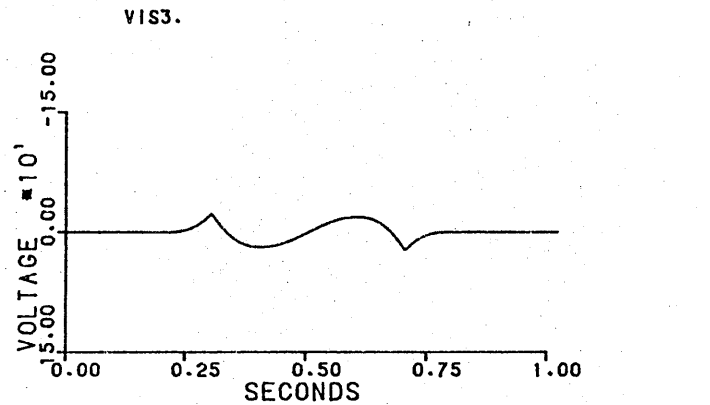

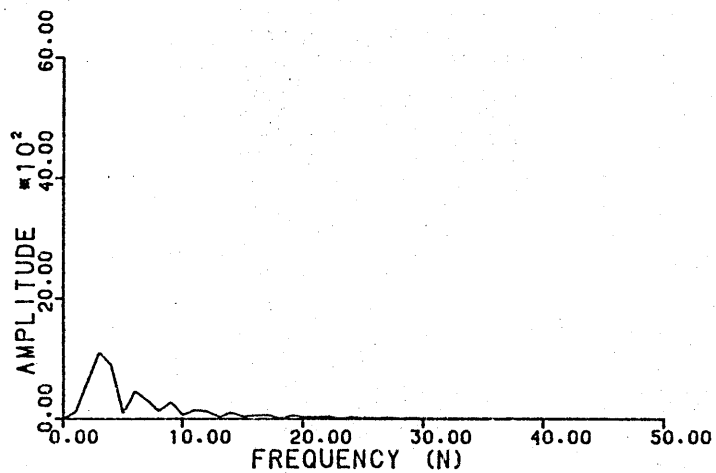

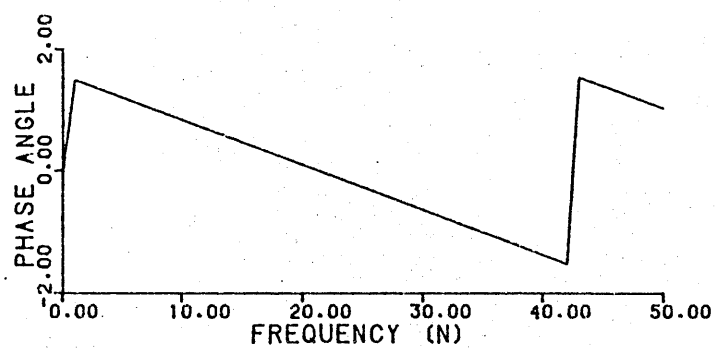

Figure 4.7. Test 1 : Removal of first order distortion from visual trace.

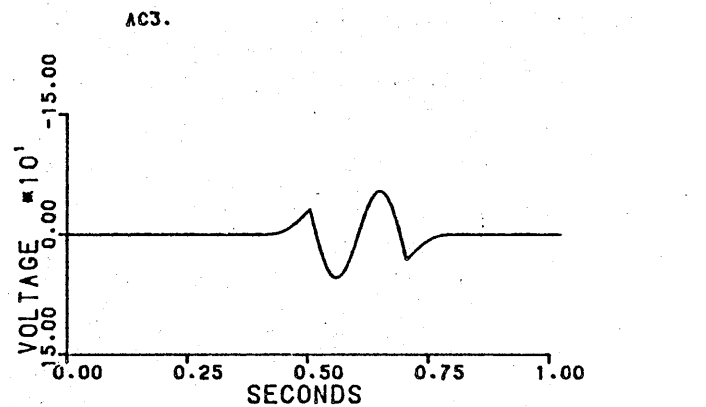

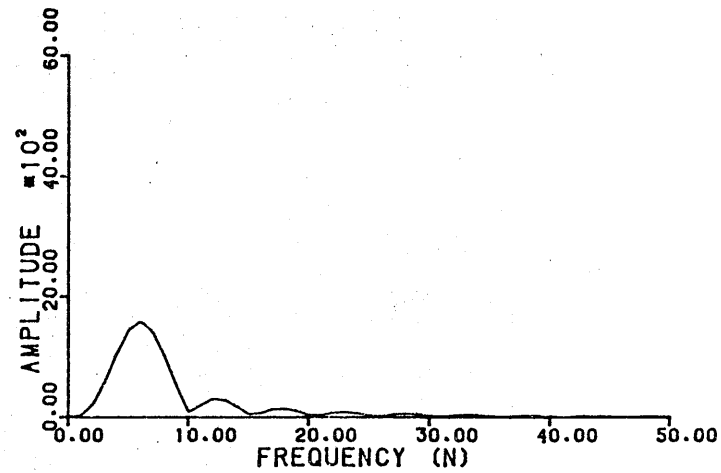

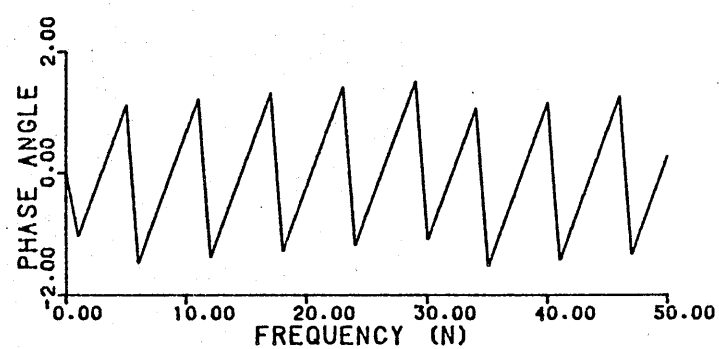

Figure 4.8. Test 1 : Removal of first order distortion from auditory trace.

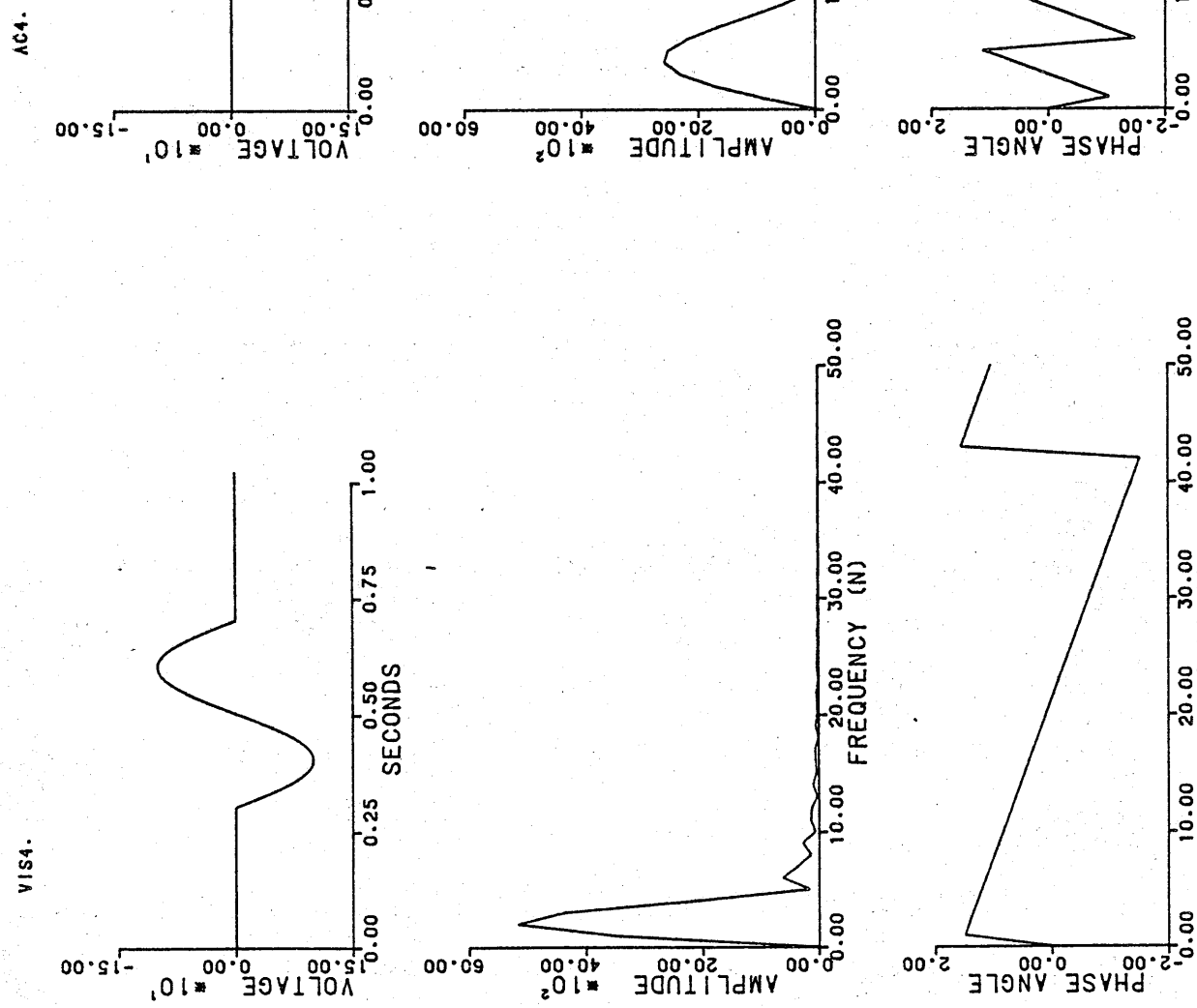

Figure 4.9. Test 1 : Recovered visual response.

Figure 4.10. Test 1 : Recovered auditory response.

The third problem, that of spectral leakage in the FFT, is less easily overcome and occurs if any component of the transformed waveform is of a frequency other than a harmonic of the fundamental frequency of the series. Figures 4.11 to 4.18 illustrate this problem using low frequency test data. VIS1, shown in Figure 4.11, consists of one cycle of a 0.977Hz sinusoid and thereby corresponds to the fundamental frequency of the series. AC1, shown in Figure 4.12, is at a frequency of 0.488Hz which is lower than the lowest frequency resolvable by the FFT. The amplitude spectra of these waveforms demonstrate that whereas the power of VIS1 is localised at the second Fourier coefficient, the power of AC1 is maximal at the first coefficient (OHz) and is leaked across all coefficients up to approximately n = 30.

Figures 4.13 and 4.14 show each waveform contaminated by the running average of the other waveform and Figures 4.15 and 4.16 show the effect of removing the first order distortion. Note the changes in scale of these latter plots, and the marked reduction in amplitude of the first Fourier coefficient for AC3.

Figures 4.17 and 4.18 show the restored waveforms after the application of the inverse filter. While the 'visual' waveform has been restored fully, the 'auditory' waveform is not restored accurately due to the misrepresentation of its component frequencies in the FFT combined with the loss of all 'DC' components resulting from the application of the first filter.

Test 3 (Figures 4.19 to 4.26) provides a second example of the effect of spectral leakage on the accuracy of the filtering procedure, this time using test data at frequencies representative of the highest frequency components of ERPs. The idealised traces shown in Figures 4.19 and 4.20 are of 12.5Hz and 25Hz, respectively.

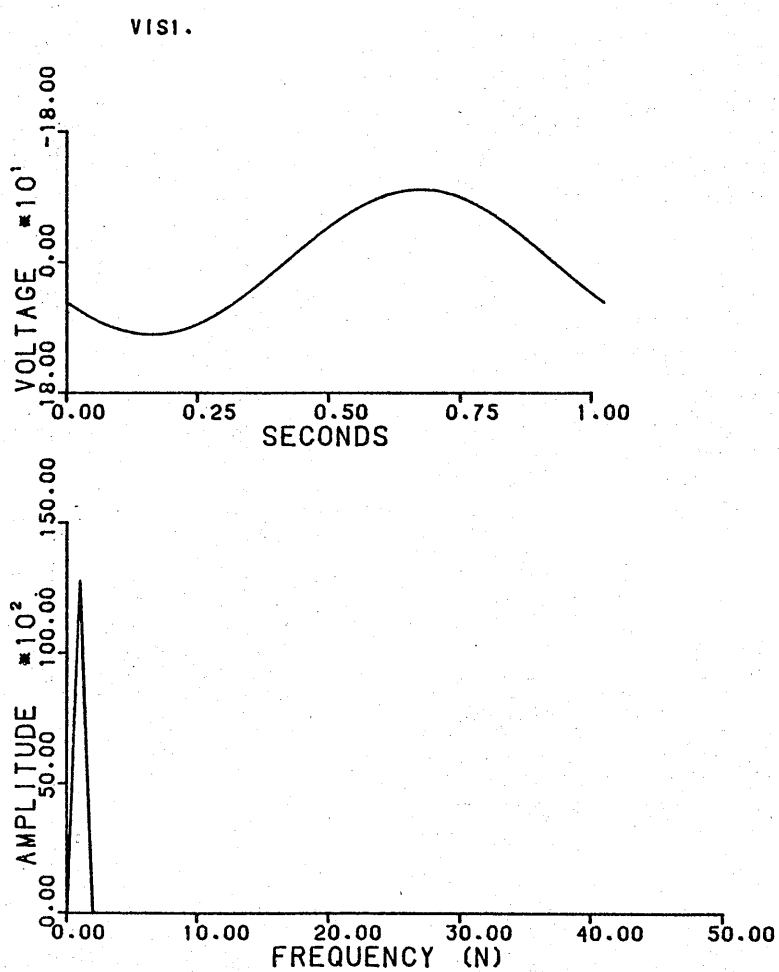

Figure 4.11. Test 2 : Idealised visual response - 0.977Hz.

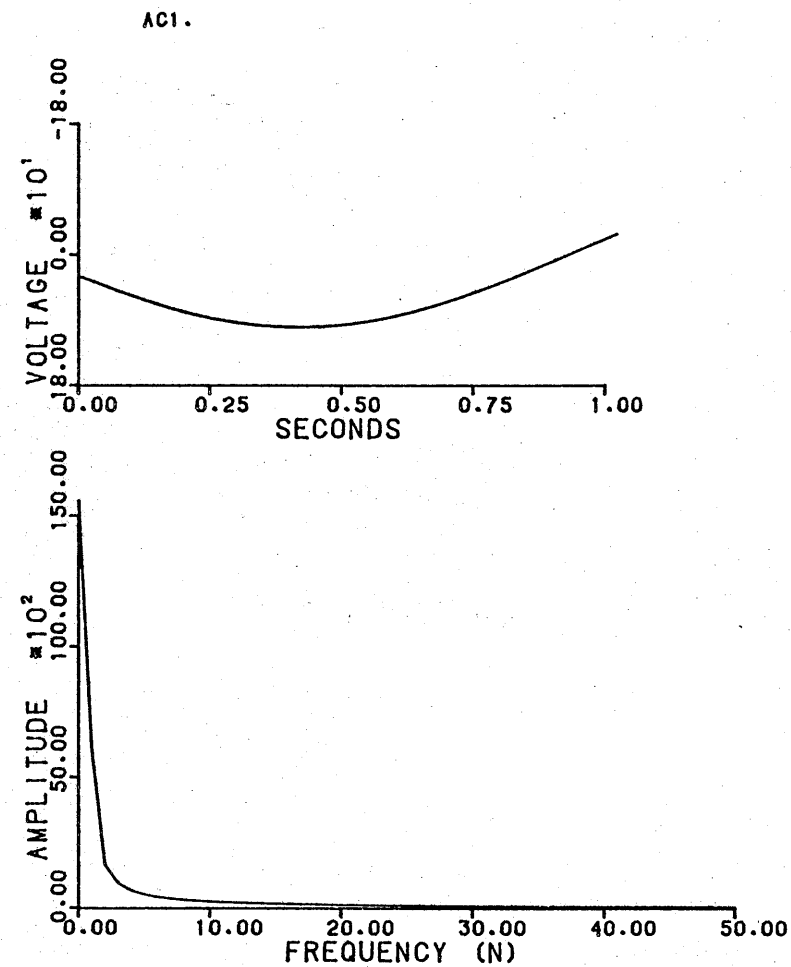

Figure 4.12. Test 2 : Idealised auditory response - 0.488Hz.

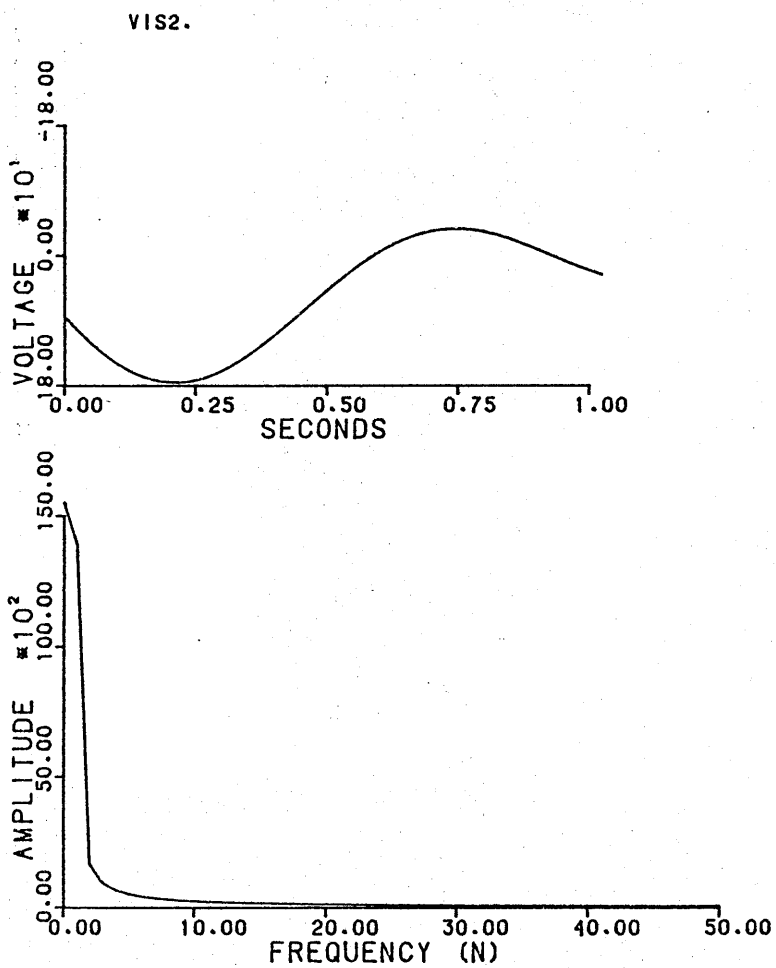

Figure 4.13. Test 2 : Visual response contaminated by the running average of the auditory response.

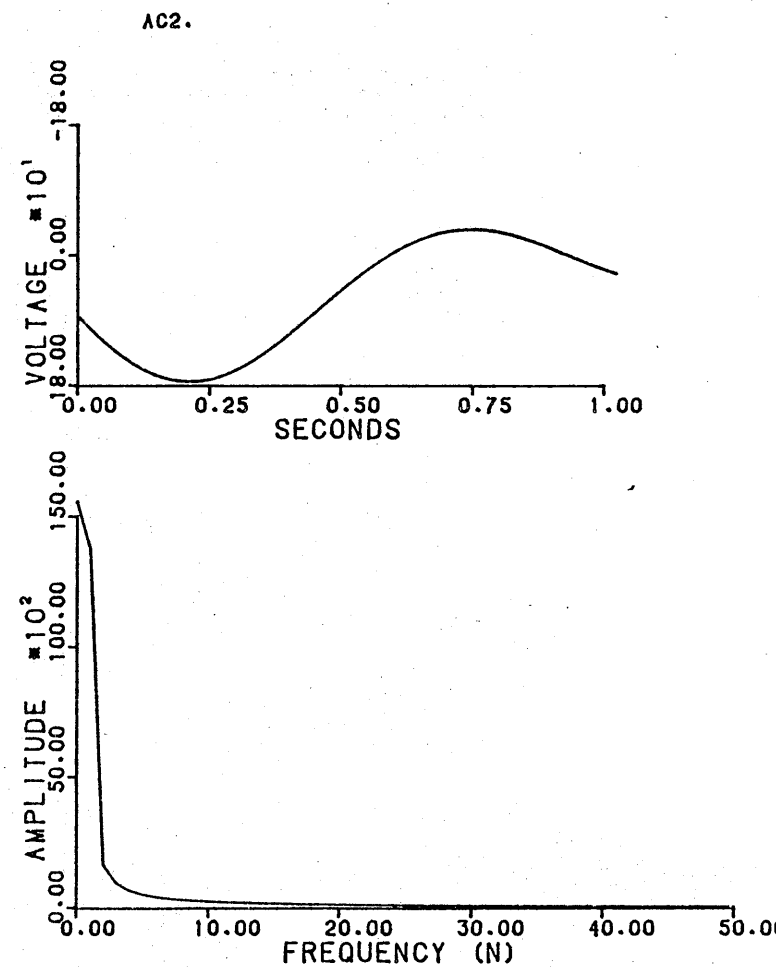

Figure 4.14. Test 2 : Auditory response contaminated by the running average of the visual response.

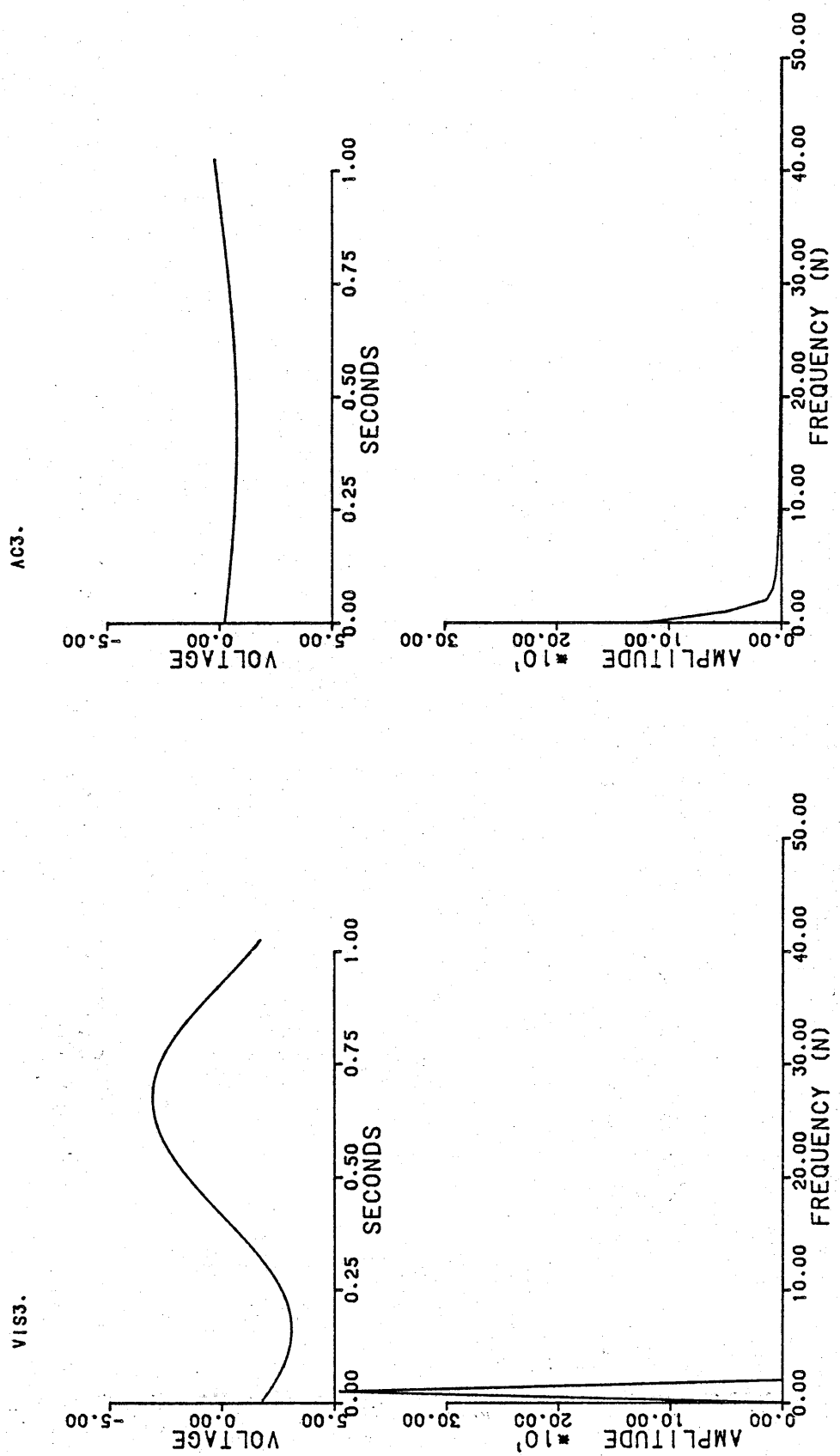

Figure 4.15. Test 2 : Removal of first order distortion from visual trace.

Figure 4.16. Test 2 : Removal of first order distortion from auditory trace.

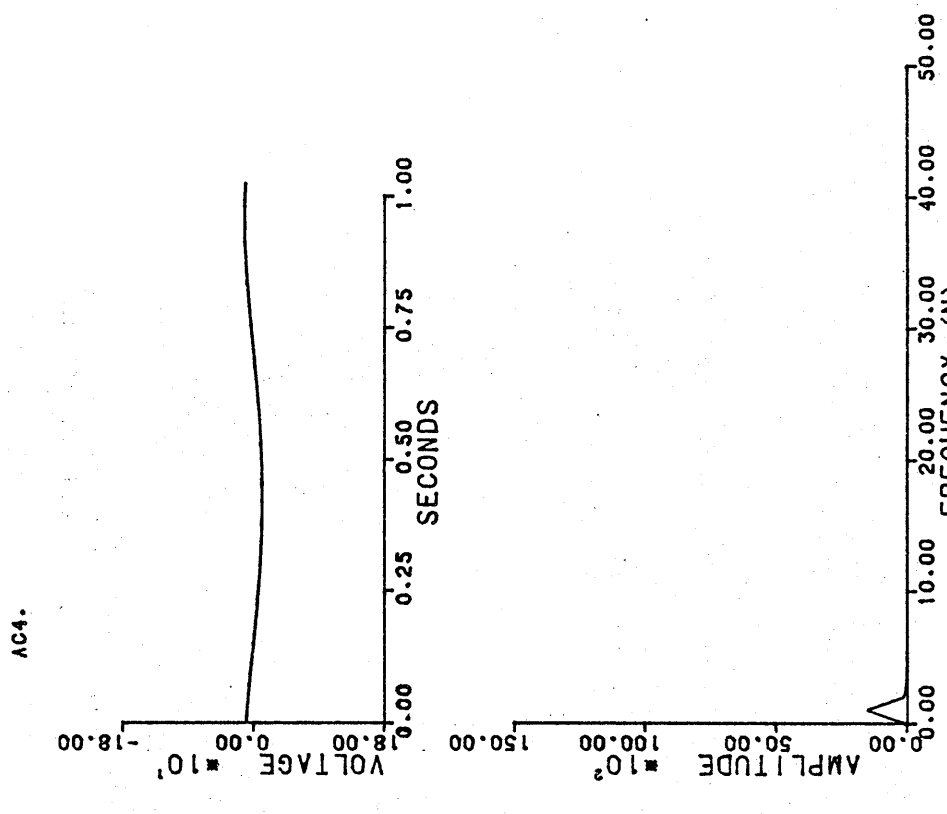

Figure 4.18. Test 2 : Recovered auditory response.

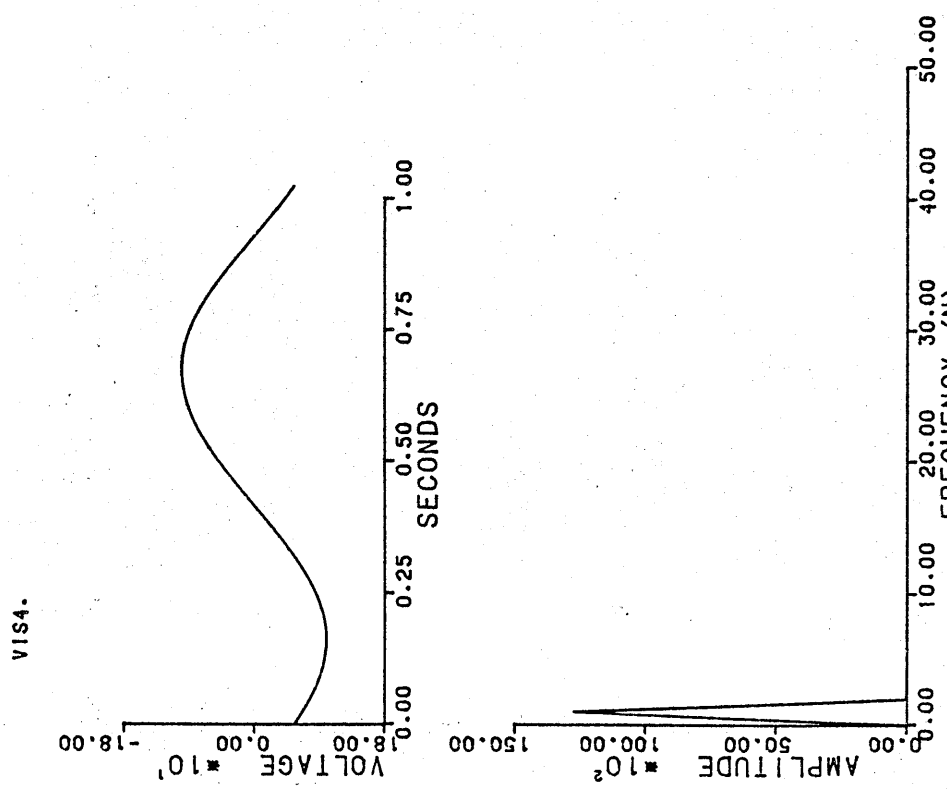

Figure 4.17. Test 2 : Recovered visual response.

Spectral leakage is evident in the amplitude spectra of both idealised waveform and the power of each waveform is leaked across all Fourier coefficients up to and beyond n = 50. Figures 4.21 and 4.22 show each trace contaminated by the staggered version of the other trace and the contribution of this 'first order' distortion is clearly evident in the corresponding amplitude spectra.

Figures 4.23 and 4.24 show the effect of removing the first order distortion. The relatively high frequencies of the original waveforms mean that these signals are only mildly affected by the double running average filter. However, application of the inverse filter (Figures 4.25 and 4.26) enhances the spurious low frequency content of the FFT and results in a gross misrepresentation of the idealised waveforms.

Therefore, spectral leakage, particularly into the lower frequency components of the FFT, constitutes a serious problem for the accurate estimation of the wanted waveforms.

The problem of spectral leakage is inherent in all procedures which depend on DFT or FFT analysis and results from the fact that the input waveform is of a finite rather than an infinite duration (see Section 4.2). Two techniques can be employed to reduce the degree of spectral leakage. The first is to increase the duration of the input time series and hence increase the frequency resolution in the FFT. As the time series approaches infinity spectral leakage will be eliminated completely. Clearly, this is an uneconomical solution, and impractical if only short data records are available. An alternative approach is to utilize 'windowing' procedures, whereby a non-uniform data window is applied to the time series. The window smoothly brings the data to zero at the boundaries and consequently forces all component frequencies to be periodic within the time span available. In the

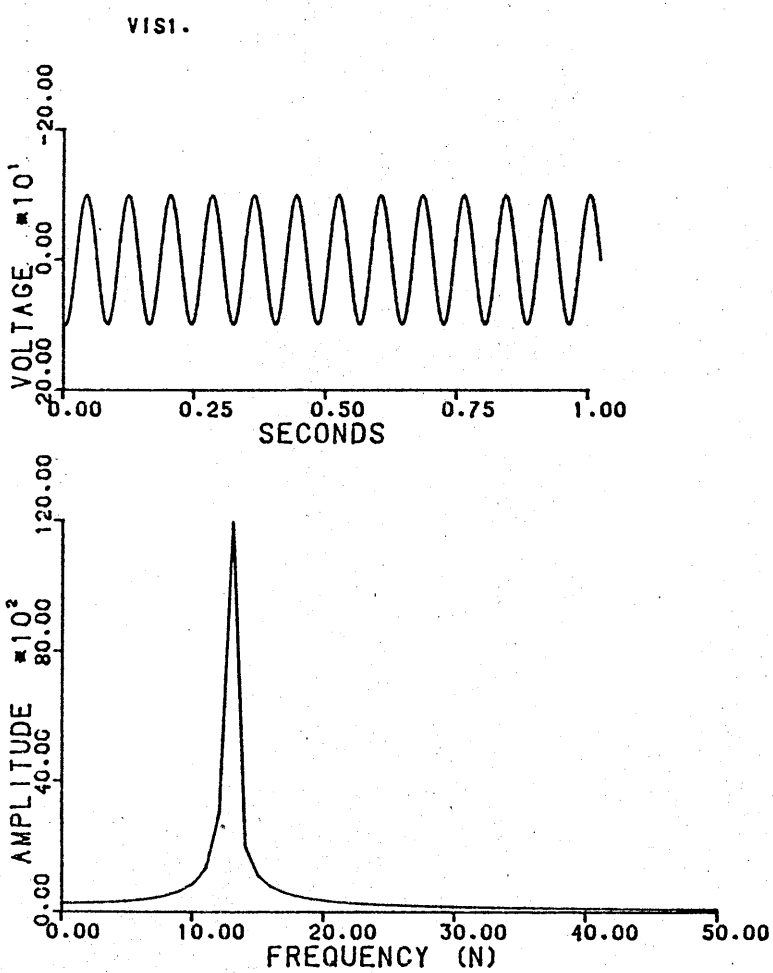

Figure 4.19. Test 3 : Idealised visual response - 12.5Hz.

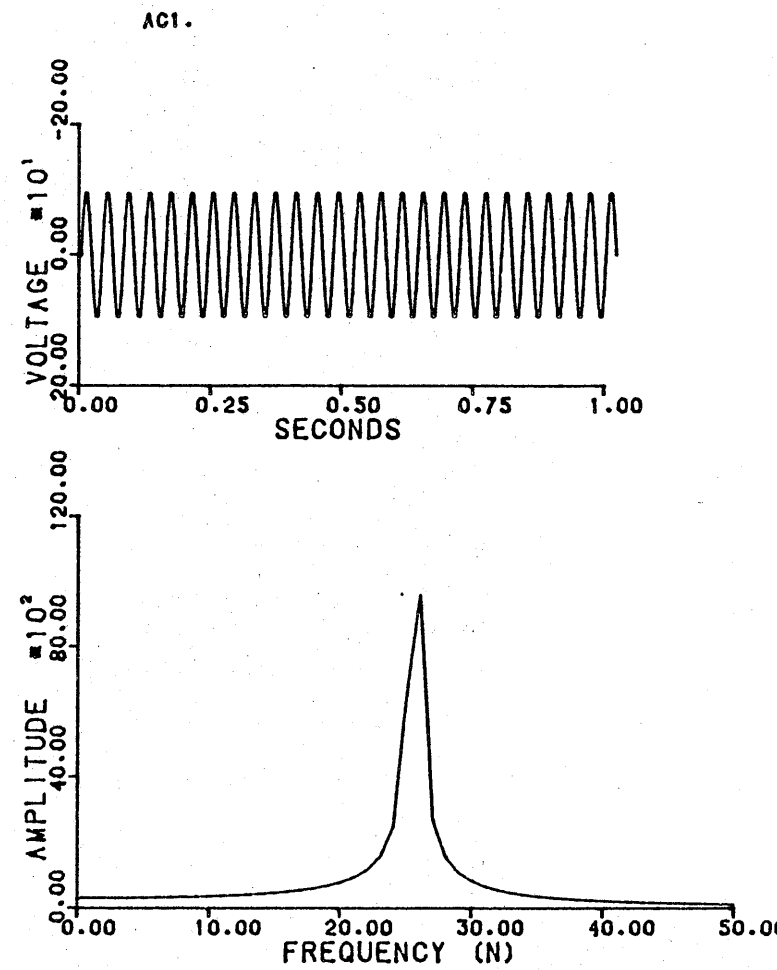

Figure 4.20. Test 3 : Idealised auditory response - 25Hz.

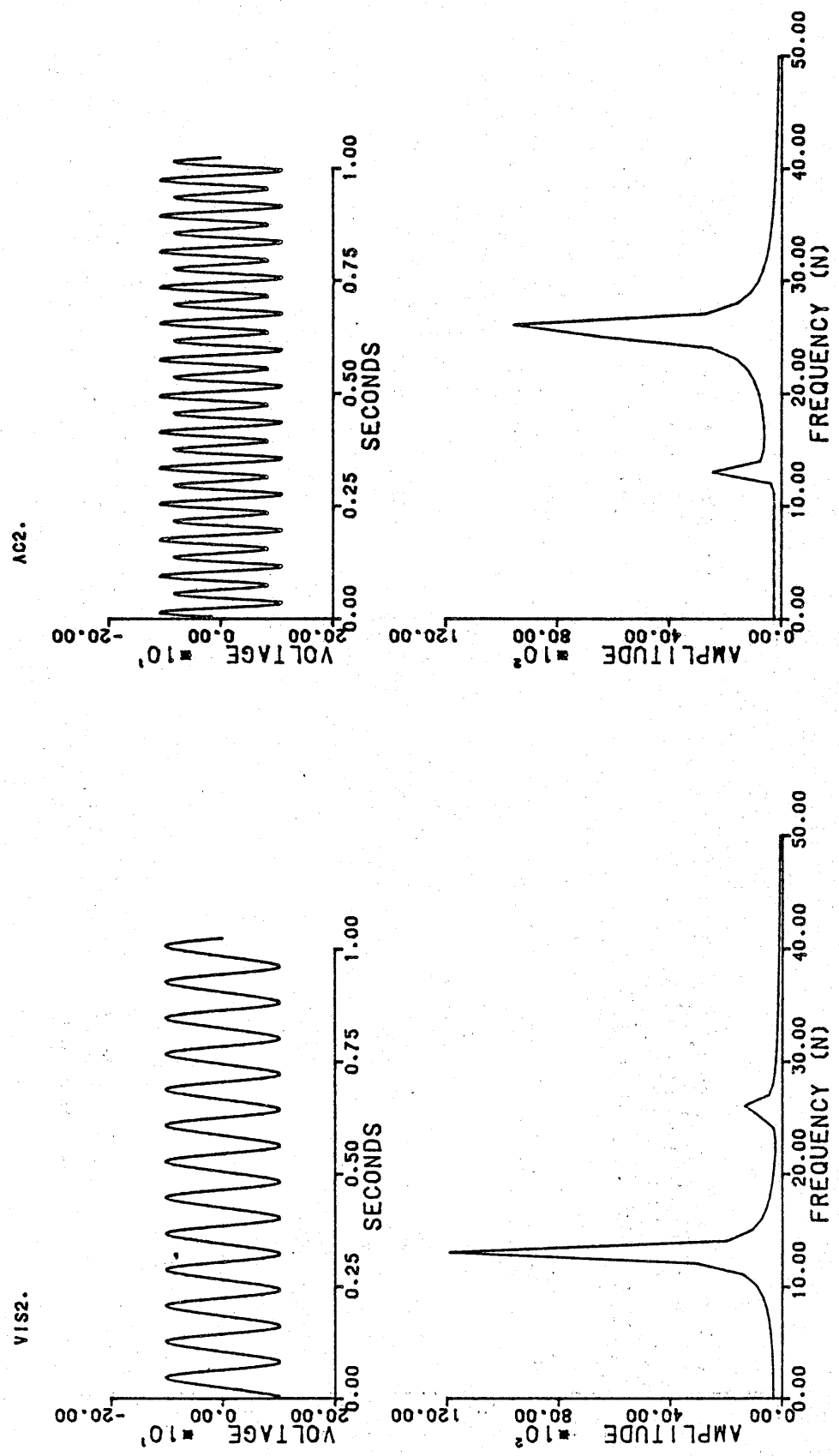

Figure 4.21. Test 3 : Visual response contaminated by the running average of the auditory response.

Figure 4.22. Test 3 : Auditory response contaminated by the running average of the visual response.

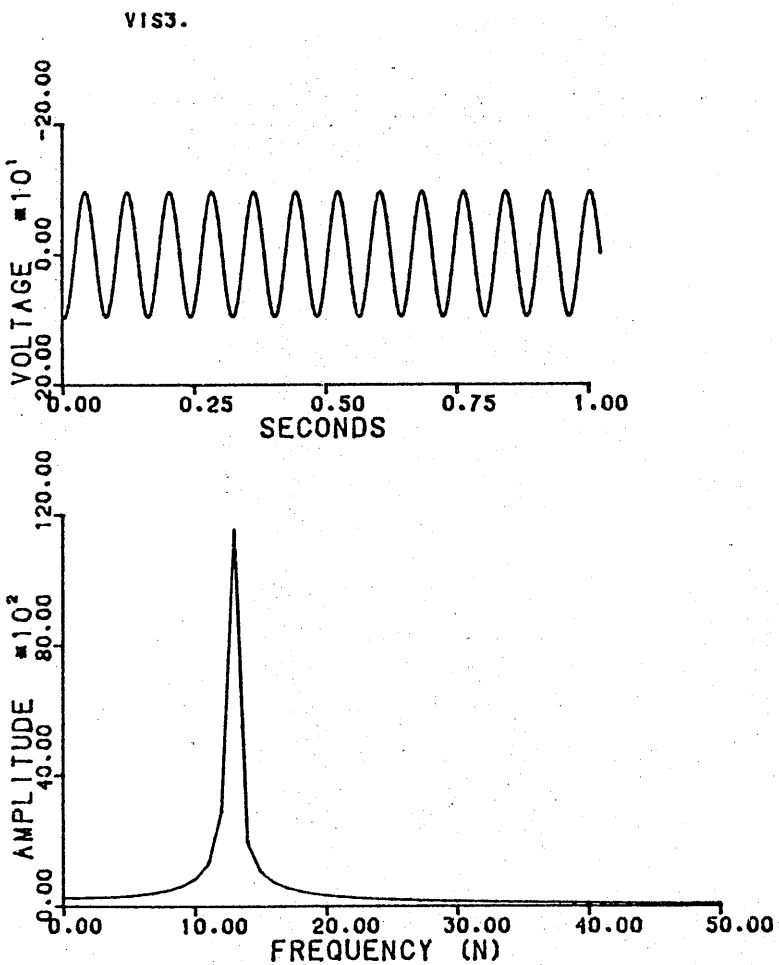

Figure 4.23. Test 3 : Removal of first order distortion from visual trace.

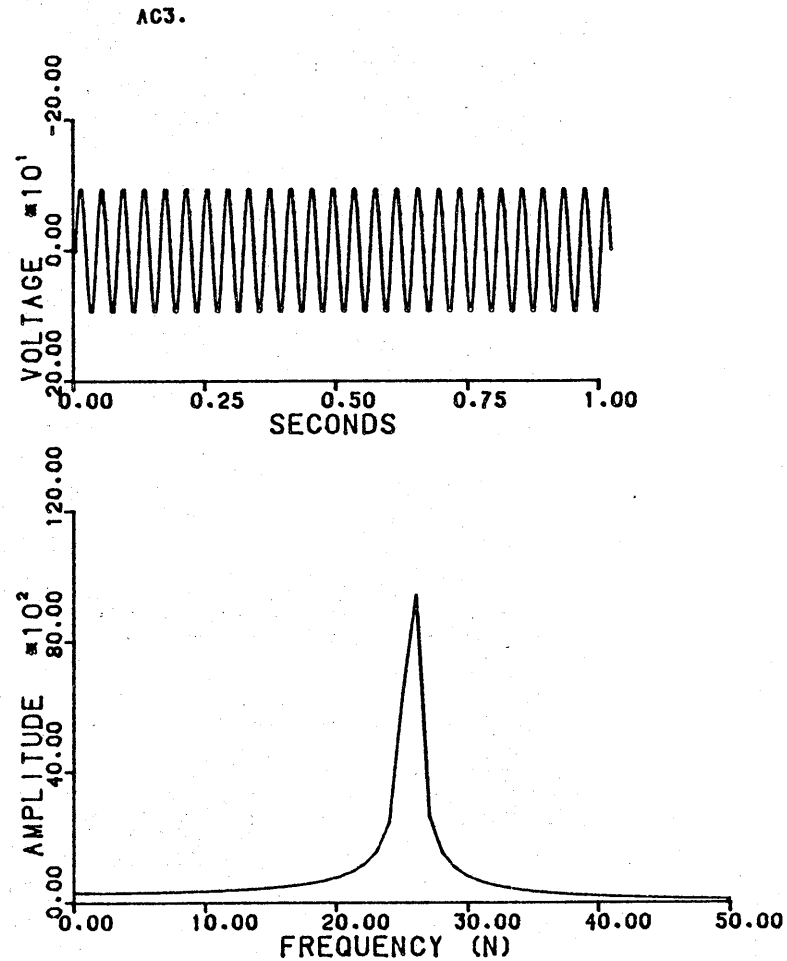

Figure 4.24. Test 3 : Removal of first order distortion from auditory trace.

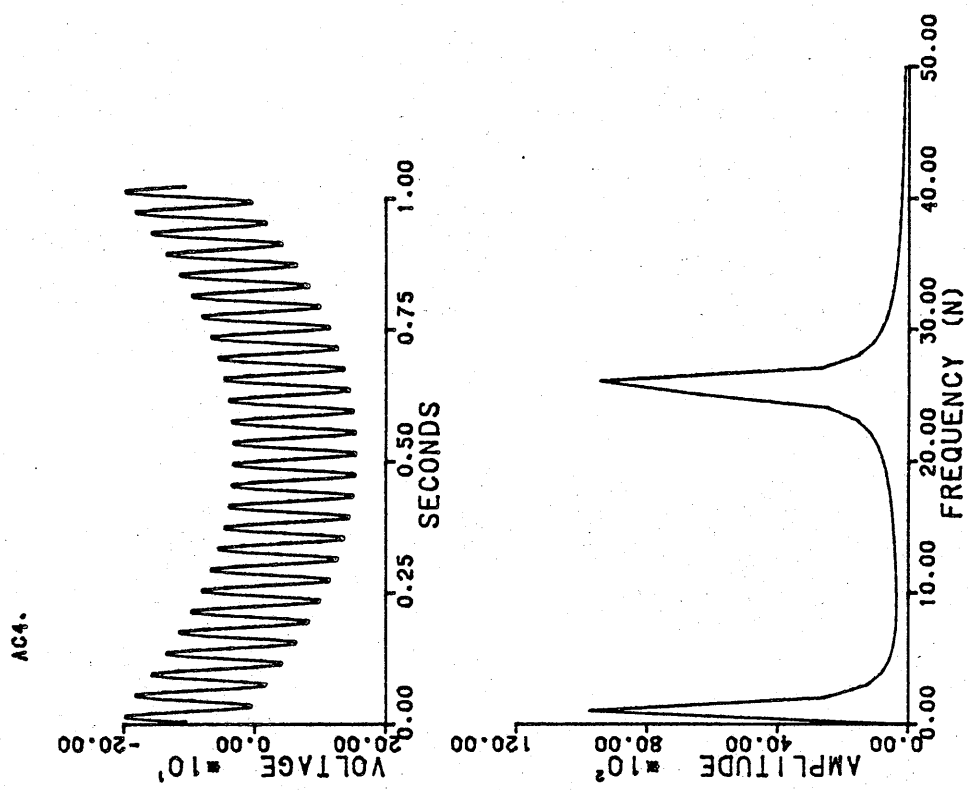

Figure 4.26. Test 3 : Recovered auditory response.

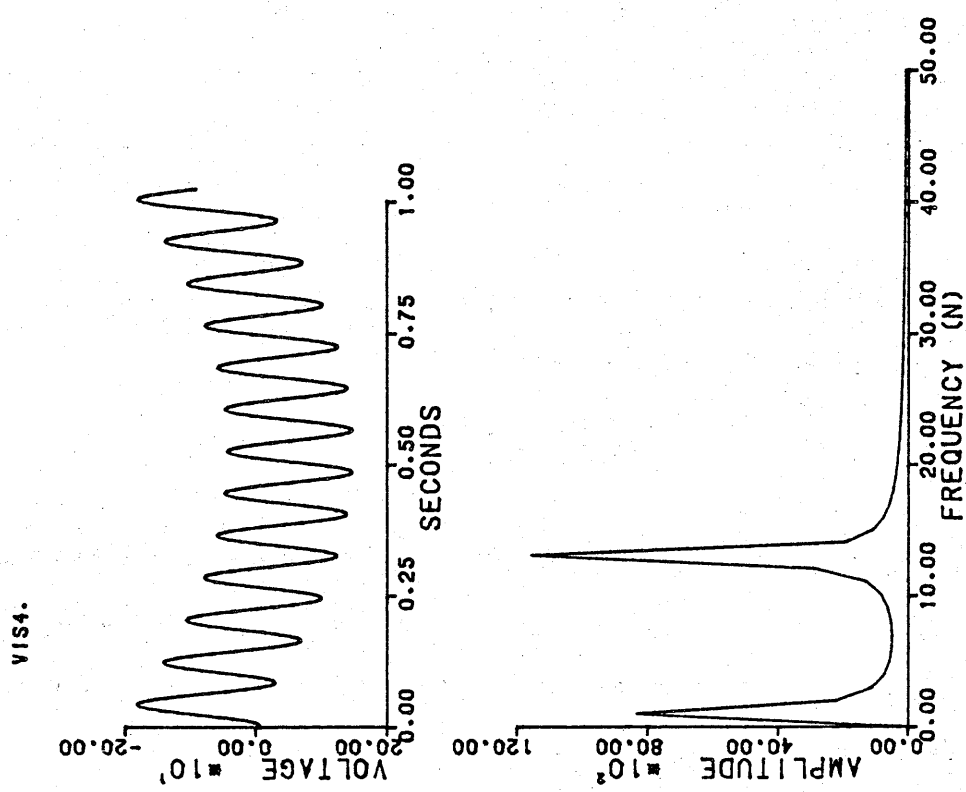

Figure 4.25. Test 3 : Recovered visual response.

frequency domain the effect of windowing is to localise the contribution of a given frequency by reducing the amount of leakage through the sidelobes of the transformed window. Hence a window is chosen which has lower sidelobes in the frequency domain than the rectangular data window. The penalty for the reduction in sidelobes, however, is a broadening of the mainlobe of the window transform which results in a decrease in the resolution of the spectral estimate.

Harris (1978) provides a comprehensive description and comparison of the performance of data windows for use with the DFT or FFT. A data window commonly used for the application of digital filters is the Hanning or raised cosine window as it can be applied to data conveniently either in the time domain or the frequency domain (Harris, 1978, p.62). Figures 4.27 and 4.28 present the time domain and frequency domain representation of the rectangular and Hanning data windows, respectively. The spectral transform of the Hanning window demonstrates a marked decrease in sidelobe levels when compared with that of the rectangular window, but also shows an increase in the width of the main lobe, indicating its poorer resolution.

The Hanning window for application in the time domain prior to the DFT or FFT is defined by:

$$w(n) = \sin^2\left[\frac{n}{N}\pi\right] = 0.5\left[1.0-\cos\left[\frac{2n}{N}\pi\right]\right] \qquad n = 0,1,2,\ldots,N-1 \qquad \{4.16\}$$

Figures 4.29 and 4.30 demonstrate the application of the Hanning window to those time series presented in Figures 4.23 and 4.24. Each value of these latter traces was multiplied by the corresponding value of the Hanning window calculated from equation {4.16} for N = 256. The data then were filtered in the usual way.

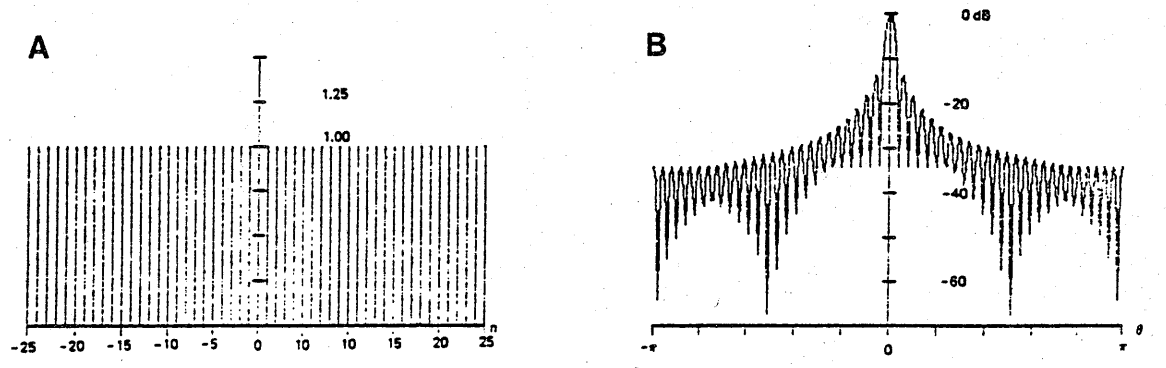

Figure 4.27. A: Rectangular window; B: Log-magnitude of Fourier transform (After Harris, 1978).

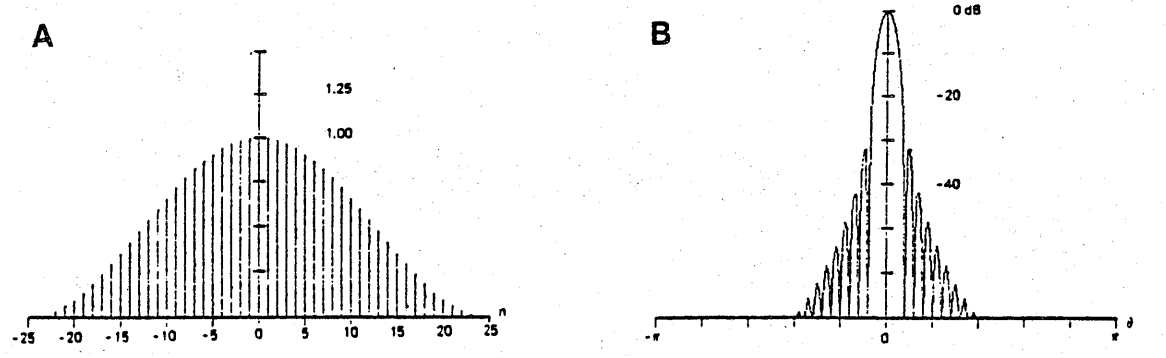

Figure 4.28. A: Hanning window; B: Log-magnitude of Fourier transform (After Harris, 1978).

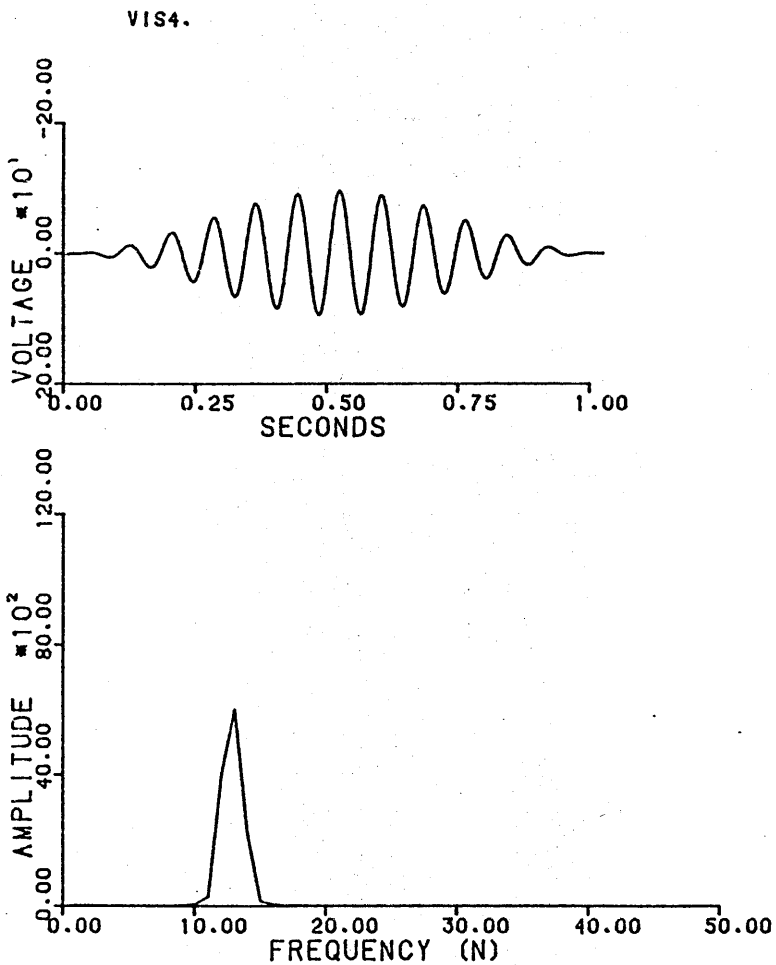

Figure 4.29. Test 3 : Recovered visual response following application of the Hanning data window.

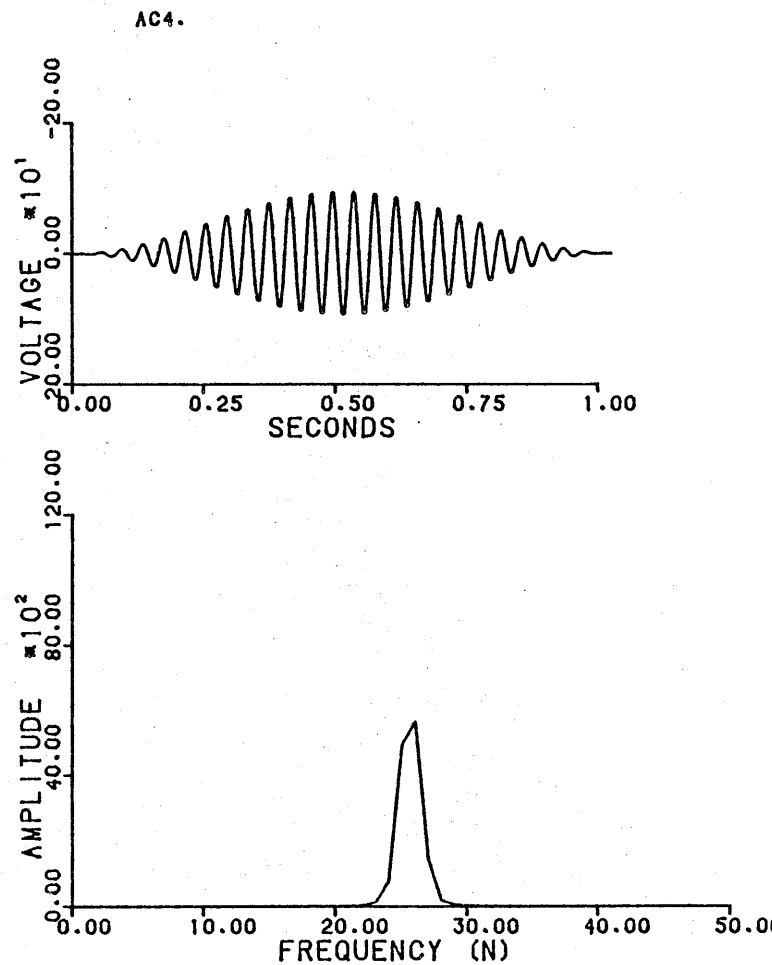

Figure 4.30. Test 3 : Recovered auditory response following application of the Hanning data window.

A striking effect due to the application of the window is that a significant proportion of the recovered time series is 'lost' due to the window progressively reducing the input series to zero at the boundaries. This loss, however, can be partially overcome through the use of overlapping analysis (see Harris, 1978, p.56).

More importantly, the application of the Hanning window has effectively confined the spectral estimates to frequencies above those affected by the inverse filter. Note, however, that the frequency representation of the recovered waveforms is still biased. The spectral estimates are not restricted to a single Fourier coefficient but rather are spread over a range of approximately 5Hz. This results from the decreased resolution due to the data window, together with the residual effects of spectral leakage through its sidelobes. This misrepresentation is of little importance in the present example, but does have serious implications for the accurate recovery of low frequency signals such as those characterized by the middle and late components of the ERP.

4.3.4 Test 4: The effects of the solution on the noise component of ERP waveforms

The above tests considered the limitations of the filtering solution using simulated data which were noise-free. The present test was designed specifically to examine the ways in which random disturbances due to interference and noise are affected by the filtering procedures.

The first part of the test considered the effects of the filtering procedures on noise alone, with no signal added. The second part of the test involved the recovery of idealised visual and auditory responses following the addition of noise to those simulated time-locked visual and auditory traces used in Test 1 (Figures 4.5 and 4.6).

Random normal deviates having a mean of zero and a standard deviation of 50 were generated using pseudo-random number generator routines from the Numerical Algorithms Group subroutine library. Twenty-five different sequences of 304 random numbers were generated, each sequence simulating the noise component recorded over a single experimental trial. The noise contribution to time-locked visual traces was derived simply by aligning the twenty-five sequences and then calculating the average value of every coincident ordinate. The resultant trace is presented in Figure 4.31, labelled VIS2. The same twenty-five sequences then were used to simulate noise contributing to time-locked auditory traces. This was achieved by staggering the start of each sequence with respect to the previous sequence over a window of twenty-five samples. The average of every coincident ordinate then was calculated and the resultant trace of 328 values was truncated to 304 values by removing the last 24 data points. Figure 4.32, labelled AC2, show this 'auditory' noise component. Both visual and auditory noise components, therefore, were derived from identical data but the latter trace was subjected to the same data collection procedures used to generate time-locked auditory averages.

The Fourier representation of both traces is generally uniform across all frequencies, reflecting the 'white noise' structure of these processes, and the only obvious effect due to the staggering procedure is the alteration in phase of AC2 compared with that of VIS2. Due to the frequency characteristics of the noise, however, it can be assumed that both Fourier representations are contaminated by spectral leakage at all frequencies.

The traces presented in Figures 4.31 and 4.32 were staggered over twenty-five samples and each staggered trace was subtracted from the unstaggered version of the other trace. The results of these

subtractions are shown in Figures 4.33 and 4.34. It is evident that the double running average filter, applied through the subtraction process, only midly affects the frequency composition of both traces below 10Hz, but that the application of the inverse filter (Figures 3.35 and 3.36) introduces a low frequency distortion of differing phase into both noise processes. The effect of the filtering solution on noise, therefore, is to amplify low frequency components resulting from spectral leakage into the FFT.

Figures 4.37 and 4.38 show the addition of the simulated noise processes presented in Figures 4.31 and 4.32 to those simulated time-locked visual and auditory traces presented in Figures 4.5 and 4.6, respectively. Figures 4.39 and 4.40 show the visual and auditory traces following removal of the first order distortion through the subtraction process, and Figures 4.41 and 4.42 show the recovered visual and auditory responses following the application of the inverse filter. Distortion in both recovered waveforms is evidenced by a low frequency baseline shift. The source of these low frequency distortions was assessed by subtracting the respective idealised waveform (Figures 4.3 and 4.4) from these recovered visual and auditory responses. The results of these subtractions were identical to the 'recovered' visual and auditory noise submitted to the filtering procedure in the absence of any signal (Figures 3.35 and 3.36). Thus the filtering procedures act independently on both the signal and noise components of waveforms submitted to the solution, and both outputs combine additively to produce the recovered waveforms. The implication of this finding is that distortions in the recovered waveforms resulting from noise and interference will be inversely related to the signal to noise ratio of those waveforms submitted to the filtering solution.

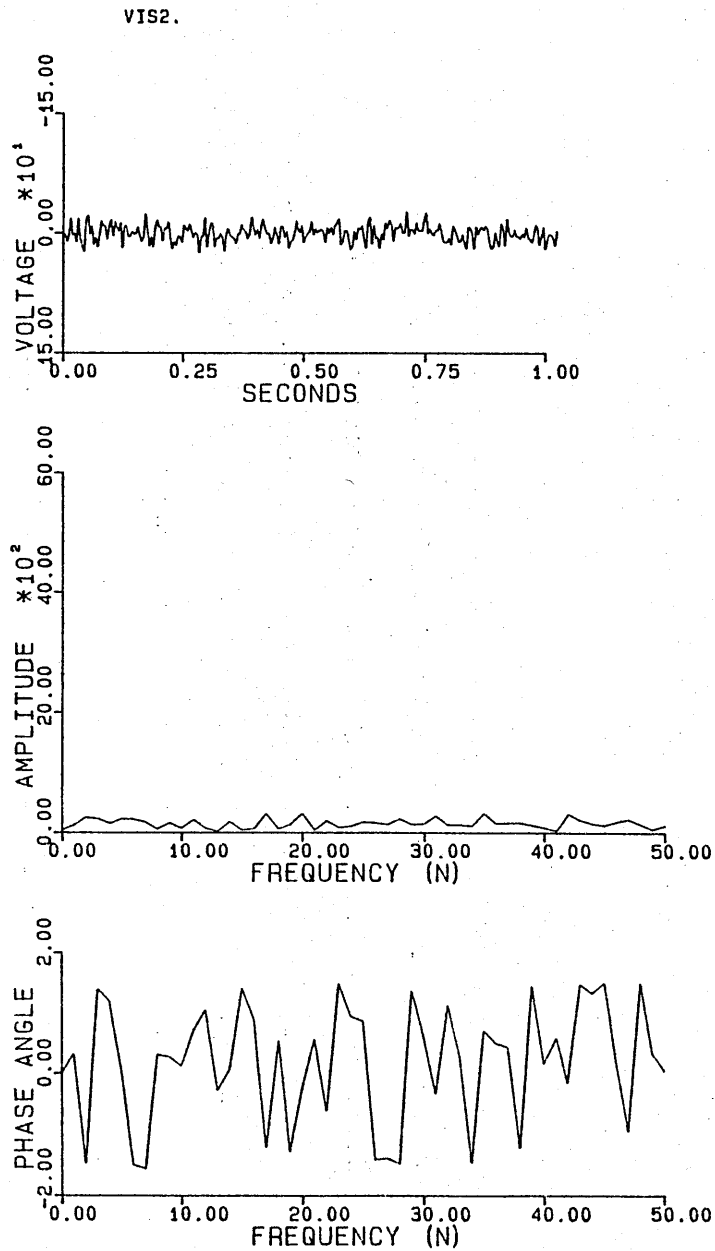

Figure 4.31. Test 4 : Simulated noise contributing to time-locked visual trace.

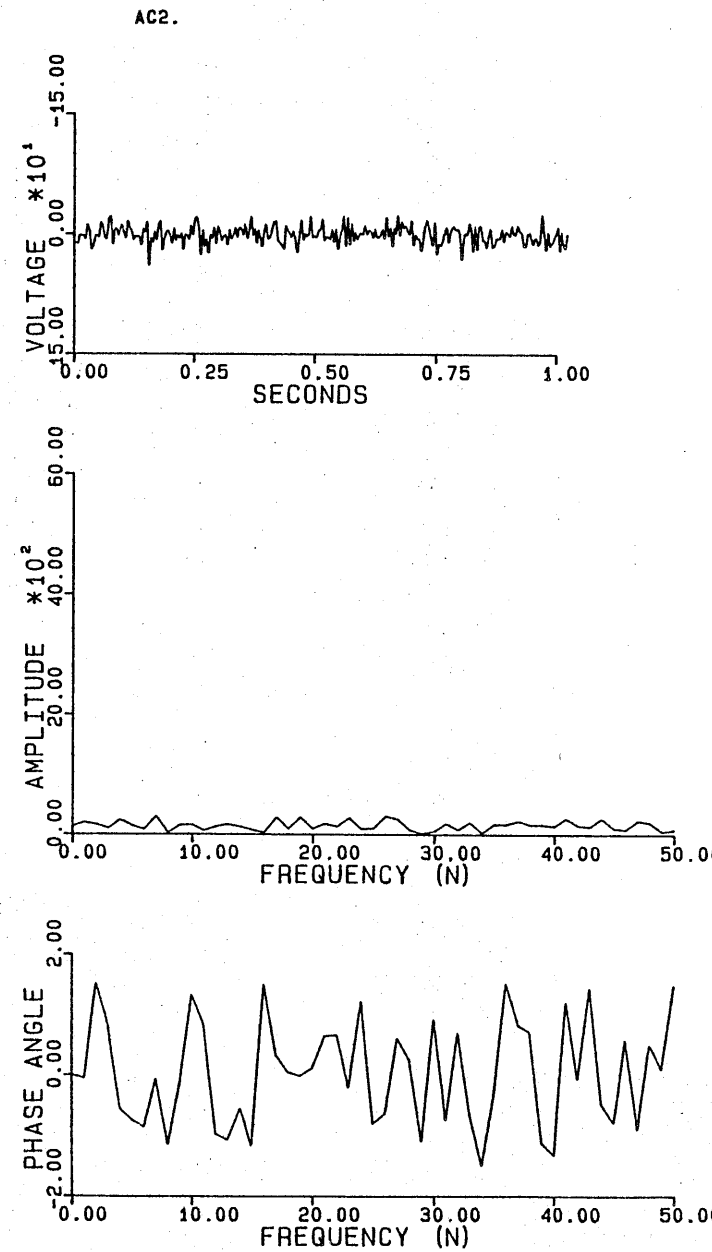

Figure 4.32. Test 4 : Simulated noise contributing to time-locked auditory trace.

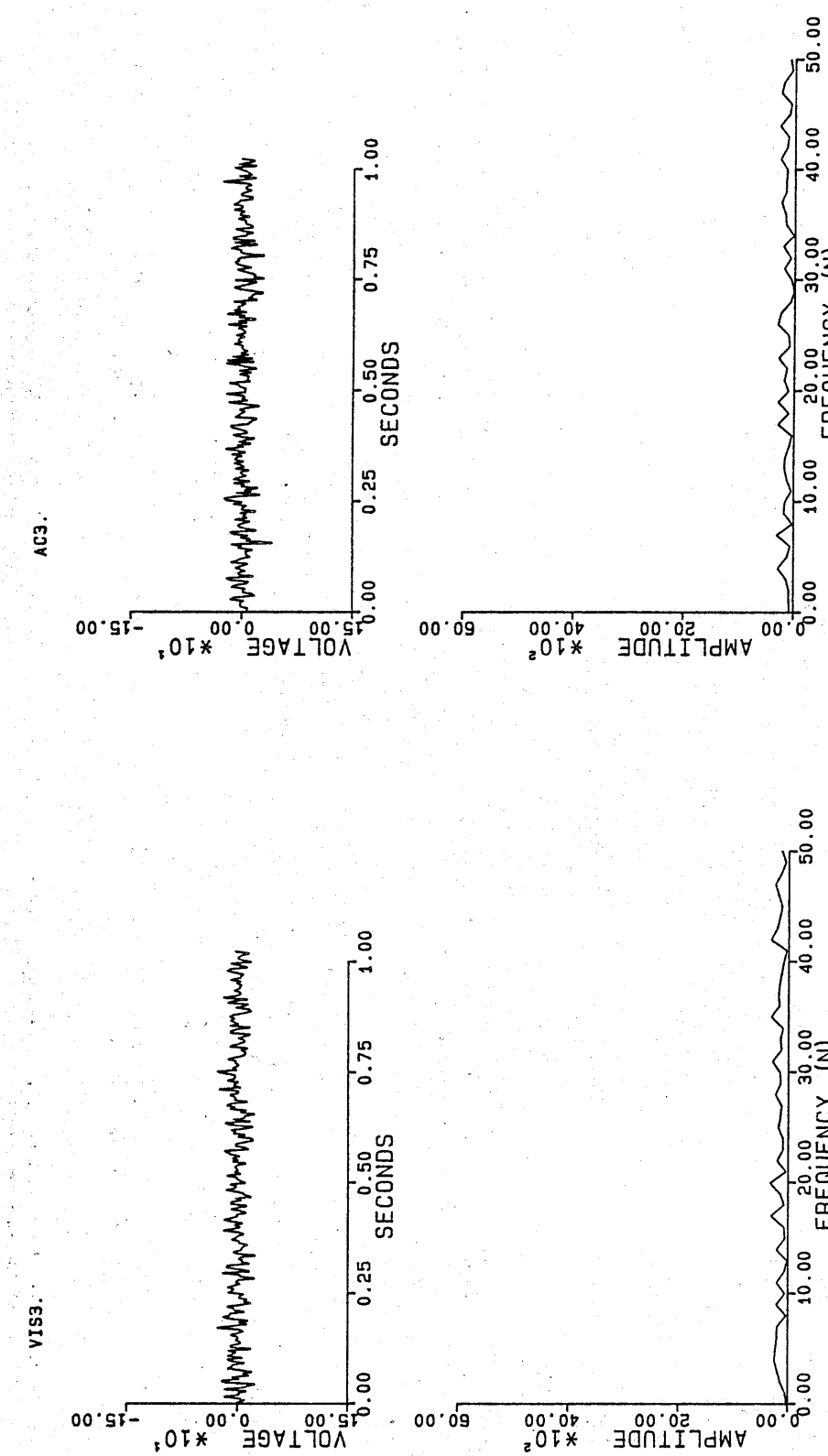

Figure 4.33. Test 4 : Visual noise following the removal of first order distortion.

Figure 4.34. Test 4 : Auditory noise following the removal of first order distortion.

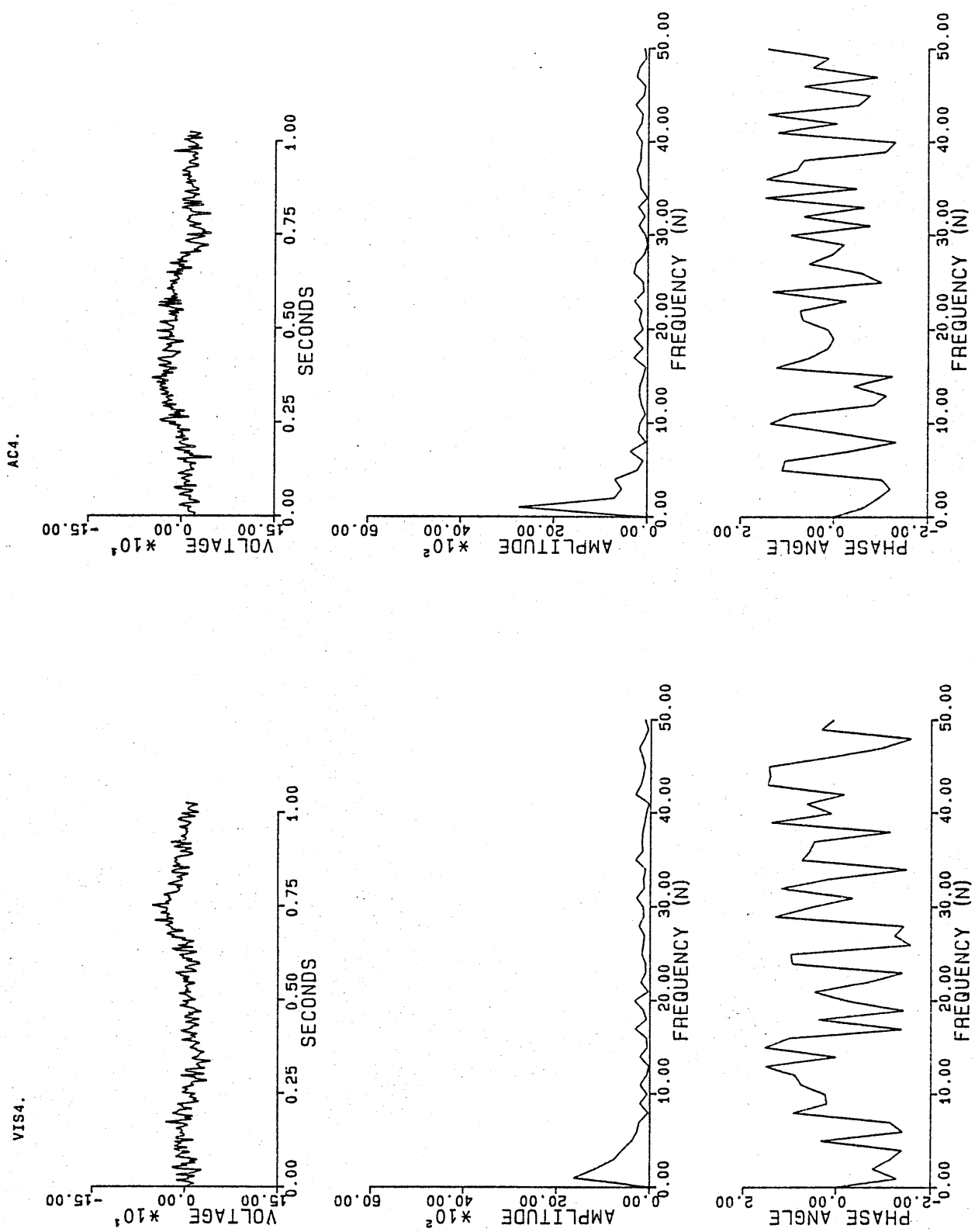

Figure 4.35. Test 4 : Visual noise following application of the inverse filter.

Figure 4.36. Test 4 : Auditory noise following application of the inverse filter.

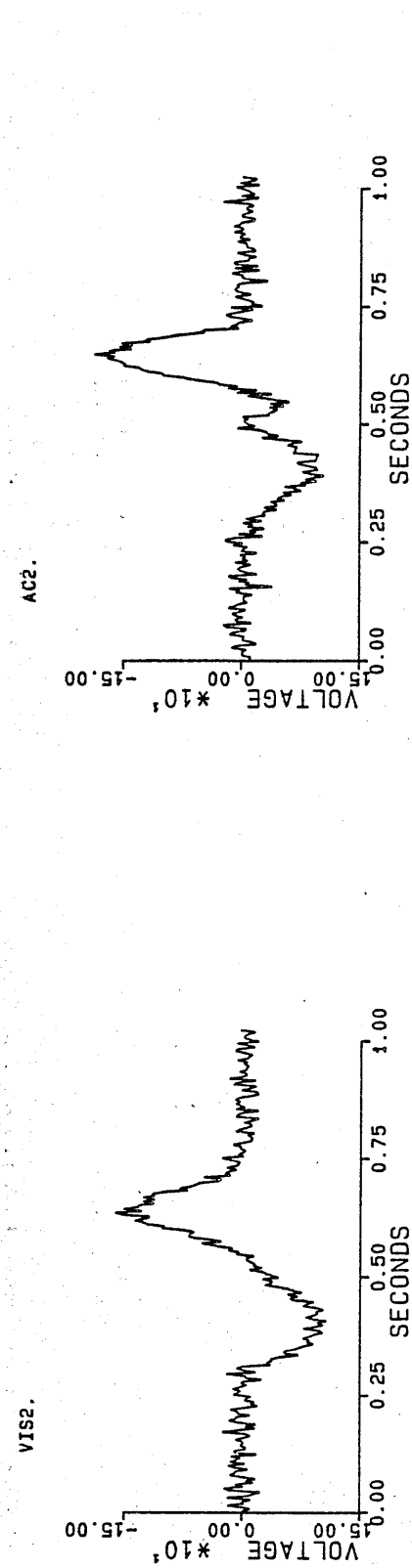

Figure 4.37. Test 4 : Time-locked visual trace plus visual noise.

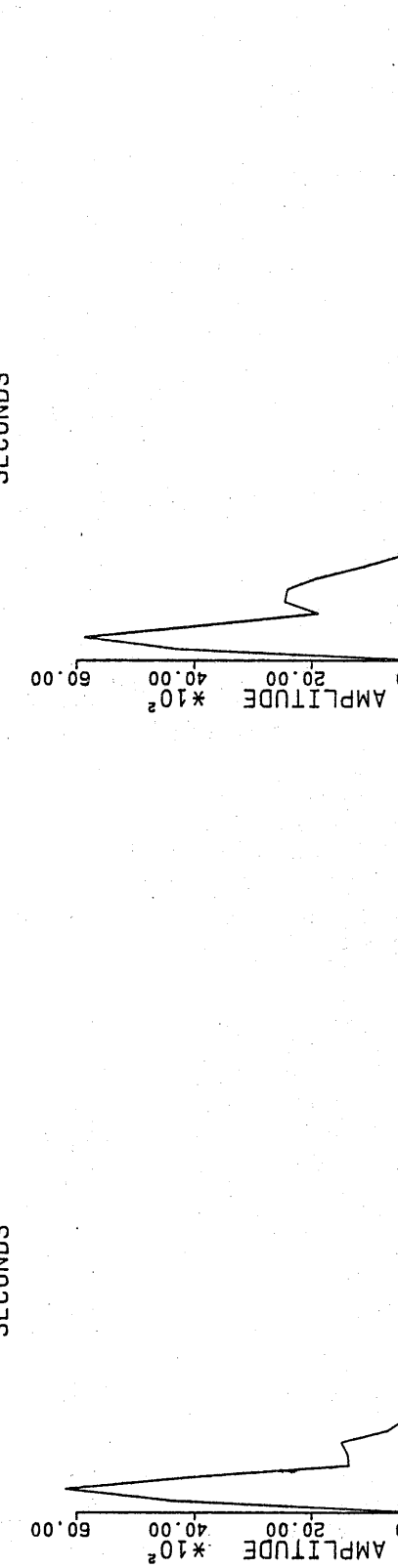

Figure 4.38. Test 4 : Time-locked auditory trace plus auditory noise.

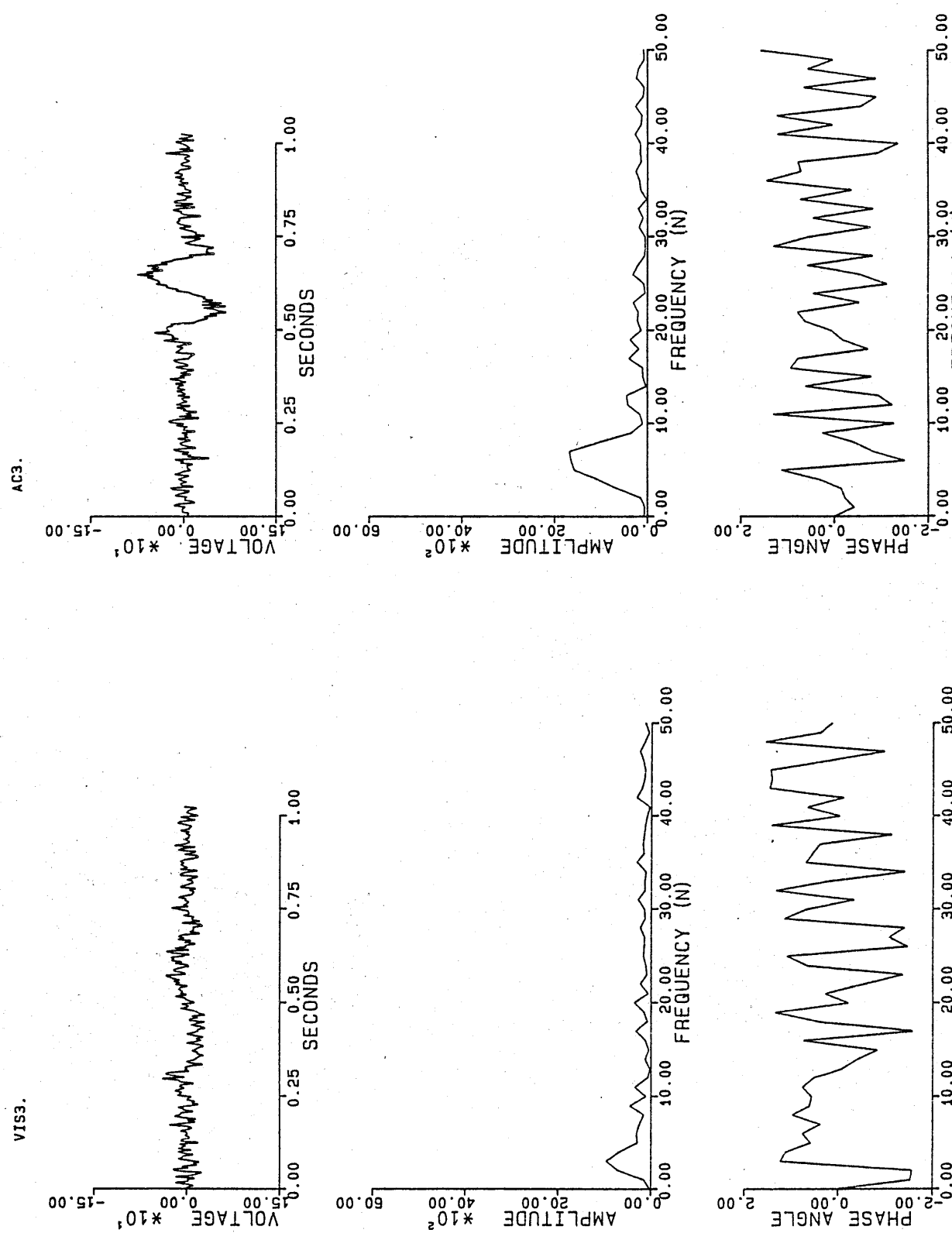

Figure 4.39. Test 4 : Visual trace plus noise following the removal of first order distortion.

Figure 4.40. Test 4 : Auditory trace plus noise following the removal of first order distortion.

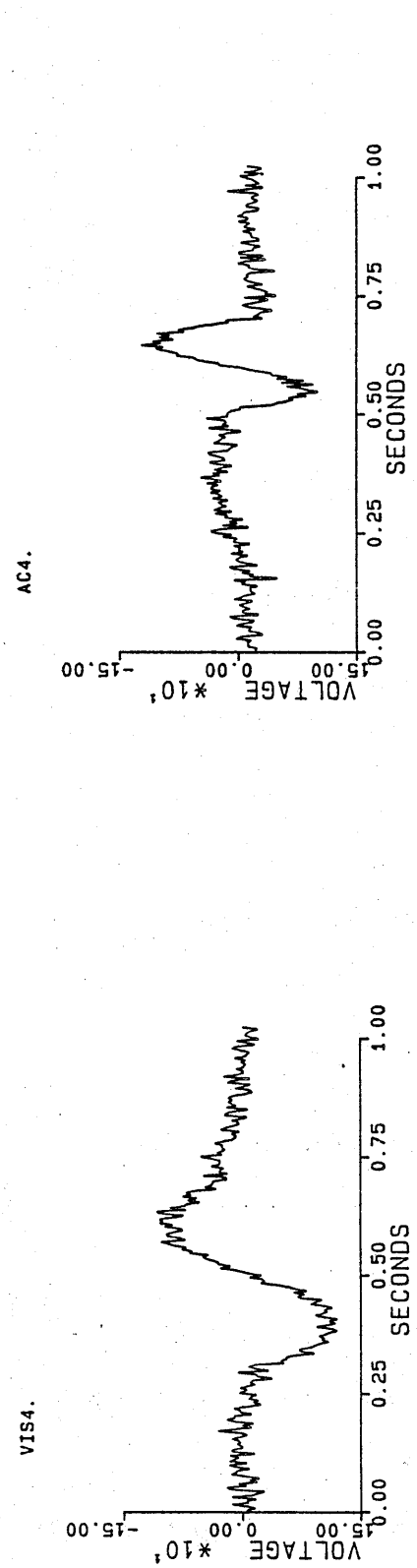

Figure 4.41. Test 4 : Recovered visual response.

Figure 4.42. Test 4 : Recovered auditory response.

The following section describes the application of the filtering procedures to dual-task data.

4.4 Application of the filtering procedures to dual task-data

The first stage in the application of the filtering procedures to dual-task data involved removing the 'first-order' distortion from time-locked visual and auditory traces.

Removal of the running average of auditory activity from time-locked visual traces was achieved by staggering the time-locked auditory averages and then subtracting these staggered traces from appropriate sections of the corresponding time-locked visual traces. The running average of every auditory trace was calculated according to the algorithm given by equations {3.3} to {3.6}, and the first and last 24 data points were truncated to remove spurious values at the beginning and end of each trace. To ensure sufficient data points for application of the inverse filter, the staggered auditory traces included those data values recorded prior to the onset of the auditory stimuli. A total of 351 data values was thus available for subtraction.

The staggered waveforms were subtracted from corresponding visual traces following an interval equal to the minimum delay between the onset of the fixation cross and the onset of the auditory stimuli in that condition, plus an additional delay of 24 samples to allow for truncation of the staggered auditory trace. The full complement of 351 samples was subtracted from visual traces recorded over signal conditions 1-5. A total of 339, 301 and 264 data values were subtracted from traces recorded over signal conditions 6, 7 and 8 respectively, being limited by the length of the visual traces. The results of these subtractions for averages

recorded from the Cz lead under the physical match condition are shown in Figure 4.43. Each section of trace is shown padded out with nulls at its relative position within the three second epoch.

A symmetrical procedure was followed for removal of the 'first order' distortion from time-locked auditory traces. Every time-locked visual trace was staggered over its entire length and the first and last 24 data values were truncated. Appropriate sections of these staggered traces were then subtracted from corresponding auditory traces. For signal conditions 1-5 a total of 375 data points were subtracted, for signal conditions 6, 7 and 8 a total of 339, 301 and 264 data points were subtracted, respectively. The results of these subtractions for averages recorded from the Cz lead over physical match trials are shown in Figure 4.44.

The traces presented in Figures 4.43 and 4.44 indicate that the double running average filter, applied through the subtraction process, has effectively removed the 'first order' distortion from time-locked visual and auditory averages. Removal of the resultant 'second order' distortion was achieved by application of the inverse filter to 256 data values taken from each of the waveforms obtained from the subtraction process. The FFT routine described in Section 4.2 was used to mediate conversion between the time domain and the frequency domain, and the filter constants by which each Fourier coefficient was multiplied are those presented in Figure 4.2.

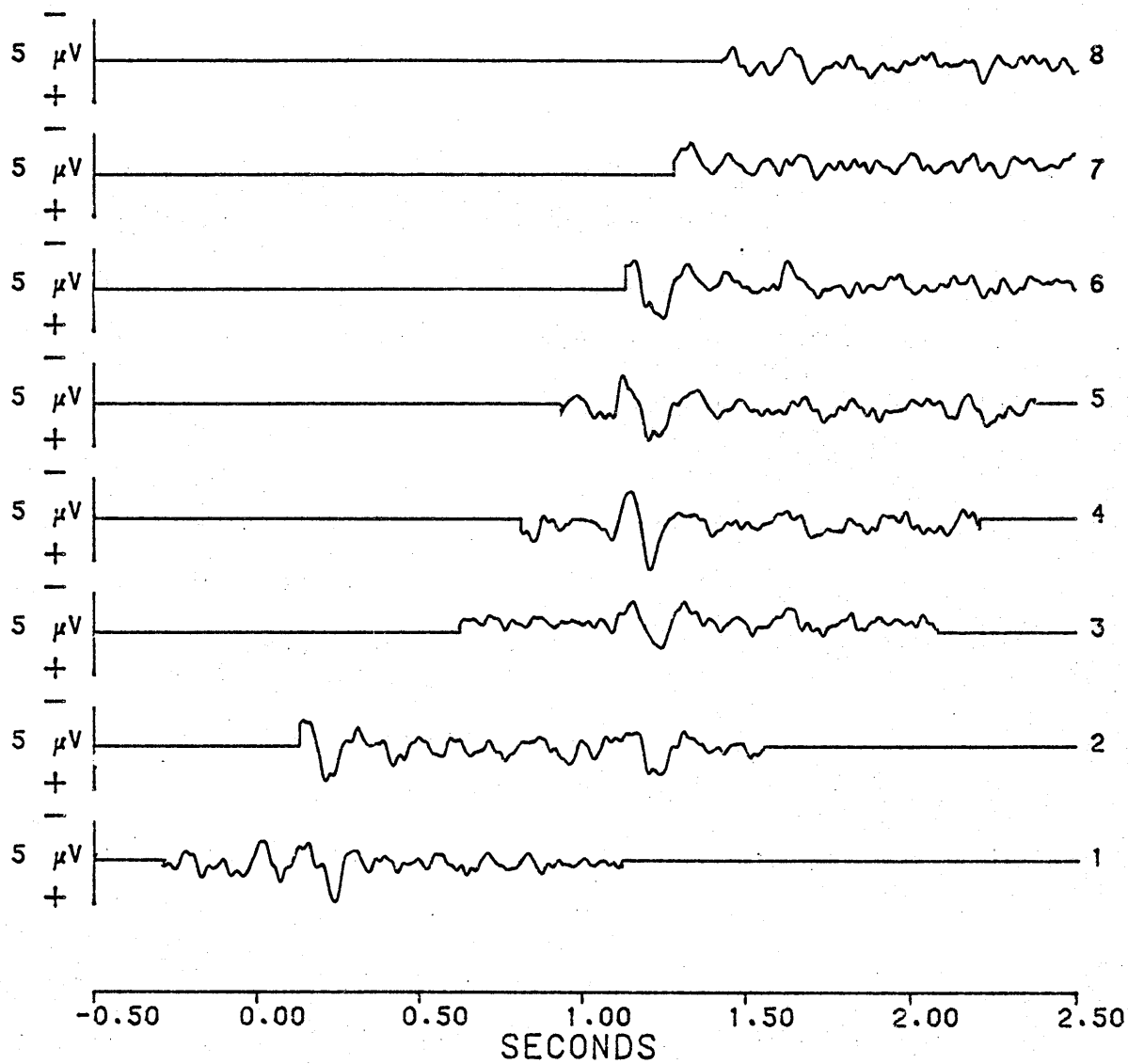

Figure 4.43. Removal of first order distortion from visual averages (CzPM).

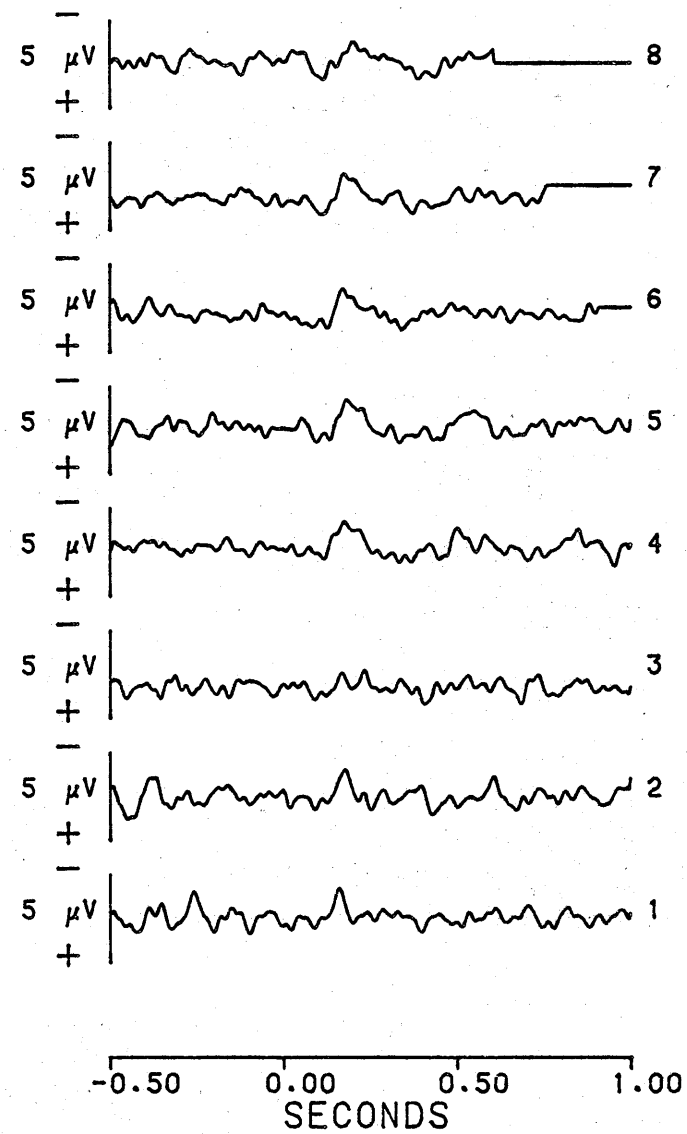

Figure 4.44. Removal of first order distortion from auditory averages (CzPM).

A number of windows were applied to the data, prior to the application of the inverse filter, in an attempt to reduce the effects of spectral leakage in the FFT. These windows included the Hanning, the 20% and 40% cosine taper windows and the Blackman-Harris window (see Harris, 1978). The results of these procedures were less than satisfactory as the recovered waveforms all exhibited low frequency distortions which could be attributed to spectral leakage in the FFT. For example, Figures 4.45 and 4.46 show the waveforms recovered from those data presented in Figures 4.43 and 4.44 following the application of the 20% cosine taper window. The recovered visual waveforms (Figure 4.45) are those sections of trace bounded by the arrow heads which have been inserted at their relative positions within the original time-locked visual traces. The pure visual average recorded over non-signal trials has been included also for purposes of comparison. In Figure 4.46, the recovered auditory waveforms are shown padded out with nulls at their relative positions within the 1.5second epoch.

Low frequency distortions are evident in both sets of traces. In particular, note the distortion of those recovered visual traces which include the very low frequency components associated with the onset of the second letter stimuli (visual traces recorded under signal conditions 3-8). Note also the distortion of the pre-stimulus baseline of auditory ERPs recorded under signal conditions 7 and 8, and the lack of resolution of the positive-going (P_3) component of the auditory ERP recorded under the first signal condition.

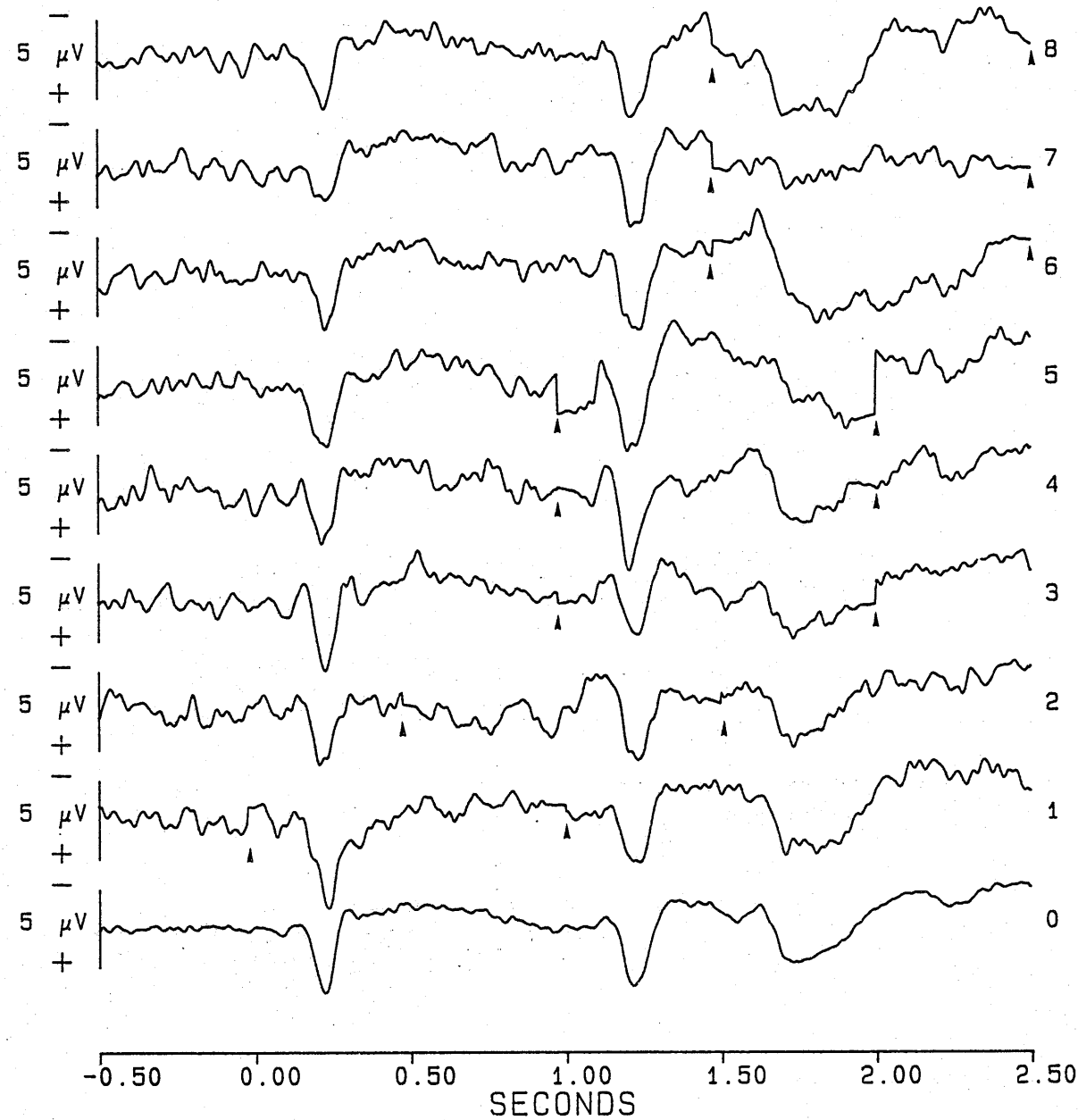

Figure 4.45. Recovered visual averages following application of the 20% cosine taper window (CzPM).

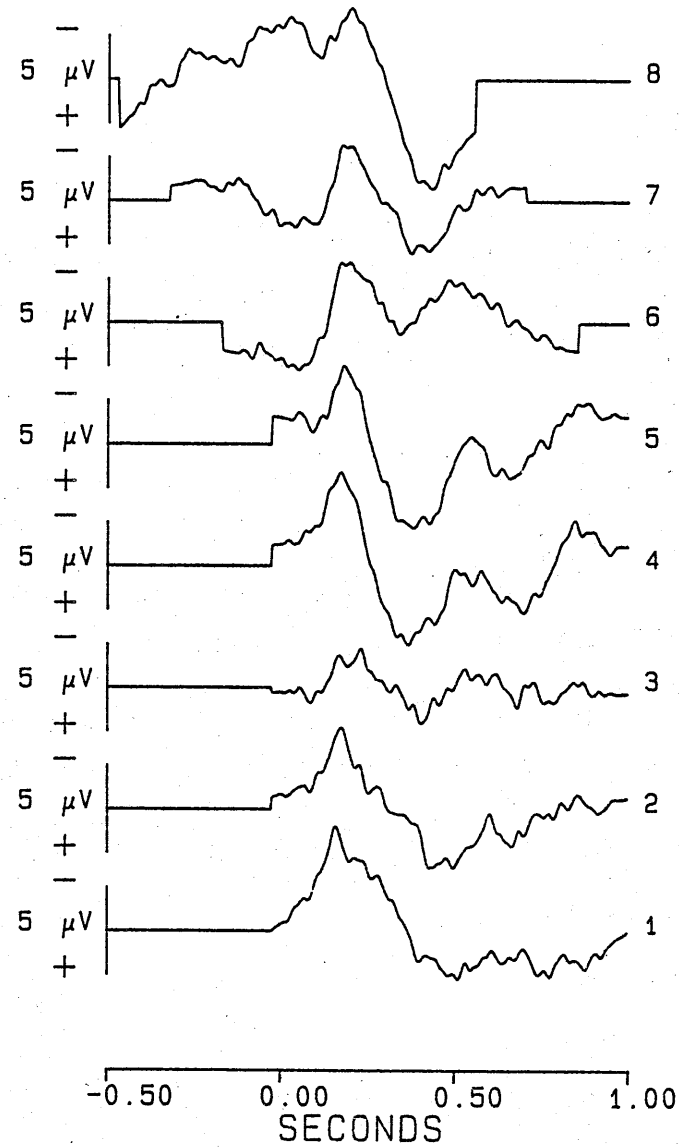

Figure 4.46. Recovered auditory averages following application of the 20% cosine taper window (CzPM).

As the inverse filter has its greatest effect on frequencies of 0.977Hz, corresponding tc the second Fourier coefficient (see Figure 4.2), the major source of distortion in the recovered waveforms results from spectral leakage into this component of the FFT. A method of avoiding this obvious source of distortion is to modify the inverse filter by setting the second filter constant to unity. This has the effect of 'filtering out' both wanted and unwanted component frequencies of 0.977Hz from the recovered waveforms.

Figures 4.47 to 4.58 show the results of applying the 20% cosine taper window and the modified inverse filter to visual and auditory traces recorded from Cz and Pz leads over all conditions of the dual-task experiment, following removal of the first order distortion. All recovered visual traces, bounded by the arrow-heads, are inserted within the corresponding original time-locked visual averages. The use of the modified filter results in a much more acceptable signal recovery. Overlays 1 and 2 can be used on these recovered waveforms to check for the removal of the first order distortion resulting from the running average of activity to stimuli in the other modality.

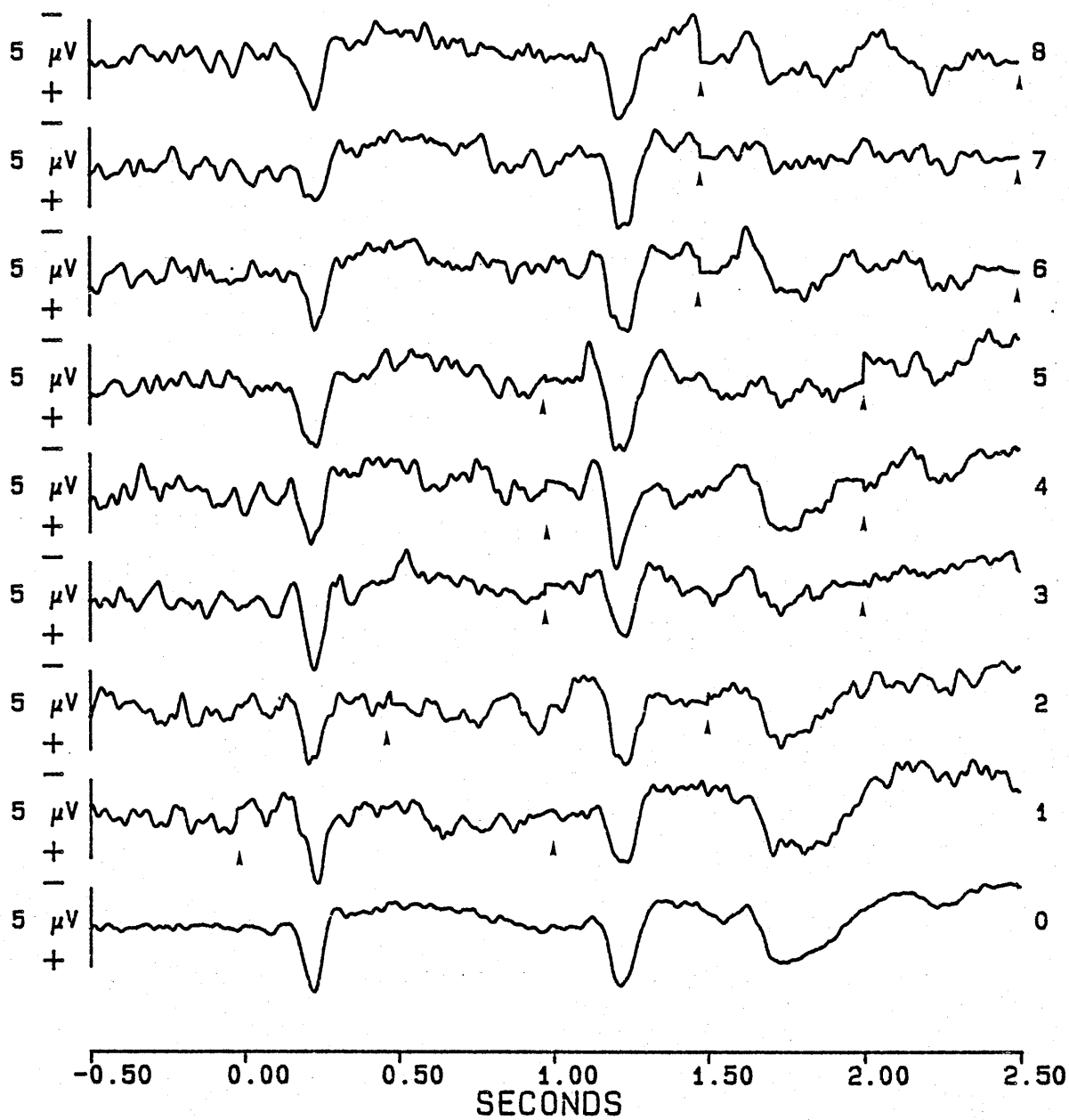

Figure 4.47. Recovered visual averages following application of the 20% cosine taper window and modified filter (CzPM).

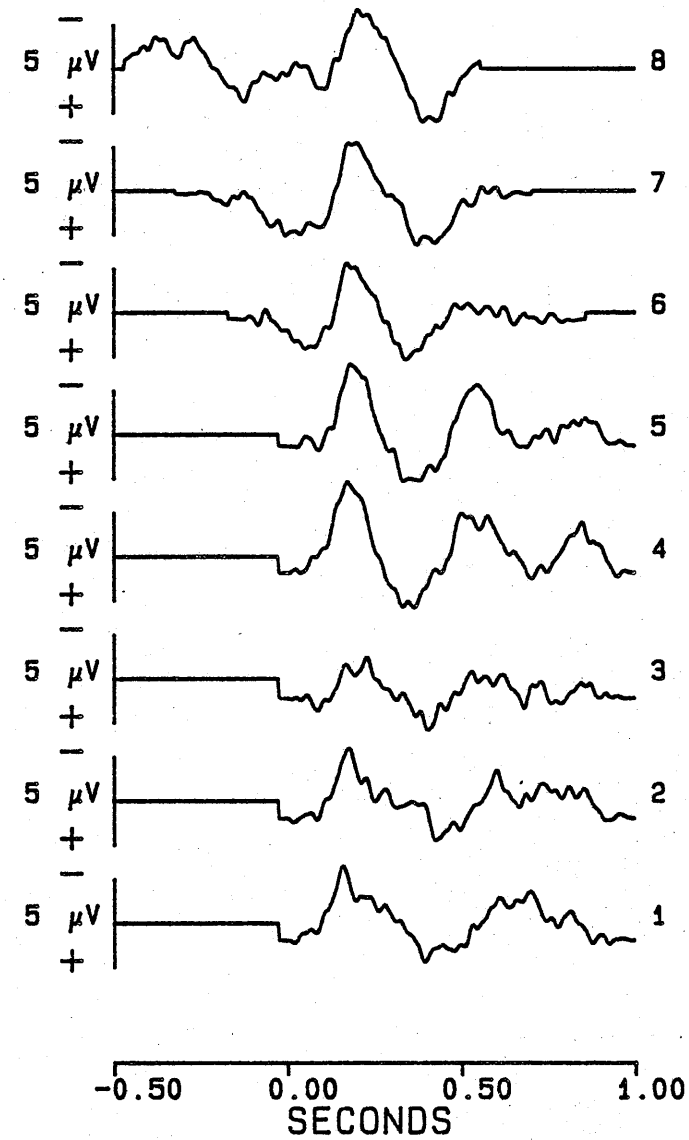

Figure 4.48. Recovered auditory averages following application of the 20% cosine taper window and modified filter (CzPM).

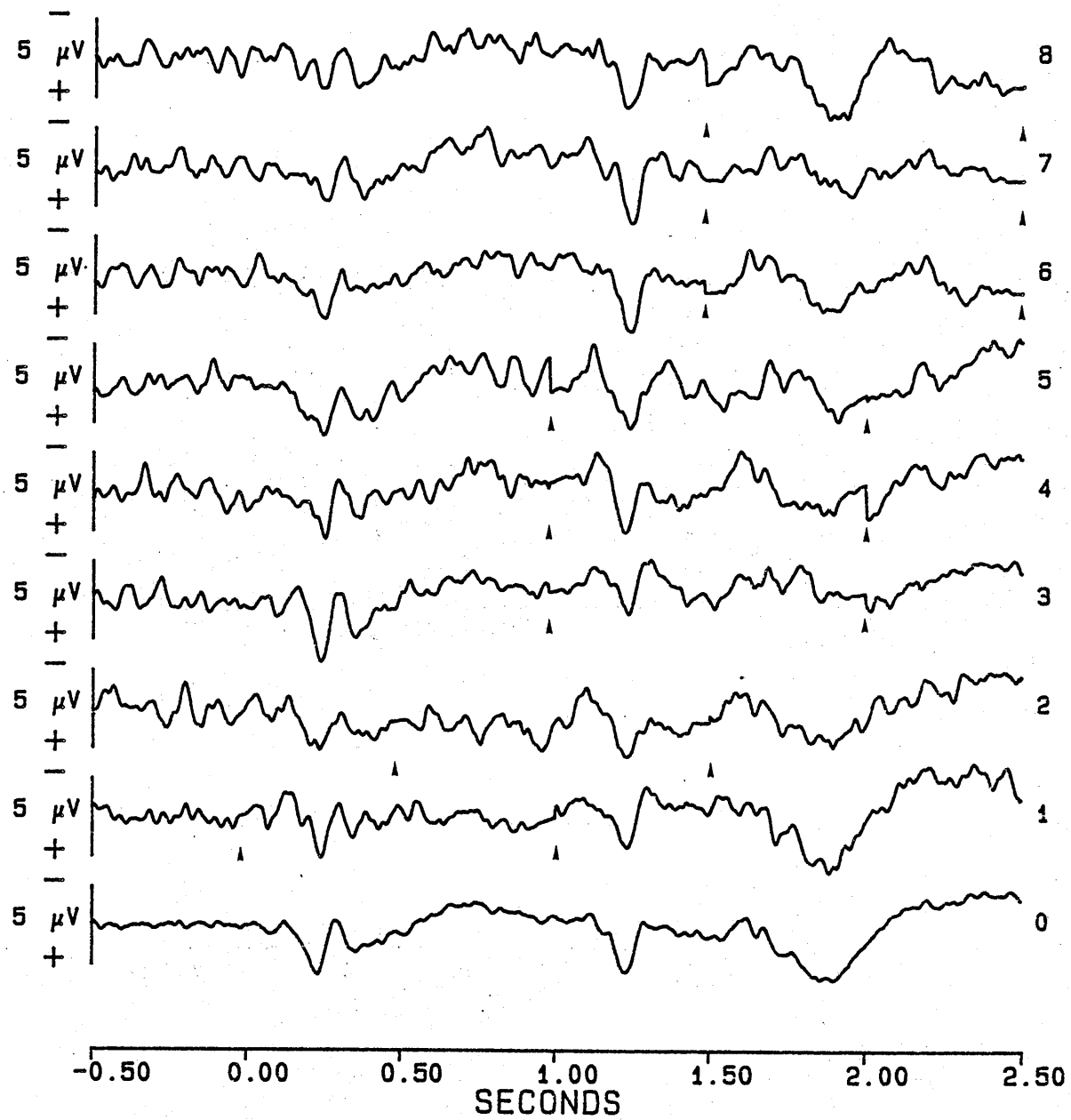

Figure 4.49. Recovered visual averages following application of the 20% cosine taper window and modified filter (PzPM).

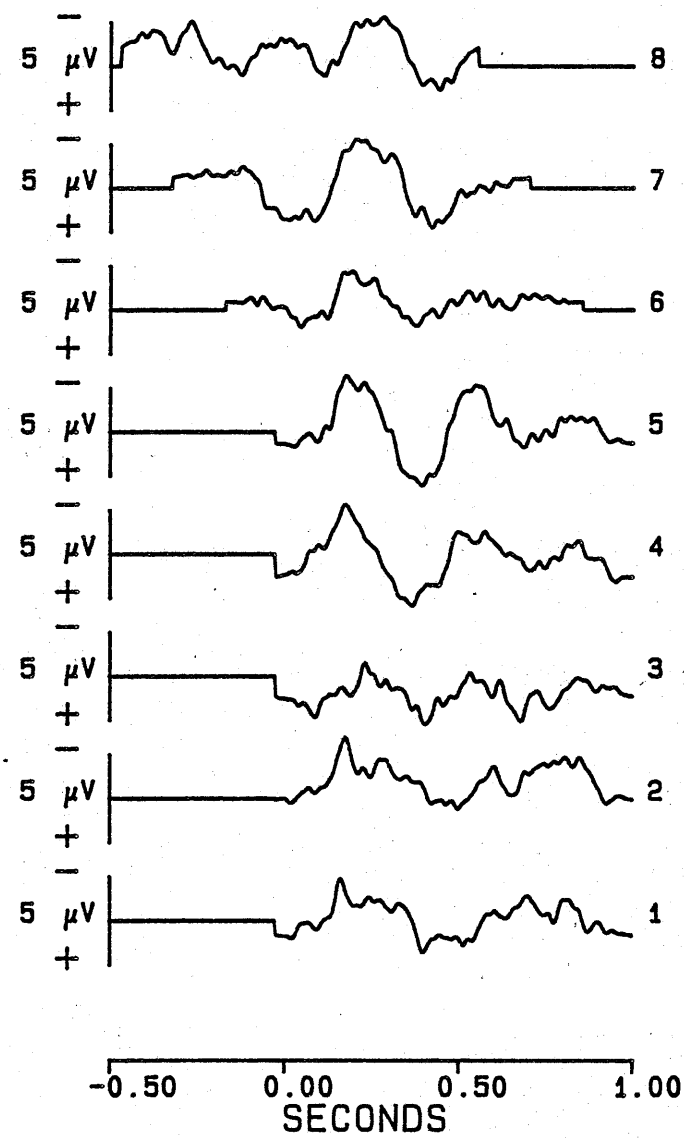

Figure 4.50. Recovered auditory averages following application of the 20% cosine taper window and modified filter (PzPM).

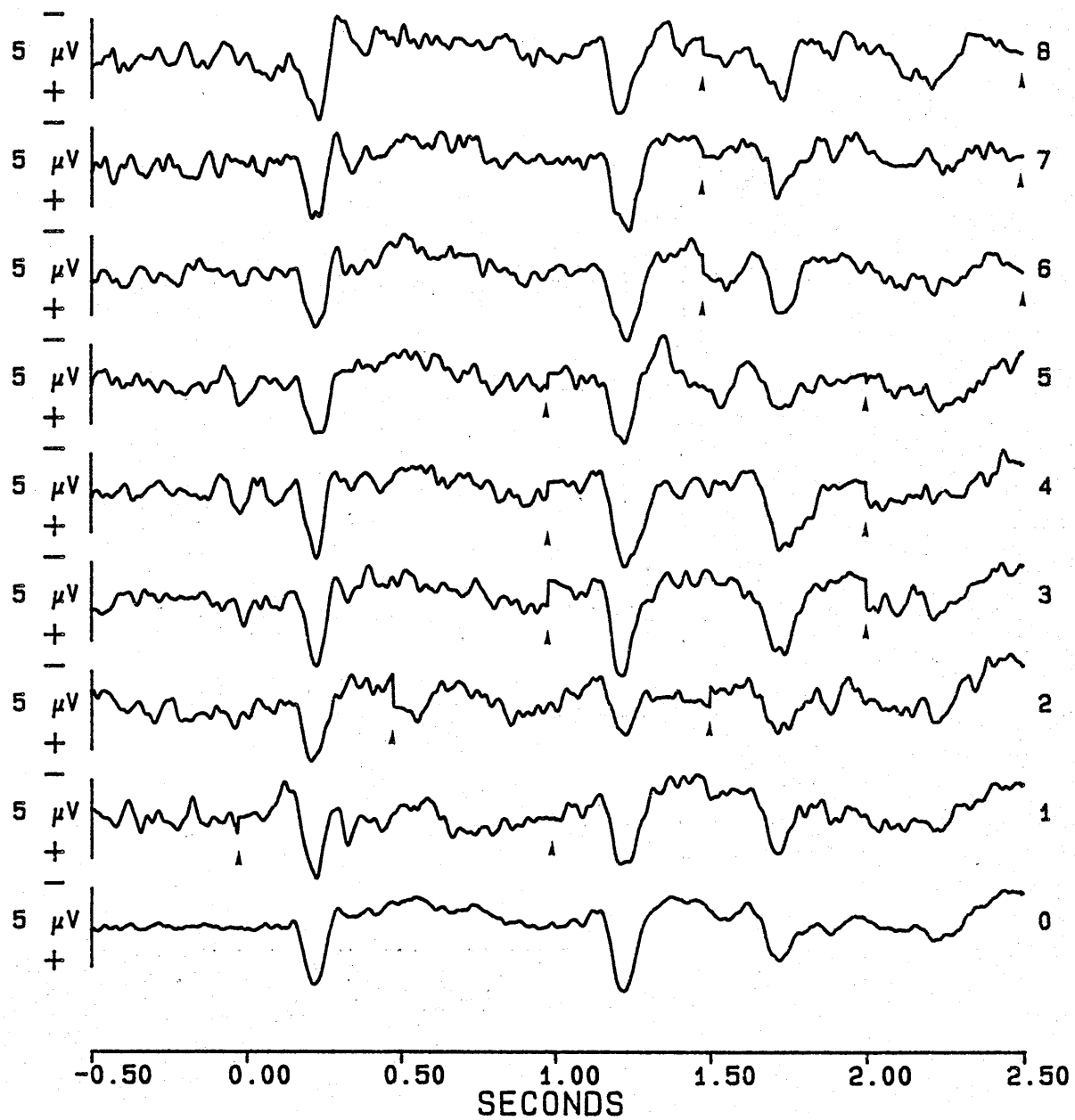

Figure 4.51. Recovered visual averages following application of the 20% cosine taper window and modified filter (CzRM).

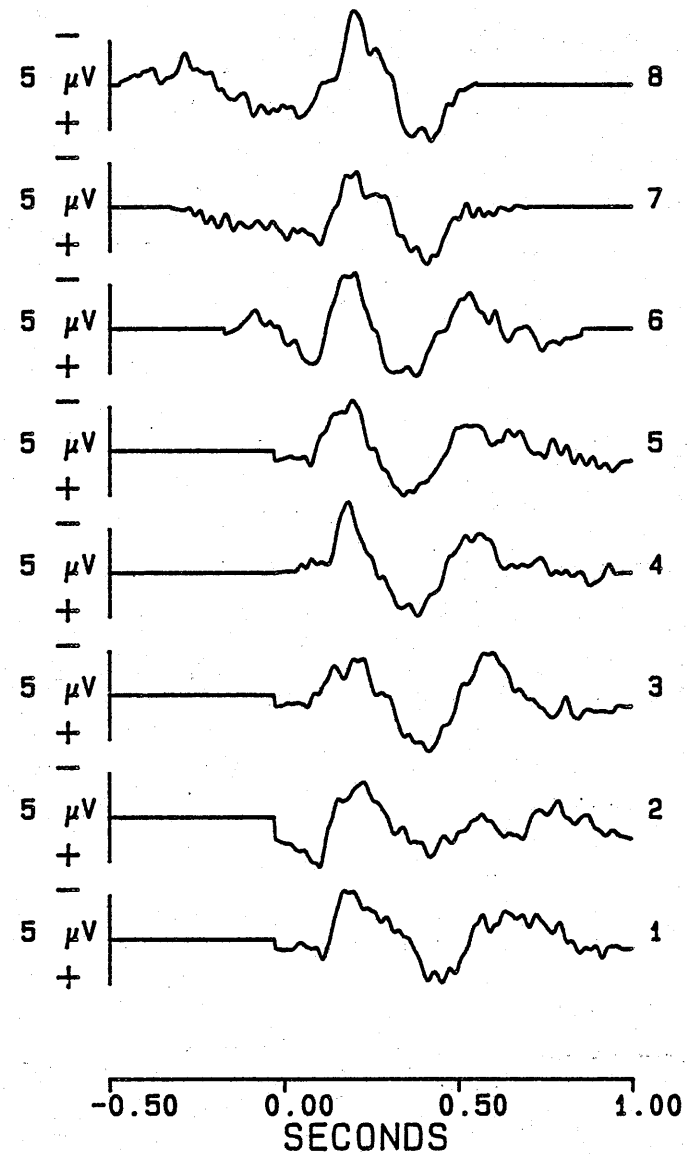

Figure 4.52. Recovered auditory averages following application of the 20% cosine taper window and modified filter (CzRM).

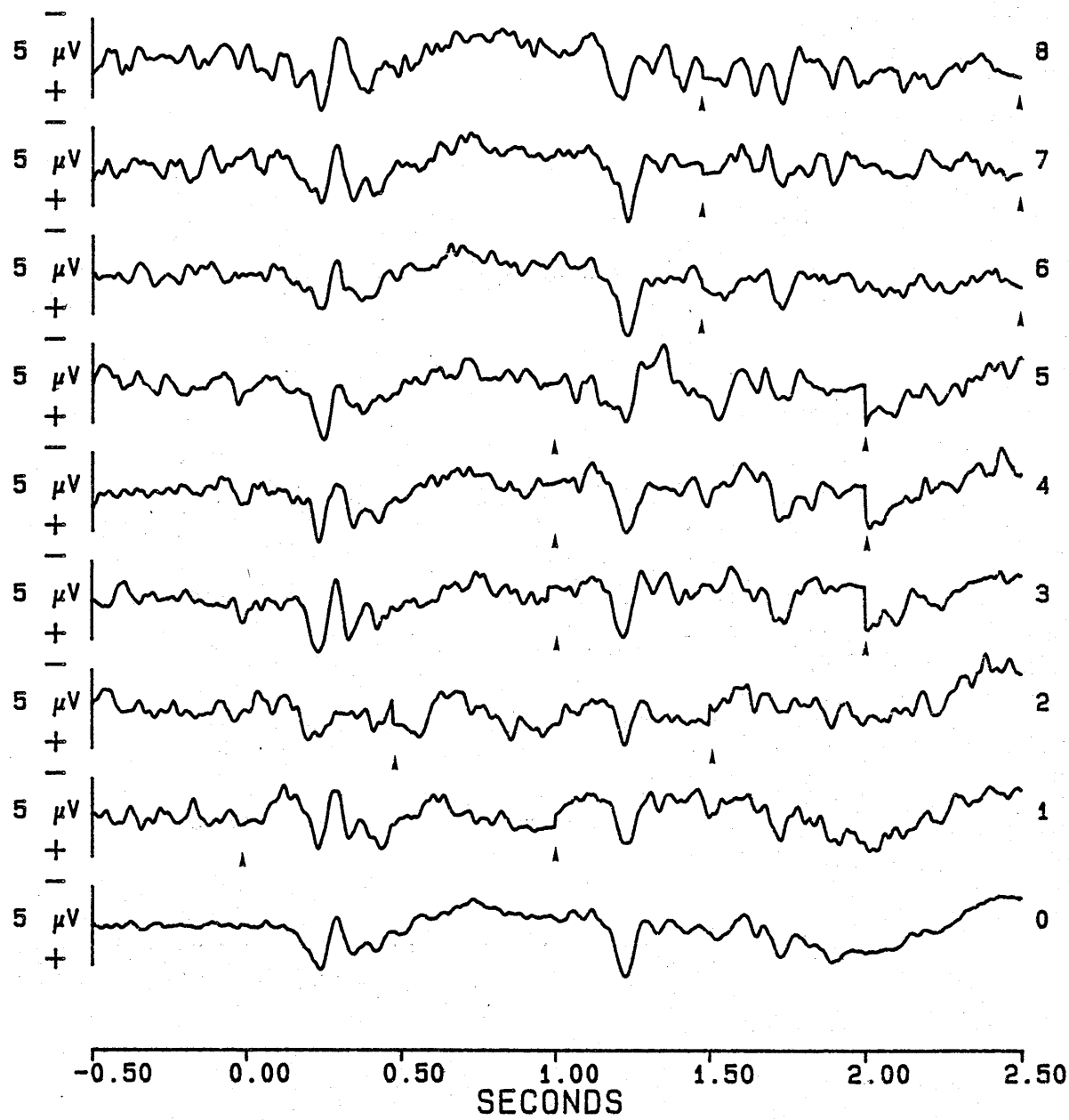

Figure 4.53. Recovered visual averages following application of the 20% cosine taper window and modified filter (PzRM).

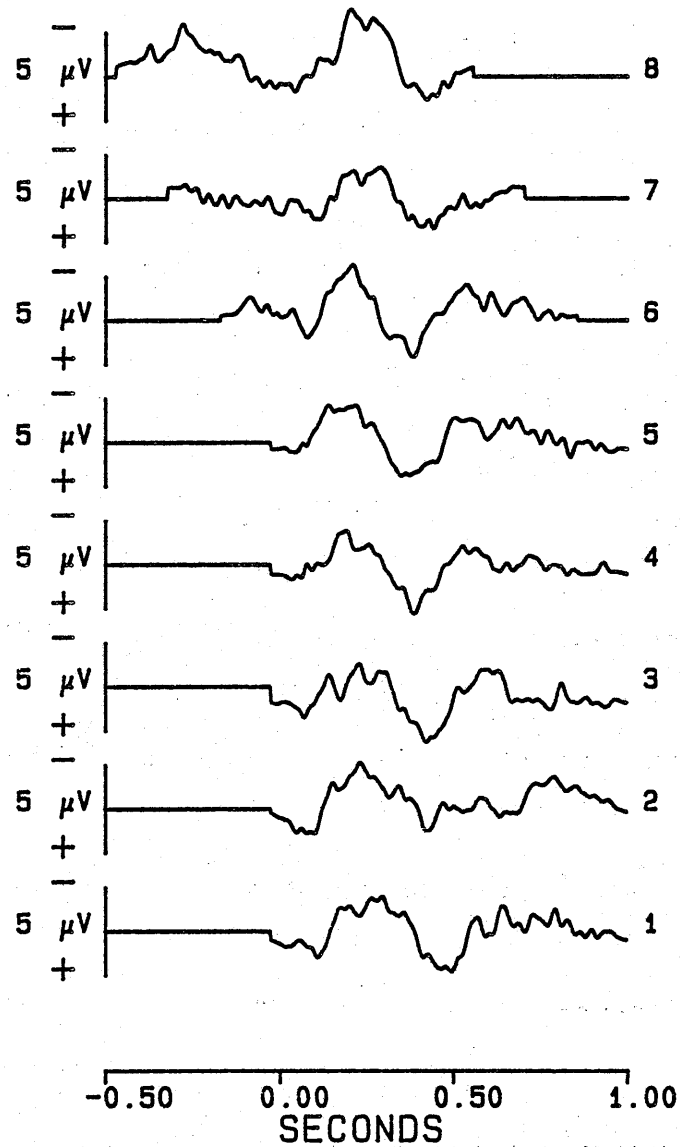

Figure 4.54. Recovered auditory averages following application of the 20% cosine taper window and modified filter (PzRM).

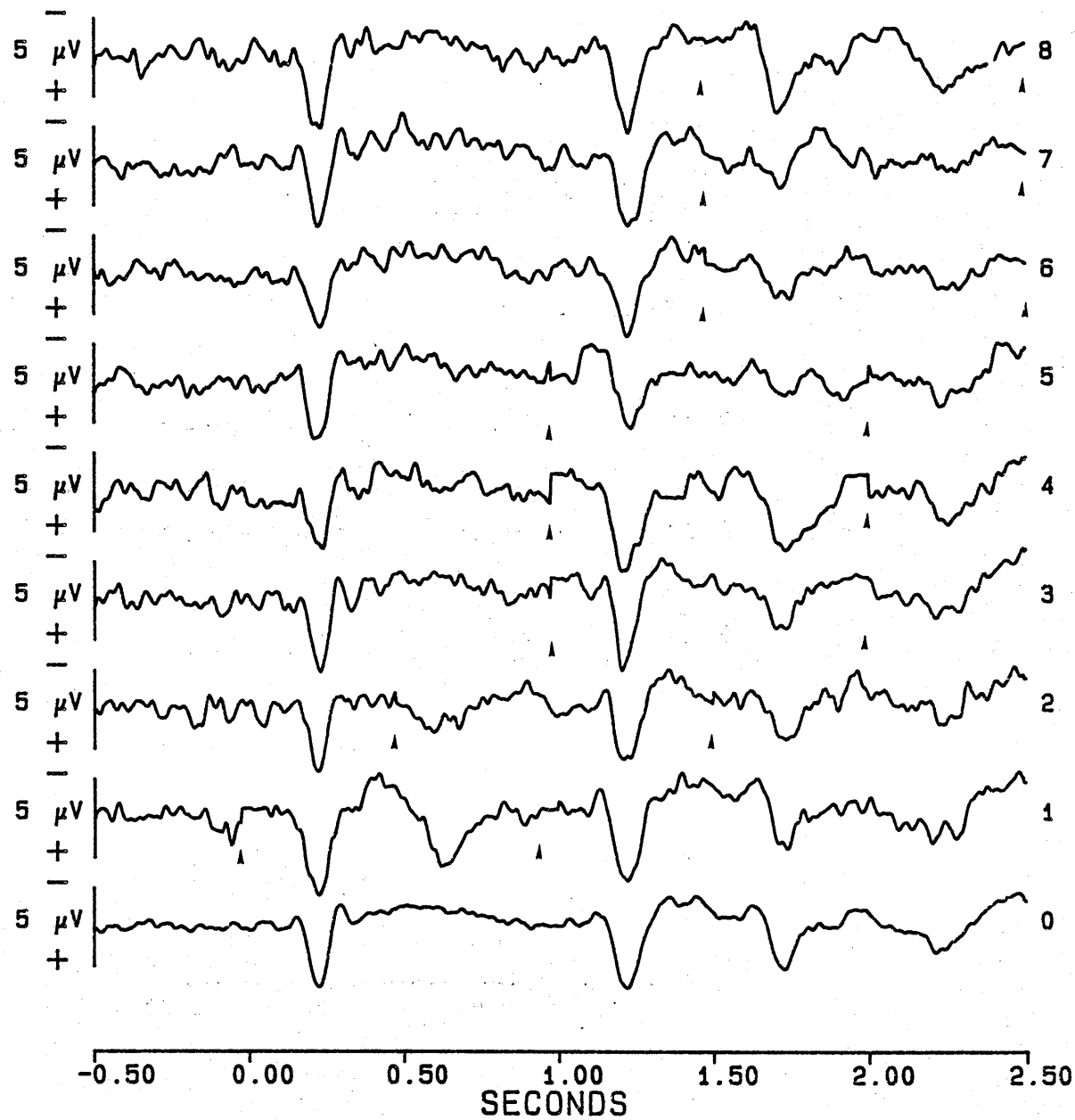

Figure 4.55. Recovered visual averages following application of the 20% cosine taper window and modified filter (CzMM).

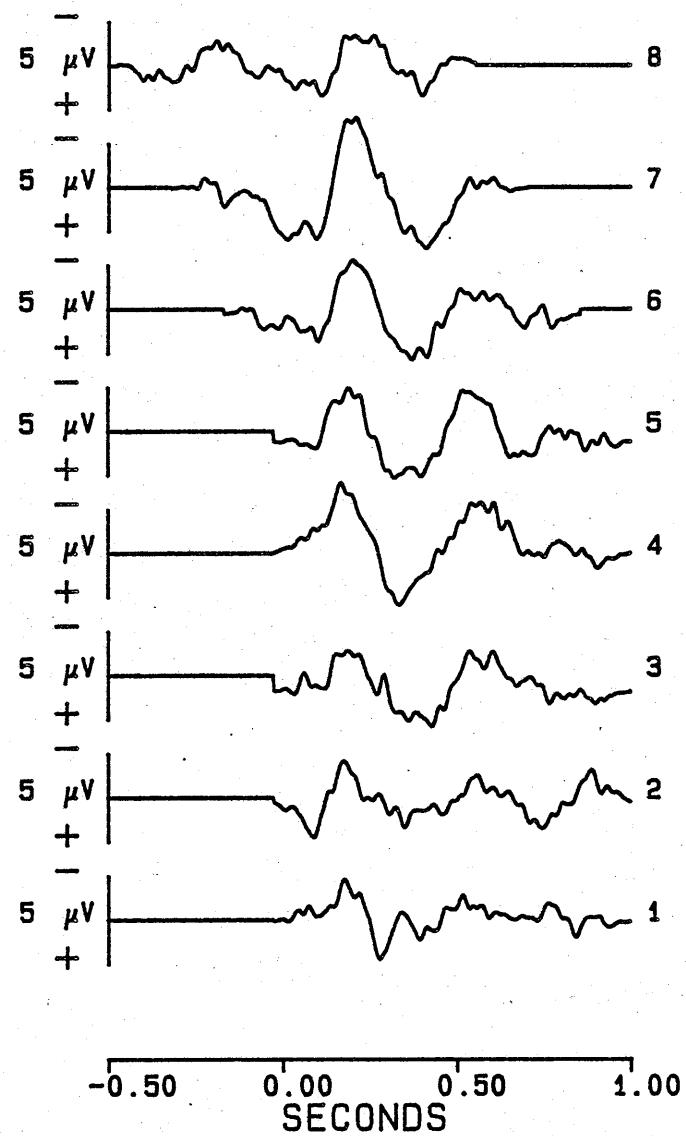

Figure 4.56. Recovered auditory averages following application of the 20% cosine taper window and modified filter (CzMM).

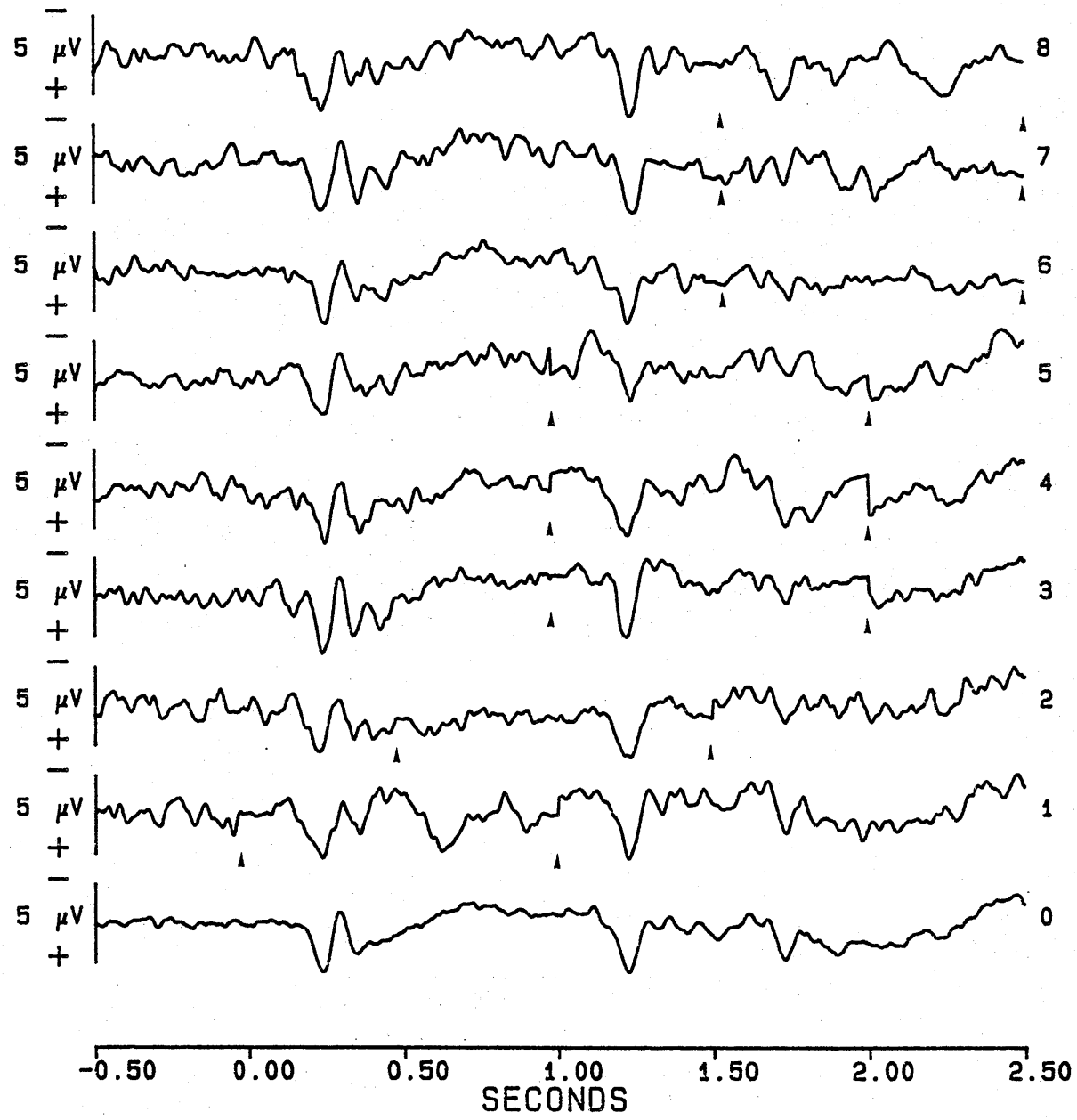

Figure 4.57. Recovered visual averages following application of the 20% cosine taper window and modified filter (PzMM).

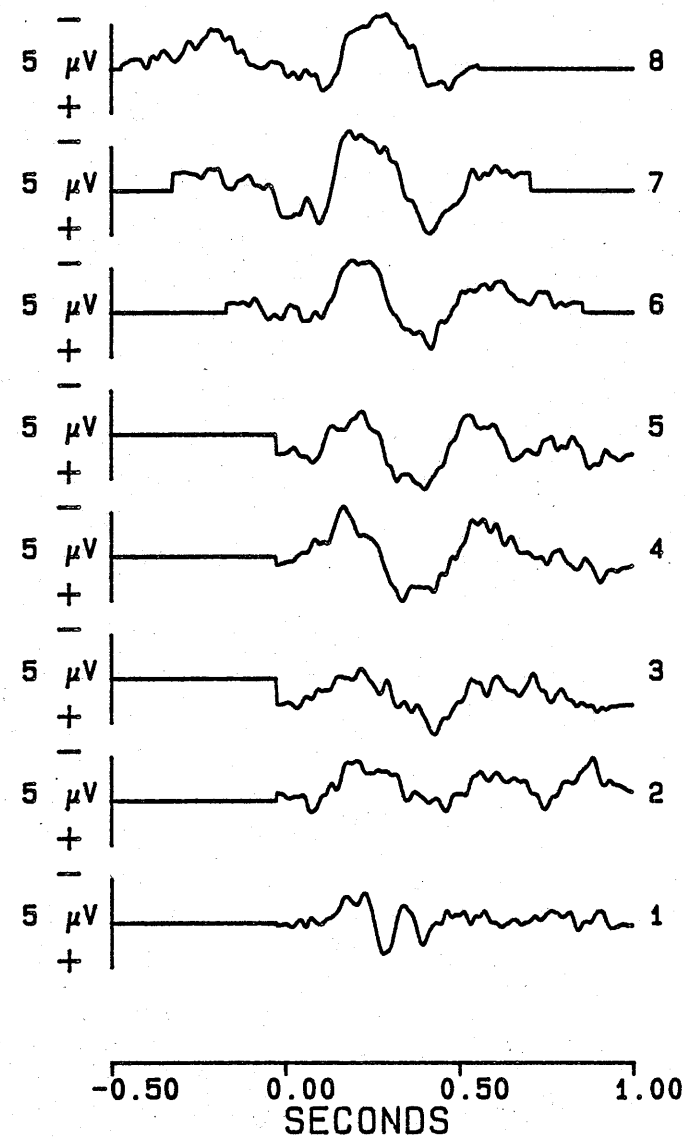

Figure 4.58. Recovered auditory averages following application of the 20% cosine taper window and modified filter (PzMM).

4.5 Discussion

The previous sections demonstrate that the digital filtering procedure provides a powerful technique for separating out overlapping waveforms to near-simultaneous stimuli. Central to the solution is the method of staggering the presentation of stimuli in one modality with respect to stimuli in the other modality to effect the partial time-unlocking of average ERPs. The solution hinges on the fact that the effect of this staggering can be defined precisely. If the assumptions inherent in the analysis hold, then the distortion present in each complex waveform must be completely removed by subtraction of the appropriately positioned running average of the other complex waveform. Further, the fact that the filter responsible for the 'second order' distortion can be defined precisely, means that its inverse is capable of precisely recovering the original waveforms, with the exception of those limitations outlined in Sections 4.3.3 and 4.3.4.

What are the assumptions inherent in this procedure? The first is that the electrical output of the visual and auditory processors sum linearly, as previously discussed in Section 3.3 of Chapter 3. This does not mean that the two processors are assumed not to interact. Indeed, a major use of this technique is to allow the detection of such interactions (cf. Section 3.3). Only the electrical output of the processors is assumed to add.

The second major assumption is that the electrical activity of the two processors, that is the visual and auditory ERPs, do not vary over the duration of the staggering window. To the extent that this technique is useful in detecting interactions which occur between the processors, this assumption, in the limit, must be false. That is, the wanted signals could be expected

to vary systematically according to the temporal interval between the two stimuli. Clearly, if this happens to any great extent, then the analytic technique is suspect.

However, this problem is minimised, if not completely overcome, by good experimental technique. For example, in the dual-task experiment, physiological data were saved only if subjects responded correctly to both visual and auditory tasks in order to minimise the variation in ERPs to stimuli presented at different positions within the staggering interval (see Section 2.6.1). Furthermore, the smaller the window used to create the two signals, the less will be the distortion due to systematic variations in the shape of the underlying waveforms. Thus, if the window size is kept small in comparison to the time over which interactions are being examined, then differences can be attributed to these interactions if they are large enough and systematic enough. Care is needed, however, to detect residual distortion which may appear from the interfering signal, as a result of its changing its nature over the staggering window. A way of validating the technique further is to use windows of different sizes so that the time course of changes in the underlying signals can be accurately mapped.

While in theory the present technique provides an optimal solution to the problem of separating out overlapping waveforms, a serious limitation in its use concerns the accuracy of the signals recovered through the application of the inverse filter in the frequency domain. The previous sections demonstrated that spectral leakage, particularly into the lowest frequency range of the FFT where the filter has its greatest effect, can result in severe distortions in the recovered waveforms. Setting the second filter coefficient to unity avoids the more obvious distortions but does not eliminate any misrepresentation

resulting from spectral leakage into or from other frequency components, and the frequency composition of the recovered waveforms can be expected to be biased to some degree. Furthermore, the modified filter fails to restore the wanted 0.977Hz component of the idealised responses. This may result in reduced peak to peak amplitudes and/or a change in peak latencies (see, for example, Goff, 1974, p.126).

The following chapter considers an alternative method of analysis in an attempt to overcome the limitations of the present technique. Again, the time-locked visual and auditory averages provide the basis for the analysis, but the following solution estimates the idealised waveforms by means of a regression analysis carried out in the time domain.

CHAPTER 5: GENERALISED LEAST SQUARES ESTIMATION

5.1 Introduction

The third method of analysis to be considered employs the classical linear regression model and estimation of the idealised visual and auditory responses is achieved through the method of least squares. This approach has an immediate advantage over the filtering procedure in that the analysis is carried out in the time domain and hence obviates the problems of spectral leakage associated with analysis in the frequency domain.

The derivation of the equation which provides the basis for estimation of the idealised visual and auditory responses is provided in the following section. The adequacy of the model hinges on the accurate specification of the transformations applied to the idealised responses through the method of stimulus presentation and data collection. It should be noted that the model to be presented incorporates some departures from the actual methods used during the dual-task experiment. These departures are discussed in Section 5.4.

5.2 Specification of the regression equation

The data recorded over signal trials of the dual task experiment can be described in the following simplified way. Every trial in a particular signal condition provides the record of event-related activity to two stimuli, a visual stimulus and an auditory stimulus, and the delay between the onset of the visual and auditory stimuli is

different for every trial as a result of the staggering procedure. Over the whole set of trials, however, every time delay that is an integral multiple of the sample interval and lies between a minimum delay of k samples and a maximum delay of l samples is used once. The staggering window can be defined as extending over $(l-k+1)$ sample intervals.

For the following data compression it is assumed that on every trial a record of N samples following the onset of the visual stimulus is saved. It is further assumed that the responses to the two stimuli are invariant over the duration of the staggering window. That is, they can be represented by separate time series which are individually unaltered by the time delay between the stimuli. An additional assumption is that the two responses add linearly at the site of the recording electrode.

The idealised response to the visual stimulus can be written as h_n where N-1 is the number of sample intervals after the onset of the stimulus and the terms h_1, h_2, h_3, h_4 up to h_N are the time series representation of the 'idealised' visual response. Similarly, the idealised response to the auditory stimulus can be written as g_n where this time the suffix represents the number of sample intervals after the onset of the auditory stimulus. The record from any one trial can thus be divided into two parts: the first after the onset of the visual stimulus but before the onset of the auditory stimulus, and the second after the onset of the auditory stimulus, when both visual and auditory responses overlap. If the experimental response from one trial is written as y_n where the onset of the visual stimulus is represented by y_1 then:

$$y_n = h_n + \varepsilon_n \qquad m+1 > n \geq 1$$

$$y_n = h_n + g_{n-m} + \varepsilon_n \qquad N \geq n \geq m+1$$

where: n is the number of the sample interval,

m is the delay between the onset of the visual and auditory stimuli ($l \geq m \geq k$), and

ε_n is the error in the observations due to interference and noise.

The above equations can be written in matrix notation as follows:

$$\underset{Nx1}{\begin{bmatrix} y_1 \\ y_2 \\ \cdot \\ \cdot \\ \cdot \\ y_N \end{bmatrix}} = \underset{NxN}{\begin{bmatrix} I \end{bmatrix}} \underset{Nx1}{\begin{bmatrix} h_1 \\ h_2 \\ \cdot \\ \cdot \\ \cdot \\ h_N \end{bmatrix}} + \underset{NxN-k}{\left[\begin{array}{c|c} & \\ 0 & \\ & \\ \hline I & 0 \\ (N-m \times N-m) & (N-m \times m-k) \end{array}\right]} \underset{N-kx1}{\begin{bmatrix} g_1 \\ g_2 \\ \cdot \\ \cdot \\ \cdot \\ g_{N-k} \end{bmatrix}} + \underset{Nx1}{\begin{bmatrix} \varepsilon_1 \\ \varepsilon_2 \\ \cdot \\ \cdot \\ \cdot \\ \varepsilon_N \end{bmatrix}} \qquad \{5.1\}$$

where I is the identity matrix and sub-matrix and

0 is the null sub-matrix.

Note that the effect of staggering the onset of the auditory stimulus with respect to the visual stimulus is incorporated in equation {5.1} through the (NxN-k) matrix which modulates the contribution of the elements within the vector $\underline{g}$. The maximum idealised auditory response of N-k samples is recorded when the delay between the onset of the visual and auditory stimuli is at a minimum ($m=k$), while the minimum auditory contribution of N-l samples is recorded when $m=l$.

Using the suffix m to indicate that the equation refers to the trial with a delay of m sample intervals between stimuli, the above equation can be written in a more compact form:

$$\underline{y}_m = [I]\underline{h} + [Q_m]\underline{g} + \underline{\varepsilon}_m \qquad \{5.2\}$$

where $\underline{y}_m$ is the vector of observations,

$\underline{h}$ is the vector of the time series representation of the idealised response to the visual stimulus,

Q_m represents the (NxN-k) matrix which specifies the contribution of the idealised auditory response,

$\underline{g}$ is the vector of the time series representation of the idealised response to the auditory stimulus, and

$\underline{\varepsilon}_m$ is the vector of observation errors.

The results of all trials presented under a particular signal condition can now be ordered in a sequence according to the delay between stimuli and combined in a new vector equation:

$$\begin{bmatrix} \underline{y}_k \\ \underline{y}_{k+1} \\ . \\ . \\ . \\ \underline{y}_{l-1} \\ \underline{y}_l \end{bmatrix} = \begin{bmatrix} I \\ I \\ . \\ . \\ . \\ I \\ I \end{bmatrix} \underline{h} + \begin{bmatrix} Q_k \\ Q_{k+1} \\ . \\ . \\ . \\ Q_{l-1} \\ Q_l \end{bmatrix} \underline{g} + \begin{bmatrix} \underline{\varepsilon}_k \\ \underline{\varepsilon}_{k+1} \\ . \\ . \\ . \\ \underline{\varepsilon}_{l-1} \\ \underline{\varepsilon}_l \end{bmatrix} \qquad \{5.3\}$$

The data defined by equation {5.3} were saved in two ways, and the two records created are the data from which the time series h_n and g_n are to be estimated. For simplicity the summation rather than averaging of data records will be assumed.

The first data saving process involved lining up each record so that the instant at which the visual stimulus occurred was coincident in all records. Then at each time interval a sum of all the coincident ordinates from each record was created over the intervals 1 to N. The resulting trace of N samples is thus the 'average' recorded time-locked to the visual events of the dual-task.

In the second data saving process the instant at which the auditory stimulus occurred in each record was aligned with the same instant in the other records. A new trace of N samples was created by summing the ordinates of each record, starting k samples prior to the auditory stimulus onset and continuing for N-k samples following the onset of the auditory stimulus. The resulting trace is thus the 'average' recorded time-locked to the auditory events of the dual-task.

Table 5.1 illustrates the two data collection processes using simulated data. In this example a total of 19 samples following the onset of the visual stimulus is recorded on every trial. The data for each trial provide a separate time series for the idealised visual response (upper row) and a separate time series for the idealised auditory response (lower row). The minimum delay between the onset of the visual stimulus and the onset of the auditory stimulus is 5 samples (trial T1), and the maximum delay is 9 samples (trial T5). Therefore, in terms of equations {5.1} and {5.3}, N = 19, k = 5 and l = 9.

The upper portion of Table 5.1 illustrates the alignment of data records so that the onset of the visual stimulus is coincident across records. The row of figures labelled r_1 provides the summation of all coincident ordinates from each record. This represents the time-locked visual trace.

Table 5.1: Simulated data illustrating transformations applied during data collection

Time-locked visual trace

T1	30	58	80	95	100	95	80	58	30	0	-30	-58	-80	-95	-100	-95	-80	-58	-30
m=5=k						40	74	95	99	86	58	20	-20	-58	-86	-99	-95	-74	-40
T2	30	58	80	95	100	95	80	58	30	0	-30	-58	-80	-95	-100	-95	-80	-58	-30
m=6							40	74	95	99	86	58	20	-20	-58	-86	-99	-95	-74
T3	30	58	80	95	100	95	80	58	30	0	-30	-58	-80	-95	-100	-95	-80	-58	-30
m=7								40	74	95	99	86	58	20	-20	-58	-86	-99	-95
T4	30	58	80	95	100	95	80	58	30	0	-30	-58	-80	-95	-100	-95	-80	-58	-30
m=8									40	74	95	99	86	58	20	-20	-58	-86	-99
T5	30	58	80	95	100	95	80	58	30	0	-30	-58	-80	-95	-100	-95	-80	-58	-30
m=9=l										40	74	95	99	86	58	20	-20	-58	-86
r_1	150	290	400	475	500	515	514	499	458	394	262	68	-157	-389	-586	-718	-758	-702	-544

Time-locked auditory trace

T1	30	58	80	95	100	95	80	58	30	0	-30	-58	-80	-95	-100	-95	-80	-58	-30
m=5=k						40	74	95	99	86	58	20	-20	-58	-86	-99	-95	-74	-40
T2	30	58	80	95	100	95	80	58	30	0	-30	-58	-80	-95	-100	-95	-80	-58	-30
m=6						40	74	95	99	86	58	20	-20	-58	-86	-99	-95	-74	
T3	30	58	80	95	100	95	80	58	30	0	-30	-58	-80	-95	-100	-95	-80	-58	-30
m=7						40	74	95	99	86	58	20	-20	-58	-86	-99	-95		
T4	30	58	80	95	100	95	80	58	30	0	-30	-58	-80	-95	-100	-95	-80	-58	-30
m=8						40	74	95	99	86	58	20	-20	-58	-86	-99			
T5	30	58	80	95	100	95	80	58	30	0	-30	-58	-80	-95	-100	-95	-80	-58	-30
m=9=l						40	74	95	99	86	58	20	-20	-58	-86				
r_2	363	428	450	428	363	463	508	475	357	167	-73	-328	-550	-718	-793	-659	-453	-236	-70

N = 19 Upper rows: idealised visual response

k = 5 Lower rows: idealised auditory response

l = 9

$l \geq m \geq k$

The lower portion of Table 5.1 illustrates the alignment of data records so that the onset of the auditory stimulus is coincident across all records. The row of figures labelled r_2 provides the summation of all ordinates from each record and represents the time-locked auditory trace. Note the truncation of data preceding the onset of the auditory stimulus by more than k samples, and the effect that the collection process has on the last $l-k$ samples of the r_2 trace.

The action of these two data transformations can be shown formally by premultiplying equation {5.3} by appropriate matrices.

The first transformation, the alignment and summation of data records coincident with the onset of the visual stimulus, involves premultiplication by the matrix W_1'

where $W_1' = [\omega_1' \; \omega_1' \; \ldots\ldots \; \omega_1']$ (Nx(l-k+1)N)

and $\omega_1' = [I]$ (NxN), the identity matrix.

The result of this transformation is:

$$[\underline{y}_k + \underline{y}_{k+1} \ldots\ldots + \underline{y}_l] = (l-k+1)[I]\,\underline{h} + [Q_k + Q_{k+1} \ldots\ldots Q_l]\underline{g} + W_1' \begin{bmatrix} \underline{\varepsilon}_k \\ \underline{\varepsilon}_{k+1} \\ \cdot \\ \cdot \\ \cdot \\ \underline{\varepsilon}_l \end{bmatrix} \qquad \{5.4\}$$

The second transformation, the alignment and summation of data records coincident with the onset of the auditory stimulus, involves pre-multiplying by the matrix W_2'

where $W_2' = [\omega_{2k}' \quad \omega_{2k+1}' \cdots \omega_{2l}']$

$Nx(l-k+1)N$

and

$$\omega_{2m}' = \left[\begin{array}{c|c} 0 & I \\ N+(k-m) \times m-k & N+(k-m) \times N+(k-m) \\ \hline 0 \quad m-k \times N & \end{array}\right]$$

Applying this transformation gives the equation:

$$[\omega_{2k}' \underline{y}_k + \omega_{2k+1}' \underline{y}_{k+1} + \cdots + \omega_{2l}' \underline{y}_l'] = [P_k + P_{k+1} \cdots + P_l]\underline{h}$$

$$+ [\omega_{2k}' Q_k + \omega_{2k+1}' Q_{k+1} + \cdots + \omega_{2l}' Q_l]\underline{g} + W_2' \begin{bmatrix} \underline{\varepsilon}_k \\ \underline{\varepsilon}_{k+1} \\ \cdot \\ \cdot \\ \cdot \\ \varepsilon_l \end{bmatrix}$$

where $P_m = \omega_{2m}'$,

and writing:

$$S_m = \omega_{2m}' Q_m = \left[\begin{array}{c|c} 0 & I \\ N+(k-m) \times m-k & N+(k-m) \times N+(k-m) \\ \hline 0 \quad m-k \times N & \end{array}\right] \left[\begin{array}{c} 0 \\ m \times N-k \\ \hline I \quad 0 \\ N-m \times N-m \quad N-m \times m-k \end{array}\right]$$

$NxN \qquad NxN-k$

$$= \left[\begin{array}{c} 0 \\ k \times N-k \\ \hline I \quad 0 \\ N-m \times N-m \quad N-m \times m-k \\ \hline k-m \times N-k \end{array}\right]$$

$N \times N-k$

allows $[\omega'_{2k}\, Q_k + \omega'_{2k+1}\, Q_{k+1} \cdots \omega'_{2l}\, Q_l]$

to be rewritten as:

$$[S_k + S_{k+1} \cdots S_l]$$

The result of this second transformation can now be written as:

$$[\omega'_{2k}\, \underline{y}_k + \omega'_{2k+1}\, \underline{y}_{k+1} + \ldots + \omega'_{2l}\, \underline{y}_l] = [P_k + P_{k+1} + \ldots + P_l]\underline{h} + [S_k + S_{k+1} + \ldots + S_l]\underline{g} + W'_2 \begin{bmatrix} \underline{\varepsilon}_k \\ \underline{\varepsilon}_{k+1} \\ \cdot \\ \cdot \\ \cdot \\ \underline{\varepsilon}_l \end{bmatrix} \qquad \{5.5\}$$

If the result of the first transformation is the N length vector $\underline{r}_1$ and the result of the second transformation is the N length vector $\underline{r}_2$ then the results of the two transformations can be incorporated into one matrix equation:

$$\left[\begin{array}{c} \underline{r}_1 \\ (Nx1) \\ \hline \underline{r}_2 \\ (Nx1) \end{array}\right] = \left[\begin{array}{c|c} (l-k+1)\ I & \sum_{m=k}^{l} Q_m \\ (NxN) & (NxN-k) \\ \hline \sum_{m=k}^{l} P_m & \sum_{m=k}^{l} S_m \\ (NxN) & (NxN-k) \end{array}\right] \left[\begin{array}{c} \underline{h} \\ (N \times 1) \\ \hline \underline{g} \\ (N-kx1) \end{array}\right] + \left[\begin{array}{c} W'_1 \\ \hline W'_2 \end{array}\right] \left[\begin{array}{c} \underline{\varepsilon}_k \\ \underline{\varepsilon}_{k+1} \\ \cdot \\ \cdot \\ \cdot \\ \underline{\varepsilon}_l \end{array}\right] \qquad \{5.6\}$$

The transformations applied to the idealised visual and auditory responses are specified completely by the (2N x N+N-k) design matrix of equation {5.6}. The design matrix appropriate to those data presented in Table 5.1 is given in Table 5.2.

Table 5.2: Design matrix for data given in Table 5.1

5000000000000000000	00000000000000
0500000000000000000	00000000000000
0050000000000000000	00000000000000
0005000000000000000	00000000000000
0000500000000000000	00000000000000
0000050000000000000	10000000000000
0000005000000000000	11000000000000
0000000500000000000	11100000000000
0000000050000000000	11110000000000
0000000005000000000	11111000000000
0000000000500000000	01111100000000
0000000000050000000	00111110000000
0000000000005000000	00011111000000
0000000000000500000	00001111100000
0000000000000050000	00000111110000
0000000000000005000	00000011111000
0000000000000000500	00000001111100
0000000000000000050	00000000111110
0000000000000000005	00000000011111
1111100000000000000	00000000000000
0111110000000000000	00000000000000
0011111000000000000	00000000000000
0001111100000000000	00000000000000
0000111110000000000	00000000000000
0000011111000000000	50000000000000
0000001111100000000	05000000000000
0000000111110000000	00500000000000
0000000011111000000	00050000000000
0000000001111100000	00005000000000
0000000000111110000	00000500000000
0000000000011111000	00000050000000
0000000000001111100	00000005000000
0000000000000111110	00000000500000
0000000000000011111	00000000050000
0000000000000001111	00000000004000
0000000000000000111	00000000000300
0000000000000000011	00000000000020
0000000000000000001	00000000000001

Equation {5.6} can be adjusted to describe the averaging rather than summation of data records, by dividing through by $(l-k+1)$:

$$\frac{1}{(l-k+1)}\begin{bmatrix}\underline{r}_1\\ \hline \underline{r}_2\end{bmatrix} = \left[\begin{array}{c|c} I & \frac{1}{(l-k+1)}\sum_{m=k}^{l} Q_m \\ \hline \frac{1}{(l-k+1)}\sum_{m=k}^{l} P_m & \frac{1}{(l-k+1)}\sum_{m=k}^{l} S_m \end{array}\right]\left[\begin{array}{c}\underline{h}\\ \hline \underline{g}\end{array}\right]$$

$$+ \frac{1}{(l-k+1)}\begin{bmatrix}W_1'\\ \hline W_2'\end{bmatrix}\begin{bmatrix}\underline{\varepsilon}_k\\ \underline{\varepsilon}_{k+1}\\ \vdots\\ \underline{\varepsilon}_l\end{bmatrix} \qquad \{5.7\}$$

Note that this equation assumes that every value represented by $\underline{r}_1$ and $\underline{r}_2$ is divided by $(l-k+1)$, which results in the inappropriate normalisation of the last $l-k$ samples of the vector $\underline{r}_2$ (refer to Table 5.1). The equation can easily be modified to accommodate the correct normalisation of actual data if necessary. For the following applications, however, the above equation is appropriate.

Equation {5.6} or {5.7} can now be used as the basis for estimating the idealised visual and auditory responses. Equation {5.8} expresses the general linear regression model in matrix notation (Kendall and Stuart, 1967, p.76), and the correspondence between this equation and equations {5.6} and {5.7} is noted:

$$Y = X\beta + \varepsilon \qquad \{5.8\}$$

where Y is a vector of observations corresponding to $\underline{r}_1$ and $\underline{r}_2$ in equations {5.6} and {5.7}

X is a matrix of known coefficients corresponding to the design matrix of equations {5.6} and {5.7}

β is a vector of unknown parameters which corresponds to the idealised visual and auditory responses represented by $\underline{h}$ and $\underline{g}$ in equations {5.6} and {5.7}, and

ε is the vector of 'error' random variables.

The parameters β of the model can be estimated through the method of ordinary least squares (OLS) (Kendall and Stuart, 1967):

$$\hat{\beta} = (X'X)^{-1} X'Y \qquad \{5.9\}$$

where, in addition to the above definitions,

X' is the transpose of the design matrix X, and

$(X'X)^{-1}$ is the inverse of the sums of squares and cross-products of the elements within X.

Note that an intercept term β_o can be added to the model by incorporating a vector of 1s in the first column position of the X matrix (Neter and Wasserman, 1974, p.234).

The OLS estimators are unbiased and of minimum variance if a number of assumptions are satisfied (see Bennett, 1979, p.244 for a comprehensive account of these assumptions). The major assumptions include:

1. That the model is correctly specified. That is, the design matrix must accurately describe the relationship between the observations and the parameters of the model.

2. That the disturbances or errors $\{\varepsilon\}$ in the equation are random and have an expected value of zero ($E\{\varepsilon\} = 0$).
3. That the errors are of constant variance (the homoscedasticity condition), with a variance-covariance matrix $E\{\varepsilon\varepsilon'\} = \sigma_\varepsilon^2 I$.
4. That the errors are independent of each other, $E\{\varepsilon_t, \varepsilon_{t-\tau}\} = 0$, for all $\tau \neq 0$.

The importance of the assumptions concerning the error term of the model is realised if we consider that the basis of least squares parameter estimation is to minimize the sum of the squared residuals which are a linear function of the unknown disturbances. It will be noted that the comparison made between the proposed model (equations {5.6} and {5.7}) and the general linear model (equation {5.8}) failed to take into account the effect of the transformation matrices W_1' and W_2', on the error term of the proposed model. These transformations may result in departures from either or both of assumptions 3 and 4 given above.

Departures from the homoscedasticity condition will result in OLS estimators which are still unbiased and consistent but which are no longer minimum variance estimators (Neter and Wasserman, 1974, p.131). Similarly, OLS estimation in the presence of autocorrelated disturbances will be asymptotically unbiased and consistent, but the estimator will be inefficient and hence no longer minimum variance. Also, the estimates of the parameter variance, $var(\hat{\beta})$ and error variance, $\hat{\sigma}_\varepsilon^2$ will be biased (Hibbs, 1974, p.256). The important implication for the present solution is that departures from these assumptions, resulting from the transformations applied through the data saving process, will yield OLS estimates of idealised visual and auditory responses which have needlessly large variances.

The assumptions of homoscedasticity and independence of the error process imply that the error variance-covariance matrix is constant in the diagonal elements (homoscedasticity) and zero in the off-diagonal elements (no autocorrelation). That is:

$$E\{\varepsilon\varepsilon'\} = \sigma_\varepsilon^2 I \qquad \{5.10\}$$

where σ_ε^2 is the population error variance and

I is the identity matrix.

In cases where the disturbances depart from either of these assumptions the dispersion matrix can no longer be described as above but rather corresponds to $\sigma_\varepsilon^2 V$, where the diagonal elements of V reflect the variance of the error terms while the off-diagonal elements reflect the mechanism generating the disturbance time dependence.

If prior information about V is available then parameter estimation can be undertaken using Aitken's (1935) method of generalised least squares (GLS), whereby equation {5.9} generalises to:

$$\hat{\beta} = (X'V^{-1}X)^{-1} X'V^{-1}Y \qquad \{5.11\}$$

Hibbs (1974, p.260) provides proof that the GLS estimator is asymptotically unbiased, minimum variance and provides unbiased estimates of the parameter variance and error variance. Therefore, GLS provides in theory the optimum solution to the problems created by departures from those assumptions concerning the error term of the general linear model.

In general prior knowledge of the disturbance variance-covariance matrix is not available and, in the case of autocorrelated disturbances, the character of V must be deduced from sample data by identifying the static model which best describes the noise process (Hibbs, 1974). In the present case, however, knowledge of the form of W_1' and W_2' allows the error variance-covariance matrix resulting from these transformations to be specified. The dispersion matrix of the transformed errors from equation {5.6} can be written:

$$\sigma_\varepsilon^2 V = \begin{bmatrix} W_1' \\ W_2' \end{bmatrix} E(\varepsilon\varepsilon') \begin{bmatrix} W_1 & W_2 \end{bmatrix}$$

Since, from equation {5.10}, σ_ε^2 is a scalar quantity and the identity matrix can be suppressed, the above becomes:

$$V = \begin{bmatrix} W_1' \\ W_2' \end{bmatrix} \begin{bmatrix} W_1 & W_2 \end{bmatrix} = \begin{bmatrix} W_1' W_1 & W_1' W_2 \\ W_2' W_1 & W_2' W_2 \end{bmatrix} \qquad \{5.12\}$$

and the component matrices of the error variance-covariance matrix can be specified as follows:

$$W_1' W_1 = \begin{bmatrix} \omega_1' & \omega_1' & \omega_1' & \cdots & \omega_1' \end{bmatrix} \begin{bmatrix} \omega_1 \\ \omega_1 \\ \omega_1 \\ \cdot \\ \cdot \\ \cdot \\ \omega_1 \end{bmatrix}$$

$$= (\ell-k+1) \underset{NxN}{\begin{bmatrix} & I & \end{bmatrix}} ,$$

$$W_2' W_2 = \begin{bmatrix} \omega_{2k}' & \omega_{2k+1}' & \cdots & \omega_{2\ell}' \end{bmatrix} \begin{bmatrix} \omega_{2k} \\ \omega_{2k+1} \\ \vdots \\ \omega_{2\ell} \end{bmatrix} = \sum_{m=k}^{\ell} \omega_{2m}' \omega_{2m}$$

where $\omega_{2m}' \omega_{2m} =$

$$\left[\begin{array}{c|c} \begin{matrix} 0 \\ N+(k-m) \\ xm-k \end{matrix} & \begin{matrix} I \\ N+(k-m) \\ xN+(k-m) \end{matrix} \\ \hline \multicolumn{2}{c}{\begin{matrix} 0 \\ m-kxN \end{matrix}} \end{array}\right] \left[\begin{array}{c|c} \begin{matrix} 0 \\ m-kx \\ N+(k-m) \end{matrix} & \begin{matrix} \\ 0 \\ Nx \end{matrix} \\ \hline \begin{matrix} I \\ N+(k-m) \\ xN+(k-m) \end{matrix} & \begin{matrix} \\ \\ m-k \end{matrix} \end{array}\right]$$

$$= \left[\begin{array}{c|c} \begin{matrix} I \\ N+(k-m)\,x \\ N+(k-m) \end{matrix} & \begin{matrix} 0 \\ N+(k-m) \\ xm-k \end{matrix} \\ \hline \multicolumn{2}{c}{\begin{matrix} 0 \\ m-kxN \end{matrix}} \end{array}\right] ,$$

$$W_2' W_1 = \begin{bmatrix} \omega_{2k}' & \omega_{2k+1}' & \cdots & \omega_{2\ell}' \end{bmatrix} \begin{bmatrix} \omega_1 \\ \omega_1 \\ \vdots \\ \omega_1 \end{bmatrix} = \sum_{m=k}^{\ell} \omega_{2m}' \omega_1$$

where $\omega'_{2m}\ \omega_1 =$

$$\left[\begin{array}{c|c} 0 & I \\ N+(k-m) & N+(k-m) \\ xm-k & x \\ & N+(k-m) \\ \hline 0 & \\ m-k\,xN & \end{array}\right] \left[\begin{array}{c} I \\ NxN \end{array}\right]$$

$$= \left[\begin{array}{c|c} 0 & I \\ N+(k-m) & N+(k-m) \\ xm-k & x \\ & N+(k-m) \\ \hline 0 & \\ m-k\,xN & \end{array}\right] ,$$

and

$$W'_1\ W_2 = \left[\omega'_1\ \omega'_1 \cdots \omega'_1\right] \left[\begin{array}{c} \omega_{2k} \\ \omega_{2k+1} \\ \vdots \\ \omega_{2l} \end{array}\right] = \sum_{m=k}^{l} \omega'_1\ \omega_{2m}$$

where $\omega'_{1m}\ \omega_{2m} =$

$$\left[\begin{array}{c} I \\ NxN \end{array}\right] \left[\begin{array}{c|c} 0 & \\ m-k\,x & 0 \\ N+(k-m) & Nx \\ \hline I & m-k \\ N+(k-m)\,x & \\ N+(k-m) & \end{array}\right]$$

$$= \left[\begin{array}{c|c} 0 & \\ m-k\,x & 0 \\ N+(k-m) & Nx \\ \hline I & m-k \\ N+(k-m) & \\ xN+(k-m) & \end{array}\right] .$$

The division of each element of the above sub-matrices by $(l-k+1)$ is appropriate if the transformations involve the averaging rather than summation of data.

The error variance-covariance matrix, V, for those data presented in Table 5.1 is given in Table 5.3. Note that the transformations remove the assumed independence of the errors and result also in a mild departure from the homoscedasticity condition.

The following Section uses simulated data to test the assumption that the design matrix of the proposed model is correctly specified. The effect of the transformations on the error term of the model and the implications for parameter estimation are also considered further.

5.3 Testing the model

For the following tests the idealised visual and auditory responses are represented by a single cycle of a sinusoid comprising 45 data values and 40 data values respectively. These idealised traces are shown in Figure 5.1A.

The first stage in testing involved simulating time-locked visual and auditory averages by calculating the running average of each idealised trace and adding the resultant waveform to the unstaggered version of the other trace. A staggering window of 5 samples was used while the minimum delay between the onset of the visual response and the onset of the auditory response was 5 samples, and the maximum delay was 9 samples. Thus, N = 45, k = 5 and l = 9. Note that all data values of each running sum were divided by $(l-k+1)$ = 5 to produce averages appropriate to the model specified by equation {5.7}. The simulated time-locked visual and auditory responses are shown in Figure 5.1B, each consisting of 45 data values.

Table 5.3: Error variance-covariance matrix for data given in Table 5.1

5000000000000000000	1000000000000000000
0500000000000000000	1100000000000000000
0050000000000000000	1110000000000000000
0005000000000000000	1111000000000000000
0000500000000000000	1111100000000000000
0000050000000000000	0111110000000000000
0000005000000000000	0011111000000000000
0000000500000000000	0001111100000000000
0000000050000000000	0000111110000000000
0000000005000000000	0000011111000000000
0000000000500000000	0000001111100000000
0000000000050000000	0000000111110000000
0000000000005000000	0000000011111000000
0000000000000500000	0000000001111100000
0000000000000050000	0000000000111110000
0000000000000005000	0000000000011111000
0000000000000000500	0000000000001111100
0000000000000000050	0000000000000111110
0000000000000000005	0000000000000011111

1111100000000000000	5000000000000000000
0111110000000000000	0500000000000000000
0011111000000000000	0050000000000000000
0001111100000000000	0005000000000000000
0000111110000000000	0000500000000000000
0000011111000000000	0000050000000000000
0000001111100000000	0000005000000000000
0000000111110000000	0000000500000000000
0000000011111000000	0000000050000000000
0000000001111100000	0000000005000000000
0000000000111110000	0000000000500000000
0000000000011111000	0000000000050000000
0000000000001111100	0000000000005000000
0000000000000111110	0000000000000500000
0000000000000011111	0000000000000050000
0000000000000001111	0000000000000004000
0000000000000000111	0000000000000000300
0000000000000000011	0000000000000000020
0000000000000000001	0000000000000000001

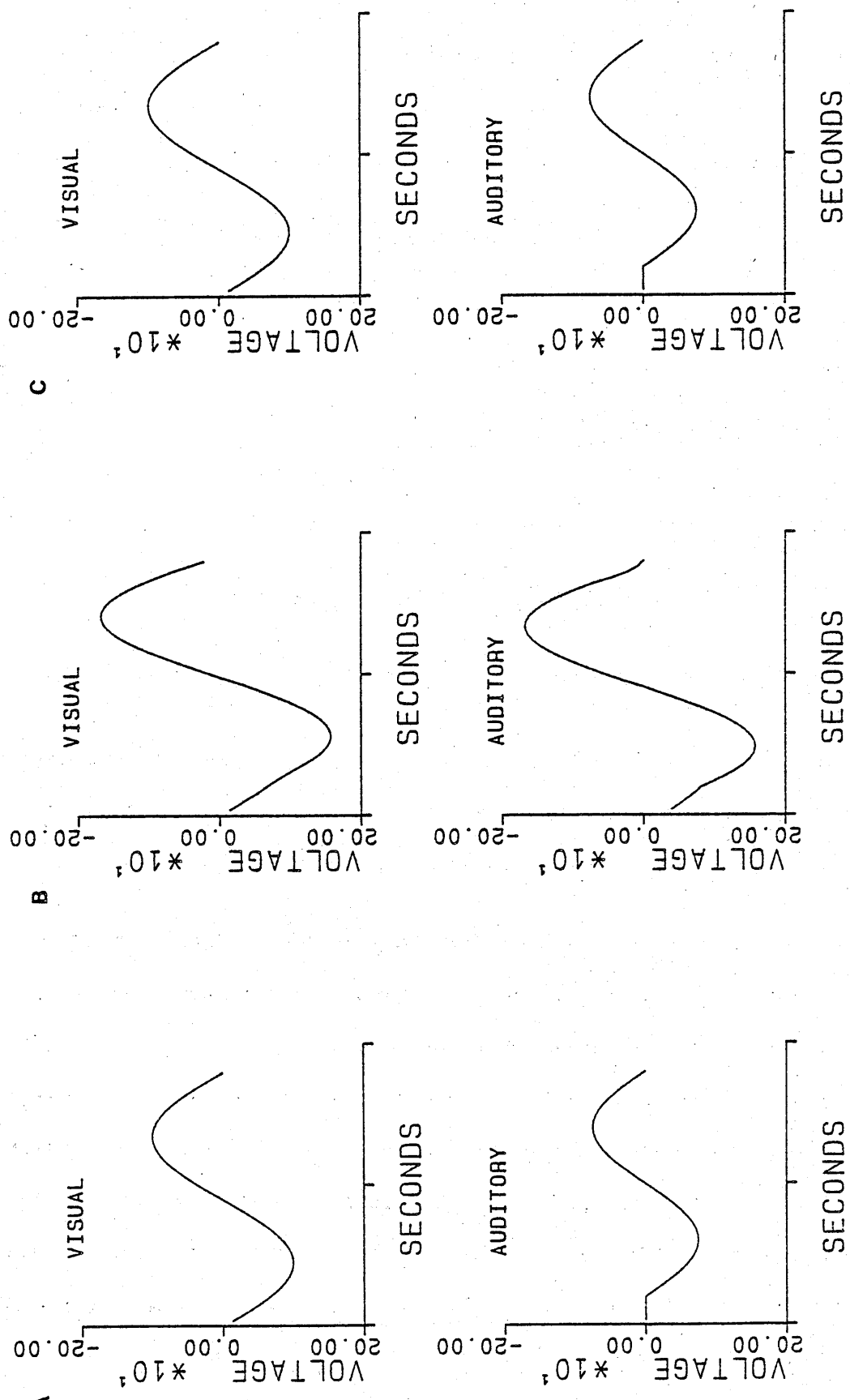

Figure 5.1. A: Idealised visual and auditory responses. B: Time-locked visual and auditory traces. C: Recovered waveforms following OLS estimation.

OLS estimation of the idealised responses was achieved through the use of the regression analysis program provided as part of the GENSTAT software package (Numerical Algorithms Group Ltd., 1980). The simulated time-locked visual and auditory responses were combined into a single vector of 90 elements for input into the program, and the design matrix for the analysis was generated from equation {5.7} with an additional column of 1s to allow estimation of the intercept term. The order of the design matrix was thus 90 x 86. A total of 85 parameter estimates (excluding β_0) was returned from the analysis, the first 45 values corresponding to the estimated idealised visual response and the latter 40 values corresponding to the estimated idealised auditory response. These are plotted separately in Figure 5.1C. Each recovered waveform replicates the original exactly and confirms the accurate specification of the design matrix for these data.

A second test was conducted to compare OLS and GLS parameter estimation following the addition to those input data presented in Figure 5.1B of random normal deviates which had been transformed to simulate the effect of the transformation matrices W_1' and W_2'.

Random normal deviates having a mean of zero and a standard deviation of 5 were generated using pseudo-random number generator routines from the Numerical Algorithms Group subroutine library. Five different sequences of 45 random numbers were generated, each sequence representing the error component recorded over a single trial. The transformations, W_1' and W_2', were then applied to these sequences to simulate the disturbances contributing to the time-locked visual trace and time-locked auditory trace, respectively. Firstly, the initial values of the five error sequences were aligned and the average value of each coincident ordinate was calculated. This average was added to the simulated time-locked visual trace presented in Figure 5.1B and the result is shown as the upper

trace in Figure 5.2A. Secondly, the error sequences were staggered according to the transformation W_2' and all coincident ordinates were averaged together to simulate the errors contributing to the time-locked auditory response. This average was added to the auditory trace presented in Figure 5.1B and the result is shown as the lower trace in Figure 5.2A.

OLS estimation of the idealised responses was achieved using the GENSTAT program described above. The estimated idealised visual and auditory responses are presented in Figure 5.2B. GLS estimation involved generating the 90 by 90 variance-covariance matrix from equation {5.12}. Note that every element of the V matrix was divided by $(\ell-k+1)$ as the input data represented the average rather than sum of data values. GLS estimates of the idealised responses were calculated according to equation {5.11} using the matrix operation subroutines supplied as part of the GENSTAT software package. The recovered waveforms are shown in Figure 5.2C.

Visual inspection of Figure 5.2B and Figure 5.2C suggests that both OLS and GLS solutions provide a satisfactory estimation of the idealised visual and auditory responses. The differences waves shown in Figure 5.3, however, demonstrate that the GLS estimates correspond more closely to the original waveforms. Figure 5.3A and Figure 5.3B show the results of subtracting the idealised waveforms presented in Figure 5.1A from the OLS estimates (Figure 5.2B) and the GLS estimates (Figure 5.2C), respectively. These 'residuals' indicate that OLS progressively overestimates the negativity of the recovered visual response and underestimates the negativity of the recovered auditory response. The 'residuals' involving the GLS estimates on the other hand fluctuate more or less randomly about zero, indicating the near perfect recovery of the idealised waveforms.

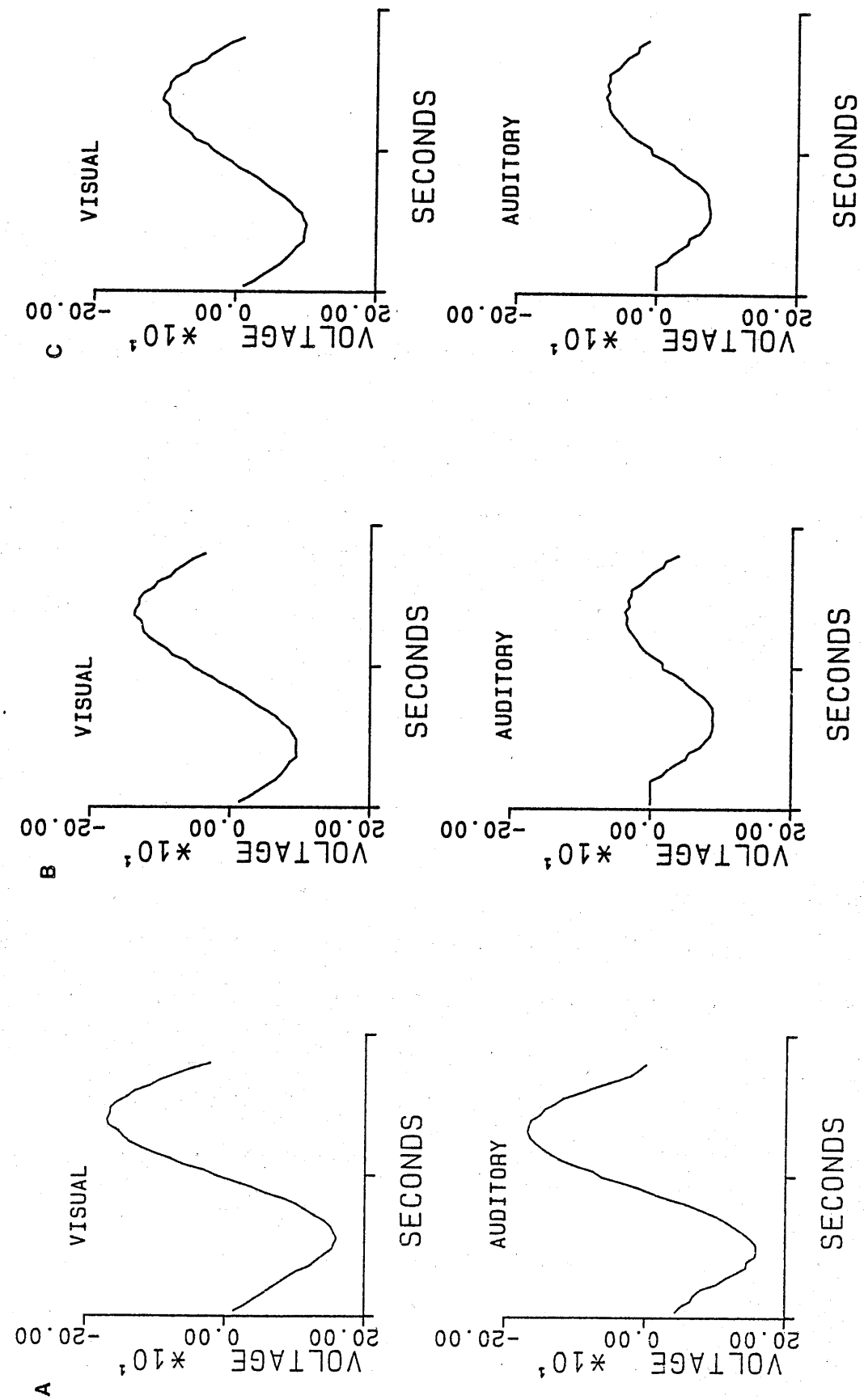

Figure 5.2. A: Time-locked visual and auditory traces following the addition of transformed random normal deviates. B: Recovered waveforms following OLS estimation. C: Recovered waveforms following GLS estimation.

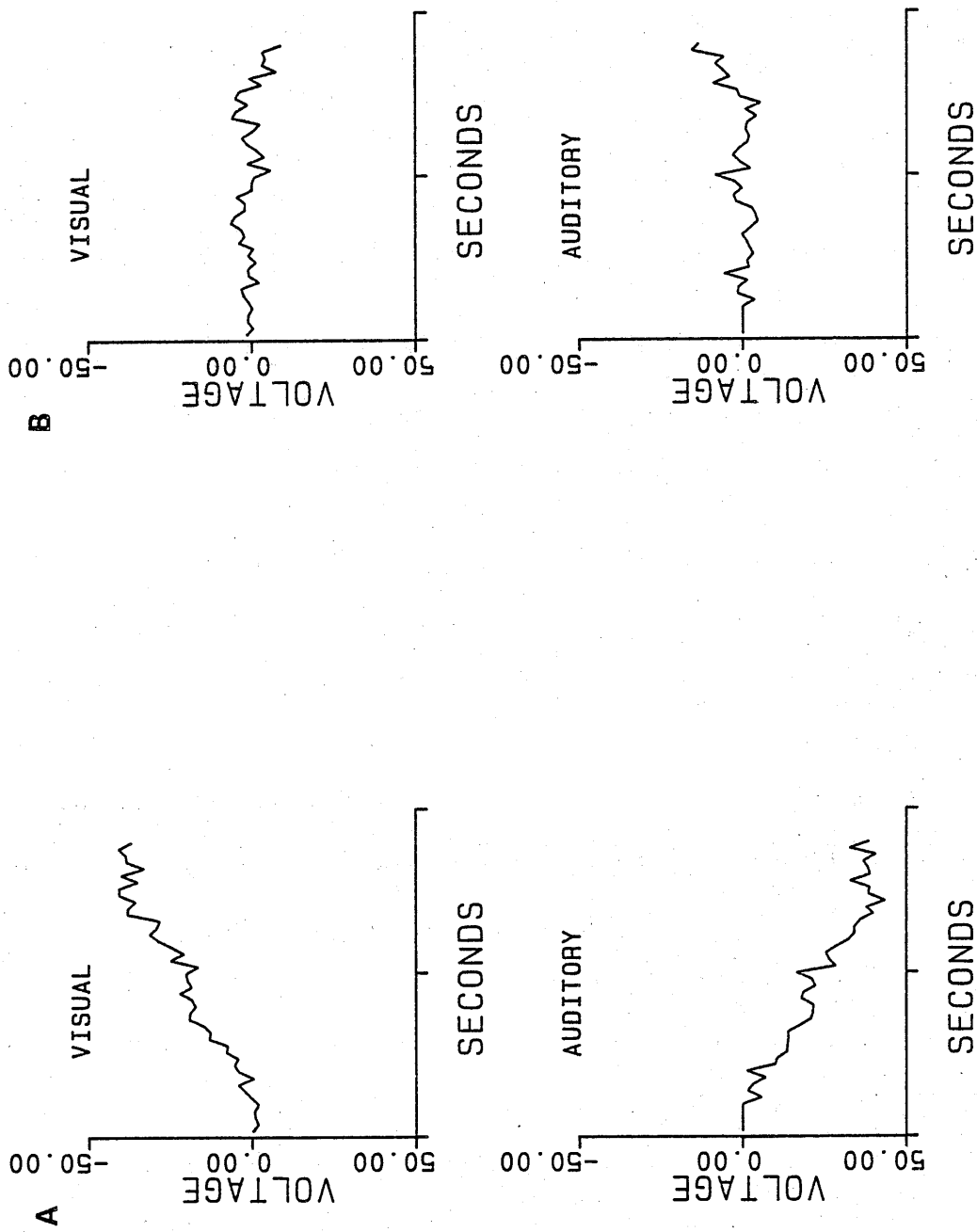

Figure 5.3. Differences between recovered waveforms and idealised waveforms following A: OLS and B: GLS estimation.

Note also that the variance of the estimated parameters can be obtained by taking the square of these difference values (Hibbs, 1974, p.255):

$$\text{var}(\hat{\beta}) = E[(\hat{\beta} - \beta)(\hat{\beta} - \beta)']$$

Figure 5.3 therefore provides confirmation that, in the presence of transformed errors, the variances of estimates secured through GLS are appreciably smaller than those of estimates derived through OLS.

5.4 Comparison between the proposed model and dual-task experimental procedures

As indicated in Section 5.1 the proposed model assumes some departures from the actual methods of stimulus presentation and data collection used in the dual-task experiment. These are as follows:

1. The proposed model assumes that, under a particular signal condition, the auditory stimulus is presented once at each interval within the staggering window. In the dual-task experiment, however, each signal was in fact presented twice to each subject. This departure can be considered trivial as the model represented by equation {5.7} is still valid if the input data consists of the averages of data records. Alternatively, the design matrix given in equation {5.6} can be readily adjusted to accommodate any duplication of stimulus presentations if the input data represent the summation of individual data records.
2. A more serious departure is that the proposed model assumes that an equal number of auditory stimuli are presented at every sample interval over the staggering window. In the dual-task experiment, however, data were not saved for those trials on which subjects responded incorrectly or made excessive eye movements, resulting in the rejection of approximately 30% of trials under every experimental condition (cf. Section 2.6.1). If this rejection

differentially affected trials corresponding to signals presented at particular sample intervals within the staggering window, then estimates of visual and auditory responses will be less than optimal. In future experiments replacement trials should be included to ensure a full complement of data and to maximise the accuracy of the solution.

3. A third departure from the proposed model concerns the method of data saving employed in the dual-task experiment to generate the time-locked auditory traces. Reference to Table 5.1 will help illustrate this difference. The model presented in equations {5.6} and {5.7} assumes that the time-locked visual and auditory responses are generated from traces comprising a maximum of N samples following the onset of the visual stimulus. This results in the progressive reduction in the number of data values contributing to the final l-k samples of the time-locked auditory response, and ultimately to the departure from the homoscedasticity condition evident in the error variance-covariance matrix. In the dual-task experiment, however, it will be recalled that a total of 375 data values (1.5 seconds duration) was always averaged into the time-locked auditory traces, irrespective of the delay between the onset of the visual and auditory stimuli. While this departure from the proposed model can easily be rectified in future experiments by truncating data values occurring beyond N samples, the failure to do so in the present experiment means that the last 24 points of the time-locked auditory traces do not conform to the specification of the design matrix, and this could lead to biased estimates of the idealised responses. Inspection of Table 5.2 will confirm that the method of data saving used in the dual-task experiment cannot be accurately described by any modification to the design

matrix which does not introduce linear dependencies into the matrix. That is, the only configuration which can accurately describe the present data is a matrix which has a greater number of columns than rows and hence will be singular. The last 24 samples of the present data, however, can be weighted in an attempt to compensate for the departure from the model specifications. Note that the correct method of data saving (as specified by the proposed model) requires an *a priori* decision concerning the length of the time series to be entered into the regression analysis for estimation of the idealised responses.

5.5 Application of the GLS solution to dual-task data

GLS estimation was achieved using Fortran-callable matrix subroutines available as part of the Numerical Algorithm Group subroutine library. The design matrix was calculated from equation {5.7} for N=170, k = 25 and l = 49. A non-intercept model was utilized as previous tests had resulted in a negligible intercept term. The order of the design matrix was thus 340 by 315, while the order of the corresponding variance-covariance matrix was 340 by 340. These matrices were the largest that could be accommodated within the program-size restrictions governing users of the Univac 1100.

The input data for the analysis consisted of 340 data values, 170 values taken from the time-locked visual trace and 170 values taken from the corresponding time-locked auditory trace. Prior to collecting these data a comparison was made between the mean value of the visual trace calculated from 100 samples prior to the start of the auditory signal window, and the mean value of the auditory trace, also calculated

from 100 samples immediately prior to the auditory signal onset. The difference in these values was added to every value of the time-locked auditory trace to ensure that the initial offsets of both sections of trace submitted to the analysis were equivalent. This adjustment is crucial to the success of the analysis as differential offsets can result in highly spurious estimates of the idealised responses.

Following the above adjustment the visual component of the input data was collected starting 25 samples before the onset of the signal window and the auditory data were similarly collected, starting 25 samples prior to the auditory stimulus onset. Note that the visual input into the analysis does not need to start at the point of onset of a visual stimulus, but rather must start k samples prior to the onset of the first auditory stimulus within the signal window. Hence the design matrix used in the present analysis is appropriate for analysing data recorded under all signal conditions of the dual-task.

Finally, the last 24 values of the auditory data were weighted in an attempt to compensate for the departure of these data from the specified model. Each data value was scaled by a factor equal to a multiple of 0.04 which represents the proportional contribution of one trace to an average based on a total of 25 traces. That is, the twenty-fourth data value from the end of the auditory trace was multiplied by 0.96, the next was multiplied by 0.92, the next by 0.88, and so on, while the final value was multiplied by 0.04. Hence the last l-k data values were progressively reduced in magnitude to provide a closer correspondence to the specifications of the proposed model (see Table 5.1).

Figure 5.4 provides examples of the data submitted to the GLS analysis. Each trace shows data recorded from the Cz placement under physical match trials. The vertical line separates the visual component of the input data from the auditory component. Figure 5.5 shows the GLS estimates of those data presented in Figure 5.4. The idealised visual response consists of 170 data values (680mS) while the idealised auditory response consists of 145 data values (580mS). Again, the responses are separated by a vertical line.

The first 25 values of the estimates visual traces are identical to the initial 25 values of the input data as they represent activity recorded prior to the onset of any auditory stimulus. These values were used to fit the estimated visual responses at their appropriate positions within the time-locked visual trace. Figure 5.6 shows the visual components of the GLS estimates from Figure 5.5, positioned within the time-locked visual traces recorded from the Cz placement over physical match trials of the dual task. The estimated sections of trace are bounded by arrow heads.

The baseline of every estimated auditory response was adjusted by subtracting the mean of the first 20 data values from every value comprising the trace, and then the trace was padded out with nulls and fitted within a 1.5 second epoch. Figure 5.7 shows the auditory components of the GLS estimates from Figure 5.5.

Figures 5.8 to 5.17 show the results of applying the analysis to visual and auditory traces recorded from Cz and Pz placements over all remaining conditions of the dual-task experiment. Overlays 1 and 2 can be used to check for the removal of the distortion resulting from the running average of activity recorded to stimuli in the other modality.

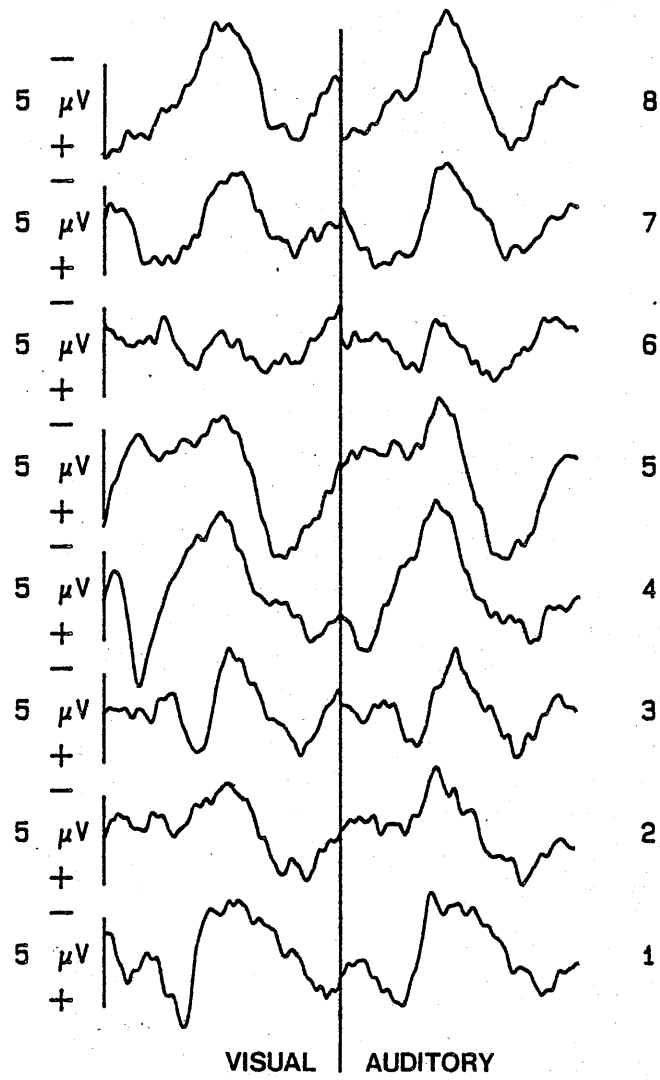

Figure 5.4. Example input data for GLS estimation (CzPM).

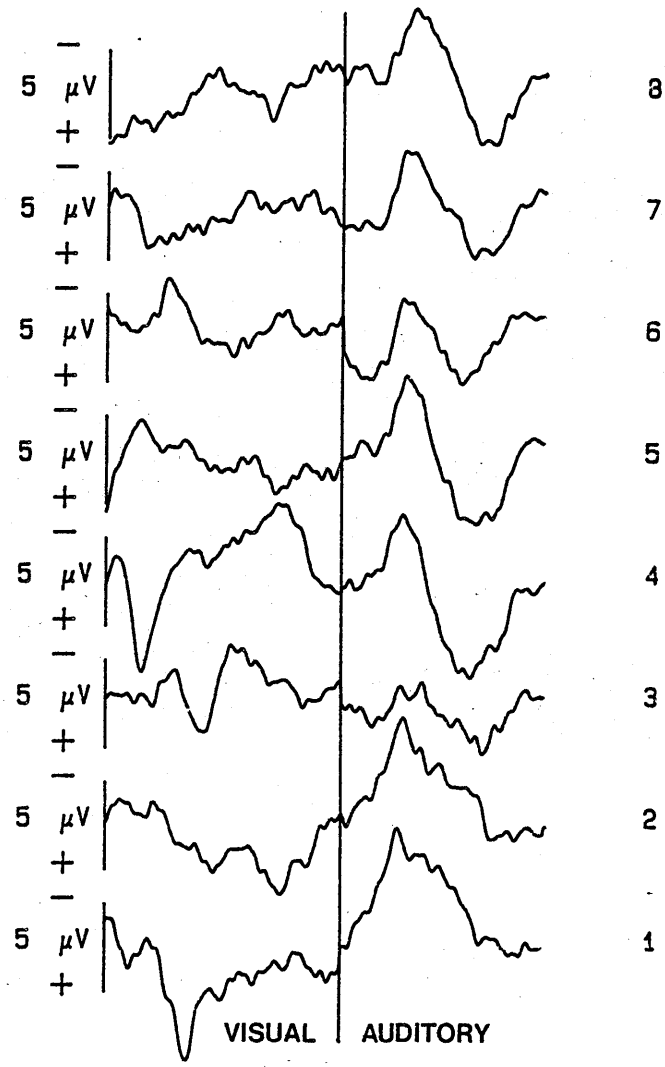

Figure 5.5. Example output following GLS estimation (CzPM).

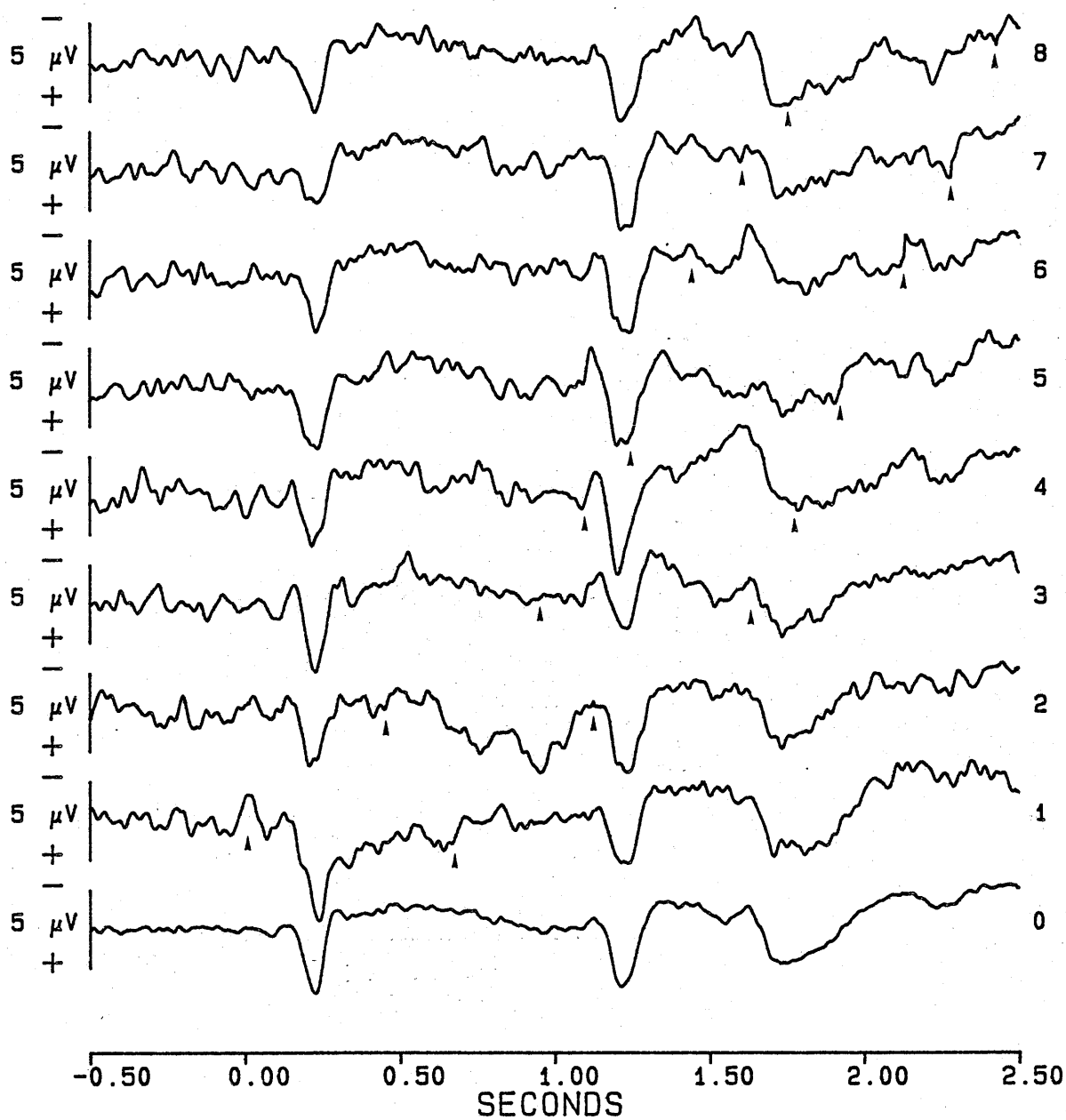

Figure 5.6. GLS estimates of visual responses (CzPM).

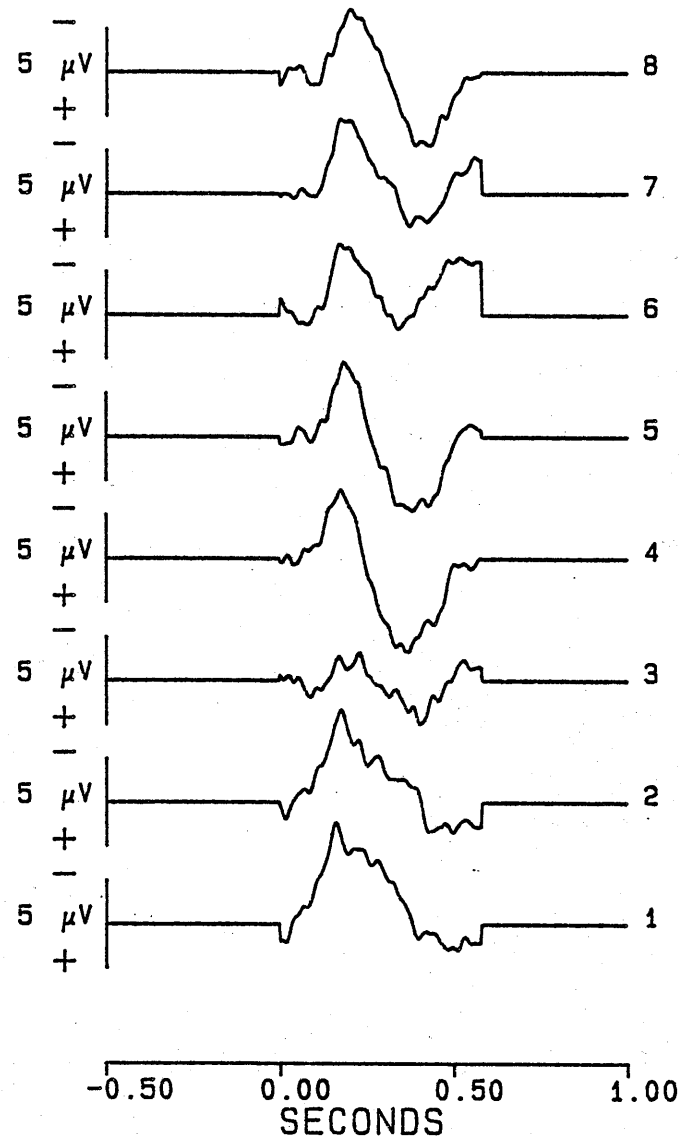

Figure 5.7. GLS estimates of auditory responses (CzPM).

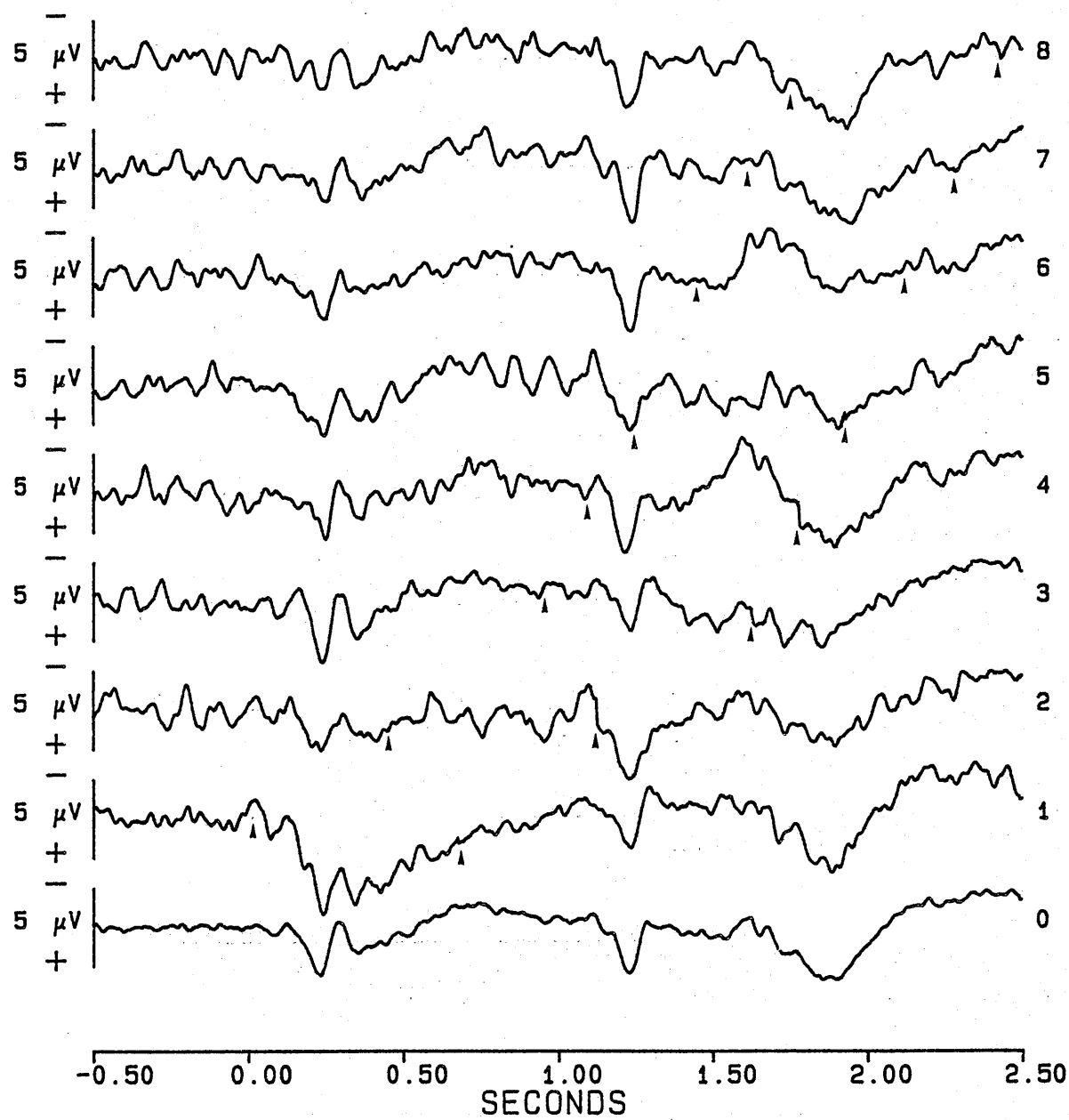

Figure 5.8. GLS estimates of visual responses (PzPM).

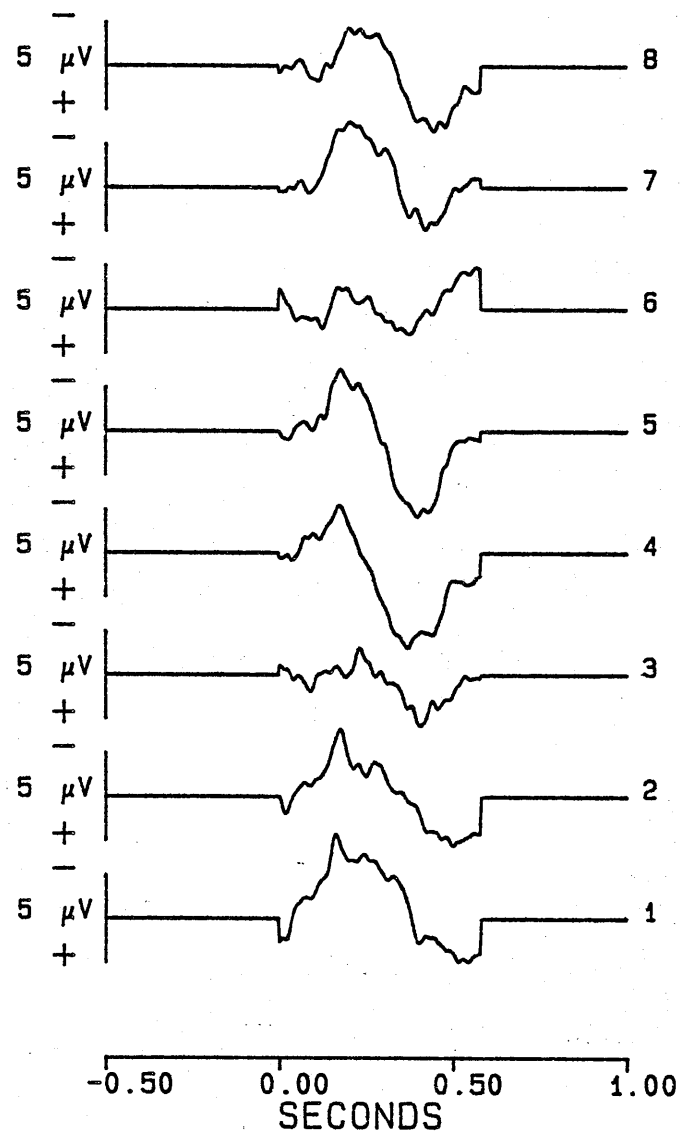

Figure 5.9. GLS estimates of auditory responses (PzPM).

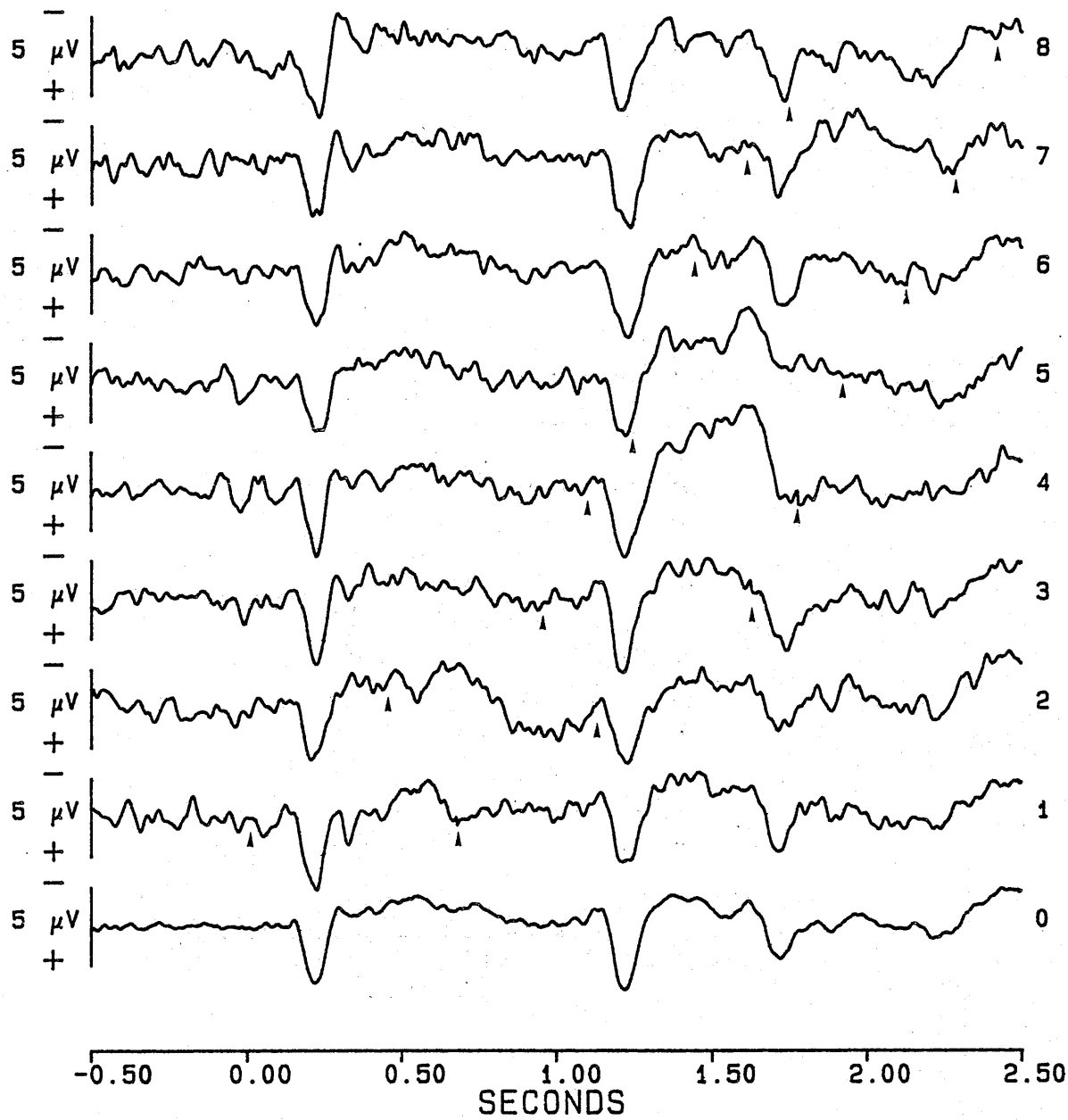

Figure 5.10. GLS estimates of visual responses (CzRM).

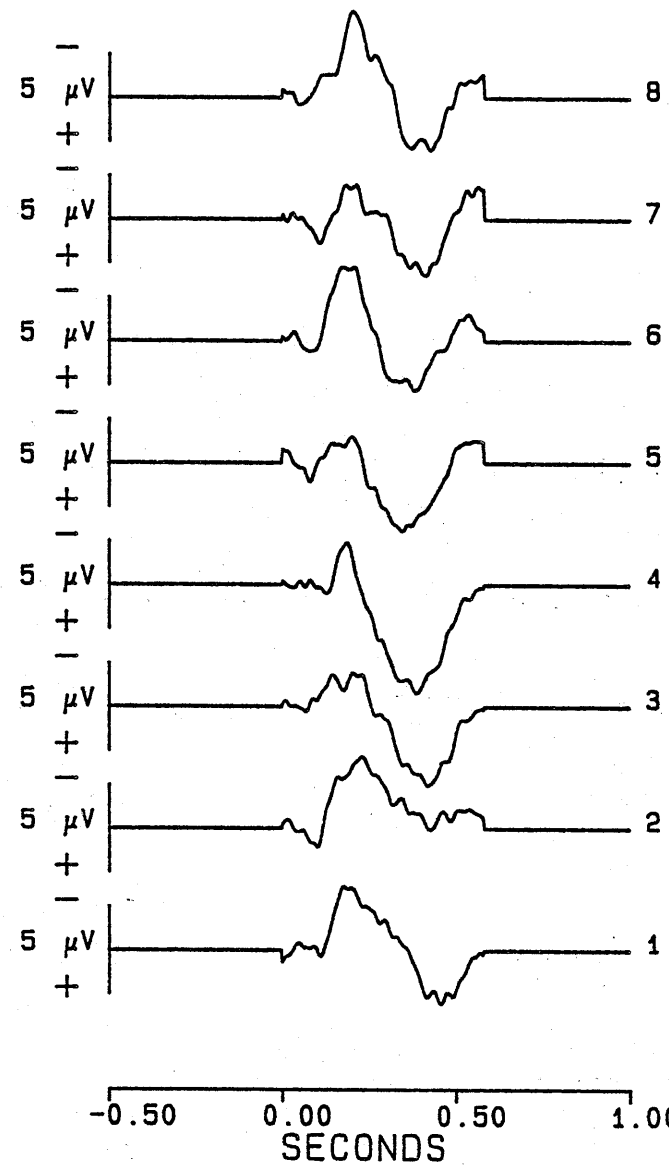

Figure 5.11. GLS estimates of auditory responses (CzRM).

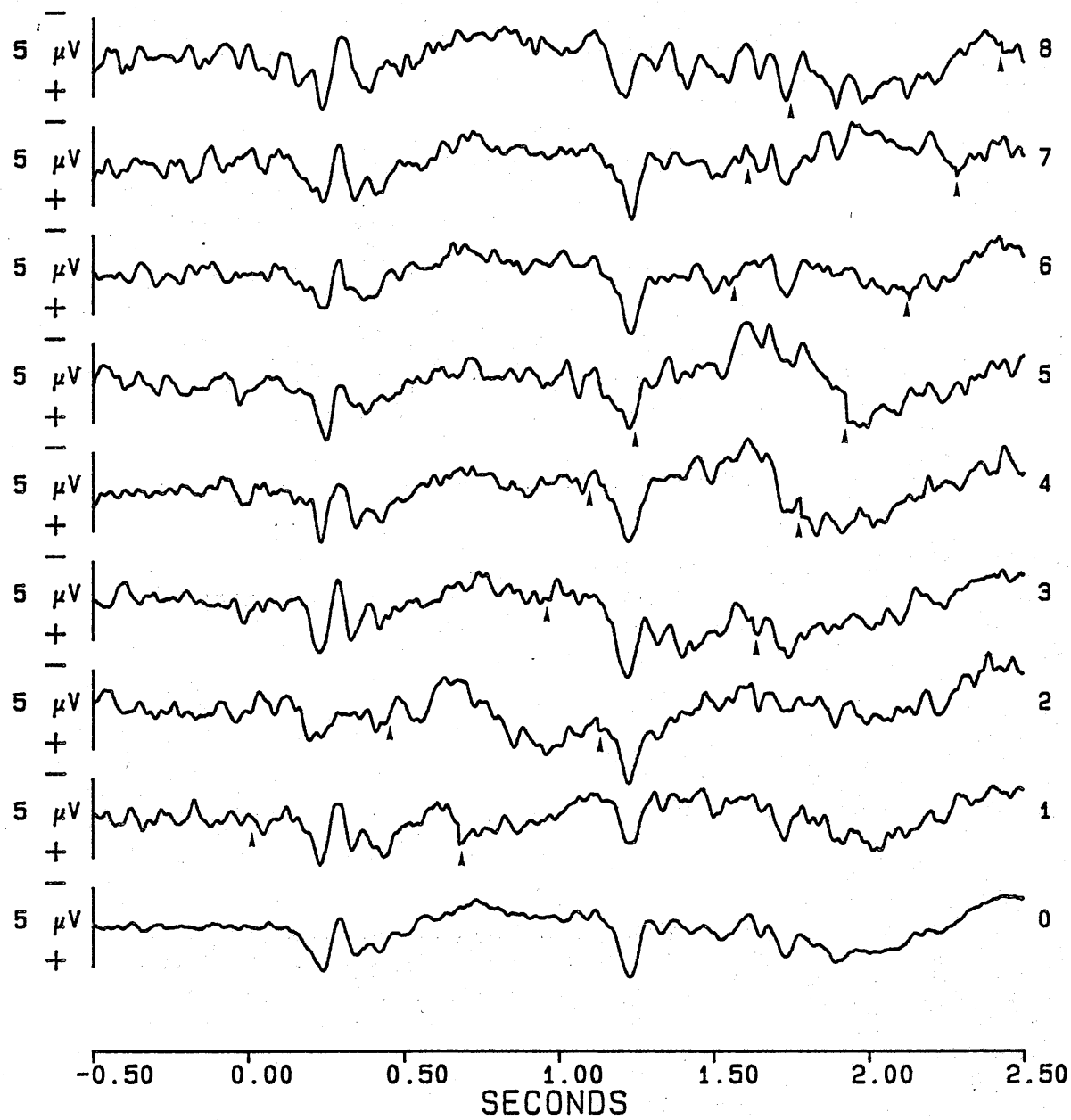

Figure 5.12. GLS estimates of visual responses (PzRM).

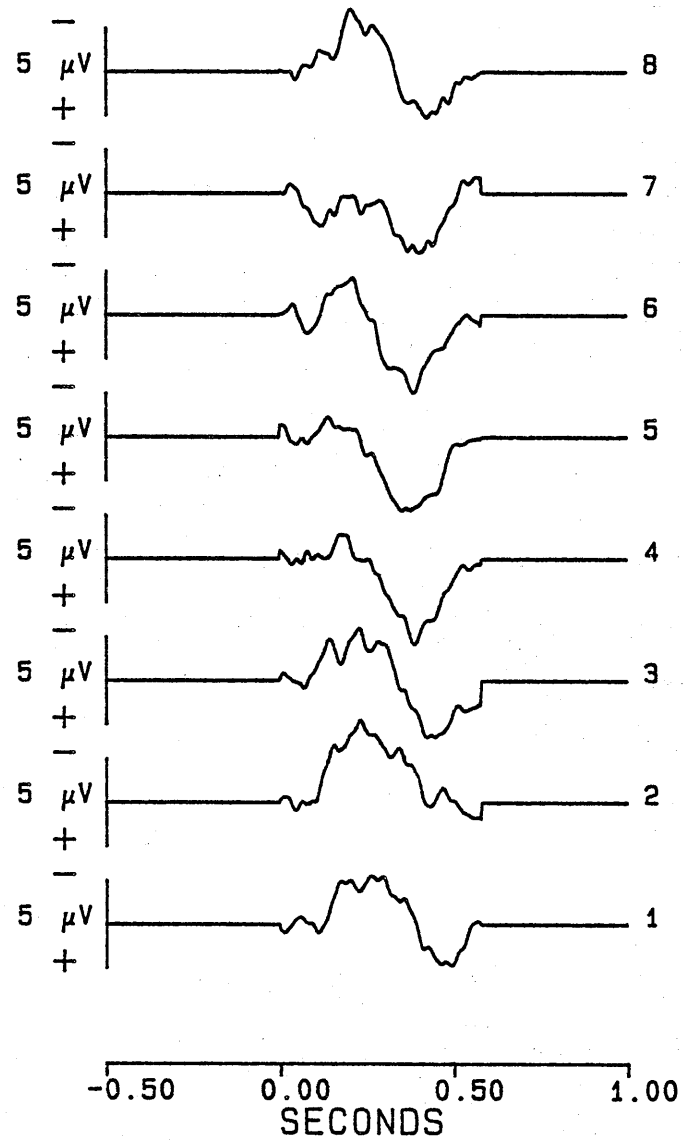

Figure 5.13. GLS estimates of auditory responses (PzRM).

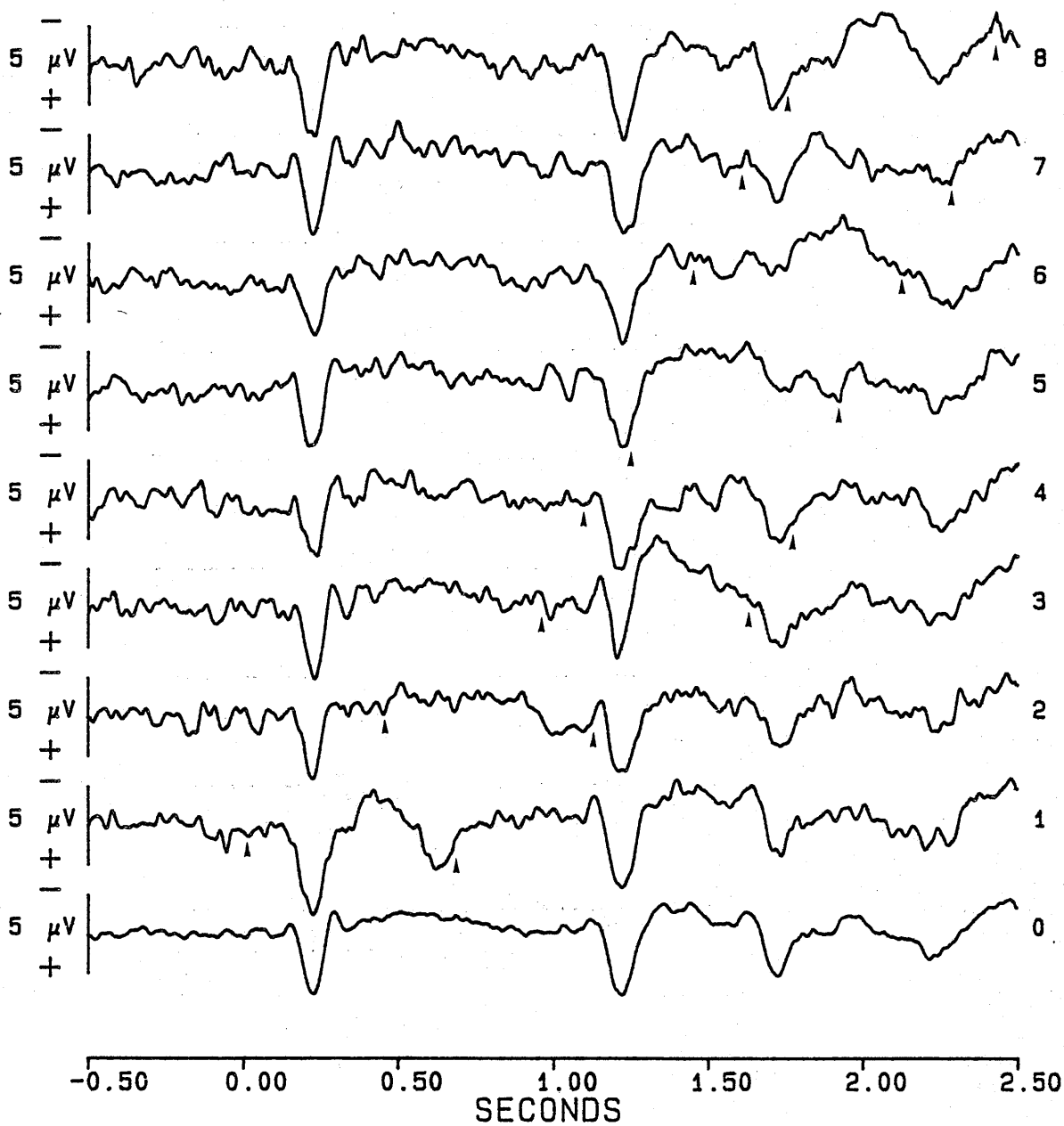

Figure 5.14. GLS estimates of visual responses (CzMM).

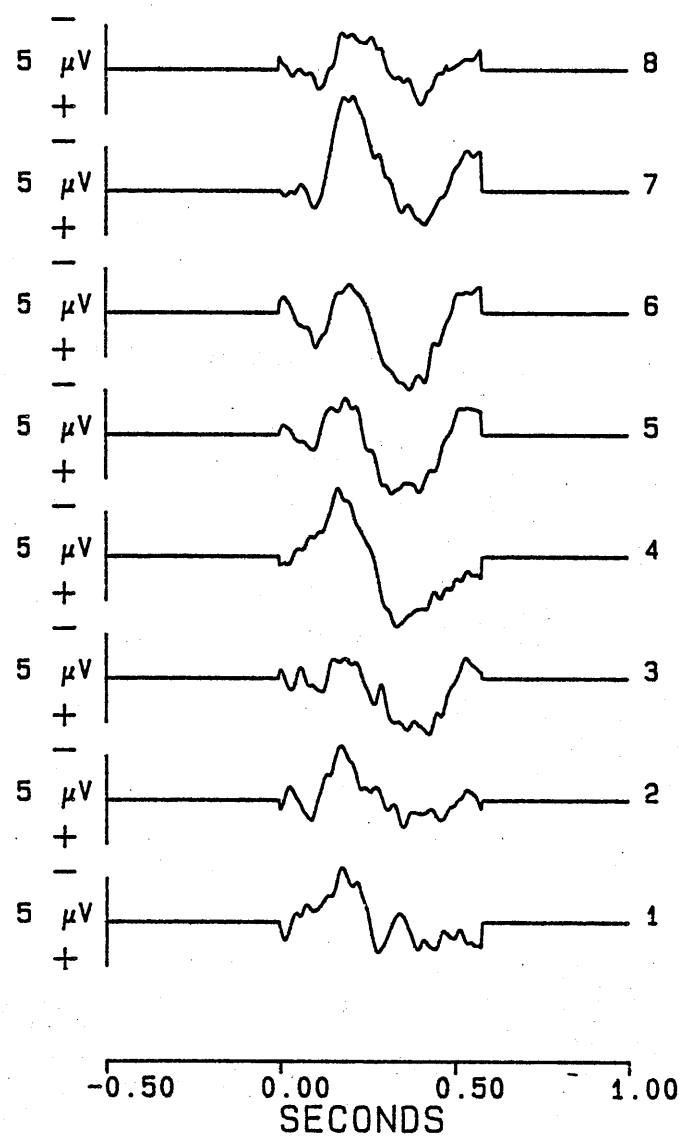

Figure 5.15. GLS estimates of auditory responses (CzMM).

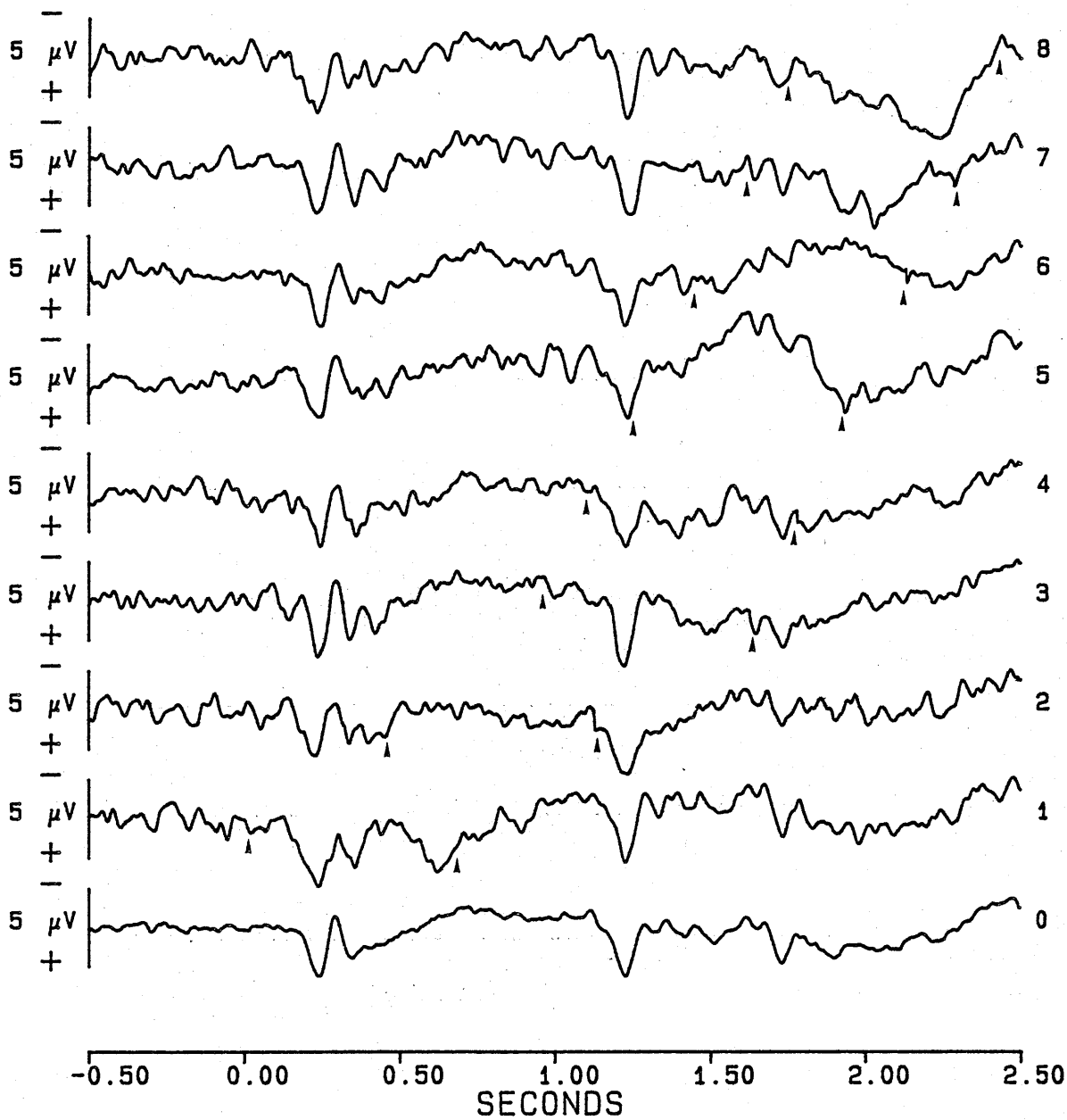

Figure 5.16. GLS estimates of visual responses (PzMM).

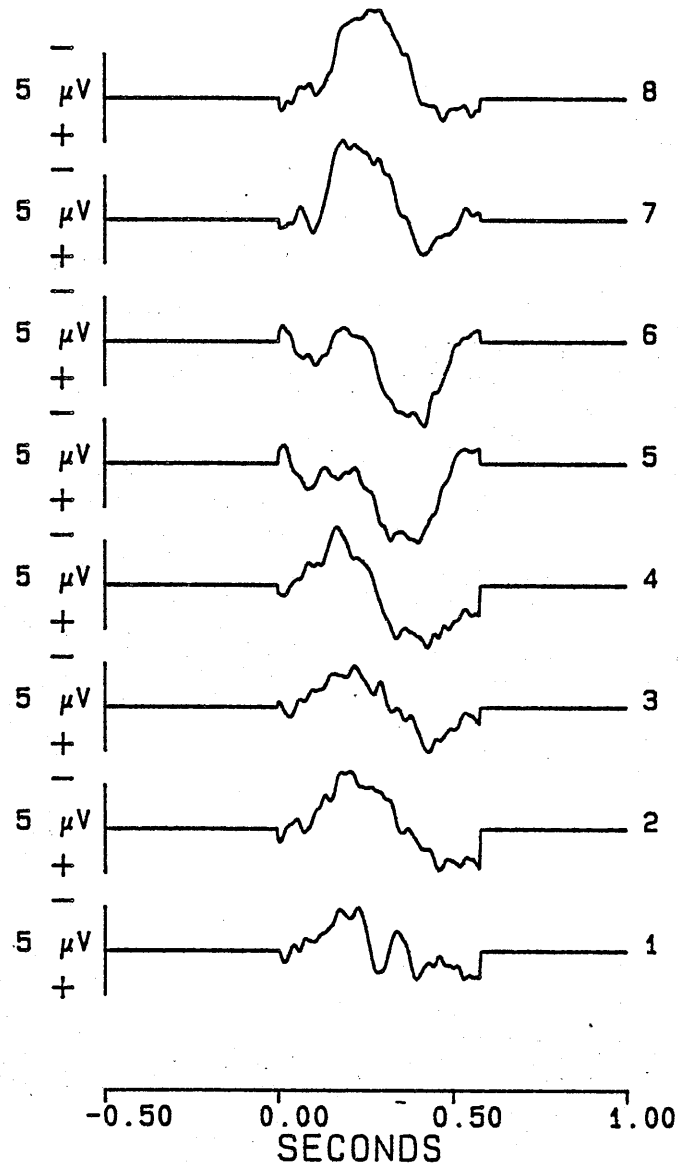

Figure 5.17. GLS estimates of auditory responses (PzMM).

5.6 Discussion

The present chapter has explored the use of regression analysis to separate overlapping components of waveforms recorded to near-simultaneous stimuli. The solution hinges on the fact that the transformations applied to the time-locked visual and auditory traces during the data collection process, can be defined precisely and incorporated into a design matrix which expresses the relationship between the observed data and the idealised visual and auditory responses.

The assumptions which underlie the analysis are identical to those which underlie the filtering procedures discussed in Chapter 4. That is, the idealised visual and auditory responses are assumed to combine additively and to be invariant over the duration of the staggering window. As previously discussed, this latter assumption must in the limit be false although the problem can be minimised through good experimental technique and by using staggering windows of short duration. For example, an optimal solution was obtained with test data using a staggering window of only five samples (see Section 5.3).

The advantage of the present solution over the filtering procedures presented in Chapter 4 is that it obviates those problems of spectral leakage inherent in the use of frequency domain analysis. Furthermore, the solution can readily be adjusted to control for problems created by autocorrelated disturbances and departures from homoscedasticity. Inspection of Figures 5.6 to 5.17, however, indicates that the GLS solution is less than optimal when applied to the present dual-task data. For example, reference to Figure 5.14 shows that the solution has only partially removed the auditory distortion from traces 1, 3 and 8 and this is reflected in the small

amplitudes of the corresponding auditory waves presented in Figure 5.15. Conversely, the recovery of visual and auditory waveforms presented in traces 2, 4 and 5 of Figures 5.14 and 5.15 is acceptable.

The GLS solution is in fact itself a filtering procedure whereby each value of the idealised waveforms is derived through the summation of weighted contributions from every data value comprising the input time series. Inaccuracies in one part of the input time series can, therefore, adversely affect the estimation of large sections of the 'idealised' responses. Section 5.4 has discussed the ways in which the methods of data collection used in the dual-task experiment depart from the model used as the basis for GLS estimation. The most serious of these departures results from the lack of replacement trials during the dual-task experiment to ensure the full complement of trials at each sample interval within the staggering window, and the failure to truncate data values at the tails of the time-locked auditory responses. While a weighting procedure was applied to the last 24 data values of all auditory sections of trace submitted to the analysis, this clearly results in a crude approximation of the true input data values, and is likely to yield a less than optimal solution. The accuracy of the solution can be maximised by the close adherence to the specifications of the proposed model.

It could be argued that the dissimilarity between recovered visual traces and those pure visual traces recorded over non-signal trials results from an interaction between visual and auditory stimuli presented on signal trials, and that the recovered traces are thus a faithful representation of the component visual and auditory waveforms.

This interpretation, however, is unlikely on three counts. Firstly, the departures of the dual-task data from the specifications of the proposed model militate against such an explanation; secondly, the effects are not systematic (for example, compare the recovered visual trace under signal condition 1 over letter-match condition and electrode placement); and thirdly, the previous treatment of these data by both elementary subtraction procedures and filtering procedures supports the assumption of visual response invariance over signal and non-signal trials for these particular data.

The following chapter presents the behavioural results of the dual-task experiment, and analyses those ERPs recovered by means of elementary subtraction procedures. Chapter 7 presents a comparison between those waveforms recovered through the traditional method of elementary subtraction and those ERPs recovered by means of the filtering procedures and GLS solution.

CHAPTER 6: EVALUATION OF THE DUAL-TASK EXPERIMENT

6.1 Introduction

An important assumption underlying the use of elementary subtraction procedures to separate overlapping visual and auditory ERPs is that of visual ERP invariance over non-signal and signal trials. The behavioural data support this assumption (see Table 3.1) and confirm that subjects managed to maintain their primary task performance following the introduction of the secondary task, and under all conditions of the secondary task. More importantly, the difference traces presented in Figures 3.17 to 3.22 indicate that visual ERPs recovered through elementary subtraction procedures have the same form as visual ERPs recorded over non-signal trials. This is particularly convincing as visual ERPs were estimated from time-locked visual averages by an indirect method which involved subtracting the staggered version of auditory responses which themselves had been estimated through the subtraction process. If the assumption of visual response invariance is incorrect, then the recovered auditory responses would be biased and this would be reflected in the subsequent recovery of the idealised visual ERPs.

A further method of assessing the similarity of visual ERPs recorded over non-signal trials and visual ERPs estimated through the subtraction process is to calculate the Pearson product-moment correlation coefficient between every recovered visual trace and the pure visual average recorded under the same visual task condition (see John, Ruchkin and Villegas, 1964; Donchin and Lindsley, 1965). A correlation coefficient of unity will be obtained if a pair of waveforms is identical in shape while a correlation approaching zero will result if there is no similarity in the shape of the waves.

Table 6.1 shows the correlation coefficients calculated between every recovered visual average and the respective pure visual average.

Table 6.1. Pearson correlation coefficients between visual averages estimated through elementary subtraction procedures and pure visual averages recorded under the same letter-match conditions (group data).

Signal Condition	C_z			P_z		
	Physical Match	Rule Match	Mismatch	Physical Match	Rule Match	Mismatch
1	.924	.905	.897	.891	.826	.736
2	.923	.904	.908	.783	.704	.619
3	.919	.935	.914	.872	.876	.844
4	.918	.921	.904	.919	.925	.900
5	.943	.909	.923	.926	.873	.863
6	.933	.938	.932	.923	.891	.915
7	.916	.910	.916	.926	.922	.890
8	.948	.897	.921	.882	.828	.882
Average	.928	.915	.914	.890	.856	.831

All correlations are based on group averages (averaged across all subjects) and derived from a total of 750 pairs of data values comprising the 3 second epochs over which averages were saved. These coefficients indicate a high degree of consistency between recovered visual waveforms and pure visual averages. The average coefficients presented in the lower row of Table 6.1 represent the mean correlation coefficient for each level of letter match and electrode placement, averaged across signal condition. The generally lower correlations obtained from the Pz placement can be attributed to the poorer signal to noise ratio of recordings made from this location.

The above data indicate that the use of elementary subtraction to separate overlapping visual and auditory ERPs is a valid procedure when applied to the present data. Consequently, the following Sections evaluate the results of the dual-task experiment by assessing the relationship between behavioural measures of dual-task performance and visual and auditory ERPs estimated through the subtraction process. For the purpose of this evaluation, visual and auditory ERPs were estimated separately for each subject through the procedures outlined in Chapter 3.

6.2 Visual letter-matching task

6.2.1 Behavioural measures of visual task performance

The behavioural data for the visual task component of the dual-task experiment were presented in Chapter 3 (see Table 3.1). Visual task performance was near perfect under all conditions of the dual-task with an overall error rate of approximately 1.3%. A 2-way repeated measures analysis of variance (ANOVA) on the arcsin transformation of the proportion of correct visual responses indicated a significant effect due to visual task condition, no

significant effect due to signal condition, and no significant interaction. A Newman-Keuls test of multiple comparisons showed that performance on physical match trials was significantly better than performance on either rule match or mismatch trials. The magnitude of the effect of letter match condition is minimal, however, as it accounts for only 3.72% of the total variance (see Winer, 1971; p428) and the mean improvement in terms of proportion of correct responses is 1.1% for physical matches when compared with rule matches, and 0.7% for physical matches when compared with mismatches.

6.2.2 Visual ERP measures

Due to the similarity of visual traces recorded over signal and non-signal trials, an assessment of visual ERPs recorded under different letter match conditions was conducted on pure visual averages recorded over non-signal trials. Figure 2.4 indicates that, irrespective of letter-match condition, visual ERPs recorded at a particular electrode placement are identical prior to second letter onset (see Section 2.9). This finding is to be expected as subjects could not determine the type of letter match a particular trial conformed to until after the onset of the second letter.

In general the long latency components of ERPs to second letter stimuli are characterised as follows (refer to Figure 2.4): a negative component (N_1) having a peak latency at approximately 120mS, a positive component (P_2) having a peak latency at approximately 230mS, and a second positive component (P_3) peaking at approximately 400mS. While a second negative component (N_2) is evident in some traces, peaking at approximately 300mS, it is difficult to identify in ERPs recorded to physical matches. The N_2 wave either is evident as a small inflection on the positive-going wave which resolves to become the P_3 (see the PzPM trace of Figure 2.4), or cannot be individually identified as the P_2 and P_3 waves combine to form one extended positive wave (see the CzPM trace of Figure 2.4).

Due to the inconsistent nature of the N_2 component it was not measured for the following analyses.

ERP components are traditionally measured in terms of peak amplitudes and peak latencies. An alternative measure, however, is that of area (see Hillyard, Squires, Bauer and Lindsay, 1973). Area measures are taken as the total area contained in either a positive or negative deflection within a particular latency range and are calculated by multiplying the sum of all positive or negative values by the duration of the latency range. Thus the measure is expressed in terms of μV x mS. These measures are useful in reducing the variability inherent in determining a single peak value on broad ERP components such as the P_3 wave, and complement the information provided by pure amplitude measures.

The following measures were taken for each subject from pure visual averages recorded over non-signal trials:

a) N_1 amplitude: taken as the value of the most negative deflection within the interval 100-140mS following second letter onset, measured relative to the mean value of the 500mS pre-fixation cross baseline. Expressed in μVs.

b) N_1 area: taken as the total area contained in the negative deflection within the interval 100-140mS following second letter onset. Expressed in μV x mS.

c) P_2 amplitude: taken as the value of the most positive deflection within the interval 212-252mS following second letter onset, measured relative to the mean value of the 500mS pre-fixation cross baseline.

d) P_2 area: taken as the total area contained in the positive deflection within the interval 212-252mS.

e) P_3 amplitude: taken as the value of the most positive deflection within the interval 260-560mS following second letter onset, measured relative to the mean value of the 500mS pre-fixation cross baseline.

f) P_3 area: taken as the total area contained in the positive deflection within the interval 300-500mS.

g) Peak latencies: the latencies of N_1, P_2 and P_3 peak amplitudes, measured with respect to second letter onset. Expressed in mS.

Table 6.2 presents the mean values, averaged across subjects, of ERP components recorded under the three letter match conditions for both Cz and Pz placements. Separate 2-way repeated measured ANOVAS were used to assess the effects of type of letter match and the effects of electrode placement on each ERP component. The results of these analyses are provided in the following Sections.

6.2.2.1 N_1 amplitude and area measures. A significant effect due to electrode placement was found for both N_1 amplitude ($F_{1,11} = 7.515$; $p < .02$) and N_1 area measures ($F_{1,11} = 7.001$; $p < .05$), with mean values of both measures being significantly larger (in terms of absolute values) at Cz than Pz. There were no effects due to type of letter match and no significant interactions for either measure.

6.2.2.2 P_2 amplitude and area measures. No significant effect due to electrode placement or type of letter match, and no significant interaction was found for either P_2 amplitude or P_2 area measures.

6.2.2.3 P_3 amplitude and area measures. For P_3 amplitude a significant placement effect ($F_{1,11} = 16.470$; $p < .003$) and a significant letter match effect ($F_{2,2} = 4.638$; $p < .025$) were evident. P_3 amplitudes were significantly larger at Pz than at the Cz placement, the mean amplitude at Pz being 4.057μV and at Cz being 2.429μV, collapsed across letter match conditions. A Newman-Keuls analysis indicated that mean P_3 amplitudes were significantly larger under the physical match condition than either the rule match or mismatch condition ($p < .05$ for both comparisons). Mean P_3 amplitudes, collapsed across

Table 6.2. Mean values of visual ERP components following second letter presentation at each level of letter-match. Measures taken from pure visual averages recorded at Cz and Pz placements.

	Cz			Pz		
	Physical Match	Rule Match	Mismatch	Physical Match	Rule Match	Mismatch
N_1 amplitude	-1.702	-1.889	-1.767	-0.910	-0.975	-0.910
N_1 area	-56.7	-66.7	-60.7	-30.2	-37.8	-31.6
P_2 amplitude	2.993	2.717	3.262	2.373	2.499	2.748
P_2 area	110.0	91.6	114.3	90.1	89.2	96.8
P_3 amplitude	2.992	2.171	2.123	4.421	4.058	3.694
P_3 area	241.3	134.3	134.7	567.3	362.1	327.9
N_1 latency	122	123	127	116	116	117
P_2 latency	237	230	228	232	238	234
P_3 latency	330	432	425	399	417	395

Cz and Pz placements, were 3.706, 3.115 and 2.908μV for physical matches, rule matches and mismatches respectively.

For P_3 area, a significant placement effect ($F_{1,11} = 19.809$; $p < .002$), a significant letter match effect ($F_{2,11} = 8.320$; $p < .005$) and a significant interaction ($F_{2,22} = 9.354$; $p < .001$) were obtained. Tests of simple main effects (Kirk, 1968; p179, p240, p265) revealed that P_3 areas were larger at the Pz placement than at the Cz placement under all levels of letter match ($p < .001$ for all comparisons); but that a significant effect due to letter match was evident at the Pz placement only ($p < .001$). Newman-Keuls tests showed that at Pz, P_3 area was significantly larger under the physical letter match condition than either the rule match or mismatch conditions ($p < .01$ for both comparisons).

6.2.2.4 N_1, P_2 and P_3 latency measures. A significant placement effect was found for N_1 latency ($F_{1,11} = 5.645$; $p < .05$) with the mean N_1 latency at Cz being 124mS and at Pz being 116mS, collapsed across letter match conditions. No significant effect of letter match or significant interaction was found. P_2 latency was found to be stable across both electrode placements, and across letter match condition, and no interaction effect was evident.

For P_3 latency, a significant effect of type of letter match ($F_{2,22} = 4.198$; $p < .05$) and a significant placement by letter match interaction ($F_{2,22} = 4.554$; $p < .05$) were found. Tests of simple main effects revealed a significant placement effect under the physical match condition ($p < .005$) with P_3 latency being shorter at the Cz placement than at the Pz placement. A significant effect of letter match was found at Cz ($p < .001$), and a Newman-Keuls test showed that at this placement, P_3 latency was significantly reduced

under the physical match condition when compared with both the rule match and mismatch conditions ($p < .01$ for both comparisons).

In summary, the main differences between ERP components measured from pure visual averages following second letter onset were as follows:

- N_1 amplitude and area measures were found to be significantly larger (in terms of absolute values) at Cz when compared with Pz; while P_3 amplitude and area measures were consistently larger at the Pz placement when compared with those recorded at the Cz placement.
- P_3 amplitude was consistently larger over physical matches than either rule matches or mismatches; while P_3 area followed this trend significant differences were obtained at Pz only.
- N_1 latency was significantly longer at Cz than at Pz, while P_3 latencies recorded from the Cz placement were significantly reduced over physical match conditions when compared with the rule match and mismatch conditions. There were no differences between P_3 latencies recorded from the Pz placement.

6.2.3 Discussion

Performance on sequential letter-matching tasks, such as that used in the present dual-task experiment, is usually measured in terms of speed of responding to second letter stimuli. A consistently reported finding is that RTs to physically same judgements are significantly faster than those to physically different judgements, be they rule matches or mismatches. Moreover, those studies which have reported error rates as well as RTs, have indicated that the relative efficiency of physically same judgements is reflected in significantly fewer errors associated with these judgements when compared with

physically different judgements (Posner and Mitchell, 1967; Posner and Boies, 1971; Posner, Klein, Summers and Buggie, 1973).

The behavioural data from the present matching task, therefore, are consistent with those of previous studies and, while RTs were not measured, it may be assumed that physical matches are evaluated more quickly than either rule matches or mismatches[1]. This assumption is consistent with the differences found between ERPs recorded to second letter stimuli under the three letter match conditions of the visual task.

While both N_1 and P_3 components of visual ERPs showed differences as a function of electrode placement, the manipulation of type of letter match was manifested only by changes in the endogenous P_3 component. P_3 amplitude and area were found to be generally larger under the physical match condition than under the rule match and mismatch conditions and, at the Cz placement, P_3 latency under the physical match condition was on average at least 95mS shorter than under the other conditions.

These findings are consistent with those of Posner, Klein, Summers and Buggie (1973) who presented subjects with a sequential letter-matching task, with physically same and physically different letter pairs occurring with equal probability. Subjects were required to make a manual 'same' or 'different' response 0.5S following the onset of the second letter. The P_3 component of ERPs recorded from the Cz placement was found to be of larger amplitude and shorter latency when second letter stimuli conformed

[1]Support for the assumption that subjects were evaluating PMs more quickly as well as more accurately than RMs and MMs is provided by the results of a follow-up study in which subjects each received two blocks (192 trials) of the visual letter-matching task and were requested to respond as quickly as possible following the onset of the second letter. All other conditions were identical to the non-signal trials of the dual-task experiment. Mean RTs for PM, RM and MM trials were 556 ± 163mS, 835 ± 200mS and 828 ± 128mS, respectively. While error rates were generally higher when responses were speeded than when they were delayed, errors for PMs were substantially lower than for RMs and MMs (0.4%, 3.1% and 3.4%, respectively).

to a 'same' judgement than when they conformed to a 'different' judgement. Evidence that these effects were related to cognitive manipulations rather than to stimulus parameters was provided by a further experiment in which subjects were presented with a word-matching task. Word pairs were either the same or different with equal probability. In separate runs subjects were required to count either matches or mismatches, and a comparison was made between ERPs recorded under the same letter-match condition when task relevant (counted) and when task irrelevant (not counted). It was found that the P_3 component elicited by the counted stimulus was substantially larger than that elicited by the uncounted stimulus. Furthermore, this amplitude difference emerged 100mS earlier when the second stimulus matched the first stimulus than when it was physically different. This time difference is consistent with the difference in P_3 latency observed at the Cz placement in the present experiment. The lack of a reduced P_3 latency at the Pz placement may be due to a greater variability in the latency of this component over individual trials of the dual-task experiment. For seven subjects P_3 latency was shorter on physical match trials than rule match or mismatch trials, while for five subjects P_3 latency was either the same over all conditions or longer on physical match trials.

Posner and his colleagues concluded from their experiments that the P_3 component for physical matches is shifted forward in latency from its value for mismatches, and that the difference in P_3 latency and the facilitation of RTs to matches are both consequences of an increase in the rate of encoding in the sensory-memory system due to the presentation of the first letter. This explanation is similar to that of Proctor (1981) who proposes that encoding and identification of a second stimulus is facilitated if it is identical to the first stimulus. In addition Proctor suggests that while mismatches lose the benefits of facilitation they are delayed further due to inhibition in the identification of a second

stimulus which has a name code different from that already activated.

Some indication of the processes which account for the slower response to mismatches when compared with matches is provided by a study of Duncan-Johnson and Donchin (1982). They measured RT and P_3 latency to letter stimuli which followed three types of stimuli: an identical letter, a neutral (non-letter) stimulus or a different letter. A comparison between mismatch and neutral trials (a cost analysis) revealed an increase in both RT and P_3 latency on mismatch trials. As evidence suggests that P_3 latency reflects stimulus evaluation and identification rather than response-related processes (Squires, Donchin, Squires and Grossberg, 1977; Donchin, 1978; Duncan-Johnson and Donchin, 1982), it was proposed that the cost of a mismatch results from an increase in stimulus processing as well as a delay due to response competition. A comparison between match trials and neutral trials (a benefit analysis), however, found no difference in RT or P_3 latency. The authors pointed out that the failure to find a benefit on match trials could be due to match and neutral trials being equally facilitated through extensive practice (p. 40). An alternative explanation may relate to the requirements of their task, as subjects were asked only to perform a choice reaction time task in response to second letter stimuli, rather than make any comparison between first and second stimuli.

In summary, the results from the visual task component of the dual-task experiment indicate that subjects process physical matches more accurately and more quickly than physical mismatches. Although type of letter match produced only minimal differences in behavioural measures of task performance, visual ERPs prove to be extremely sensitive to this manipulation.

Dual-task methodology is designed to assess the processing demands of a primary task by reference to performance on a secondary task, and in the present experiment two aspects of secondary task performance are of

interest. These are, firstly the extent to which different stages of the primary task affect performance on the secondary task, and, secondly, the extent to which manipulations of the primary task affect performance on the secondary task. In the present paradigm, any effect due to type of letter match would be expected to be evidenced by behavioural and/or ERP data associated with auditory stimuli presented under signal conditions 6, 7 and 8, which coincide with the evaluation of the second letter and the selection of an appropriate visual task response. The following Sections provide the results of the auditory signal detection task.

6.3 Auditory signal detection task

6.3.1 Behavioural measures of signal detection performance

Subjects' responses to the signal detection task were categorised according to four possible outcomes. These were, hits: correctly reporting the presence of a signal; misses: incorrectly reporting the absence of a signal; correct rejections: correctly reporting the absence of a signal; and false alarms: reporting the presence of a signal when in fact no signal was presented. The rates of these possible outcomes are determined by two distinct processes: the sensitivity of the subject in terms of his or her ability to discriminate between signal and noise, and all other factors which influence a particular response, that is, the subject's response bias or decision criterion. The use of measures from signal detection theory (Green and Swets, 1966) allows the separation of these processes. The signal detection measure, d', provides an index of perceptual sensitivity, uncontaminated by response bias while the likelihood ratio, β, provides information about the subject's decision criterion. Both measures are derived from a knowledge of the proportion of hits and false alarms given under a particular experimental condition.

While in the present experiment the number of hits reported by every subject under a particular combination of signal condition and letter match condition can be calculated, a unique false alarm rate cannot be derived for every combination of conditions. This is because non-signal trials were common to all auditory task conditions associated with a particular type of letter match. Consequently, performance on the signal detection task cannot be evaluated using measures of d' and β. However, if subjects demonstrate a stable response criterion over the different levels of letter match, hit rates can be assumed to provide a relatively pure index of perceptual sensitivity.

To test the stability of subjects' response criteria, three β values were calculated for every subject by taking the ratio of the proportion of misses to that of false alarms associated with each type of letter match. The proportion of misses was determined from the 400 signal trials presented to each subject under the eight signal conditions associated with a particular type of letter match, while the proportion of false alarms was derived from the 400 non-signal trials associated with a particular level of letter match. Mean values of β for physical match, rule match and mismatch trials were 1.35, 1.21 and 1.14, respectively, averaged across all subjects. A 1-way repeated measures ANOVA confirmed that these values were not significantly different ($F_{2,22} = 2.303$; $p > 0.12$).

Signal detection performance was assessed by calculating the proportion of correct detections (hits) for every subject under the twenty-four combinations of signal condition and letter match condition. As visual task performance was near perfect under all signal conditions, the calculation of hit rates included those trials on which visual task errors were made. Figure 6.1 shows the mean proportion of correct detections averaged across subjects for each signal condition and letter match condition.

A 2-way repeated measures ANOVA on the proportion of correct detections[1] indicated no effect due to letter match condition ($F_{2,22} = 0.099$; $p > 0.90$), a significant effect due to signal condition ($F_{7,77} = 9.464$; $p < 0.001$) and no visual task by auditory

[1] To assess the homogeneity of variance of the proportion of correct detections, the mean and variance for each of the twenty-four experimental conditions were calculated. As the correlation between these values was not significant, no transformation was applied to the data.

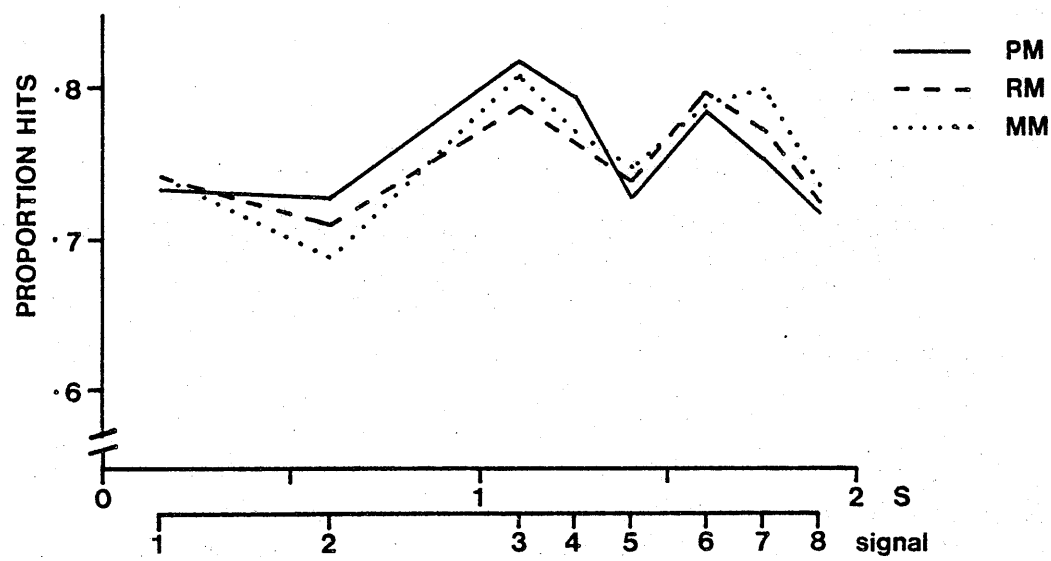

Figure 6.1. Mean proportion of correct detections (hits) averaged across all 12 subjects as a function of letter-match condition and signal condition.

task interaction ($F_{14,154} = 0.843$; $p > 0.620$). Newman-Keuls analysis showed that there was no difference in the detection of signals presented at positions 1, 2, 5 and 8, but that signal detection at these positions was significantly worse than detection performance at positions 3, 4 and 6 ($p < 0.05$ for all comparisons). Detection at signal position 7 was signficantly better than performance at positions 2 and 8 ($p < 0.05$ for both comparisons).

Signal detection performance, therefore, improves by approximately 10% following the onset of the first letter (signal conditions 3 and 4), falls sharply at signal position 5 prior to the onset of the second letter, increases again during the exposure of the second letter (signal condition 6), and finally drops back to the level of performance achieved for those signals presented in the warning interval.

6.3.2 Auditory ERP measures

For average auditory ERPs a negative component (N_1) with a peak latency of approximately 200mS, and a positive component (P_3) with a peak latency of approximately 430mS could readily be identified. A second positive component (P_2), preceding the P_3 component, was generally undetected although for some ERPs it was discernable as a small inflection on the positive-going wave, with a latency ranging between 250 and 300mS. Due to the inconsistent nature of this component, however, its measurement was excluded from the present analysis.

The following measures were taken for every subject, from auditory ERPs recorded from the Cz and Pz placements under all signal conditions of the dual-task experiment and estimated through the elementary subtraction process (see Chapter 3).

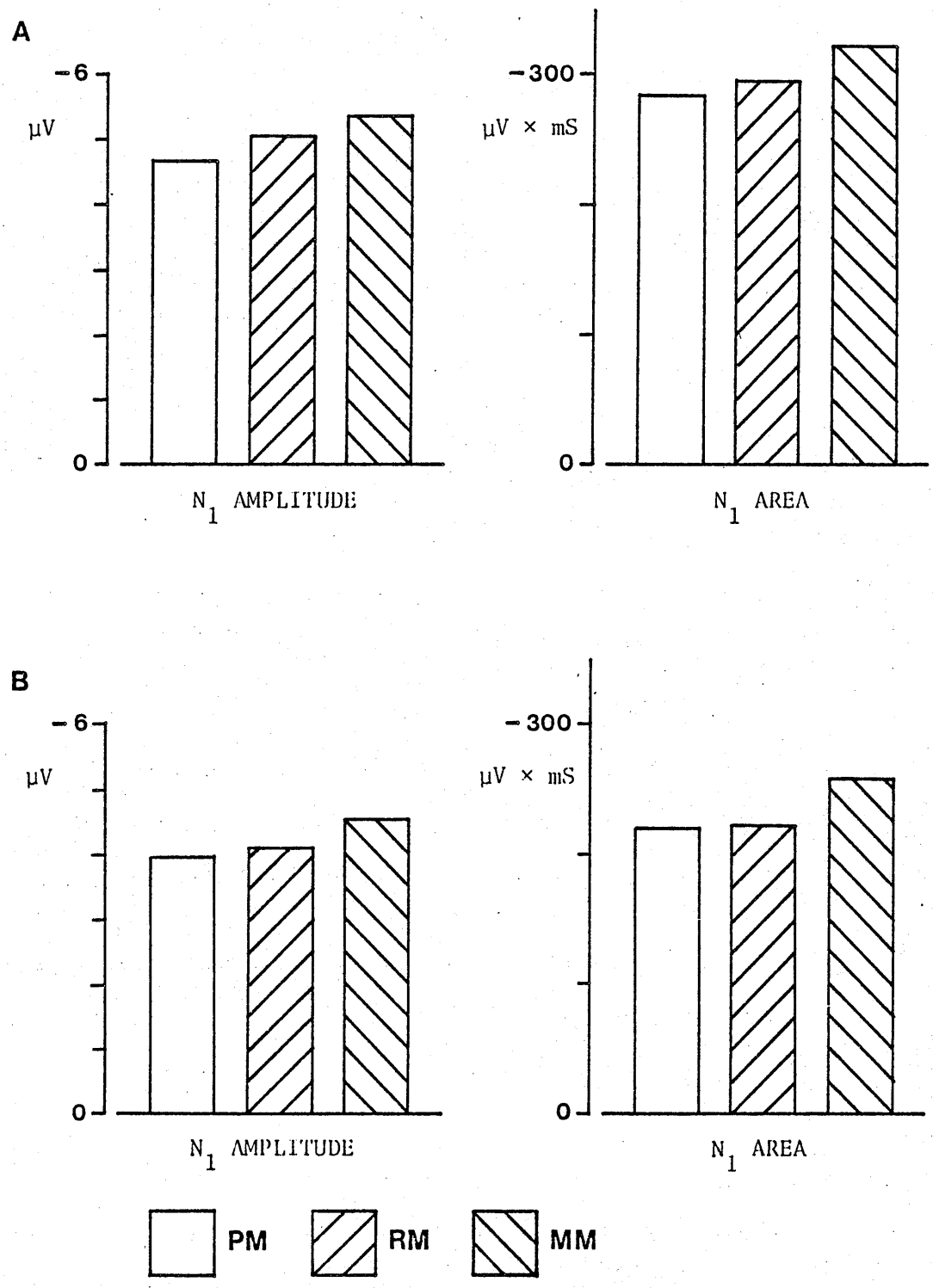

Figure 6.2. Mean N_1 amplitude and N_1 area measures from auditory ERPs for each level of letter-match, collapsed across signal condition. A: Cz placement; B: Pz placement.

a) N_1 amplitude: taken as the value of the most negative deflection within the interval 100-300mS following signal onset, measured relative to the mean baseline value calculated over the first 80mS following stimulus onset.

b) N_1 area: taken as the total area of the negative deflection within the interval 160-260mS following signal onset.

c) P_3 amplitude: taken as the value of the most positive deflection within the interval 320-540mS following signal onset, measured relative to the 80mS post-stimulus baseline.

d) P_3 area: taken as the total area of the positive deflection within the interval 336-536mS following signal onset.

e) Peak latencies: the latencies of N_1 and P_3 peak amplitudes, measured with respect to stimulus onset.

Treatment effects of letter match and signal condition, and differences between electrode placements were assessed for every auditory ERP measure by means of a 3-way repeated measures ANOVA. The results of these analyses are detailed in the following Sections.

6.3.2.1 N_1 amplitude and area measures. A significant effect due to electrode placement ($F_{1,11} = 13.25$; $p < .005$) and type of letter match ($F_{2,22} = 4.950$; $p < .020$) was found for N_1 amplitude. There was no significant effect due to signal condition, and no significant interactions. The mean absolute N_1 amplitude was significantly larger when recorded from the Cz placement (mean value collapsed over all other conditions = -5.018μV) than the Pz placement (mean value collapsed over all other conditions = -4.196μV). A Newman-Keuls test showed that the mean absolute N_1 amplitude recorded on mismatch trials was significantly larger than that recorded on physical match trials ($p < 0.05$), while there was no significant difference between N_1 amplitudes recorded on mismatch and rule match trials, or rule match and physical match trials.

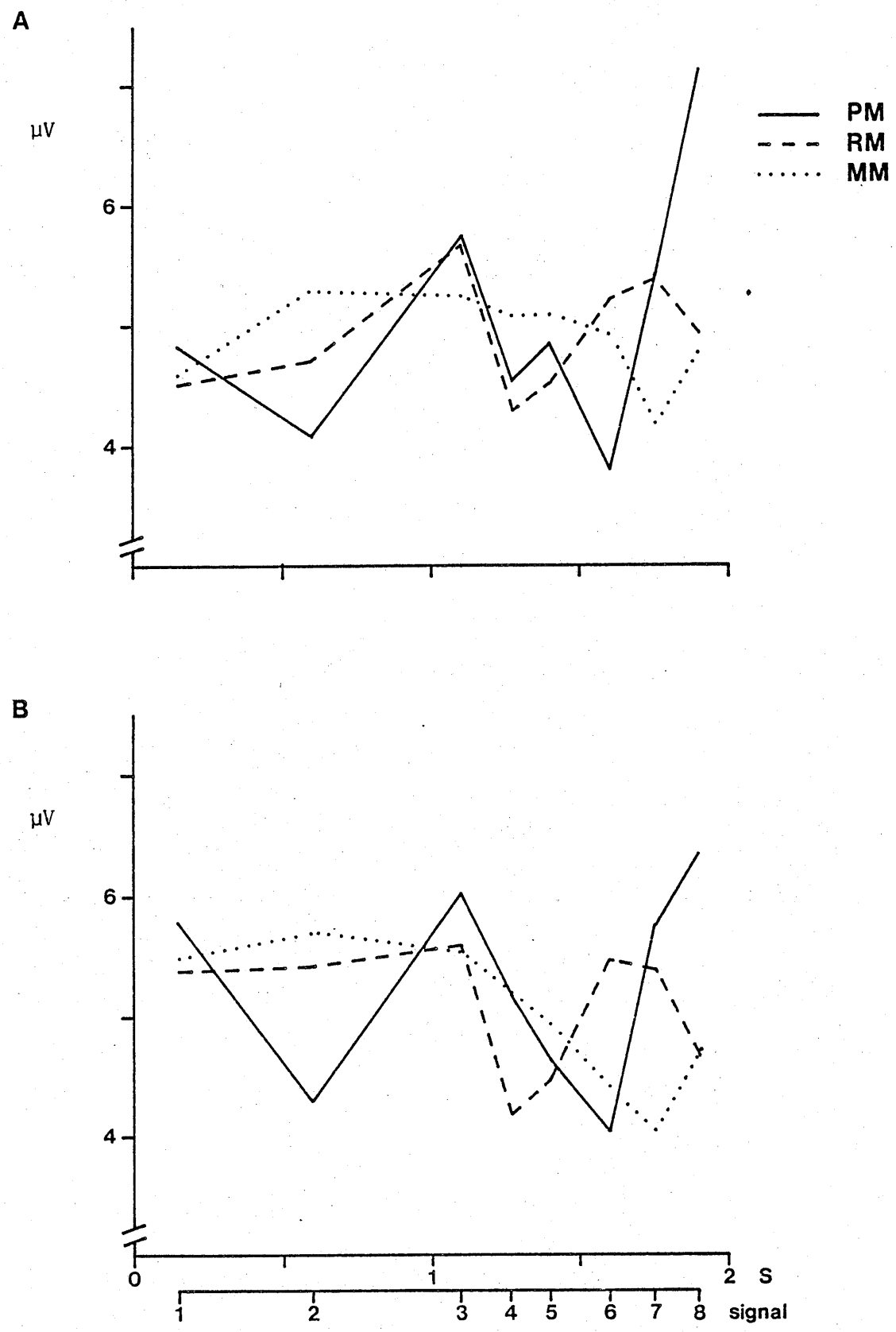

Figure 6.3. Mean P_3 amplitudes of auditory ERPs as a function of letter-match condition and signal condition. A: Cz placement; B: Pz placement.

Figure 6.2 shows the mean values of N_1 amplitudes and N_1 area for each level of letter match averaged across signal condition, for A:Cz and B:Pz. While N_1 area measures follow the same trend as N_1 amplitude measures, and display a significant effect of electrode placement ($F_{1,11} = 16.622$; $p < .003$), there was no significant effect due to letter match or signal condition and no significant interactions.

6.3.2.2 P_3 amplitude and area measures. Figure 6.3 shows the mean P_3 amplitudes of auditory ERPs recorded from A:Cz and B:Pz. Analysis of variance revealed a significant electrode placement by signal condition interaction ($F_{7,77} = 2.626$; $p < .02$) and a significant signal condition by type of letter match interaction ($F_{14,154} = 2.092$; $p < .02$).

Tests of simple main effects indicated that differences in P_3 amplitudes due to electrode placement were evident only under signal condition 1 ($F_{1,88} = 11.239$; $p < .005$), P_3 amplitudes being significantly larger at the Pz placement than at the Cz placement. Analysis of the signal condition by type of letter match interaction indicated that an effect due to type of letter match was evident only under signal condition 8 ($F_{2,176} = 5.983$; $p < .005$) and Newman-Keuls analysis confirmed that, under this signal condition, P_3 amplitudes on physical match trials were significantly larger than P_3 amplitudes on rule match or mismatch trials ($p < .01$ for both comparisons).

Analysis of variance on P_3 area measures also showed a significant signal condition by type of letter match interaction ($F_{14,154} = 1.833$; $p < .05$) and tests of simple main effects revealed a significant effect due to letter match condition under signal conditions 7 ($F_{2,176} = 3.781$; $p < .025$) and 8 ($F_{2,176} = 4.872$, $p < .01$). Newman-Keuls tests showed

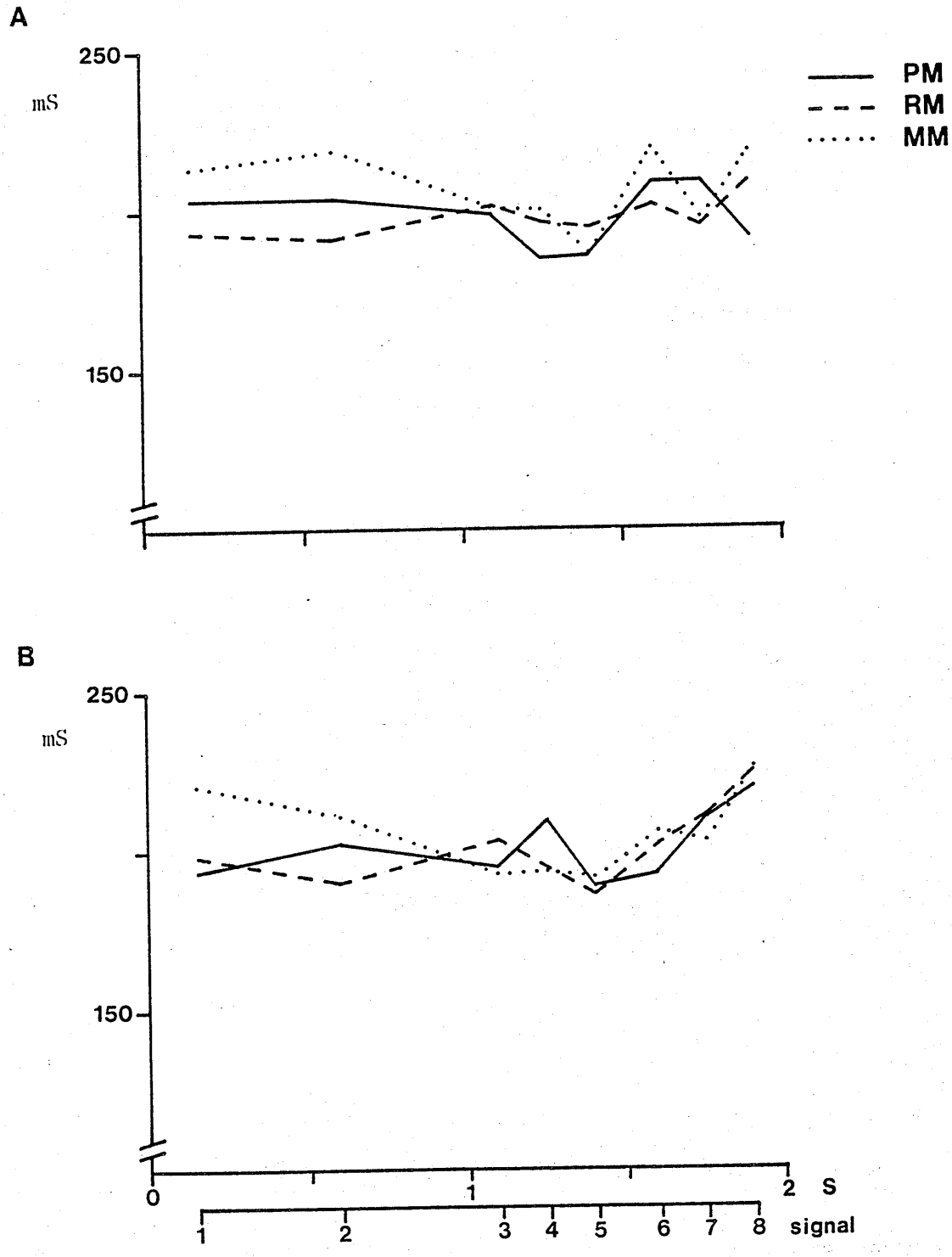

Figure 6.4. Mean N_1 latencies of auditory ERPs as a function of letter-match condition and signal condition.
A: Cz placement; B: Pz placement.

that P_3 areas measured under signal condition 7, were larger when signals were associated with physical match trials than mismatch trials ($p < .05$); while P_3 areas under signal condition 8 were larger when signals were associated with physical match trials than either rule match ($p < .05$) or mismatch ($p < .01$) trials.

6.3.2.3 N_1 and P_3 latency measures. Figure 6.4 shows mean N_1 peak latencies measured from A:Cz and B:Pz. Analysis of variance revealed no significant effects due to type of letter match, signal condition or electrode placement and no significant interactions. The mean N_1 latency averaged across experimental conditions and electrode placements is 202mS.

Figure 6.5 shows mean P_3 peak latencies recorded from A:Cz and B:Pz. Analysis of variance revealed a significant placement effect ($F_{1,11} = 16.180$; $p < .005$) with P_3 latencies being consistently longer at Pz than Cz, and a significant effect of signal condition ($F_{7,77} = 13.296$; $p < .0001$). There was no effect due to type of letter match and no significant interactions.

A Newman-Keuls test indicated that P_3 latency under signal condition 1 was significantly longer than that under signal condition 2 ($p < .05$) while the latency recorded under signal condition 2 was significantly longer than those recorded under all other signal conditions ($p < 0.05$ for all comparisons). In addition, the mean latency of the P_3 components recorded under signal conditions 3, 4 and 8 were significantly longer than that recorded under signal condition 5 ($p < 0.05$ for all comparisons). There were no further differences between any other pair of means.

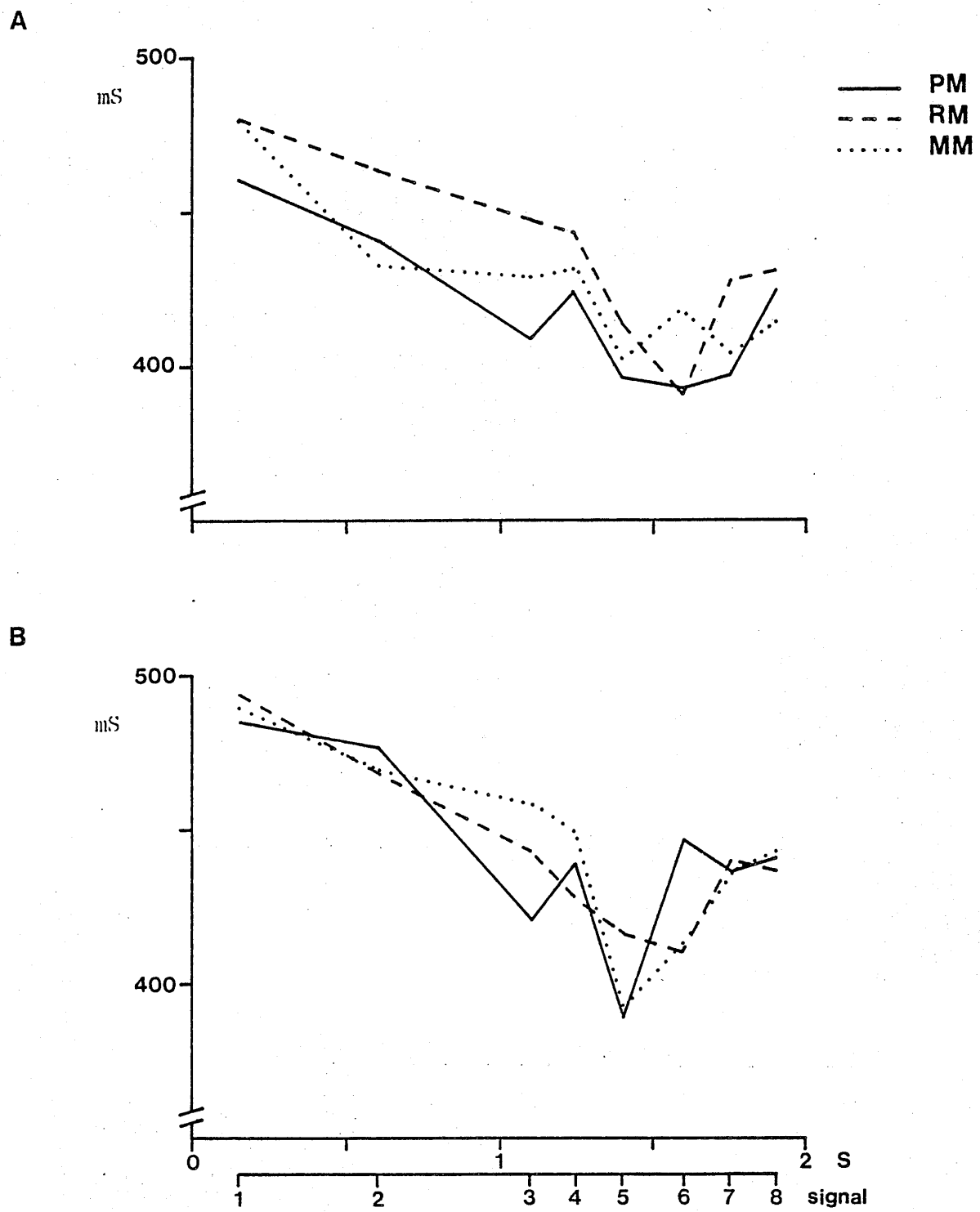

Figure 6.5. Mean P_3 latencies of auditory ERPs as a function of letter-match condition and signal condition.
A: Cz placement; B: Pz placement.

In summary, the above analyses indicate that:

- Signal detection performance varied as a function of the different stages of the primary task, but was unaffected by the manipulation of type of letter match.
- N_1 amplitude and area measures were significantly larger (in terms of absolute values) at Cz when compared with Pz; while P_3 amplitude was significantly larger at Pz than Cz, but only under the first signal condition.
- The mean absolute N_1 amplitude recorded over mismatches was significantly larger than that recorded over physical matches; this difference, however, was not significant for N_1 area.
- Under signal condition 7 P_3 area was larger for physical matches than mismatches, while under signal condition 8 both P_3 area and amplitude were significantly larger for physical matches than either rule matches or mismatches.
- N_1 latency was unaffected by all experimental manipulations.
- P_3 latency was consistently longer at Pz than Cz, and varied as a function of the different stages of the primary task, but was unaffected by the manipulation of type of letter match.

The following Section assesses the relationship between behavioural and ERP measures of signal detection performance.

6.4 Relationship between behavioural and ERP measures

Pearson product-moment correlations were calculated to assess the relationship between the mean values of auditory ERP components and the mean proportion of correct signal detections recorded under the twenty-four combinations of letter-match condition and signal condition. The resultant correlation coefficients are presented in Table 6.3, and the only values to approach significance, (using non-

Table 6.3. Pearson correlation coefficients between auditory ERP measures and the proportion of correct detections (hits).

	Cz	Pz
N_1 amplitude† with proportion hits (n=24)	.063	.257
N_1 area† with proportion hits (n=24)	-.085	.071
P_3 amplitude with proportion hits (n=24)	-.065	-.133
P_3 area with proportion hits (n=24)	-.022	-.010
N_1 latency with proportion hits (n=24)	-.099	-.227
P_3 latency with proportion hits		
signal conditions 1-8 (n=24)	-.383+	-.322++
signal conditions 1-4, 6-8 (n=21)	-.504*	-.585**

† absolute values

+ p = .064 * p = .020

++ p = .125 ** p = .005

directional tests) are those between the proportion of correct detections and P_3 latencies recorded at both Cz and Pz placements. The trend towards an inverse relationship between the proportion of hits and P_3 latency is evident from inspection of Figures 6.1 and 6.5. However, these figures also highlight a dissociation in this trend. The detection of signals presented under signal condition 5 is significantly worse than that for signals presented under condition 4 or 6, while P_3 latency approaches a minimum or is at a minimum under this signal condition. This dissociation is emphasised further by evaluating the correlation coefficient between the proportion of hits and P_3 latency when the data values associated with signal condition 5 are excluded from the analysis. The ensuing correlation coefficients are presented in the final row of Table 6.3, and exhibit an increase in statistical significance despite the loss of degrees of freedom.

6.5 Discussion

Secondary task signal detection performance shares a number of similarities with the results reported by Posner and Boies (1971).

The finding that preparation for a visual stimulus results in an improvement in performance to stimuli presented in another modality led Posner and Boies to conclude that preparation is a general process which is not selective. The present results are consistent with this interpretation as signal detection performance under signal condition 3 (following first letter onset) is significantly better than that under signal conditions 1 and 2 (presented in the warning interval). In addition, the lack of any performance decrement immediately following the onset of of the first letter is consistent with Posner and Boies' proposal that the encoding of a letter (that is, the contact between the input and long-term memory that leads to the letter name) can proceed without the

requirement for any processing capacity. This proposal, however, was based partly on the results of studies which involved very short (50mS) presentations of first letter stimuli. In the present experiment, first letter stimuli were available for 500mS and it is possible that subjects switched their attention to the auditory task during the early part of this interval.

The substantial decrement in signal detection performance immediately prior to second letter onset (signal condition 5) also is consistent with the findings of Posner and Boies. They interpreted a similar deficit in performance to auditory probe stimuli as indicating that:

> "...such mental operations as rehearsal or generation of distinctive features for testing, which follow encoding of the first letter, require processing capacity, while encoding itself does not", (p.407)

Signal detection performance following second letter onset follows a different pattern to that found for probe RTs by Posner and Boies. They observed long RTs to probes presented up to 300mS following second letter onset, and a reduced deficit in performance to probes arriving at about 400mS after the onset of the second letter. In the present experiment, a decrement in detection performance is not evident until signal condition 8, that is, 348 - 448mS following second letter onset. This difference may be attributed to the response requirements of the two dual-tasks. In Posner and Boies' study subjects were required to respond as quickly as possible to both the visual task and the auditory task, and the timing of the interference effect can be attributed to the need for processing capacity during the selection and execution of an appropriate visual task response. In the present experiment, however, subjects were requested to delay responding to both elements of the dual-task until 500mS after the offset of the second letter, and were requested to respond first to the visual task and then to the auditory task. The lack of any decrement

in auditory task performance under signal conditions 6 and 7 is consistent with these delayed response instructions, and suggests that subjects did not select and prepare for a visual response until towards the end of second letter presentation.

An alternative explanation for the behavioural results of the signal detection task is that subjects learn the distribution of the signals over the two second trial interval. That is, they generated expectancies about the time of arrival of signals within the trial interval. The shape of the signal detection function supports this interpretation, with the exception of the level of performance achieved under signal condition 5. A possible explanation for the decrement in performance under this condition is that the perception of signals presented within the 100mS interval (52 - 152mS prior to second letter onset) tends to be masked by the following visual stimulus. The shape of the P_3 latency function accords well with the interpretation that subjects have generated expectancies about the timing of auditory signals, as it has been shown that P_3 latency varies inversely with the proportion of correct detections and with the confidence subjects have about the correctness of a particular decision (Hillyard, Squires, Bauer and Lindsay, 1971; Squires, Hillyard and Lindsay, 1973; Parasuraman and Beatty, 1980). Moreover, the proposal that performance under signal condition 5 suffers from the effects of intermodality backward masking explains the dissociation between detection performance and P_3 latency. Measures of P_3 latency were taken from ERPs elicited by detected signals and, therefore, only provide information concerning successful performance. On the other hand, the behavioural data reflect the relative degree of both success and failure.

The detection of fewer signals presented in the latter half of the signal window when compared with the detection of signals presented in

the first half of the window would be consistent with the proposal that detection is impaired under signal condition 5 due to backward masking. To test this possibility, a comparison was made between the mean number of misses occurring over the first 12 and last 12 intervals of the signal window. Data for nine subjects only were available, as the information about the sequencing of signal presentation within the 100mS window was lost for three subjects during the transfer of data to the Univac 1100. For these nine subjects, however, the mean number of undetected signals in the first half of the signal interval was 17.67, while the mean number of undetected signals in the second half of the interval was 17.89. A related t-test confirmed that these values were not significantly different ($t = -0.193$, $p > .25$).

The results concerning the extent to which behavioural and ERP measures of secondary task performance reflect the processing demands of the letter-matching task, therefore, remain equivocal, and further experimentation is required to decide between these alternative interpretations.

The second question of interest in relation to these data is the extent to which the manipulation of type of letter match is reflected by behavioural and ERP measures of signal detection performance associated with second letter visual stimuli.

The analysis of the proportion of hits as a function of signal condition and visual task condition failed to reveal any interaction between these variables. Clearly, signal detection performance on the secondary task does not reflect differences in the processing requirements of the primary task under different letter match conditions. ERP data, however, do prove to be sensitive to the manipulation of type of letter match.

N_1 amplitude was found to be significantly larger over mismatch trials than physical match trials, while the amplitude of this component over rule match trials did not differ from that recorded over the other types of letter match. This finding is difficult to interpret as differences due to type of letter match would be expected to occur following the presentation of the second letter, and to be reflected by an interaction between signal condition and letter match condition. Further, N_1 area measures, while showing a similar trend, failed to reach statistical significance. It is possible that this result arises from slight differences in pre-stimulus baseline values of auditory ERPs, introduced through the elementary subtraction process.

A significant interaction between signal condition and letter match condition was found for both P_3 amplitude and area measures. Under signal condition 7 P_3 area was significantly larger for physical matches than for mismatches, while under signal condition 8 both P_3 area and amplitude were significantly larger for physical matches than either rule matches or mismatches. Inspection of Figure 6.3, however, indicates that at both Cz and Pz, P_3 amplitude tends to be smaller for physical matches under signal condition 6 than for either rule matches or mismatches. A similar trend was evident for P_3 area measures, the mean values of which were 308, 476 and 340μV x mS for physical matches, rule matches and mismatches, respectively, collapsed across subjects and electrode placement.

If we accept the proposal of Isreal *et al.* (1980), that the P_3 amplitude to secondary task stimuli provides an indirect index of the primary task's requirement for perceptual processing resources, then the above results can be interpreted as reflecting the relative timing of the evaluation and classification of second letter stimuli conforming to different types of letter match. It would seem that for physical matches the greatest processing capacity is required sometime after the interval corresponding

to signal condition 6 (48 - 148mS after second letter onset). For mismatches the greatest processing capacity requirement occurs sometime after the interval corresponding to signal condition 7 (200 - 300mS after second letter onset), while for rule matches the greatest processing capacity is required following the interval corresponding to signal condition 8 (348 - 448mS after second letter onset, see Figure 6.3). This temporal ordering of amplitude differences is consistent with the finding that RTs are faster to physical matches than to other types of letter match, and that, while not significant, RTs to mismatches tend to be marginally faster than RTs to rule matches (see footnote on p.223).

The above interpretations of the results of the dual-task experiment are necessarily speculative. It is clear, however, that ERPs are extremely sensitive to manipulations of task requirements, and in some instances are more sensitive than behavioural measures of performance. As Duncan-Johnson and Donchin (1982) state:

> " The concurrent recording of behavioral and ERP measures can illuminate the operation of the human information processing system more fully than is otherwise possible using either measure alone", (p.45).

The following Chapter provides a comparison of the three analytical procedures used to separate overlapping ERP components.

CHAPTER 7: COMPARISON OF SIGNAL RECOVERY TECHNIQUES

7.1 Introduction

The present Chapter assesses the three methods used to separate overlapping ERPs by comparing visual and auditory ERPs recorded over the dual-task experiment and estimated by each of the three signal recovery techniques. Group data provide the basis for all comparisons.

As the behavioural and electrophysiological data presented in Chapters 3 and 6 support the assumption of visual ERP invariance over non-signal and signal trials of the dual-task experiment, this assumption will provide the basis for the following comparisons. That is, the success of the filtering procedures and the GLS solution will be assessed by comparing visual ERPs estimated by means of these techniques with those visual ERPs recorded over non-signal trials. Auditory ERPs estimated through the filtering procedures and GLS solution will then be assessed by means of a comparison with auditory ERPs recovered through elementary subtraction procedures.

7.2 Visual ERPs

Table 6.1 presented Pearson correlation coefficients expressing the relationship between visual averages estimated by means of elementary subtraction procedures and pure visual averages recorded over non-signal trials. A similar procedure was carried out for visual averages estimated by filtering and GLS solutions. The entire length (750 data values) of every estimated visual trace was correlated with the pure visual average recorded under the same visual task condition, and the results of these correlations are given in Table 7.1 for the filtering solution and Table 7.2 for the GLS solution. The average coefficients, presented in the lower row of each table, represent the mean correlation coefficient for each level of letter match and electrode placement, collapsed across

Table 7.1. Pearson correlation coefficients between visual averages estimated through digital filtering procedures and pure visual averages recorded under the same letter-match condition (group data).

Signal Condition	Cz			Pz		
	Physical Match	Rule Match	Mismatch	Physical Match	Rule Match	Mismatch
1	.844	.754	.738	.795	.647	.497
2	.817	.728	.758	.656	.494	.464
3	.824	.880	.887	.513	.627	.663
4	.859	.848	.832	.732	.794	.736
5	.849	.823	.782	.721	.680	.719
6	.689	.863	.894	.545	.686	.742
7	.685	.858	.806	.535	.644	.678
8	.657	.806	.833	.492	.614	.702
Average	.778	.820	.816	.624	.648	.650

Table 7.2. Pearson correlation coefficients between visual averages estimated through the GLS solution and pure visual averages recorded under the same letter-match condition (group data).

Signal Condition	C_z			P_z		
	Physical Match	Rule Match	Mismatch	Physical Match	Rule Match	Mismatch
1	.729	.864	.754	.654	.629	.473
2	.756	.814	.859	.717	.445	.540
3	.876	.909	.815	.868	.749	.801
4	.781	.722	.840	.815	.779	.800
5	.885	.698	.838	.827	.533	.538
6	.817	.910	.660	.589	.798	.443
7	.862	.799	.862	.836	.424	.856
8	.846	.868	.806	.825	.819	.679
Average	.819	.823	.804	.766	.647	.641

signal condition. Inspection of these latter values indicates that, on average, both the filtering and the GLS solutions result in waveforms which are of similar shape to those recorded under non-signal conditions, and that a closer relationship exists for averages recorded from the Cz placement than the Pz placement.

While these findings are similar to those observed for waveforms recovered by means of elementary subtraction procedures, a comparison of average coefficients presented in Tables 7.1 and 7.2 with those presented in Table 6.1 indicates that visual ERPs recovered through the filtering and GLS solutions correspond less closely to non-signal-traces than those ERPs recovered through elementary subtraction procedures.

For waveforms recovered through the filtering procedures, these differences can primarily be attributed to distortions due to the 'filtering out' of very low frequency components resulting from setting the second filter coefficient to unity, combined with distortions arising from residual spectral leakage in the FFT. This is illustrated by reference to Table 7.1 which shows that those coefficients corresponding to signal conditions 6, 7 and 8 over physical match trials are systematically lower than those corresponding to the same signal conditions over rule match and mismatch trials. Inspection of the recovered sections of traces corresponding to these signal conditions and shown in Figures 4.47 and 4.49 reveals that the slow increase in negativity which follows the P_3 component on physical match trials is not fully recovered by the filtering procedures.

Table 7.2 indicates that the degree of correspondence between visual waveforms recovered by means of the GLS solution and visual averages recorded over non-signal trials is variable, particularly at

the Pz placement, where correlation coefficients range between 0.424 and 0.868. There is, however, no systematic effect which can be related to a particular level of letter match or a particular signal condition. Therefore, the success of the GLS procedure seems to be less clearly related to the specific frequency characteristics of those waveforms to be recovered.

7.3 Auditory ERPs

The similarity in the shape of auditory ERPs recovered by means of the three signal recovery techniques was assessed by calculating Pearson correlation coefficients between pairs of waveforms recorded under the same combination of signal condition and letter match condition and estimated by a different analytical procedure. Three sets of correlations were calculated, each set corresponding to one of the three possible pairings of signal recovery procedures. All correlations were calculated from group averages and were based on a total of 145 pairs of data values representing 580mS starting from the time of auditory signal onset. Tables 7.3, 7.4 and 7.5 show correlation coefficients calculated between auditory ERPs estimated by means of elementary subtraction and filtering procedures, elementary subtraction and GLS solutions, and filtering and GLS solutions, respectively.

In general all methods result in ERPs which are similar in form, and no two methods consistently correspond more closely to one another than to a third method. In addition, there is a tendency for waveforms recorded from the Cz placement to correspond marginally more closely than those recorded from the Pz placement.

Table 7.3. Pearson correlation coefficients between auditory ERPs estimated through elementary subtraction procedures and digital filtering procedures.

Signal Condition	Cz			Pz		
	Physical Match	Rule Match	Mismatch	Physical Match	Rule Match	Mismatch
1	.872	.896	.274	.867	.819	.301
2	.926	.771	.701	.870	.569	.715
3	.826	.903	.870	.450	.783	.853
4	.949	.817	.878	.895	.789	.788
5	.943	.927	.803	.941	.894	.812
6	.870	.853	.963	.710	.835	.976
7	.858	.919	.901	.734	.870	.897
8	.922	.941	.763	.822	.902	.792
Average	.896	.878	.769	.786	.808	.767

Table 7.4. Pearson correlation coefficients between auditory ERPs estimated through elementary subtraction procedures and the GLS solution.

Signal Condition	Cz			Pz		
	Physical Match	Rule Match	Mismatch	Physical Match	Rule Match	Mismatch
1	.956	.979	.792	.952	.940	.827
2	.844	.703	.921	.922	.717	.967
3	.867	.984	.824	.924	.941	.984
4	.961	.823	.971	.941	.854	.973
5	.987	.817	.861	.959	.857	.687
6	.638	.972	.874	.232	.949	.853
7	.920	.850	.942	.927	.512	.945
8	.977	.978	.890	.973	.981	.857
Average	.894	.888	.884	.854	.844	.887

Table 7.5. Pearson correlation coefficients between auditory ERPs estimated through digital filtering procedures and GLS solution.

Signal Condition	Cz			Pz		
	Physical Match	Rule Match	Mismatch	Physical Match	Rule Match	Mismatch
1	.900	.948	.705	.924	.957	.695
2	.892	.961	.835	.864	.884	.667
3	.955	.915	.971	.733	.798	.878
4	.877	.892	.842	.833	.844	.765
5	.903	.923	.964	.839	.857	.833
6	.926	.935	.884	.655	.871	.810
7	.978	.859	.987	.931	.505	.963
8	.977	.972	.908	.917	.934	.940
Average	.926	.926	.887	.837	.831	.819

While the correlation coefficients presented in Tables 7.3, 7.4 and 7.5 provide information about the similarity of the shape of waveforms recovered by means of the different procedures, they fail to provide information about differences in the overall sizes of ERPs or about differences in amplitudes and latencies of ERP components. In order to make these assessments the amplitudes and latencies of N_1 and P_3 components were derived according to the method described in Section 6.3.2 from auditory ERPs estimated through each of the three signal recovery techniques. ERP measures were taken from group averages and hence the values derived from auditory ERPs estimated by means of elementary subtraction procedures differ somewhat from mean values presented in Chapter 6 which were based on measures derived separately for every subject.

A total of 48 measures of a particular ERP component amplitude or latency was taken from each set of auditory traces estimated by a particular analytical procedure. These 48 measures comprised values corresponding to each of the 24 combinations of signal condition and visual task condition, taken from both Cz and Pz placements.

As a first stage in the analysis, the means and variances of ERP components estimated through the three analytical procedures were calculated separately for each placement and these are presented in Table 7.6. Note that every mean was derived from the 24 values associated with each combination of signal condition and visual task condition. Inspection of Table 7.6 indicates that the variances associated with N_1 and P_3 amplitudes and latencies estimated through the filtering and GLS solutions are generally larger than those associated with estimates derived through subtraction procedures. For each ERP measure a series of three t-tests for equality of

Table 7.6. Means and variances of auditory ERP components estimated by each of the three signal recovery techniques.

		Cz			Pz		
		Subtraction	Filtering	GLS	Subtraction	Filtering	GLS
N_1 amplitude (μV)	$\bar{x}$	-3.547	-3.748	-3.359	-2.640	-2.950	-2.681
	σ^2	0.380	1.238	1.907	0.285	0.663	2.233
P_3 amplitude (μV)	$\bar{x}$	2.917	1.809	2.961	3.114	1.516	3.126
	σ^2	0.392	0.605	2.207	0.496	0.491	1.652
N_1 latency (mS)	$\bar{x}$	192	191	190	201	212	198
	σ^2	115	189	216	403	699	714
P_3 latency (mS)	$\bar{x}$	414	393	405	431	420	435
	σ^2	998	1206	1628	1292	1175	2482

variances of dependent samples[1] (Kirk, 1978; p.277) was used to compare variances associated with the three analytical procedures.

For the Cz placement, N_1 amplitudes taken from both filtering and GLS estimates were significantly more variable than those derived from subtraction procedures ($p < .01$ for both comparisons). For the Pz placement, however, the variability in N_1 amplitudes was significantly different for all signal recovery procedures ($p < .05$ for all comparisons), with GLS providing the most variable estimates and the subtraction procedures providing the least variable estimates. Similarly, comparisons of the variability of P_3 amplitudes recorded from the Cz placement all proved to be significantly different ($p < .01$ for all comparisons) ; while at the Pz placement the GLS solution yielded more variable P_3 estimates than either subtraction or filtering procedures ($p < .01$ for both comparisons). No signficant differences were found between the variances of N_1 or P_3 latency estimates at either Cz or Pz.

Separate 2-way repeated measures ANOVAs were used to assess the effects of signal recovery method and electrode placement on N_1 and P_3 amplitudes and latencies. Note that the 24 data values corresponding to each combination of letter match and signal condition were used as 'subjects' or 'blocks' within these analyses.

While ANOVA procedures are relatively insensitive to violations of the assumption of homogeneity of variance, heterogeneity of both variances and covariances in a design having repeated measures on the

[1] dependency between ERP components estimated by means of the three signal recovery techniques was assumed as the estimates corresponding to a particular experimental condition were all derived from identical data.

same subjects can result in a positive bias in the F test and hence an unacceptable number of type 1 errors. To guard against this possibility, Geisser-Greenhouse conservative F tests (Kirk, 1968,p.142) with degrees of freedom for treatment and error terms of 1 and 23, respectively, were applied to these data as well as conventional F tests. Consistent outcomes were obtained for both types of test and consequently the results of the conventional F tests are reported.

ANOVA on N_1 amplitudes indicated a significant placement effect ($F_{1,23} = 37.00$; $p < .001$), no significant effect due to method of signal recovery ($F_{2,46} = 1.25$; $p > .300$) and no significant interaction ($F_{2,46} = 0.74$; $p > .400$). From Table 7.6 it can be seen that N_1 amplitudes of ERPs recorded from Cz are larger than those measured from ERPs at Pz.

For P_3 amplitudes ANOVA indicated no significant placement effect ($F_{1,23} = 0.10$; $p > .800$), a significant method effect ($F_{2,46} = 26.02$; $p < .001$) and a significant placement by method interaction ($F_{2,46} = 6.63$; $p < .005$). Tests of simple main effects showed a significant method effect at both Cz and Pz ($F_{2,92} = 15.91$; $p < .001$ and $F_{2,92} = 32.02$; $p < .001$, respectively), and a Newman-Keuls analysis showed that at both placements P_3 amplitudes of ERPs estimated through subtraction and GLS procedures are significantly larger than those of ERPs estimated through the filtering process ($p < .01$ for all comparisons). Note, however, that the trend for P_3 amplitudes to be larger at Pz than at Cz is reversed for those amplitudes measured from ERPs estimated through the filtering process.

For N_1 latencies, ANOVA revealed a significant effect due to electrode placement ($F_{1,23} = 24.71$; $p < .05$) and a significant method by placement interaction ($F_{2,46} = 3.72$; $p < .05$). Tests of simple main

effects showed that there was a significant effect due to signal recovery method at the Pz placement only ($F_{2,92} = 5.62$; $p < .005$), and a Newman-Keuls test showed that, at this placement, N_1 latencies of ERPs estimated by the filtering procedures were significantly longer than those recovered by either the elementary subtraction or the GLS solutions ($p < .05$ for both comparisons).

For P_3 latencies, ANOVA revealed a significant effect due to method of signal recovery ($F_{2,46} = 4.44$; $p < .025$) and electrode placement ($F_{1,23} = 36.79$; $p < .001$). There was no significant interaction ($F_{2,46} = 2.60$; $p > .08$). A Newman-Keuls test indicated that P_3 latencies of ERPs recovered through the filtering process were significantly shorter than those recovered through the subtraction or GLS procedures ($p < .05$ for both comparisons). Inspection of Table 7.6 shows that the latencies of P_3 waves recorded from Pz were consistently longer than those recorded from Cz.

In summary, the above analyses on auditory ERP components indicate that:

- the GLS and, to a lesser extent, the filtering solutions resulted in significantly more variable N_1 and P_3 amplitudes than the elementary subtraction procedure. While the variances of latency measures followed this trend, they were not found to differ significantly;
- there were no differences between mean N_1 amplitudes estimated through the three signal recovery techniques. However, P_3 amplitudes estimated through the filtering procedures were significantly reduced when compared with those estimated through elementary subtraction and GLS solutions;
- at the Pz placement, N_1 latencies were significantly longer when estimated through the filtering process, while at both placements,

P_3 latencies were significantly shorter when recovered by the filtering procedure. There were no differences between the mean latencies of either N_1 or P_3 components estimated by subtraction or GLS solutions.

The above analyses have investigated differences in overall mean values of auditory ERP components estimated through each of the signal recovery techniques. An important consideration in the comparison of the analytical procedures, however, is the extent to which ERP amplitudes and latencies exhibit similar trends as a function of manipulations of the independent variables. Figures 7.1 to 7.8 allow these comparisons as each figure presents a component amplitude or latency estimated through A: elementary subtraction, B: digital filtering and C: GLS, as a function of signal condition and visual task condition.

Figures 7.1 and 7.2 show N_1 amplitudes from Cz and Pz placements, respectively. While these figures illustrate the increased variability in the estimates obtained through the GLS and filtering procedures compared with those obtained through elementary subtraction procedures, the graphs exhibit trends which are similar for all methods of signal recovery and which are consistent across electrode placement.

Figures 7.3 and 7.4 show P_3 amplitudes taken from Cz and Pz placements, respectively. These figures illustrate the increased variability in values estimated through the GLS and filtering procedures when compared with the subtraction process, and the reduced amplitudes of P_3 components recovered through the filtering procedures. While some differences are evident between the relative amplitudes of P_3 components corresponding to the first 5 signal conditions, a common feature of all methods of signal recovery is the

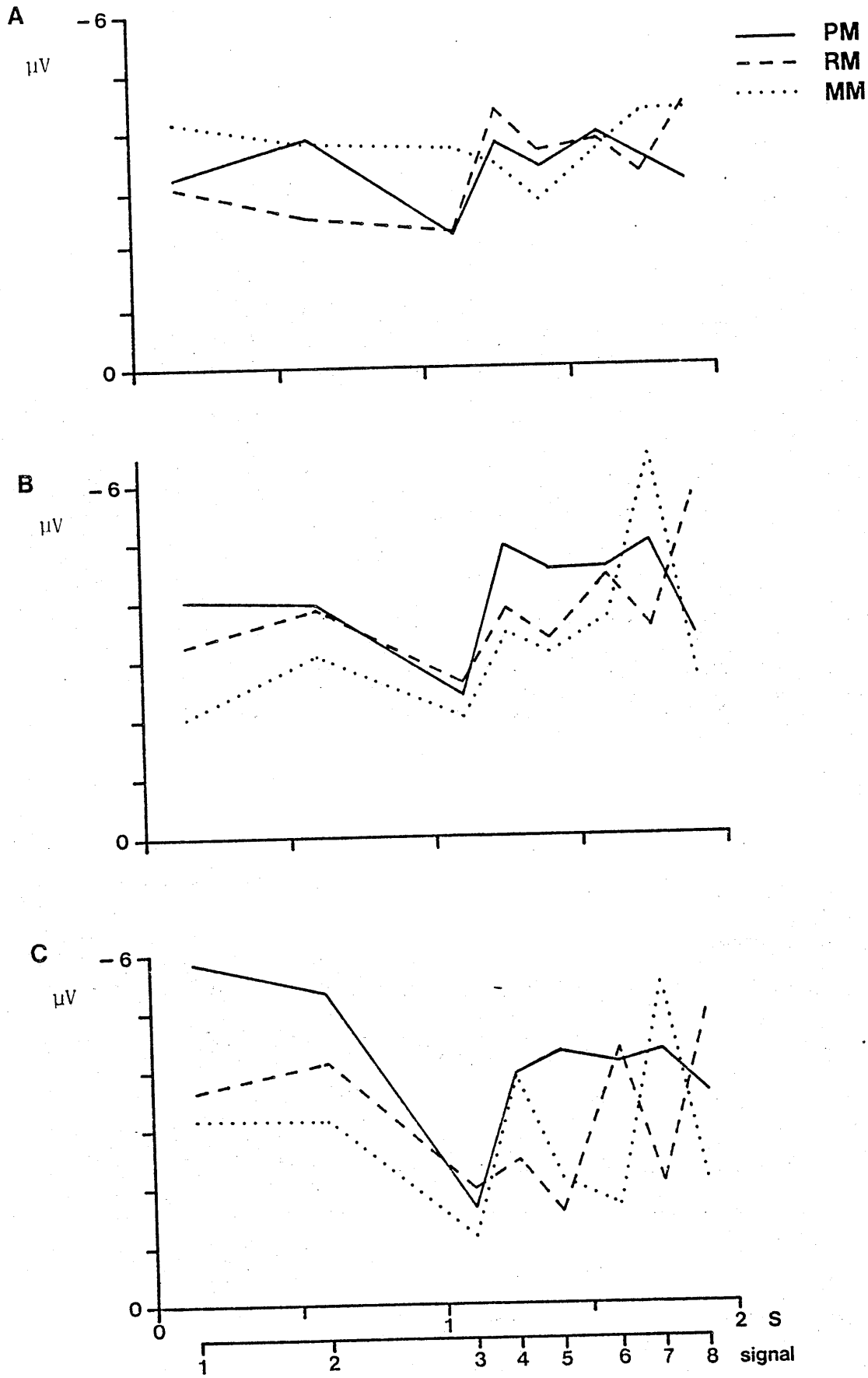

Figure 7.1. N_1 amplitudes of auditory ERPs recorded from Cz and estimated by means of A: elementary subtraction, B: digital filtering and C: GLS.

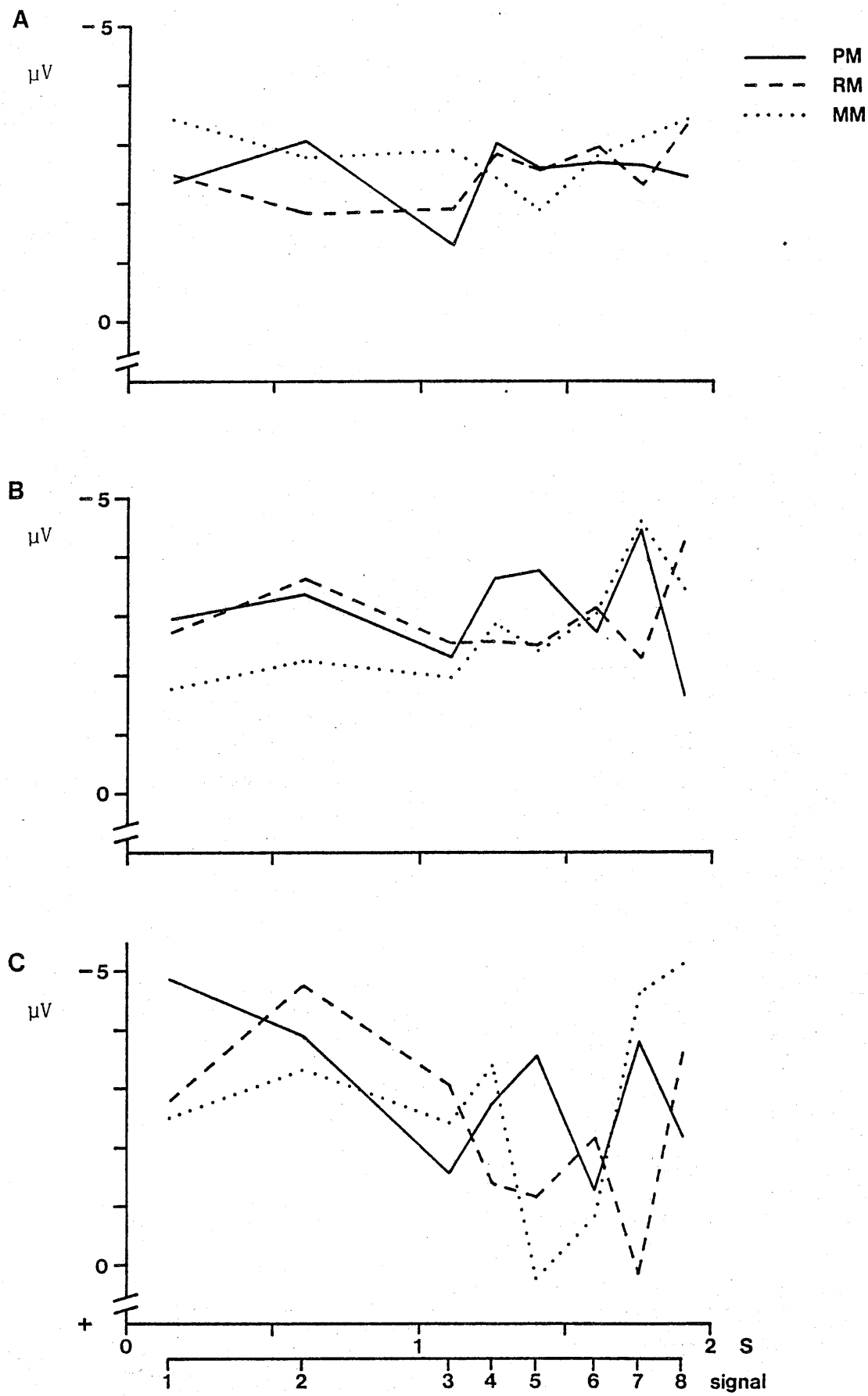

Figure 7.2. N_1 amplitudes of auditory ERPs recorded from Pz and estimated by means of A: elementary subtraction, B: digital filtering and C: GLS.

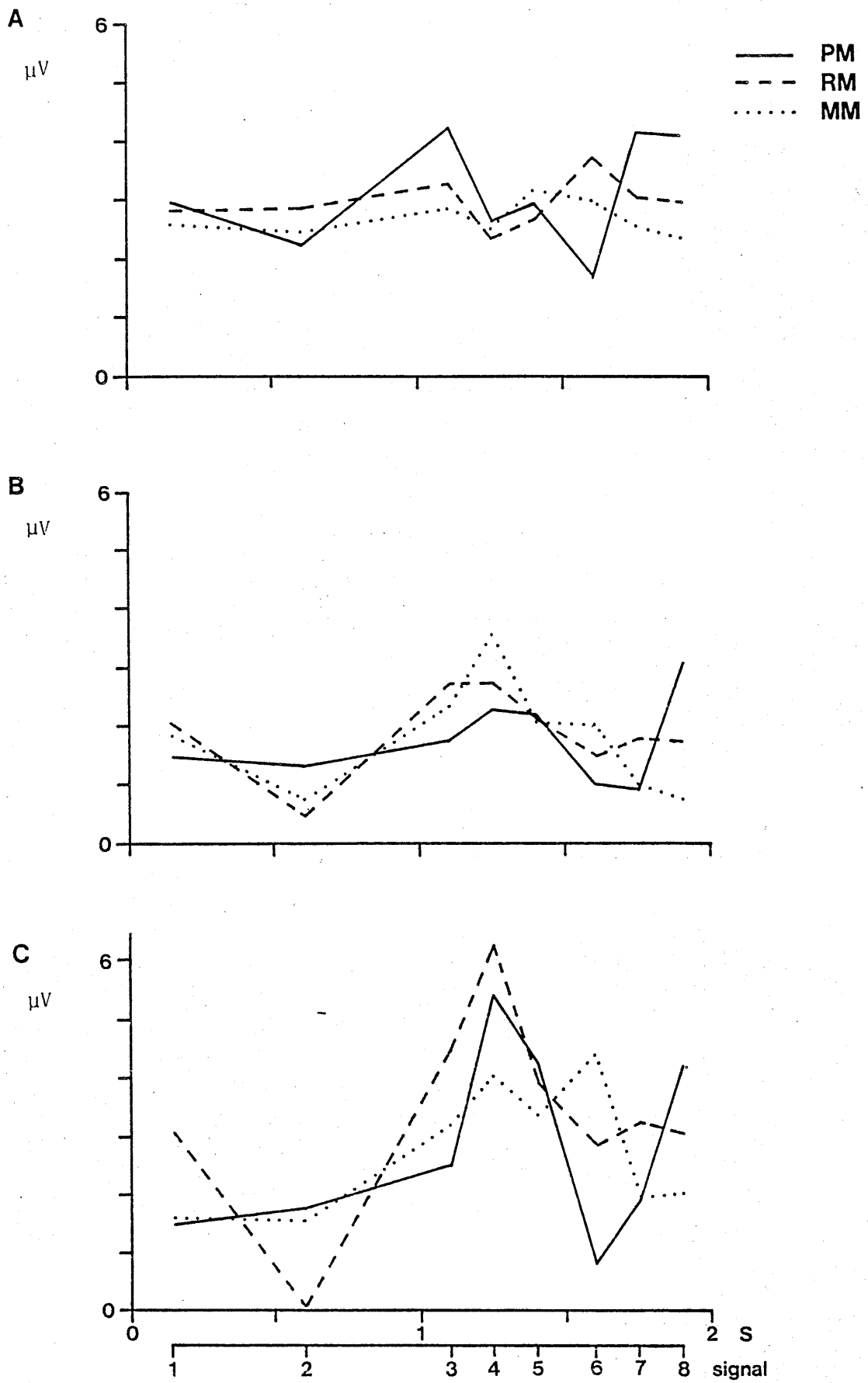

Figure 7.3. P_3 amplitudes of auditory ERPs recorded from Cz and estimated by means of A: elementary subtraction, B: digital filtering and C: GLS.

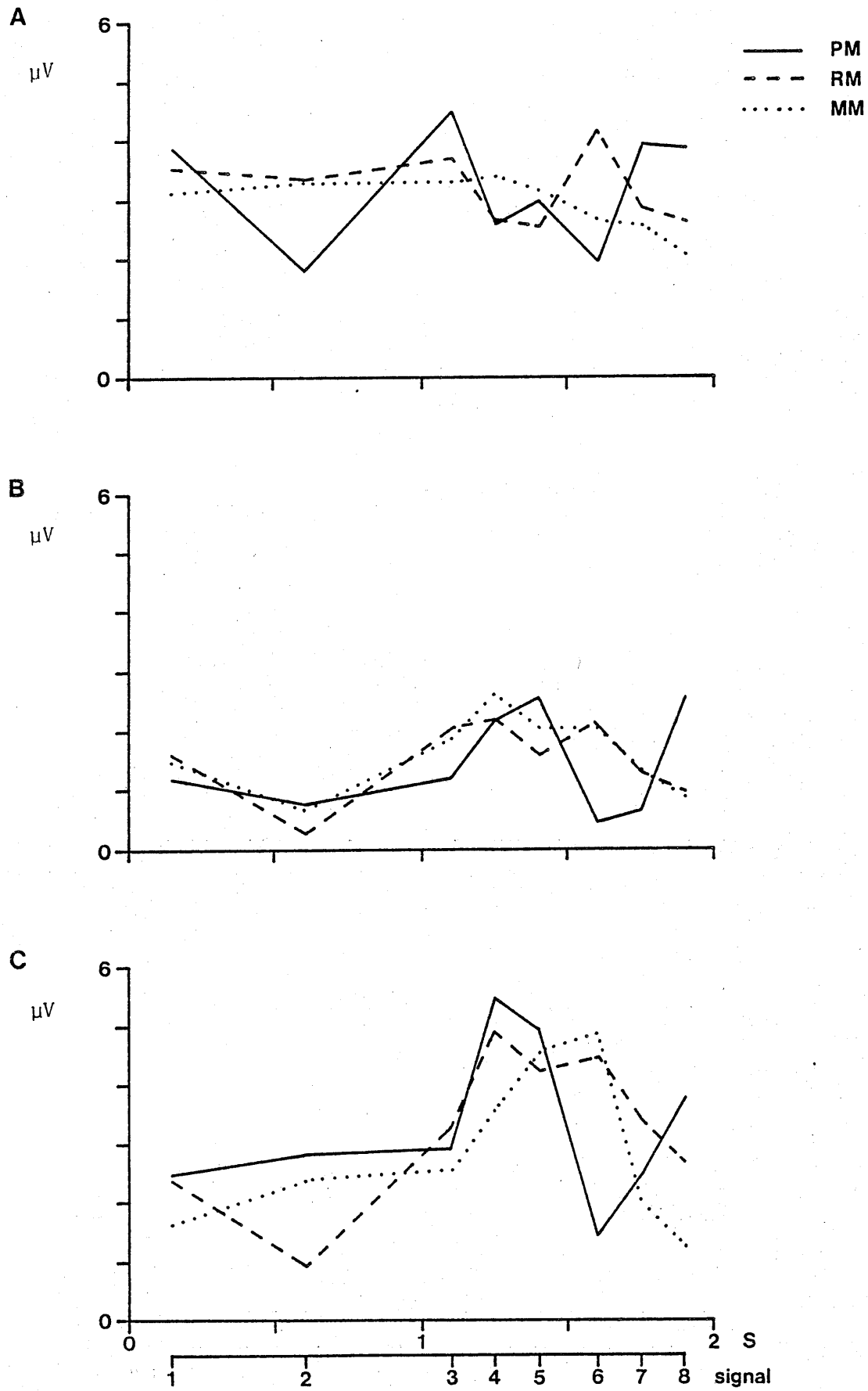

Figure 7.4. P_3 amplitudes of auditory ERPs recorded from Pz and estimated by means of A: elementary subtraction, B: digital filtering and C: GLS.

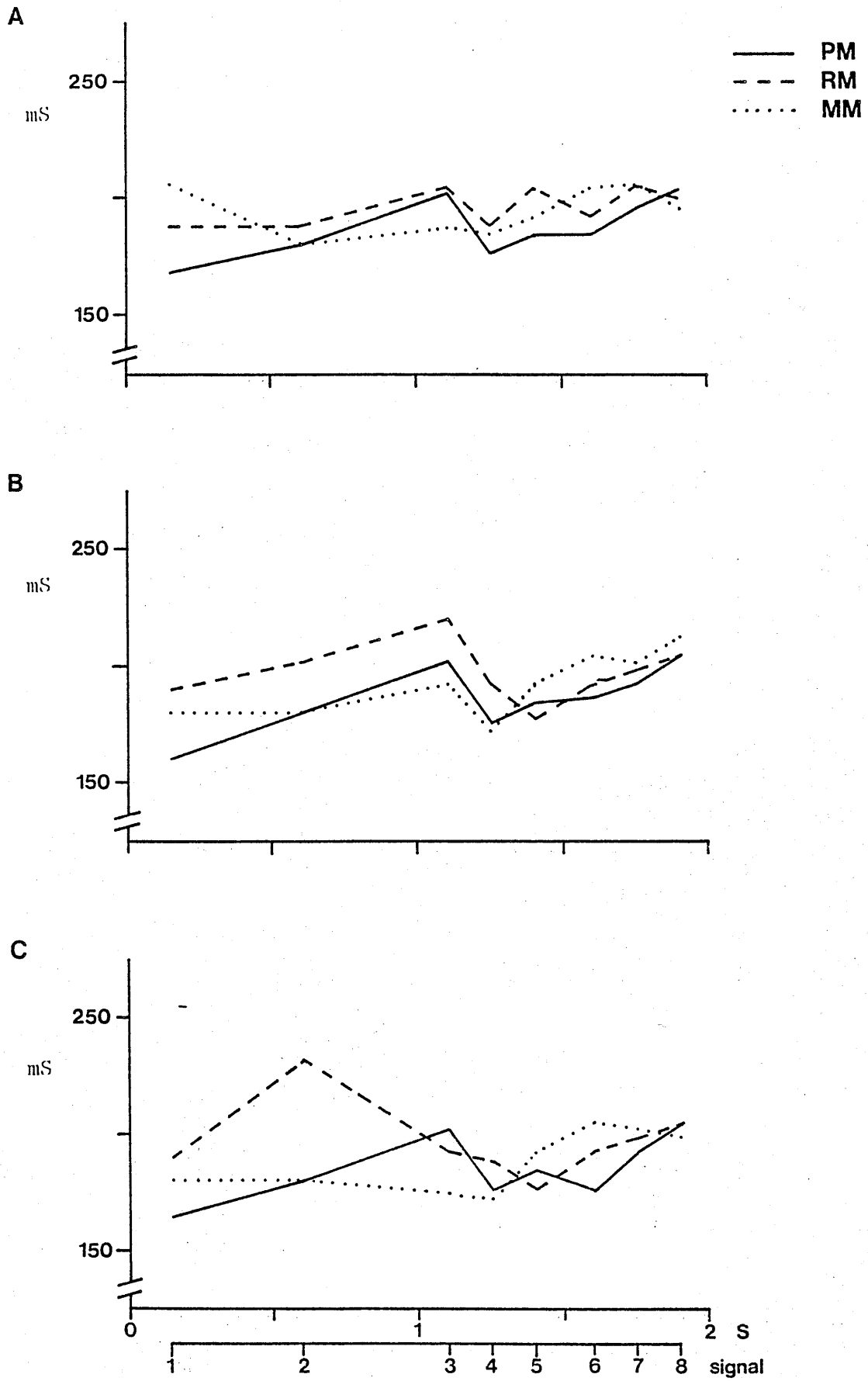

Figure 7.5. N_1 latencies of auditory ERPs recorded from Cz and estimated from A: elementary subtraction, B: digital filtering and C: GLS.

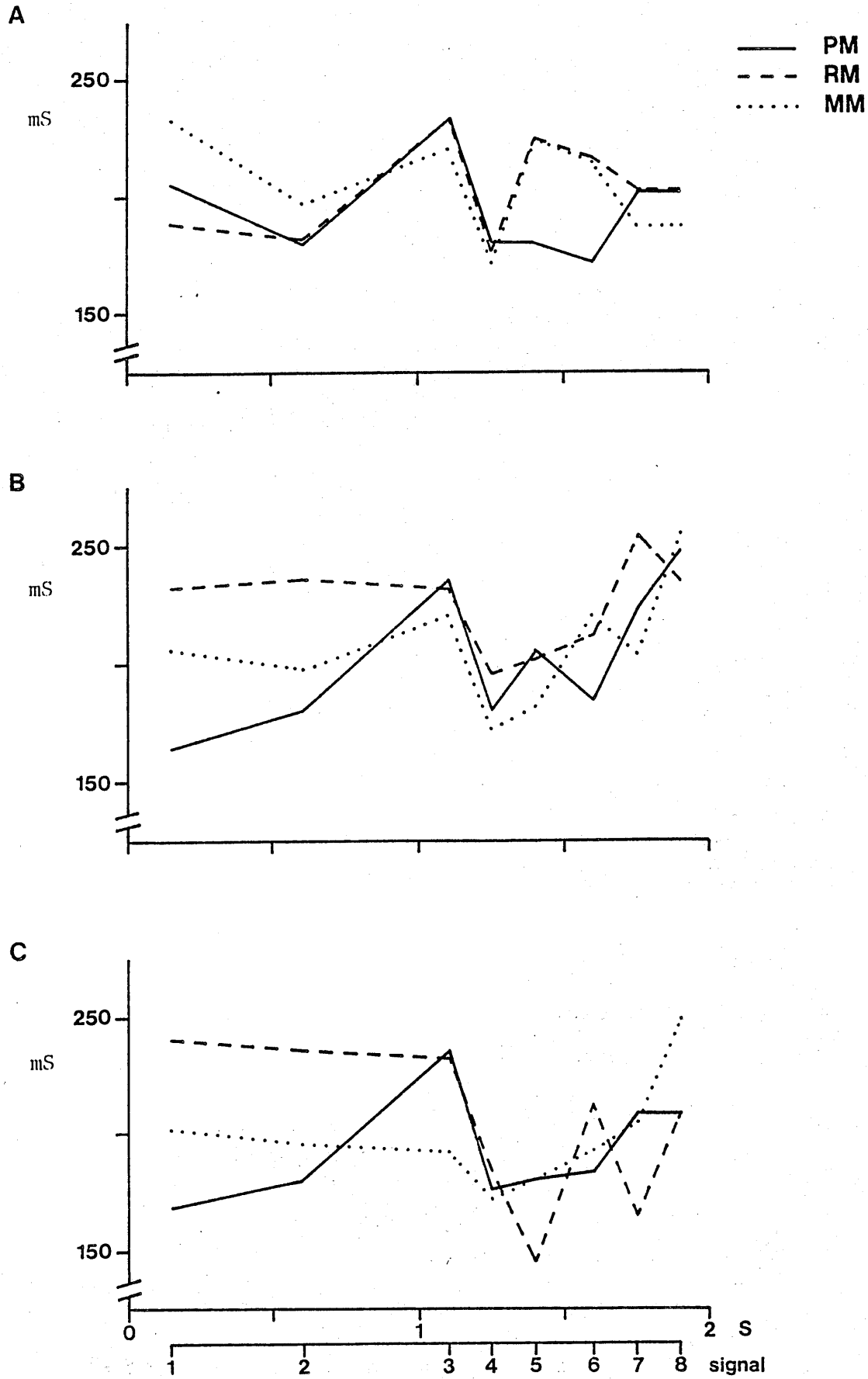

Figure 7.6. N_1 latencies of auditory ERPs recorded from Pz and estimated by means of A: elementary subtraction, B: digital filtering and C: GLS.

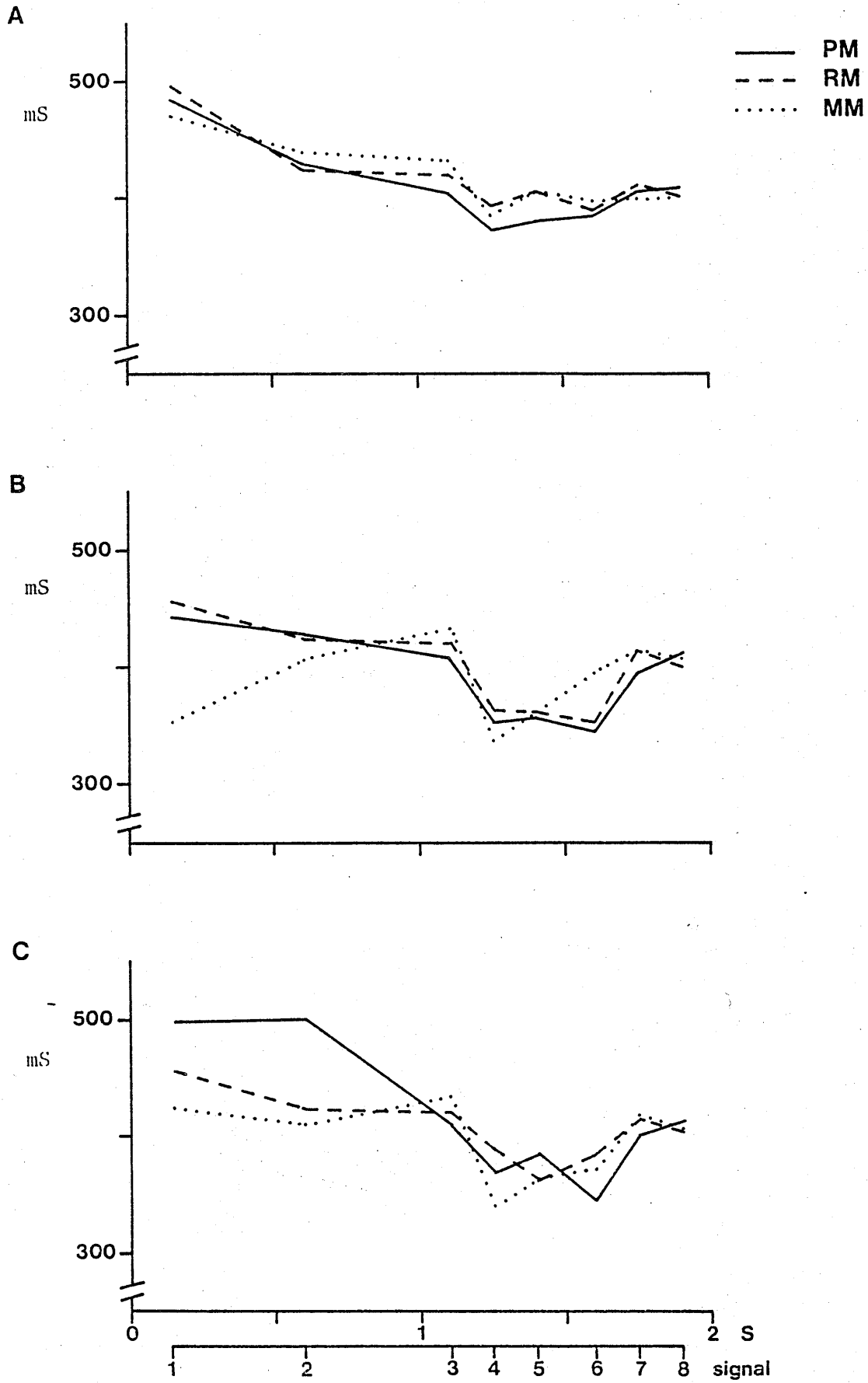

Figure 7.7. P_3 latencies of auditory ERPs recorded from Cz and estimated by means of A: elementary subtraction, B: digital filtering and C: GLS.

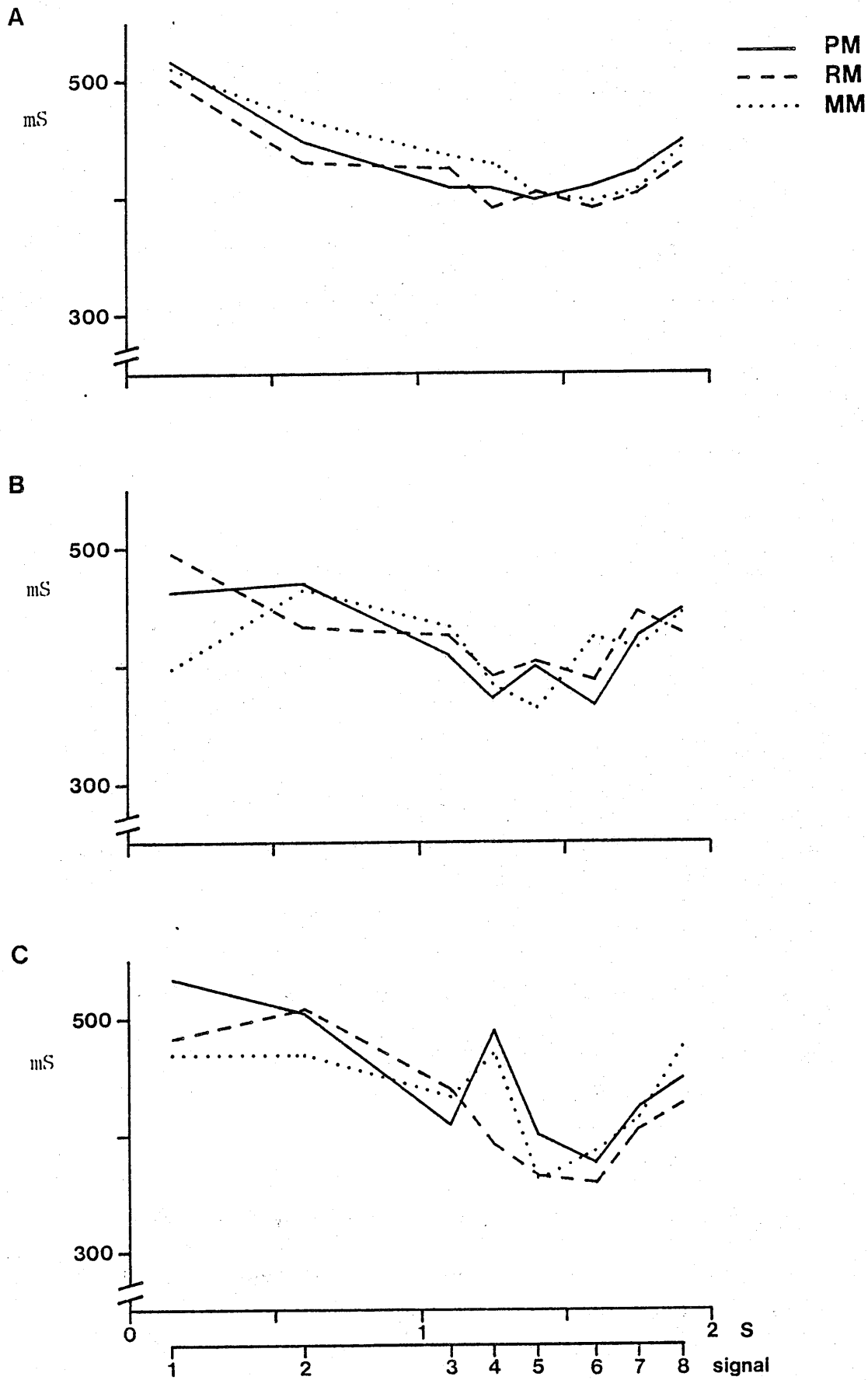

Figure 7.8. P_3 latencies of auditory ERPs recorded from Pz and estimated by means of A: elementary subtraction, B: digital filtering and C: GLS.

interaction which occurs between visual and auditory tasks over signal conditions 6, 7 and 8. Under signal condition 6, P_3 amplitudes to signals presented during physical match trials are consistently reduced when compared with those presented during rule match and mismatch trials. In contrast, under signal condition 8, auditory P_3 amplitudes associated with physical match trials are consistently larger than those associated with the other types of letter match. This patterning of P_3 amplitudes is consistent with those results reported in Section 6.3.2.

Figures 7.5 and 7.6 present N_1 latencies for Cz and Pz placements, respectively. All graphs exhibit similar profiles with N_1 latencies tending to be marginally longer under signal condition 3 than signal condition 4. For all methods of signal recovery, N_1 estimates at Pz are more variable than those at Cz.

Figures 7.7 and 7.8 show P_3 latencies measured from Cz and Pz placements, respectively. While the latencies of P_3 components recovered by the filtering procedures are noticeably reduced when compared with those estimated through the other techniques, all graphs exhibit similar trends which are consistent with the results reported in Section 6.3.2.

In general, therefore, the profiles of amplitude and latency measures taken from ERPs estimated by the filtering and GLS solutions correspond well with the trends of ERP components estimated through the elementary subtraction procedure.

A further important consideration in the comparison of the analytical procedures is the relationship between signal detection performance and components of auditory ERPs estimated through each procedure. Table 7.7 presents the correlation coefficients calculated

Table 7.7. Pearson correlation coefficients between auditory ERP components estimated by each of the three signal recovery techniques and the proportion of correct detections (hits).

	Cz			Pz		
	Subtraction	Filtering	GLS	Subtraction	Filtering	GLS
N_1 amplitude† with proportion hits (n=24)	-.043	.014	-.321	-.107	-.033	-.366
P_3 amplitude with proportion hits (n=24)	.132	.282	.359	.105	.318	.282
N_1 latency with proportion hits (n=24)	.213	.209	-.088	.187	-.035	.004
P_3 latency with proportion hits						
signal conditions 1-8 (n=24)	-.375	-.195	-.295	-.502*	-.470*	-.441*
signal conditions 1-4, 6-8 (n=21)	-.464*	-.312	-.402	-.616**	-.601**	-.620**

† absolute values

* $p < .05$

** $p < .005$

between the mean proportion of correct signal detections and auditory ERP components recorded under the twenty-four combinations of signal condition and letter match condition. These data are consistent with those presented in Table 6.3, and indicate an inverse relationship between P_3 latency and signal detection which is strengthened when the data values associated with signal condition 5 are excluded from the analyses. The tendency towards larger correlation coefficients for N_1 amplitudes estimated by the GLS solution, and for P_3 amplitudes estimated by both the filtering and GLS solutions can be attributed to the greater variability in the values of components derived through these procedures.

7.4 Discussion

This chapter has compared the success of the three signal recovery techniques following their application to 'real' data which are typical of those requiring some estimation procedure to separate overlapping ERPs to near-simultaneous stimuli. The invariance of visual ERPs recorded over signal and non-signal trials of the dual-task experiment has allowed waveforms recovered through elementary subtraction procedures to be used as a model against which to assess the adequacy of the digital filtering and GLS solutions.

The comparison between the mean amplitudes and latencies of ERP components recovered through the different techniques showed that the digital filtering process resulted in significantly reduced P_3 amplitudes and P_3 latencies when compared with the other procedures. Further, the latencies of N_1 components at the Pz placement were delayed when estimation was achieved through the filtering process.

These differences can be attributed to the effects of setting

the second coefficient of the inverse filter to unity in an attempt to reduce distortions arising from spectral leakage in the FFT. While this modification eliminates the more obvious effects of spectral leakage, it also results in the attenuation of the wanted frequency component corresponding to approximately 0.977Hz. The attenuation of this frequency is manifested in the recovered waveforms by amplitude and latency distortions of the low frequency P_3 and N_1 components. Goff (1974, p.126) provides an example of such distortions of the vertex potentials resulting from progressive decreases in the low frequency response of the recording amplifier.

While the mean amplitudes and latencies of ERPs recovered through the filtering process were significantly affected by the modification made to the inverse filter, the shape of the recovered waveforms generally provided a good correspondence with those recovered through the elementary subtraction process. In addition, the trends in ERP component amplitudes and latencies as a function of signal condition and visual task condition, also corresponded well with those obtained through elementary subtraction procedures.

Various methods can be employed to minimise the degree of spectral leakage in the FFT and hence optimise the digital filtering solution. For example, in the present experiment a low frequency amplifier setting of 0.4Hz (50% cut off) was used for EEG recordings. The use of a higher setting, such as 1Hz, would result in little or no distortion of the vertex potentials, but would help attenuate the very low frequencies which prove to be particularly problematic for the technique. More importantly, increasing the length of the time series submitted to the FFT would reduce the fundamental frequency and result in less spectral leakage as the harmonics of the series will be more closely spaced. The use of windowing procedures and the application

of the techniques to data which have a high signal to noise ratio will further reduce the degree of distortion resulting from the effects of spectral leakage.

Although methods are available for optimising the digital filtering solution, the procedure clearly is unsuitable if slow potential changes such as the CNV, which require either DC recording or the use of long time constants in the order of 8 seconds, are of interest. Further, while every precaution may be taken to reduce distortion resulting from spectral leakage, its effects cannot be eliminated completely, and estimates returned by the solution must be expected to be biased to some degree.

The GLS solution is potentially a more reliable technique for separating overlapping ERP components, primarily because it is applied in the time domain and hence obviates the effects of spectral leakage associated with manipulations in the frequency domain. The comparison of visual and auditory waveforms recovered through this procedure with those recovered through elementary subtraction indicated a generally good, although variable, correspondence. Further, the overall elevation of ERP component amplitudes and latencies estimated through these two procedures was found not to differ. The amplitudes of ERP components derived from GLS estimates, however, were found to be significantly more variable than those derived through the subtraction process. Three factors may be responsible for this increased variability.

As indicated in Chapter 4, the method of data collection during the dual-task experiment resulted in time-locked visual and auditory averages which departed from the model of the GLS solution in two significant ways: the time-locked averages were not based on the full complement of trials assumed by the model, and the last 24 samples of

the time-locked auditory trace were weighted inappropriately. While attempts were made to compensate for this latter departure, the solution should be optimised by ensuring the appropriate methods of data collection.

The third factor which may have contributed to the variable nature of GLS estimates relates to the offsets of the sections of visual and auditory time-locked averages submitted to the analysis. It will be recalled that the time-locked auditory traces were adjusted so that the mean of the 100mS prior to the onset of the auditory signal was equivalent to the mean of the 100mS section of visual trace prior to the start of the auditory signal window. This method of adjustment appeared to work well, but as previously noted, the GLS solution is extremely sensitive to differential offsets, which can result in highly spurious estimates. A more appropriate procedure would be to apply the solution immediately following data collection, before any adjustment is made to prestimulus baselines and prior to scaling procedures used to convert averages to microvolt equivalents (see Section 2.7).

In conclusion, this thesis has investigated the use of three analytical procedures for separating overlapping waveforms recorded following near-simultaneous stimuli. Traditional elementary subtraction procedures have been found to provide highly reliable estimates when the assumptions underlying their application are met. Their use is questionable, however, in situations where the composite waveform may reflect any interaction between the evoking stimuli.

Both digital filtering and GLS procedures allow the detection and assessment of interactions between task stimuli by virtue of the fact that estimates are derived directly from the composite waveforms. Estimates obtained by the filtering solution, however, are subject to

severe distortions arising from spectral leakage in the FFT. Methods used to eliminate the more obvious effects of spectral leakage result in residual distortions of the low frequency, late components of the ERP.

A potentially more useful procedure than either elementary subtraction or digital filtering is that of GLS estimation. The advantage over that of the digital filtering procedures is that estimation is carried out in the time domain, thus obviating the problems associated with analysis in the frequency domain.

REFERENCES

Aitken, A.C. On least squares and linear combination of observations. *Proceedings of the Royal Society of Edinburgh*. 1935, 55, 42.

Andreassi, J.L., De Simone, J.J., and Mellers, B.W. Amplitude changes in the visual evoked cortical potential with backward masking. *Electroencephalography and Clinical Neurophysiology*, 1976, 41, 387-398.

Andreassi, J.L., Stern, M., and Okamura, H. Visual cortical evoked potentials as a function of intensity variations in sequential blanking. *Psychophysiology*, 1974, 11, 336-345.

Beauchamp, K., and Yuen, C. *Digital Methods for Signal Analysis*. London: George Allen and Unwin, 1979.

Begleiter, H. (Ed.). *Evoked Brain Potentials and Behaviour*. New York and London: Plenum Press, 1979.

Bennett, R.J. *Spatial Time Series*. London: Pion, Ltd., 1979.

Berger. H. On the electroencephalogram of man. 1929. In: Gloor, P. (Ed.). *Hans Berger on the electroencephalogram of man. Electroencephalography and Clinical Neurophysiology Supplement*, 1969, 28, 38.

Bergland, G.D. A guided tour of the fast Fourier transform. *Institute of Electrical and Electronics Engineering, IEEE Spectrum*, 1969, 6, 41-52.

Buchsbaum, M., and Coppola, R. Computer use in bioelectric data collection and analysis. In: Thompson, R.F., and Patterson, M.M. (Eds.), *Bioelectric Recording Techniques Vol. 1 - Part B: Electroencephalography and Human Brain Potentials*. New York: Academic Press, 1974.

Callaway, E., Tueting, P., and Koslow, S.H. (Eds.). *Event-Related Brain Potentials in Man*. New York and London: Academic Press, 1978.

Caton, R. The electrical currents of the brain. *British Medical Journal*, 1875, 2, 278.

Clynes, M., and Kohn, M. The use of the Mnemotron for biological data storage, reproduction, and for an average transient computer. *Abstracts of 4th Annual Meeting of the Biophysics Society*, 1960, 23. Philadelphia, Pennsylvania.

Cogan, D.G. *Neurology of the Visual System*. Springfield, Illinois: Charles C. Thomas, 1966.

Corby, J.C., and Kopell, B.S. Differential contributions of blinks and vertical eye movements as artifacts in EEG recording. *Psychophysiology*, 1972, 9, 640-644.

Davis, H., Osterhammel, R.A., Weir, C.C., and Gjerdingen, D.B. Slow vertex potentials: interactions among auditory, tactile, electric and visual stimuli. *Electroencephalography and Clinical Neurophysiology*, 1972, 33, 537-545.

Dawson, G.D. Cerebral responses to electrical stimulation of peripheral nerve in man. *Journal of Neurology, Neurosurgery and Psychiatry*, 1947, 10, 134-140.

Dawson, G.D. A summation technique for detecting small signals in a large irregular background. *Journal of Physiology*, 1951, 115, 2-3.

Desmedt, J.E. (Ed.). Cognitive components in cerebral event-related potentials and selective attention. *Progress in Clinical Neurophysiology, Vol. 6*. Basel: Karger, 1979.

Donchin, E. Event-related brain potentials: a tool in the study of human information processing. In: Begleiter, H. (Ed.). *Evoked Brain Potentials and Behaviour*. New York and London: Plenum Press, 1979.

Donchin, E., (Ed.). *Cognitive Psychophsiology*. Hillsdale, New Jersey: Erlbaum Press, 1982.

Donchin, E., and Lindsley, D.B. Visually evoked response correlates of perceptual masking and enhancement. *Electroencephalography and Clinical Neurophysiology*, 1965, 19, 325-335.

Donchin, E., Ritter, W., and McCallum, W.C. Cognitive psychophysiology: the endogenous components of the ERP. In: Callaway, E., Tueting, P., and Koslow, S.H. (Eds.). *Event-Related Brain Potentials in Man*. New York and London: Academic Press, 1978.

Duncan, J. The demonstration of capacity limitation. *Cognitive Psychology*, 1980, 12, 75-96.

Duncan-Johnson, C.C., and Donchin, E. The P300 component of the event-related brain potential as an index of information processing. *Biological Psychology*, 1982, 14, 1-52.

Freides, D. Human information processing and sensory modality: cross-modal functions, information complexity, memory, and deficit. *Psychological Bulletin*, 1974, 81, 284-310.

Galambos, R., and Hillyard, S.A. Electrophysiological approaches to human cognitive processing. *Neuroscience Research Program Bulletin*, 1981, 20, 141-265.

Galton, F. Composite portraits. *Journal of the Anthropological Institute*, 1878, 8, 132-142.

Gilden, L., Vaughan, H.G. and Costa, L.D. Summated human EEG potentials associated with voluntary movement. *Electroencephalography and Clinical Neurophysiology*, 1966, 20, 433-438.

Glaser, E.M., and Ruchkin, D.S. *Principles of Neurobiological Signal Analysis*. New York and London: Academic Press, 1976.

Goff, W.R. Human average evoked potentials: procedures for stimulating and recording. In: Thompson, R.F., and Patterson, M.M. (Eds.). *Bioelectric Recording Techniques Vol. 1. Part B: Electroencephalography and Human Brain Potentials*. New York: Academic Press, 1974.

Goff, W.R., Allison, T., and Vaughan, H.G. The functional neuroanatomy of event-related potentials. In: Callaway, E., Tueting, P., and Koslow, S.H. (Eds.). *Event-Related Brain Potentials in Man.* New York and London: Academic Press, 1978.

Green, D.M., and Swets, J.A. *Signal Detection Theory and Psychophysics.* New York: Wiley, 1966.

Haber, R.N. Information processing. In: Carterette, E.C., and Friedman, M.P. (Eds.). *Handbook of Perception Vol 1,* New York: Academic Press, 1974.

Hansen, J.C., and Hillyard, S.A. Endogenous brain potentials associated with selective auditory attention. *Electroencephalography and Clinical Neurophysiology,* 1980, 49, 277-290.

Harris, F.J. On the use of windows for harmonic analysis with the discrete Fourier transform. *Proceedings of the IEEE,* 1978, 66, 51-83.

Hibbs, D.A. Problems of statistical estimation and causal inference in time-series regression models. In: Costner, H.L. (Ed.). *Sociological Methodology 1973-1974.* San Francisco: Jossey-Bass, 1974.

Hillyard, S.A. Selective auditory attention and early event-related potentials: a rejoinder. *Canadian Journal of Psychology,* 1981, 35, 159-174.

Hillyard, S.A., and Galambos, R. Eye movement artifact in the CNV. *Electroencephalography and Clinical Neurophysiology,* 1970, 28, 173-182.

Hillyard, S.A., Hink, R.F., Schwent, V.L., and Picton, T.W. Electrical signs of selective attention in the human brain. *Science,* 1973, 182, 177-180.

Hillyard, S.A., and Kutas, M. Electrophysiology of cognitive processing. *Annual Review of Psychology,* 1983, 34, 33-61.

Hillyard, S.A., Picton, T.W., and Regan, D. Sensation, perception, and attention: analysis using ERPs. In: Callaway, E., Tueting, P., and Koslow, S.H. (Eds.). *Event-Related Brain Potentials in Man.* New York and London: Academic Press, 1978.

Hillyard, S.A., Squires, K.C., Bauer, J.W. and Lindsay, P.H. Evoked potential correlates of auditory signal detection. *Science,* 1971, 172, 1357-1360.

Isreal, J.B., Chesney, G.L., Wickens, C.D., and Donchin, E. P300 and tracking difficulty: Evidence for multiple resources in dual-task performance. *Psychophysiology,* 1980, 17, 259-273.

Isreal, J.B., Wickens, C.D., Chesney, G.L. and Donchin, E. The event-related brain potential as an index of display-monitoring workload. *Human Factors,* 1980, 22, 211-224.

Jasper, H.H. The ten twenty electrode system of the International Federation. *Electroencephalography and Clinical Neurophysiology,* 1958, 10, 371-375.

Jewett, D.L., and Williston, J.S. Auditory-evoked far fields averaged from the scalp of humans. *Brain*, 1971, 94, 681-696.

John, E.R., Ruchkin, D.S., and Vidal, J.J. Measurements of event-related potentials. In: Callaway, E., Tueting, P., and Koslow, S.H. (Eds.). *Event-Related Brain Potentials in Man.* New York and London: Academic Press, 1978.

John, E.R., Ruchkin, D.S., and Villegas, J. Experimental background: signal analysis and behavioural correlates of evoked potential configuration in cats. *Annals of the New York Academy of Sciences*, 1964, 112, 362-420.

Kahneman, D. Method, findings and theory in studies of visual masking. *Psychological Bulletin*, 1968, 70, 404-425.

Kahneman, D. *Attention and Effort.* New Jersey: Prentice-Hall, 1973.

Karrer, R., Cohen, J., and Tueting, P. *Brain and Information: Event-Related Potentials.* New York: New York Academy of Sciences, 1984.

Kendall, M.G., and Stuart, A. *The Advanced Theory of Statistics. Vol. 2: Inference and Relationship.* London: Charles Griffin and Co., 1967.

Kerr, B. Processing demands during mental operations. *Memory and Cognition*, 1973, 1, 401-412.

Kirk, R.E. *Experimental Design: Procedures for the Behavioural Sciences.* Belmont, California: Wadsworth, 1968.

Kirk, R.E. *Introductory Statistics.* Belmont, California: Wadsworth, 1978.

Klinke, R., Fruhstorfer, H., and Finkenzeller,P. Evoked responses as a function of external and stored information. *Electroencephalography and Clinical Neurophysiology*, 1968, 25, 119-122.

Kornhuber, H.H., and Deeke, L. (Eds.). Motor and sensory processes of the brain: Electrical potentials, behaviour and clinical use. *Progress in Brain Research, Vol. 54.* Amsterdam: Elsevier/ North-Holland Biomedical Press, 1980.

Kuhn, T.S. *The Structure of Scientific Revolutions.* Chicago: University of Chicago Press, 1962.

Lehmann, D., and Callaway, E. (Eds.). *Human Evoked Potentials: Applications and Problems.* New York: Plenum Press, 1979.

Loveless, N.E., Brebner, J., and Hamilton, P. Bisensory presentation of information. *Psychological Bulletin*, 1970, 73, 161-199.

McLeod, P. Does probe RT measure central processing demand? *Quarterly Journal of Experimental Psychology*, 1978, 30, 83-89.

Moray, N. Where is capacity limited? A theory and a model. *Acta Psychologica*, 1967, 27, 84-92.

Näätänen, R. Selective attention and evoked potentials in humans - a critical review. *Biological Psychology*, 1975, 2, 237-307.

Näätänen, R. Processing negativity: an evoked-potential reflection of selective attention. *Psychological Bulletin*, 1982, 92, 605-640.

Näätänen, R., and Michie, P.T. Early selective attention effects on the evoked potential: a critical review and reinterpretation. *Biological Psychology*, 1979, 8, 81-136.

Nash, A.J. and Williams, C.S. Effects of preparatory set and task demands on auditory event-related potentials. *Biological Psychology*, 1982, 15, 15-31.

Navon, D., and Gopher, D. On the economy of the human-processing system. *Psychological Review*, 1979, 86, 214-255.

Navon, D., and Gopher, D. Task difficulty, resources and dual-task performance. In: Nickerson, R.S. (Ed.). *Attention and Performance, Vol. VIII*. New Jersey: Lawrence Erlbaum Assoc., 1980.

Neter, J., and Wasserman, W. *Applied Linear Statistical Models*. Homewood, Illinois: Richard D. Irwin, Inc., 1974.

Norman, D.A., and Bobrow, D.G. On data-limited and resource-limited processes. *Cognitive Psychology*, 1975, 7, 44-64.

Ogden, G.D., Levine, J.M., and Eisner, E.J. Measurement of workload by secondary tasks. *Human Factors*, 1979, 21, 529-548.

Otnes, R.K., and Enochson, L. *Digital Time Series Analysis*. New York and London: John Wiley and Sons, 1972.

Otto, D.A. (Ed.). *Multidisciplinary Perspectives in Event-Related Potential Research*. EPA-600/9-77-043, US Government Printing Office: Washington, DC, 1978.

Parasuraman, R., and Beatty, J. Brain events underlying detection and recognition of weak sensory signals. *Science*, 1980, 210, 80-83.

Picton, T.W., and Hillyard, S.A. Human auditory evoked potentials. II: Effects of attention. *Electroencephalography and Clinical Neurophysiology*, 1974, 36, 191-200.

Picton, T.W., Hillyard, S.A., Krausz, H.I., and Galambos, R. Human auditory evoked potentials. I: evaluation of components. *Electroencephalography and Clinical Neurophysiology*, 1974, 36, 179-190.

Picton, T.W., and Hink, R.F. Evoked potentials: how? what? and why? *American Journal of EEG Technology*, 1974, 14, 9-44.

Picton, T.W., Woods, D.L., and Proulx, G.B. Human auditory sustained potentials. I: The nature of the response. *Electroencephalography and Clinical Neurophysiology*, 1978, 45, 186-197.

Posner, M.I., and Boies, S.J. Components of attention. *Psychological Review*, 1971, 78, 391-408.

Posner, M.I., Klein, R.M., Summers, J., and Buggie, S. On the selection of signals. *Memory and Cognition*, 1973, 1, 2-12.

Posner, M.I., and McLeod, P. Information processing models - in search of elementary operations. *Annual Review of Psychology*, 1982, 33, 477-514

Posner, M.I., and Mitchell, R.F. Chronometric analysis of classification. *Psychological Review*, 1967, 74, 392-409.

Proctor, R.W. A unified theory for matching-task phenomena. *Psychological Review*, 1981, 88, 291-326.

Ritter, W., Simpson, R., and Vaughan, H.G. Association cortex potentials and reaction time in auditory discrimination. *Electroencephalography and Clinical Neurophysiology*, 1972, 33, 547-555.

Rolfe, J.M. The secondary task as a measure of mental load. In: Singleton, W.T., Fox, J.G., and Whitfield, D. (Eds.). Measurement of Man at Work: *An Appraisal of Physiological and Psychological Criteria in Man-Machine Systems*. London: Taylor and Francis Ltd., 1971.

Roth, M., Shaw, J., and Green, J. The form, voltage distribution and physiological significance of the K-complex. *Electroencephalography and Clinical Neurophysiology*, 1956, 8, 385-402.

Ruchkin, D.S. An analysis of average response computations based upon aperiodic stimuli. *IEEE Transactions on Bio-Medical Engineering*. 1965, 12, 87-94.

Schwartz, M., and Pritchard, W.S. AERs and detection in tasks yielding u-shaped backward masking functions. *Psychophysiology*, 1981, 18, 678-685.

Segal, E.M., and Lachman, R. Complex behaviour or higher mental process: Is there a paradigm shift? *American Psychologist*, 1972, 27, 46-55.

Shannon, C.E. Communication in the presence of noise. *Proceedings I.R.E.* 1949, 37, 10-21.

Snyder, E., Hillyard, S.A., and Galambos, R. Similarities and differences among the P_3 waves to detected signals in three modalities. *Psychophysiology*, 1980, 17, 112-122.

Squires, N.K., Donchin, E., Squires, K.C., and Grossberg, S. Bisensory stimulation: inferring decision-related processes from the P300 component. *Journal of Experimental Psychology*, 1977, 3, 299-315.

Squires, K.C., Hillyard, S.A., and Lindsay, P.H. Vertex potentials evoked during auditory signal detection: Relation to decision criteria. *Perception and Psychophysics*, 1973, 14, 265-272.

Starr, A., Sohmer, H., and Celesia, G.G. Some applications of evoked potentials to patients with neurological and sensory impairment. In: Callaway, E., Tueting, P., and Koslow, S.H. (Eds.). *Event-Related Brain Potentials in Man*. New York and London: Academic Press, 1978.

Thomson, W.T. *Laplace Transformations: Theory and Engineering Applications*. London: Longmans, Green and Co., 1957.

Tueting, P. Event-related potentials, cognitive events, and information processing. In: Otto, D.A. (Ed.). *Multidisciplinary Perspectives in Event-Related Brain Potential Research*. EPA-600/9-77-043, US Government Printing Office: Washington DC, 1978.

Turvey, M.T. On peripheral and central processing in vision: inferences from an information-processing analysis of masking with patterned stimuli. *Psychological Review*, 1973, 80, 1-52.

Vaughan, H.G. The analysis of scalp-recorded brain potentials. In: Thompson, R.F., and Patterson, M.M. (Eds.). *Bioelectric Recording Techniques Vol. 1. Part B: Electroencephalography and Human Brain Potentials*. New York: Academic Press, 1974.

Vaughan, H.G. The neural origins of human event-related potentials. *Annals of the New York Academy of Sciences*, 1982, 388, 125-138.

Vaughan, H.G. and Ritter, W. The sources of auditory evoked responses recorded from the human scalp. *Electroencephalography and Clinical Neurophysiology*, 1970, 28, 360-367.

Weerts, T.C., and Lang, P.J. The effects of eye fixation and stimulus and response location on the contingent negative variation (CNV). *Biological Psychology*, 1973, 1, 1-19.

Wickens, C.D. The structure of attentional resources. In: Nickerson, R.S. (Ed.). *Attention and Performance, Vol. VIII*. New Jersey: Lawrence Erlbaum Assoc., 1980.

Wickens, C.D., Isreal, J.B., and Donchin, E. The event-related cortical potential as an index of task workload. In: Neal, A.S., and Palasek, R.F. (Eds.). *Proceedings of the Human Factors Society 21st Annual Meeting*. Santa Monica: Human Factors Society, 1977.

Winer, B.J. *Statistical Principles in Experimental Design*. New York: McGraw-Hill, 1971.

Wood, C.C. Application of dipole localisation methods to source identification of human evoked potentials. *Annals of the New York Academy of Sciences*, 1982, 388, 139-155.

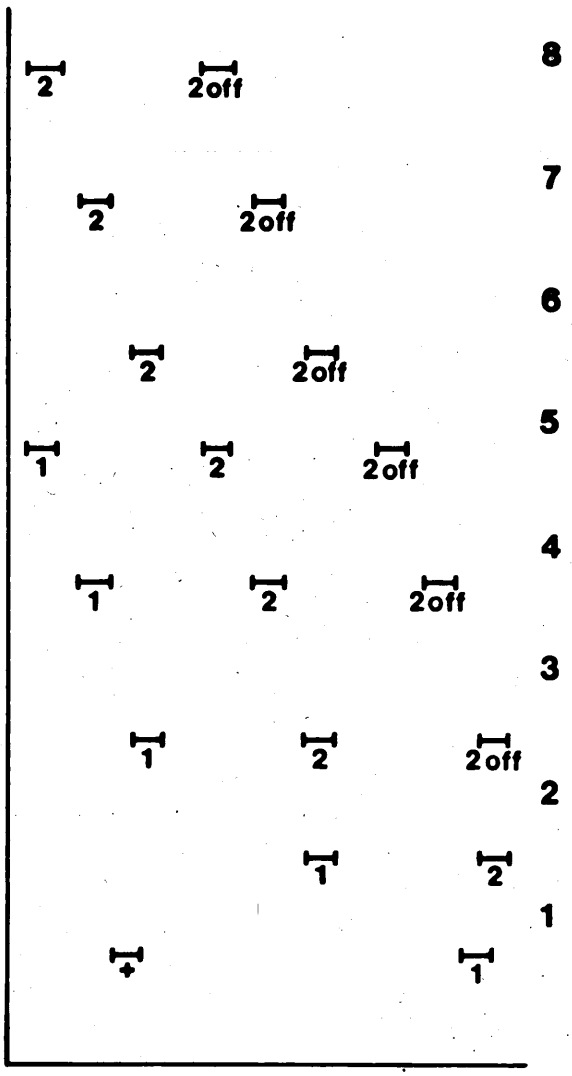

Overlay 1. Showing 100mS windows over which the onset and offset of visual task stimuli occur with respect to auditory task stimuli.

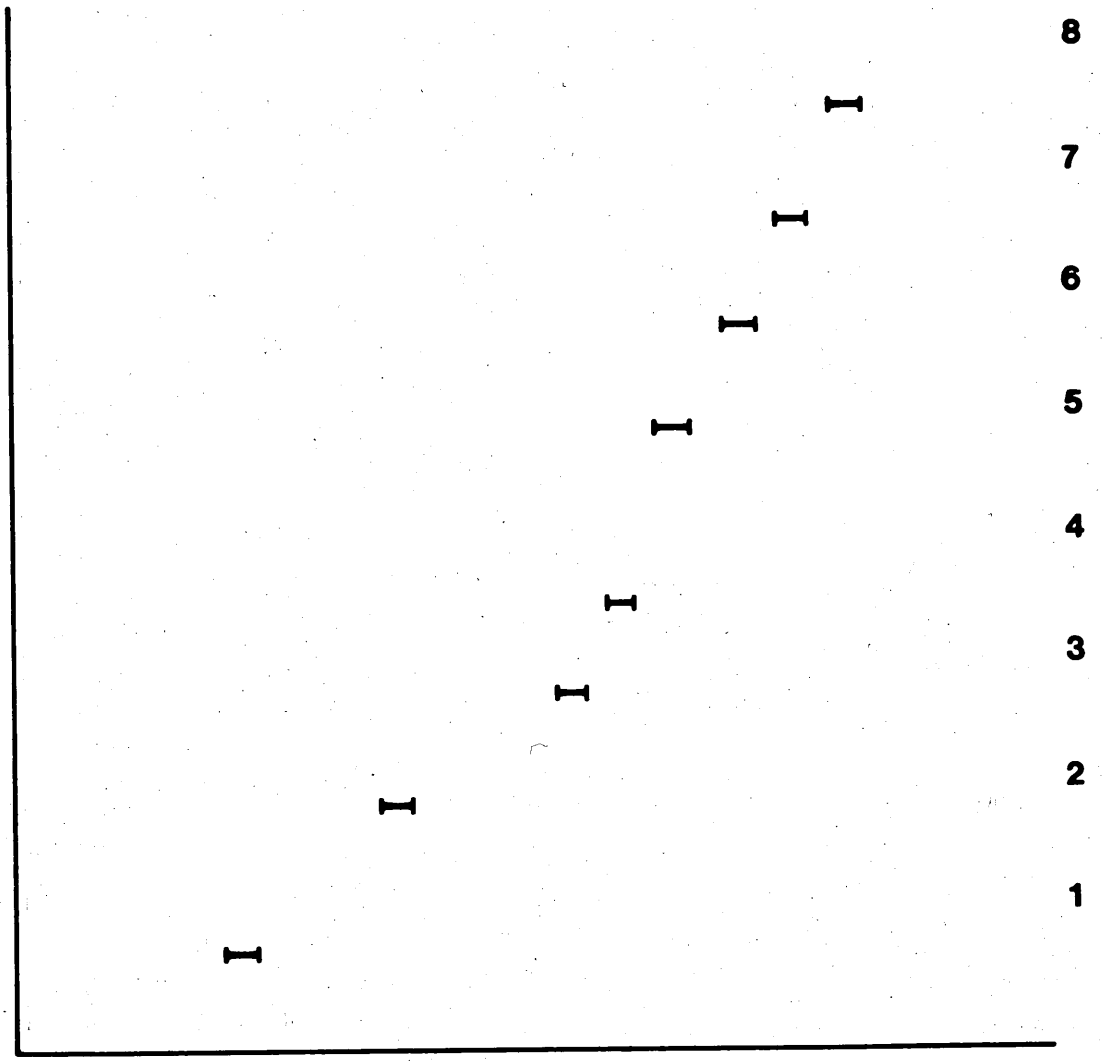

Overlay 2. Showing 100mS windows over which auditory task stimuli occur with respect to visual task stimuli.